Promotor : dr. ir. W.H. van der Molen, hoogleraar in de agrohydrologie.

Electrolytic analogue study of the effect of openings and surrounds of various permeabilities on the performance of field drainage pipes

W. DIERICKX

Electrolytic analogue study of the effect of openings and surrounds of various permeabilities on the performance of field drainage pipes

Proefschrift
ter verkrijging van de graad van
doctor in de landbouwwetenschappen,
op gezag van de rector magnificus,
dr. H.C. van der Plas,
hoogleraar in de organische scheikunde,
in het openbaar te verdedigen
op vrijdag 25 april 1980
des namiddags te vier uur in de aula
van de Landbouwhogeschool te Wageningen

Rijksstation voor Landbouwtechniek
Merelbeke 1980

D/1980/0252/1

ISN = 106891

ABSTRACT

DIERICKX, W. 1980. Electrolytic analogue study of the effect of openings and surrounds of various permeabilities on the performance of field drainage pipes.
Comm. of the Nat. Inst. for Agr. Eng. (Med. Rijksstation voor Landbouwtechniek) 77. Merelbeke (Belgium).
ISBN 90 70142 13 9. XVIII + 238 p., 90 figs., 48 tables, 104 refs. English, Dutch, French and German summaries.
Also : Doctoral thesis Wageningen.

The effect of various openings and surrounds of various permeabilities on the performance of field drainage pipes was studied by means of an electrolytic analogue. The results obtained were compared with those of analytical solutions. Rather simple and sufficiently accurate solutions exist to determine the entrance resistance of pipes with smooth outer surface. These theoretical solutions cannot be applied to pipes with corrugated outer surface provided with perforations in the valley of the corrugations for which the corrugations are filled with soil. The shape of the corrugations and the boundary of soil and corrugation present additional difficulties in obtaining an exact theoretical solution for such drains.

From the investigations performed it follows that the smallest entrance resistance is obtained at the greatest subdivision of a given perforation area or perimeter per unit drain length. The most favorable perforations which confer the lowest entrance resistance are these with the smallest area or perimeter such as circular perforations and, for rectangular slits, those with the smallest length. Except for circular perforations, an increase of the actual perforation area of 20 - 25 cm^2/m to about 50 cm^2/m will considerably reduce the entrance resistance.

Using permeable envelopes, the entrance resistance decreases considerably up to an envelope thickness of about 5 mm after which a constant value is obtained. The effective radius, however, continues to increase with increasing envelope thickness due to the decrease in radial resistance. Increasing the permeability of the envelope reduces the entrance resistance and increases the effective radius up to a permeability ratio of 20. Any further increase of the permeability ratio is of less significance. For a constant value of pipe radius plus envelope thickness much the same effective radius is obtained if the thickness of the envelope is at least 5 mm.

A less permeable drain surround increases the entrance resistance enormously and inadmissible values are quickly reached. A constant entrance resistance is obtained for thicknesses of about 10 mm and upwards. The effective radius decreases due to the increase of radial resistance and exceptionally small values are obtained. The increase of entrance resistance and decrease of effective radius are particularly marked for permeability ratios less than 0,2.

The entrance resistance only changes slightly when a drain is surrounded by an envelope which has a reduced permeability over a certain percentage of its original thickness. Due to the effect upon radial resistance, the effective radii will decrease with decreasing permeability and increasing thickness of the blocked zone. The affective radius never assumes such extremely small values as are obtained with a drain directly surrounded by a wholly less permeable layer.

The entrance resistance of a drain pipe is constant and depends only on the geometrical characteristics of the pipe itself. It is, however, important to give an exact description of the flow pattern, since its omission can result in faulty conclusions being drawn about the entrance resistance.

Due to the entrance resistance, the hydraulic gradient in the vicinity of the perforations can reach high values and massive invasion of soil particles may occur. These gradients are markedly reduced when the drain is surrounded by a permeable envelope.

Although the approach flow conditions are more favorable if water is standing above the drain, the entrance resistance which causes a certain water level above the drain will raise the water table midway between drains more than an ideal drain operating with the same head.

Free descriptors : drainage, electrolytic analogue, openings of drain pipes, drain pipe surrounds, entrance resistance, approach flow resistance, effective radius, permeability of drain surrounds, partially blocked envelopes, hydraulic gradient.

This thesis will also be published as Report 77.

National Institute for Agricultural Engineering
Van Gansberghelaan, 115
B-9220 Merelbeke (Belgium).

Stellingen

1. Het algemeen gebruikte begrip *intreeweerstand* geeft aanleiding tot heel wat verwarring. Een betere bepaling is *konvergentieweerstand van de stroomlijnen naar de perforaties.*

2. De theoretische oplossingen van MUSKAT (1942) en van KIRKHAM & SCHWAB (1951) bevatten onjuiste benaderingen die aanleiding geven tot foutieve intreeweerstanden.

   MUSKAT, M. 1942. The effect of casing perforations on well productivity. Petroleum Technology 5 : 175-187.

   KIRKHAM, D. & SCHWAB, G.O. 1951. The effect of circular perforations on flow into subsurface drain tubes. Part I, Theory. Agr. Eng. 32, 4 : 211-214.

3. De bepaling van de doorlatendheid van draineerbuizen (KLOTZ, 1973) heeft weinig of geen physische betekenis.

   KLOTZ, D. 1973. Durchlässigkeitsuntersuchungen an gewellten Kunststoff-Dränrohren. Zeitschr. f. Kult. und Flurber. 14 : 40-53.

4. De cohesie van de bodem verklaart de gunstige werking van de relatief grovere en de ongunstige werking van de relatief fijnere omhullingsmaterialen.

5. De weerstand tegen doorspoeling van een kohesieloos poreus medium doorheen een omhulling of weefsel kan het duidelijkst vastgesteld worden bij opwaarts gerichte stroming.

6. Alhoewel het gebruik van bodemkonditioneringsmiddelen bij drainage gunstige perspektieven biedt, doen zich nog een aantal problemen voor van praktische aard.

7. Verschillen in drainerende werking van vollopende en niet-vollopende draineerbuizen, al dan niet voorzien van een omhulling, kunnen niet toegeschreven worden aan verschillende intreeweerstanden.

8. Het ontwerp *ISO-aanbevelingen voor draineerbuizen uit niet-geplastificieerd PVC* wordt, ten onrechte, alleen toegepast in het Belgisch type-bestek.

   Type-bestek voor de uitvoering van de drainage van landbouwgronden. Ministerie van Landbouw, Vlaamse aangelegenheden, Nationale Landmaatschappij, B.R.B.V. nr. 34.7, uitgave 1978.

9. Het elektrolytmodel is een uitstekend hulpmiddel voor de studie van drie-dimensionale stationaire grondwaterstromingen.

10. Elektrische modellen lenen zich, ondanks hun beperkte nauwkeurigheid, uitstekend tot het toetsen van de juistheid en de nauwkeurigheid van theoretische oplossingen.

11. Alhoewel de numerieke simulatie bepaalde voordelen biedt, geniet de analoge simulatie in vele gevallen de voorkeur.

12. Globale weersvoorspellingen uit weerkundige waarnemingen op lange termijn blijven onbetrouwbaar.

13. Het toenemend verbruik van drinkwater kan aanzienlijk beperkt worden door gebruik van regenwater voor doeleinden waarvoor de aan leidingwater gestelde hoge kwaliteitseisen eigenlijk niet vereist zijn.

14. De alternatieve landbouw is een typische exponent van een maatschappij van overvloed.

15. Jeugdmisdadigheid wordt niet verminderd door het afschaffen van speelgoedwapens.

Stellingen behorende bij het proefschrift van W. DIERICKX, *Electrolytic analogue study of the effect of openings and surrounds of various permeabilities on the performance of field drainage pipes.* Wageningen, vrijdag 25 april 1980.

In de wetenschap gelijken wij op kinderen die aan de oever van de kennis hier en daar een steentje oprapen, terwijl de wijde oceaan van het onbekende zich voor onze ogen uitstrekt.

John Newton.

Aan Jacqueline
Aan Adelhard en Adelheid

CURRICULUM VITAE

De auteur werd geboren op 15 oktober 1942 te Gent (België). Hij volgde lager onderwijs aan de Gemeenteschool te Wondelgem en in juni 1961 behaalde hij het diploma van het middelbaar onderwijs (moderne humaniora, wetenschappelijke afdeling A) aan het Instituut der Broeders van Onze Lieve Vrouw van Lourdes te Oostakker. Van oktober 1961 tot juni 1966 studeerde hij aan de Landbouwhogeschool, later Fakulteit der Landbouwwetenschappen (F.L.W.) van de Rijksuniversiteit, te Gent (R.U.G.). Hij behaalde (met grote onderscheiding) het diploma van Landbouwkundig Ingenieur in de Boerderijbouw, richting Konstrukties en Kultuurtechniek met als eindwerk : *Het elektrisch netwerk als hulpmiddel bij de studie van niet-stationaire grondwaterstromingen naar drains*.

Na het vervullen van de militaire dienstplicht was hij van oktober 1967 tot januari 1970 als assistent toegevoegd aan Prof. ir. G.A. HEYNDRICKX, titularis van de Leerstoel voor Kultuurtechniek aan de F.L.W. van de R.U.G. Vanaf februari 1970 is hij, achtereenvolgens als assistent tot september 1971, als aerstaanwezend-assistent tot oktober 1977 en als werkleider tot op heden, werkzaam bij de Werkgroep voor de Studie van de Technologie der Waterbeheersingsmaterialen in de Landbouw, gehecht aan het Rijksstation voor Landbouwtechniek te Merelbeke (Direkteur : Dr. ir. A. MATON), aan onderzoeksprojekten betreffende de werking en verwerking van drainagematerialen en hun specifieke toepassingen.

DIERICKX Willy
Geraardsbergsesteenweg, 18
9233 OOSTERZELE (Landskouter)
België

VOORWOORD

Het in dit proefschrift vermelde onderzoek maakt deel uit van het onderzoekingsprogramma van de Werkgroep voor de Studie van de Technologie der Waterbeheersingsmaterialen in de Landbouw en graag wil ik iedereen bedanken die bij de totstandkoming ervan heeft bijgedragen.

Dr. ir. A. MATON, Direkteur van het Rijksstation voor Landbouwtechniek, ben ik zeer erkentelijk voor zijn belangstelling en aanmoediging bij het uitvoeren van dit onderzoek.

Bijzonder dankbaar ben ik mijn promotor Prof. dr. ir. W.H. VAN DER MOLEN voor het aanvaarden van de leiding van dit onderzoek. De talrijke besprekingen en praktische raadgevingen zijn voor mij blijvende herinneringen van bijzondere waardering.

Bijzondere steun en aanmoediging mocht ik steeds ontvangen van ir. J.A.C. KNOPS waarvoor mijn welgemeende dank. Ook dr. ir. J. WESSELING ben ik dank verschuldigd voor het kritisch bestuderen van het koncept en voor de konstruktieve suggesties van het manuskript. Voor hun belangstelling, aanmoediging en hulp dank ik eveneens ir. C. VAN SOMEREN en ir. J. CAVELAARS.

Zeer erkentelijk ben ik ir. R. MOERMANS en Mevr. B. ROEF van het Centrum voor Biometrische Verwerking waar ik nooit tevergeefs aanklopte voor de talloze computerberekeningen.

I take great pleasure in acknowledging the many helpful suggestions and advice received from Agr. Eng. C. DENNIS of the Field Drainage Experimental Unit in Cambridge.

Ook mijn medewerkers ben ik zeer erkentelijk waarbij in de eerste plaats ing. N. LEYMAN voor de plichtsbewustheid en de nauwgezetheid waarmede hij de talloze berekeningen heeft uitgevoerd en de tekeningen verzorgde. Nooit deed ik tevergeefs beroep op de heer N. VAN HAVERMAETE voor de konstruktie van diverse modellen en het uitvoeren van talloze metingen. De heer E. MOREELS leverde een belangrijke bijdrage in de praktische realisatie van de buizen met geïsoleerde kontaktpunten. Zonder hun vakbekwaamheid en nauwgezette toewijding zou dit onderzoek nooit mogelijk geweest zijn waarvoor mijn bijzondere waardering. Ook dank aan de heer F. VAN HESSCHE die behulpzaam was bij de metingen en de verwerking van de resultaten.

Voor het geduldig en zorgvuldig typen van de diverse koncepten en het uiteindelijke manuskript dank ik Mevr. D. DE CONINCK.

Verder dank ik ing. J. LAMBRECHTS voor het degelijk fotografisch werk en de heer G. VERMEULEN voor de zorg om het drukwerk.

Jacqueline, niet in het minst wens ik jou te danken voor de morele steun en het begrip dat je opbracht voor de vele vrije uren die ik aan mijn proefschrift besteedde.

CONTENTS

LIST OF SYMBOLS

A_p	= perforation area per unit drain length (cm^2/m)	L
A_{pp}	= percentage open area of the drain (%)	-
A_{pz}	= percentage open area of a partial perforated zone (%)	-
$C^1_{co}(\beta_s)$ $C^1_{dcs}(\beta_s)$	= code symbols for corrugated drains	
C_p	= perforation perimeter per unit drain length (cm/m)	-
c	= gap spacing or discontinuous circumferential slit spacing in the row (mm)	L
c_o	= soil cohesion (N/m^2)	$ML^{-1}T^{-2}$
D_o	= outer diameter of smooth drains; larger outer diameter of corrugated drains (mm)	L
D'_o	= smaller outer diameter of corrugated drains (mm)	L
d	= drain depth (m)	L
d_b	= thickness of the partially blocked envelope (mm)	L
d_c	= thickness of the less permeable drain surround (mm)	L
d_e	= thickness of the more permeable envelope (mm)	L
E	= drain spacing (m)	L
H	= depth of the impervious layer below drain level (m)	L
h_A	= hydraulic head at point A (m)	L
h_{AB}	= mean hydraulic head of h_A and h_B (m)	L
h_B	= hydraulic head at point B (m)	L
h_C	= hydraulic head at point C (m)	L
h_m	= water table height above drain level midway between drains (m)	L
h_o	= water table height above drain level at the drain (m)	L
I	= electric current (A)	I
I_{id}	= electric current for flow towards a conductor simulating an ideal drain (A)	I
I_{rd}	= electric current for flow towards a conductor simulating a real drain (A)	I
I_o	= modified Bessel function of the first kind and zero order	-
I_1	= modified Bessel function of the first kind and first order	-

i	= hydraulic gradient	-
	= integer	-
i_c	= critical hydraulic gradient	-
K_o	= modified Bessel function of the second kind and zero order	-
K_1	= modified Bessel function of the second kind and first order	-
k	= hydraulic conductivity of the soil (m/d)	LT^{-1}
k_b	= hydraulic conductivity of the partially blocked envelope (m/d)	LT^{-1}
k_c	= hydraulic conductivity of the less permeable drain surround (m/d)	LT^{-1}
k_e	= hydraulic conductivity of the more permeable envelope (m/d)	LT^{-1}
L	= conductor length (m)	L
l	= length of individual clay drain pipes (mm)	L
m	= perforation number per unit drain length (1/m)	L^{-1}
N	= flow rate per unit surface area (mm/d)	LT^{-1}
	= number of perforation rows	-
n	= integer	-
p	= $2\ \pi/\beta$	-
q	= discharge per unit drain length (m^2/d)	L^2T^{-1}
R	= circular equipotential radius (mm)	L
R'	= circular equipotential radius (mm)	L
R_o	= ideal drain radius; outer radius of a smooth drain; larger outer radius of a corrugated drain (mm)	L
R'_o	= smaller outer radius of a corrugated drain (mm)	L
R_1	= difference between equipotential radius and outer drain radius (mm)	L
R_b	= radius of drain plus envelope plus partially blocked envelope (mm)	L
R_{bi}	= inner radius of the pipe with isolated contact points at the interface of soil and partially blocked envelope (mm)	L

R_{bo}	= outer radius of the pipe with isolated contact points at the interface of soil and partially blocked envelope (mm)	L
R_c	= radius of drain plus less permeable surround (mm)	L
R_{ci}	= inner radius of the pipe with isolated contact points at the interface of soil and less permeable surround (mm)	L
R_{co}	= outer radius of the pipe with isolated contact points at the interface of soil and less permeable surround (mm)	L
R_e	= radius of drain plus envelope material (mm)	L
R_{ef}	= effective drain radius (mm)	L
R_{ei}	= inner radius of the pipe with isolated contact points at the interface of soil and envelope material (mm)	L
R_{eo}	= outer radius of the pipe with isolated contact points at the interface of soil and envelope material (mm)	L
R_m	= mean radius of the pipe with isolated contact points (mm)	L
S^1_{co}		
$S^2_{co}(\beta_s)$		
$S^1_{cp}(\delta_p)$		
$S^2_{cp}(\delta_p)$		
$S^3_{cp}(\delta_p)$	= code symbols for smooth drains	
$S^4_{cp}(\delta_p)$		
$S^1_{cls}(\beta_p)$		
$S^1_{dls}(\beta_p)$		
$S^1_{dcs}(\beta_s)$		
V_e	= electric potential component due to entrance flow (V)	$ML^2T^{-3}I^{-1}$
V_{ec}	= electric potential component due to entrance flow of the system simulating drain plus less permeable surround (V)	$ML^2T^{-3}I^{-1}$

V_{ee}	= electric potential component due to entrance flow of the system simulating drain plus envelope (V)	$ML^2T^{-3}I^{-1}$
V_r	= electric potential component due to radial flow (V)	$ML^2T^{-3}I^{-1}$
V_{rs}	= electrical potential component due to radial flow of the system simulating a drain surrounded by one or more layers having another permeability than that of the soil (V)	$ML^2T^{-3}I^{-1}$
V_t	= total electric potential due to radial flow from an equipotential with radius R towards a conductor simulating a real drain (V)	$ML^2T^{-3}I^{-1}$
V'_t	= total electric potential due to radial flow from an equipotential with radius R' towards a conductor simulating a real drain (V)	$ML^2T^{-3}I^{-1}$
W	= total flow resistance (d/m)	TL^{-1}
W_e	= entrance resistance (d/m)	TL^{-1}
W_h	= horizontal resistance (d/m)	TL^{-1}
W_r	= radial resistance (d/m)	TL^{-1}
W_t	= total resistance for radial flow towards a real drain (d/m)	TL^{-1}
W_v	= vertical resistance (d/m)	TL^{-1}
W_u	= total resistance for unsymmetrical radial flow towards an ideal drain (d/m)	TL^{-1}
X	= midpoint eccentricity of equipotential and drain pipe (mm)	L
α	= slope angle of the relation between V_t and $\ln(R/R_o)$	rad
α_{ap}	= approach flow resistance	-
α_e	= entrance resistance of the plain drain	-
α_e^*	= entrance resistance for radial flow over a sector of a circle	-
α'_e	= entrance resistance of the drain surrounded by one or more layers having another permeability than that of the soil	-
$(\alpha'_e)_{th}$	= theoretical value of α'_e	-

α_{ea}	= entrance resistance of the plain drain for arched boundary conditions	-
α_{ec}	= entrance resistance of drain plus less permeable surround	-
α_{ee}	= entrance resistance of drain plus envelope	-
$(\alpha_{ee})_W$	= entrance resistance of drain plus envelope according to WIDMOSER (1968)	-
α_{eeb}	= entrance resistance of drain plus envelope plus partially blocked envelope	-
α_{ep}	= entrance resistance of the plain drain for plane boundary conditions	-
α_h	= horizontal resistance	-
α_{0e}	= entrance resistance of ideal drain plus envelope	-
α_r	= radial resistance	-
$(\alpha_{0e})_W$	= entrance resistance of ideal drain plus envelope according to WIDMOSER (1968)	-
α_{rc}	= radial resistance of the less permeable drain surround related to the permeability of the surround itself	-
α'_{rc}	= radial resistance of the less permeable drain surround related to the permeability of the surrounding soil	-
α_{re}	= radial resistance of the envelope related to the permeability of the envelope itself	-
α'_{re}	= radial resistance of the envelope related to the permeability of the surrounding soil	-
α_{rs}	= radial resistance of the soil for flow towards a drain surrounded by one or more layers having another permeability than that of the soil	-
α_{su}	= additional resistance in accepting an imaginary radial flow	-
α_t	= total resistance for radial flow towards a real drain	-
α_u	= total resistance for unsymmetrical radial flow towards an ideal drain	-
β	= sector of the circle representing radial flow	rad

β_{en}	= entrance resistance of the pipe with isolated contact points	-
β_{en}^{ip}	= entrance resistance of the inner pipe with isolated contact points	-
β_{en}^{op}	= entrance resistance of the outer pipe with isolated contact points	-
β_{eq}	= equivalent angle	rad
β_{ex}	= exit resistance of the pipe with isolated contact points	-
β_{ex}^{ip}	= exit resistance of the inner pipe with isolated contact points	-
β_{ex}^{op}	= exit resistance of the outer pipe with isolated contact points	-
β_p	= width of continuous or discontinuous longitudinal slits (mm)	L
β_s	= width of continuous or discontinuous circumferential slits (mm)	L
β_v	= valley width of corrugated drains (mm)	L
Γ	= gamma function	-
γ	= EULER's constant (γ = 0,577 21...)	-
γ	= ratio of perforation length to perforation spacing	-
Δh	= total hydraulic head loss for flow towards drains (m)	L
Δh_e	= hydraulic head loss due to entrance flow (m)	L
Δh_m	= difference in water table height midway between drains (m)	L
Δh_r	= hydraulic head loss due to radial flow (m)	L
Δh_t	= total hydraulic head loss due to flow towards a real drain (m)	L
Δh_u	= total hydraulic head loss due to unsymmetrical radial flow towards an ideal drain (m)	L
$\Delta\alpha_r$	= difference in radial flow resistance	-
δ	= eccentricity of well midpoint to aquifer midpoint (m)	L
δ_p	= perforation diameter (mm)	L
δ_r	= corrugation height of corrugated drain pipes (mm)	L
ϵ	= ratio between eccentricity δ and the length of the aquifer	-

ζ	= $(\lambda_r + 2\delta) / 2\lambda_r$	-
θ_i	= angle to the i^{th} perforation row, measured from the base line passing through the x-axis	-
κ_b	= permeability ratio of the blocked part of the envelope to the surrounding soil	-
κ_c	= permeability ratio of less permeable drain surround to surrounding soil	-
κ_e	= permeability ratio of envelope to surrounding soil	-
λ_1	= smallest spacing of circular perforations (mm)	L
λ_2	= largest spacing of circular perforations (mm)	L
λ_c	= spacing of perforations on the drain circumference (mm)	L
λ_f	= length of the partially perforated section (mm)	L
λ_g	= spacing of the partially perforated section (mm)	L
λ_p	= length of discontinuous longitudinal slits (mm)	L
λ_r	= spacing of perforations in the row (mm)	L
λ_s	= spacing of circular perforations in a square pattern (mm)	L
ρ	= resistivity of the electrolyte (Ω.m)	$ML^3T^{-3}I^{-2}$
ρ_s	= specific mass of saturated soil (kg/m^3)	ML^{-3}
ρ_w	= specific mass of water (kg/m^3)	ML^{-3}
ρ_e	= intergranular stress (N/m^2)	$ML^{-1}T^{-2}$
τ_f	= shearing resistance per unit area (N/m^2)	$ML^{-1}T^{-2}$
φ	= largest angle of the water table with the horizontal	rad
ϕ	= angle of internal friction	rad
Ω	= total electric resistance (Ω)	$ML^2T^{-3}I^{-2}$
ω	= coefficient taking into account the boundary conditions at the perforations	-

INTRODUCTION

IMPORTANCE OF ENTRANCE RESISTANCE FOR DRAINAGE

The word *drainage* has many meanings and includes the methods and means that can be used to remove excess subsurface water from the soil. The immediate purpose of drainage for agriculture is to decrease the water content of the upper soil layers by lowering the groundwater table. The final purpose is to increase crop yield, to improve the quality of the crops or to alter the soil in such a way that crops of higher value can be grown. Moreover, other objectives such as improved soil bearing strength and cultivatibility can be envisaged.

Besides the removal of excess soil water, drainage is applied in irrigated areas to leach saline soils and to evacuate excess irrigation water. Drains are also used to intercept seepage water from catchment areas and spring lines. Drainage also contributes to the stability of slopes. Ever increasing demands are made on fields for recreation and, there also, drainage is applied successfully. Drainage is carried out on airfields, industrial estates, burial grounds and in road construction. Drains are applied to reduce water pressure on building foundations and can be efficiently applied to roof gardens.

The mathematical analysis of the problem of water flow through porous media into subsurface drains is based on DARCY's law and solutions have been obtained only after making many simplifying assumptions about the flow behaviour towards drains. One of the primary assumptions that underlies most of the formulae applied for drainage design is the assumption of an *ideal drain*, i.e. a drain with a completely pervious wall surrounded by a homogeneous soil of uniform permeability. An ideal drain could be formed by a mole channel if no compaction in the surrounding of the mole channel has occured and if no smearing of the wall has taken place. Due to the convergency of the streamlines to the inlet openings, the flow of water towards a *real drain*, i.e. a drain with a relatively small area of inlets, encounters an extra resistance and consequently an extra head loss. This extra resistance is commonly called *entrance resistance*. When clay or concrete drain pipes are used, water enters through the gaps between the pipes. Plastic

drain pipes manufactured from polyvinylchloride (P.V.C.) or polyethylene (P.E.) are generally provided with slits or perforations to allow the entrance of water.

At the beginning of the application of plastic drain pipes, smooth pipes were used. The perforations strongly influenced the strength of the pipe. These smooth plastic drains were, if they had a too thin wall, deformed by the load of the trench backfill and the width of saw slits was reduced (SEGEREN & ZUIDEMA, 1969). To obtain a low entrance resistance, a large number of perforations is required. This often weakens the pipe to such an extent that a larger wall thickness is required. An increased wall thickness means more material and a more expensive pipe. For that reason WESSELING & HOMMA (1967) propose that the highest possible number of perforations that are consistent with satisfactory crushing strength and drainage performance should be used. At the same time it was the objective to design perforations which prevented the entrance of soil particles. This was, however, impossible and impracticable for certain soil types (VAN SOMEREN, 1964).

In contrast, the more modern corrugated drain pipes had greater crushing strength and in consequence the perforation area could be increased considerably. Indeed, the larger the amount of perforations, the smaller the entrance resistance will be. Aiming for a large number of perforations can contribute to the success of the drainage. The acceptance of a minimum amount of perforations introduces considerable risk as blocking and clogging of perforations is an established phenomenon. Although the entrance resistance of drain pipes can be decreased considerably by using a good envelope material, the continuous increase in price of these materials limits the use to soils subject to erosion. Therefore stable soils are generally drained without envelope material in order to decrease the costs. This being so, the use of well-perforated pipes is of great importance. Numerous investigations have already shown that it is not only the perforation area which determines entrance resistance. Also shape, size, width, distribution and number of perforations determine the extra resistance which flow towards the drain has to overcome. Here the question is in which way the factors mentioned influence the entrance resistance.

Entrance resistances also play an important role in the construction of wells since the well screen applied largely determines the performance of

the well. Several theories on entrance resistance in fact have been developed for well screens. Since these theories assume DARCY's law to be valid, the problem is similar to that of drains and they have been considered in this research too.

In the first part of this study the entrance resistance itself forms the subject. After the definition of it, the existing theories on the subject have been reviewed. This leads to derivations of the entrance resistance for certain perforation types and patterns. Next the theoretical background and set up of model tests have been treated and the electrolytic model used has been described. The results of electrolytic model tests have been compared with theoretical solutions. This comparison allowed the choice of mathematical formulae for the entrance resistance from which it can be concluded which factors and parameters are important in determining it.

The use of envelope material considerably increases the drainage performance and its influence is studied in the second part. Besides some theoretical considerations, the definition of entrance resistance has been discussed and a review of the methods to determine the effect of envelopes has been given. Next the electrolytic analogue of envelopes has been described and the effect of envelope thickness and permeability has been systematically investigated. These investigations allowed conclusions about envelope thickness and permeability to be drawn.

The third part deals with the influence on drainage performance of less permeable drain surrounds and of partially clogged envelopes. The analogue model has been described and the results obtained used to establish their effect on entrance resistance.

Some additional aspects of entrance resistance constitute the fourth part. To investigate the effect of flow pattern and partially full drain on entrance resistance, some additional electrolytic and sand model tests have been carried out. The influence of entrance resistance on soil particle invasion could be derived from the model tests performed and has been discussed. Based on theoretical considerations, the effect of entrance resistance on water table height has been treated.

The purpose of this study is to contribute to our knowledge of drain pipe and envelope material construction with a view to improving the performance of drainage systems.

CHAPTER I

THE ENTRANCE RESISTANCE OF DRAIN PIPES

---

1. *Theoretical background*

The hydraulic head required for flow of water towards a drainage system in a homogeneous and isotropic soil is given by ERNST (1954) as

$$\Delta h = N\ E\ W = q\ W \qquad (1.1)$$

where Δh = difference in hydraulic head midway between two drains and in the drain (m)

N = flow rate per unit surface area (m/d)

E = drain spacing (m)

W = total flow resistance (d/m)

q = discharge per unit drain length (m^2/d).

The total flow resistance can be considered to consist of a vertical resistance W_v, a horizontal resistance W_h, a radial resistance W_r and an entrance resistance W_e (fig. 1.1). Both horizontal and vertical resistances only depend on the porous medium and are independent of the drain used. The magnitude of radial and entrance resistances are determined by both the

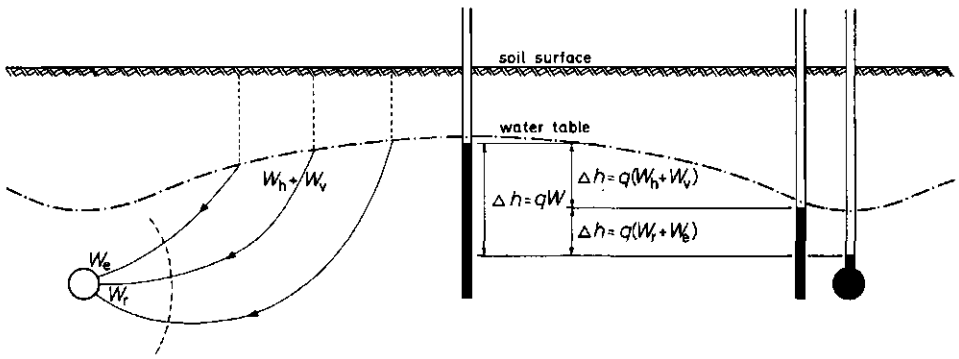

Fig. 1.1 Resistances and head losses for flow of water towards drain pipes.

porous medium and the drain used.

Considering radial flow towards an ideal drain (fig. 1.2) in an homogeneous isotropic soil, the hydraulic head loss is given by

$$\Delta h_r = \frac{q}{2 \pi k} \ln \frac{R}{R_o} = q \, W_r \qquad (1.2)$$

or

$$W_r = \frac{1}{2 \pi k} \ln \frac{R}{R_o} \qquad (1.3)$$

where Δh_r = hydraulic head loss (m)
k = hydraulic conductivity (m/d)
R = radius of a circular equipotential (m)
R_o = radius of the ideal drain (m).

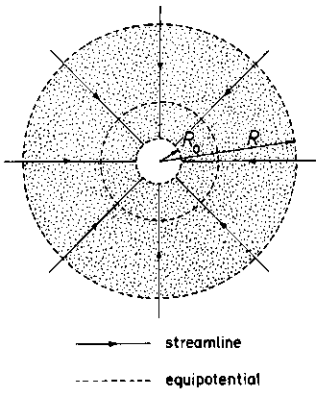

Fig. 1.2. Radial flow towards an ideal drain.

The radial resistance depends on the hydraulic conductivity of the porous medium, the radius of the equipotential considered and the radius of the ideal drain. The radial resistance increases with decreasing hydraulic conductivity and with decreasing radius of the drain. Eqn. (1.2) can be written as

$$\Delta h_r = \frac{q}{k} \alpha_r \qquad (1.4)$$

where

$$\alpha_r = \frac{1}{2\pi} \ln \frac{R}{R_o} \tag{1.5}$$

and from eqns. (1.2) and (1.4) it follows that

$$\alpha_r = W_r \, k \tag{1.6}$$

where α_r is the radial resistance for a soil with a hydraulic conductivity equal to unity. It is a dimensionless constant which decreases with increasing radius of the drain (fig. 1.3).

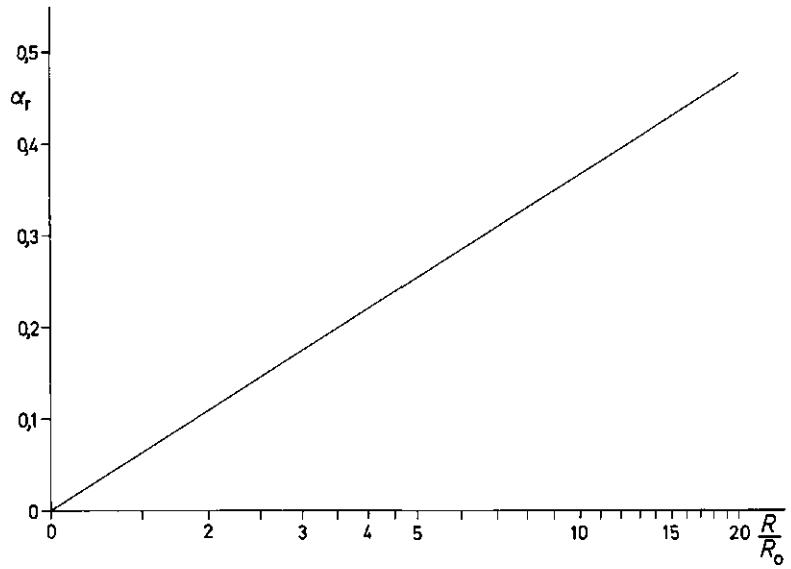

Fig. 1.3. Radial resistance as a function of the ratio R/R_o.

Ideal drain pipes have no physical reality and the additional hydraulic head loss for flow towards a real drain (fig. 1.4) can be expressed as

$$\Delta h_e = q \, W_e = \frac{q}{k} \alpha_e \tag{1.7}$$

and consequently

$$\alpha_e = W_e \, k \tag{1.8}$$

where α_e is the entrance resistance for a soil with hydraulic conductivity equal to unity. It is dimensionless and often called the *entrance constant*.

Here this entrance constant will, throughout, be called *entrance resistance*.

From their investigations, WESSELING & HOMMA (1967) found that eqn. (1.8) is valid as long as the hydraulic conductivity does not exceed 10 m/d.

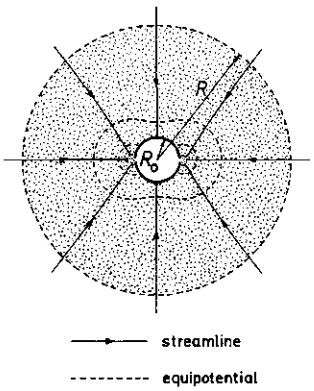

Fig. 1.4. Radial flow towards a real drain with two continuous longitudinal slits.

If radial flow only occurs towards part of the drain circumference, the entrance resistance can be modified (BOUMANS, 1963) as

$$\alpha_e^{\star} = p\ \alpha_e \qquad (1.9)$$

p being

$$p = \frac{2\pi}{\beta} \qquad (1.10)$$

where β is the angle of the sector over which radial flow takes place (fig. 1.5).

Since the flow zone will not always be a true sector of a circle, CAVELAARS (1970) introduced the concept of equivalent angle β_{eq} (fig. 1.6).

The total hydraulic head loss Δh_t for radial flow towards a real drain is given by

$$\Delta h_t = \Delta h_r + \Delta h_e \qquad (1.11)$$

or

$$\Delta h_t = q\ W_t = q\ (W_r + W_e) \qquad (1.12)$$

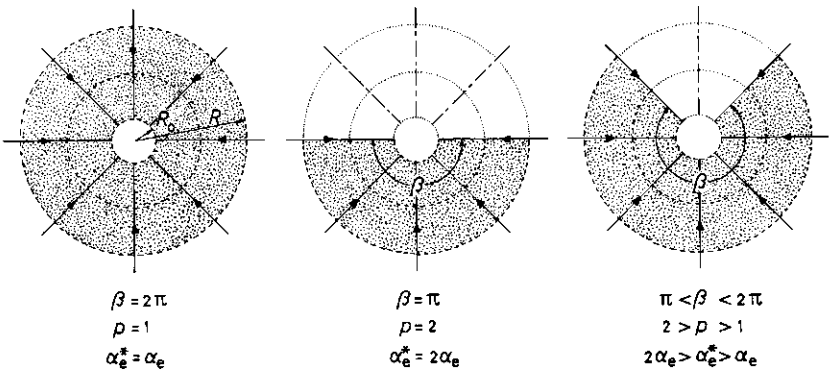

Fig. 1.5. Influence of a partially radial flow on the entrance resistance.

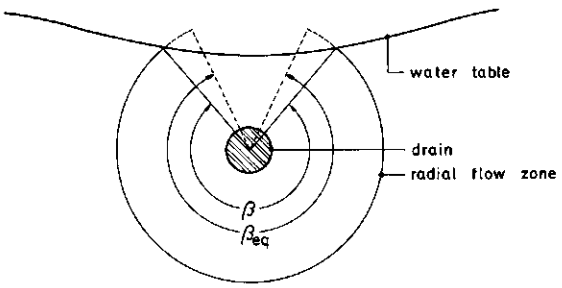

Fig. 1.6. Since the flow zone does not always cover a true sector of a circle, CAVELAARS (1970) introduced the concept of equivalent angle.

or

$$\Delta h_t = \frac{q}{k} \alpha_t = \frac{q}{k} (\alpha_r + \alpha_e) \qquad (1.13)$$

hence it appears that

$$\alpha_t = \alpha_r + \alpha_e \qquad (1.14)$$

and

$$\alpha_t = W_t \, k \qquad (1.15)$$

where W_t is the total resistance for radial flow towards a real drain and α_t is the dimensionless total flow resistance. Eqn. (1.14) allows the calculation of α_e if α_t and α_r are known.

CHILDS & YOUNGS (1958) have shown that a real drain can be replaced by an ideal drain of a smaller radius, called the *effective radius* R_{ef}. Substitution of α_r from eqn. (1.5) into eqn. (1.14) gives

$$\alpha_t = \frac{1}{2\pi} \ln \frac{R}{R_o} + \alpha_e \qquad (1.16)$$

Similar to eqn. (1.5) we can write that for the ideal substitute with the same resistance

$$\alpha_t = \frac{1}{2\pi} \ln \frac{R}{R_{ef}} \qquad (1.17)$$

It follows that

$$R_{ef} = R \, e^{-2\pi\alpha_t} \qquad (1.18)$$

or

$$R_{ef} = R_o \, e^{-2\pi\alpha_e} \qquad (1.19)$$

Eqn. (1.19) shows that a real drain with radius R_o can be replaced by an imaginary ideal drain with a smaller radius R_{ef} and that the radius of that ideal drain decreases with increasing values of α_e. From these considerations it may be concluded that :

- the entrance resistance of a real drain can be derived from the difference between total resistance and radial resistance towards an ideal drain of the same diameter;
- a real drain can be replaced by an imaginary ideal drain of smaller diameter; this diameter follows from the value of its entrance resistance.

2. *Methods to determine the entrance resistance*

2.1. Analytical solutions

In studying the flow of water towards gaps between clay drains or towards perforations in smooth plastic drains, the boundary between soil and opening can be considered differently (fig. 1.7) :

(1) soil particles penetrate into the openings;

(2) soil particles form a plane boundary at the outside of the openings (plane boundary conditions);

(3) soil particles near the openings are washed out and form an arched boundary (arched boundary conditions);

(4) soil particles near the openings are washed out and form an irregular boundary at the outside of the openings.

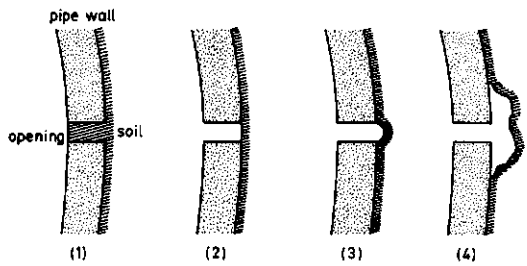

Fig. 1.7. Possible boundaries between soil and drain opening (CAVELAARS,1970).

In determining the influence of openings on drainage performance these situations are of importance. Here situations (2) and (3) are considered although the arched boundary condition is supposed to be the more likely due to washing out of soil particles (PESCHL, 1969).

Many authors determined the total head loss as a result of flow towards openings of a real drain. From this, the additional head loss due to openings and consequently the entrance resistance can be derived using eqn. (1.13). For reason of uniformity and simplicity all equations are modified in such a way that they permit the direct calculation of entrance resistances.

Due to the wide variety of types of pipes and well screens and openings or perforations applied, a large number of theoretical solutions, all pertaining to certain conditions, are available. Here the following division and codification has been made :

- Smooth drains with
  - Circumferential Openings — S_{co}
  - Circular Perforations — S_{cp}
  - Continuous Longitudinal Slits — S_{cls}
  - Discontinuous Longitudinal Slits — S_{dls}
  - Discontinuous Circumferential Slits — S_{dcs}
- Corrugated drains with
  - Circumferential Openings — C_{co}
  - Discontinuous Circumferential Slits — C_{dcs}

2.1.1. Smooth drains with circumferential openings

The first investigation of the influence of gap width was carried out by OEHLERS (1932). He established that the discharge did not increase with increasing gap width. ZUNKER (1932) attributed this remarkable result to the relatively large hydraulic conductivity of the gap. KOZENY (1933) stated, however, that an increasing gap width should result in a higher discharge rate. According to him, the conclusions of OEHLERS (1932) were based on well flow so that the gap width does not influence the groundwater table.

KOZENY (1933) derived the theoretical relationship between gap width, drain diameter, hydraulic conductivity, discharge and head loss. From his equations for the total hydraulic head loss for radial flow, the entrance resistance can be derived using eqn. (1.13). For arched boundary conditions the following result is obtained :

$$\alpha_{ea} = \frac{c}{4\,\pi^2\,R_o}\,\ln\frac{2\,R_1(\beta_s + \pi\,R_o)}{\beta_s(2\,R_1 + \pi\,R_o)}\,\frac{\ln\dfrac{\cosh^2\dfrac{R_1\,\pi}{l} - 1}{\cosh^2\dfrac{\beta_s\,\pi}{2\,l} - 1}}{\ln\dfrac{2\,R_1}{\beta_s}} - \frac{1}{2\,\pi}\,\ln\frac{R}{R_o} \qquad (1.20)$$

and for plane boundary conditions :

$$\alpha_{ep} = \frac{c}{4\,\pi^2\,R_o}\,\ln\frac{2\,R_1(\beta_s + \pi\,R_o)}{\beta_s(2\,R_1 + \pi\,R_o)}\,\frac{\ln\dfrac{\cosh^2\dfrac{R_1\,\pi}{l} - 1}{\cosh^2\dfrac{\beta_s\,\pi}{2\,l} - 1}}{\ln\dfrac{2\,R_1}{\beta_s}}$$

$$\frac{\ln\left(\dfrac{2\,R_1}{\beta_s} + \sqrt{1 + \dfrac{4\,R_1^2}{\beta_s^2}}\right)}{\ln\dfrac{2\,R_1}{\beta_s}} - \frac{1}{2\,\pi}\ln\frac{R}{R_o} \qquad (1.21)$$

in which α_{ea} and α_{ep} are the entrance resistances for arched and plane boundary conditions respectively. For the other symbols used, reference is made to fig. 1.8. KOZENY (1933) concluded that the discharge is only slightly increased with increasing gap width. ERNST (1962) established that the solution of KOZENY (1933) contained some unproper approximations. Based on the

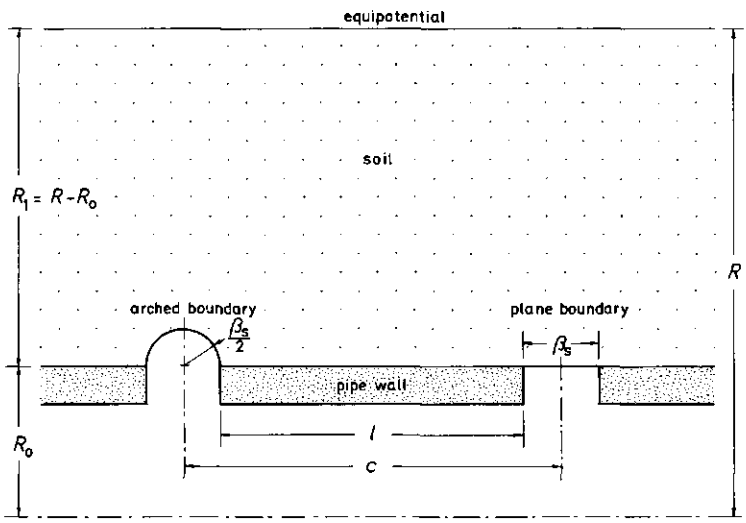

Fig. 1.8. Radial flow towards gaps between clay drain pipes.

theoretical considerations of KOZENY (1933), slightly different equations have been derived (Appendix I). For arched boundary conditions this solution results in :

$$\alpha_{ea} = \frac{c}{2\,\pi^2\,R_o} \ln \frac{2\,R_1(\beta_s + \pi\,R_o)}{\beta_s(2\,R_1 + \pi\,R_o)} + \frac{c}{\pi^2\,R_o} \sum_{n=1}^{\infty} \ln \frac{2 + \dfrac{\pi\,R_o}{n\,c}}{2 + \dfrac{\pi\,R_o}{\sqrt{(n\,c)^2 + R_1^2}}} - \frac{1}{2\,\pi} \ln \frac{R}{R_o} \qquad (1.22)$$

and for plane boundary conditions in :

$$\alpha_{ep} = \frac{c}{2\,\pi^2\,R_o} \ln \frac{2\,R_1(\beta_s + 2\,\pi\,R_o)}{\beta_s(2\,R_1 + \pi\,R_o)} + \frac{c}{\pi^2\,R_o} \sum_{n=1}^{\infty} \ln \frac{2 + \dfrac{\pi\,R_o}{n\,c}}{2 + \dfrac{\pi\,R_o}{\sqrt{(n\,c)^2 + R_1^2}}} - \frac{1}{2\,\pi} \ln \frac{R}{R_o} \qquad (1.23)$$

According to WESSELING (1958), the solution of KIRKHAM (1950) can be considered to have a more exact physical and mathematical basis than that of KOZENY (1933). For arched boundary conditions KIRKHAM (1950) states that

$$\alpha_{ea} = \frac{c^2}{4\,\pi^3\,R_o\,\beta_s} \sum_{n=1}^{\infty} \frac{1}{n^2} \frac{K_o(2\,n\,\pi\,R_o/c)}{K_1(2\,n\,\pi\,R_o/c)} \sin \frac{2\,n\,\pi\,\beta_s}{c} \qquad (1.24)$$

and for plane boundary conditions that

$$\alpha_{ep} = \frac{c^2}{2\,\pi^3\,R_o\,\beta_s} \sum_{n=1}^{\infty} \frac{1}{n^2} \frac{K_o(2\,n\,\pi\,R_o/c)}{K_1(2\,n\,\pi\,R_o/c)} \sin \frac{n\,\pi\,\beta_s}{c} \qquad (1.25)$$

in which K_o and K_1 are modified Bessel functions of the second kind and zero and first order respectively. The only difference between arched and plane boundary conditions is that β_s is replaced by $\beta_s/2$. KIRKHAM (1950) carried out the summations in eqns. (1.24) and (1.25) for $n = 1$ to $n = 44$ and he used the EULER-MacLAURIN summation formulae for $n = 45$ to ∞ taking $K_o/K_1 = 1$ for $n \geqslant 45$. These solutions are valid for $c \gg \beta_s$, a condition which is normally satisfied for flow towards clay drains.

ENGELUND (1953) proved that the additional head loss at the perforations, within certain limits, is independent of whether the perforations are placed on a plane or on a cylindrical surface. As the greater part of the hydraulic head loss will occur in the immediate vicinity of the perforations, the conditions farther away from the perforations are unimportant. From the solution of ENGELUND (1953) a very simple expression is obtained. For arched boundary conditions, the following formula holds :

$$\alpha_{ea} = \frac{c}{2\,\pi^2\,R_o}\,\ln\frac{c}{\pi\,\beta_s} \qquad (1.26)$$

and for plane boundary conditions :

$$\alpha_{ep} = \frac{c}{2\,\pi^2\,R_o}\,\ln\frac{2\,c}{\pi\,\beta_s} \qquad (1.27)$$

These equations are valid for $c \gg \beta_s$ and $2\,R_o > c$. The first condition is usually satisfied but the second one generally not.

KRUIJTZER (1971) found a solution identical to that of ENGELUND (1953) for well screens with circumferential openings and plane boundary conditions.

CHEESEMAN et al. (1974) gave a solution for the two-dimensional flow towards continuous slits with plane boundary conditions. When applied to circumferential openings, the equation of ENGELUND (1953) resulted.

Splitting up the flow towards circumferential openings with plane boundary conditions into a number of components, ERNST (1962) calculated an approximate entrance resistance :

$$\alpha_{ep} = \frac{1}{2\,\pi}\left(\frac{l^2}{90\,R_o^2} + \frac{l}{3\,R_o} + \frac{l}{3{,}3\,R_o}\,\ln\frac{R_o}{\beta_s}\right) \qquad (1.28)$$

An exact solution for plane boundary conditions, valid for $\beta_s/c \to 0$ or $c \gg \beta_s$, has been given by SNEYD & HOSKING (1976) :

$$\alpha_{ep} = \frac{c}{2\,\pi^2\,R_o}\,\ln\frac{2\,c}{\pi\,\beta_s} - \frac{1}{2\,\pi}\left(\frac{c}{2\,\pi\,R_o}\right)^2 + \frac{c}{2\,\pi\,R_o}\,g\left(\frac{2\,R_o}{c},\frac{2\,R}{c}\right) \qquad (1.29)$$

The solution for arched boundary conditions is given by SNEYD (1976) :

$$\alpha_{ea} = \frac{c}{2\,\pi^2\,R_o}\,\ln\frac{c}{\pi\,\beta_s} - \frac{1}{2\,\pi}\left(\frac{c}{2\,\pi\,R_o}\right)^2 + \frac{c}{2\,\pi\,R_o}\,g\left(\frac{2\,R_o}{c},\frac{2\,R}{c}\right) \qquad (1.30)$$

where

$$g\left(\frac{2\,R_o}{c},\frac{2\,R}{c}\right) = \frac{1}{\pi}\left[T'_1\left(\frac{2\,R_o}{c}\right) - 1 + \sum_{n=2}^{\infty}\frac{1}{n}\left\{T'_n\left(\frac{2\,R_o}{c}\right) - 1 + \frac{c}{4\,\pi\,R_o(n-1)}\right\}\right]$$

with

$$T'_n\left(\frac{2\,R_o}{c}\right) = \frac{K_o(2\,n\,\pi\,R_o/c)\;I_o(2\,n\,\pi\,R/c) - K_o(2\,n\,\pi\,R/c)\;I_o(2\,n\,\pi\,R_o/c)}{K_1(2\,n\,\pi\,R_o/c)\;I_o(2\,n\,\pi\,R/c) + K_o(2\,n\,\pi\,R/c)\;I_1(2\,n\,\pi\,R_o/c)}$$

and consequently

$$T'_1\left(\frac{2\,R_o}{c}\right) = \frac{K_o(2\,\pi\,R_o/c)\;I_o(2\,\pi\,R/c) - K_o(2\,\pi\,R/c)\;I_o(2\,\pi\,R_o/c)}{K_1(2\,\pi\,R_o/c)\;I_o(2\,\pi\,R/c) + K_o(2\,\pi\,R/c)\;I_1(2\,\pi\,R_o/c)}$$

where K_o and K_1 and I_o and I_1 are modified Bessel functions of the second and first kind and zero and first order respectively. SNEYD (1976) gives a table for the value of $g(2\,R_o/c, 2\,R/c)$ for different values of $2\,R_o/c$ and $2\,R/c$ (table 1.1).

Table 1.1. Values of $g(2\,R_o/c, 2\,R/c)$ after SNEYD (1976).

$2\,R/c \rightarrow$	0,5	1,0	1,5	2,0	2,5	3,0
$2\,R_o/c \downarrow$			$g(2\,R_o/c, 2\,R/c)$			
0,1	0,3819	0,3602	0,2990	0,2990	0,1268	0,1268
0,2	0,1440	0,1670	0,1289	0,1291	0,0038	0,0038
0,3	0,0012	0,1038	0,0792	0,0795	-0,0197	-0,0197
0,4	-0,2027	0,0606	0,0562	0,0567	-0,0257	-0,0257
0,5		0,0500	0,0427	0,0438	-0,0268	-0,0268
0,6		0,0208	0,0513	0,0355	0,0356	-0,0262
0,7		-0,0243	0,0416	0,0298	0,0299	-0,0250
0,8		-0,1062	0,0324	0,0255	0,0258	-0,0237
0,9		-0,2800	0,0273	0,0221	0,0226	-0,0224
1,0			0,0113	0,0191	0,0202	-0,0211

$$g\left(\frac{2\,R_o}{c},\frac{2\,R}{c}\right) = g\left(\frac{2\,R_o}{c},3\right) \text{ for } \frac{2\,R}{c} > 3$$

These solutions of SNEYD & HOSKING (1976) and SNEYD (1976) allow correction of the simple equations derived by ENGELUND (1953). However, as can be seen from table 1.1, the third term can be omitted for most practical situations. Hence α_{ea} can be calculated from the simple relationship :

$$\alpha_{ea} = \frac{c}{2\,\pi^2\,R_o}\left(\ln\frac{c}{\pi\,\beta_s} - \frac{c}{4\,\pi\,R_o}\right) \qquad (1.31)$$

and α_{ep} from :

$$\alpha_{ep} = \frac{c}{2\,\pi^2\,R_o}\left(\ln\frac{2\,c}{\pi\,\beta_s} - \frac{c}{4\,\pi\,R_o}\right) \qquad (1.32)$$

On further consideration of these theoretical solutions it emerges that the entrance resistance of circumferential openings mainly depends on :

- the gap spacing c
- the outer drain radius R_o

and less on :

- the gap width β_s
- the radius R of the equipotential considered.

Based on theoretical considerations, MOODY (1960) also concluded that increasing gap width between clay drain pipes is a very ineffective way of improving their water uptake capacity.

2.1.2. Smooth drains with circular perforations

Plastic drain pipes are provided with perforations for water entrance. The circular opening is one of the first shapes for which the influence of the perforation on the uptake capacity of pipes has been analytically studied.

For circular openings placed in spirals on the drain wall (fig. 1.9a) and arched boundary conditions, the solution of MUSKAT (1942) for the head loss gives the following expression for α_{ea} :

$$\alpha_{ea} = \frac{1}{2\,\pi\,N}\left[2\sum_{n=1}^{\infty} K_o\left(\frac{n\,\pi\,\delta_p}{\lambda_r}\right) + 2\sum_{i=1}^{N-1}\left\{\sum_{n=1}^{\infty} K_o\left(\frac{4\,n\,\pi\,R_o}{\lambda_r}\sin\frac{\theta\,i}{2}\right)\cos\frac{2\,n\,\pi\,i}{N}\right\} + \ln\frac{2\,R_o}{\delta_p} - \sum_{i=1}^{N-1}\ln\left(2\sin\frac{\theta\,i}{2}\right)\right] \qquad (1.33)$$

where N = number of perforation rows

δ_p = perforation diameter (m)

λ_r = perforation spacing in the row (m)

θ_i = angle to the i^{th} perforation row, measured from the base line passing through the x-axis.

When $\lambda_r \to 0$ then $K_o \to 0$ and a solution for continuous longitudinal slits is obtained :

$$\alpha_{ea} = \frac{1}{2\,\pi\,N}\left\{\ln\frac{2\,R_o}{\delta_p} - \sum_{i=1}^{N-1}\ln\left(2\,\sin\frac{\theta_i}{2}\right)\right\} \qquad (1.34)$$

or

$$\alpha_{ea} = \frac{1}{2\,\pi\,N}\ln\frac{2\,R_o}{N\,\delta_p} \qquad (1.35)$$

since it can be proved (Appendix II) that

$$\sum_{i=1}^{N-1}\ln\left(2\,\sin\frac{\theta_i}{2}\right) = \ln N \qquad (1.36)$$

If different rows of perforations all lie in parallel planes normal to the well axis, thus forming a rectangular perforation pattern (fig. 1.9b), the following expression for α_{ea} can be derived from the solution of MUSKAT (1942) :

$$\alpha_{ea} = \frac{1}{2\,\pi\,N}\left[2\sum_{n=1}^{\infty}K_o\left(\frac{n\,\pi\,\delta_p}{\lambda_r}\right) + 2\sum_{i=1}^{N-1}\left\{\sum_{n=1}^{\infty}K_o\left(\frac{4\,n\,\pi\,R_o}{\lambda_r}\sin\frac{\theta_i}{2}\right)\right\}\right.$$

$$\left. + \ln\frac{2\,R_o}{\delta_p} - \sum_{i=1}^{N-1}\ln\left(2\,\sin\frac{\theta_i}{2}\right)\right] \qquad (1.37)$$

When $\lambda_r \to 0$, then eqn. (1.37) becomes identical to eqn. (1.34). An identical expression for rectangular perforation patterns and arched boundary conditions is given by KIRKHAM & SCHWAB (1951).

MUSKAT (1942) and KIRKHAM & SCHWAB (1951) assumed that no signifant error is introduced by not taking into account the presence of an impermeable surface in which the perforations are embedded (fig. 1.10). By adding a central source of strength $q/2$ the region between the perforations is actually impermeable and an exact solution is obtained resulting in α_{ea}-values that are doubled. Hence a correction factor of 2 has to be introduced into eqns. (1.33), (1.34), (1.35) and (1.37).

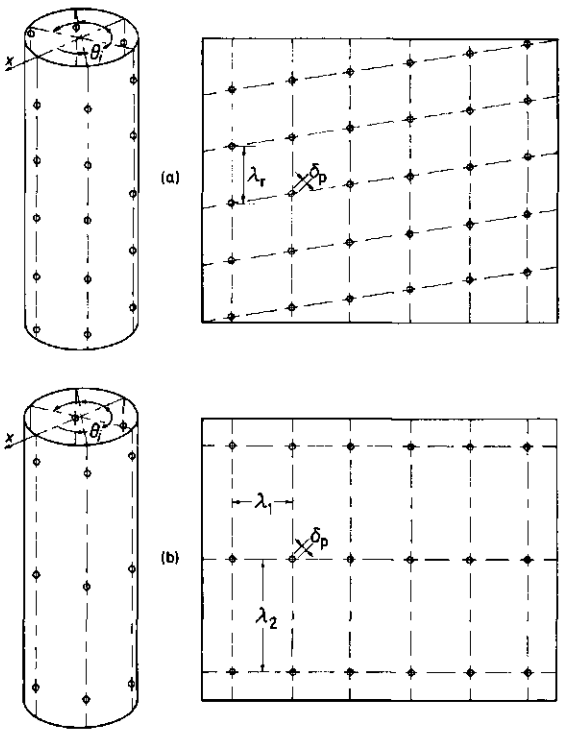

Fig. 1.9a. Spiral distribution of circular openings.
b. Rectangular distribution of circular openings.

Taking into account eqn. (1.36), eqn. (1.37) modifies into

$$\alpha_{ea} = \frac{1}{\pi N}\left[2\sum_{n=1}^{\infty} K_o\left(\frac{n\,\pi\,\delta_p}{\lambda_r}\right) + 2\sum_{i=1}^{N-1}\left\{\sum_{n=1}^{\infty} K_o\left(\frac{4\,n\,\pi\,R_o}{\lambda_r}\sin\frac{\theta_i}{2}\right)\right\} + \ln\frac{2\,R_o}{N\,\delta_p}\right] \qquad (1.38)$$

According to KIRKHAM & SCHWAB (1951), for plane boundary conditions, the discharge has to be multiplied by a factor of $2/\pi$ resulting in an entrance resistance that is given by

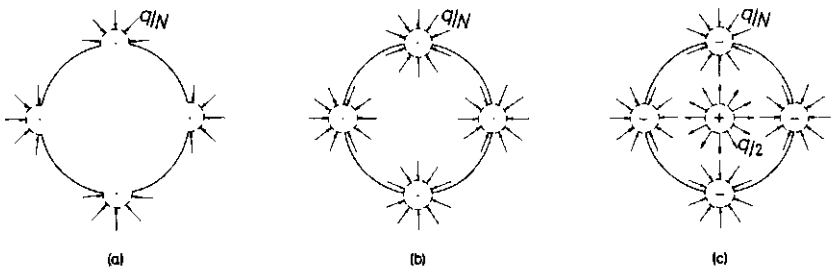

Fig. 1.10. MUSKAT (1942) and KIRKHAM & SCHWAB (1951) assumed that the situtions (a) and (b) are equivalent. This is only true for the situations (a) and (c).

$$\alpha_{ep} = \frac{1}{4\,N}\left[2\sum_{n=1}^{\infty} K_o\left(\frac{n\,\pi\,\delta_p}{\lambda_r}\right) + 2\sum_{i=1}^{N-1}\left\{\sum_{n=1}^{\infty} K_o\left(\frac{4\,n\,\pi\,R_o}{\lambda_r}\sin\frac{\theta_i}{2}\right)\right\}\right.$$

$$\left. + \ln\frac{2\,R_o}{\delta_p} - \sum_{i=1}^{N-1}\ln\left(2\sin\frac{\theta_i}{2}\right)\right] + \frac{\pi - 2}{4\,\pi}\ln\frac{R}{R_o} \qquad (1.39)$$

Since eqn. (1.39) is derived from eqn. (1.37), correction by a factor of 2 has to be made and taking into account eqn. (1.36), eqn. (1.39) becomes

$$\alpha_{ep} = \frac{1}{2\,N}\left[2\sum_{n=1}^{\infty} K_o\left(\frac{n\,\pi\,\delta_p}{\lambda_r}\right) + 2\sum_{i=1}^{N-1}\left\{\sum_{n=1}^{\infty} K_o\left(\frac{4\,n\,\pi\,R_o}{\lambda_r}\sin\frac{\theta_i}{2}\right)\right\}\right.$$

$$\left. + \ln\frac{2\,R_o}{N\,\delta_p}\right] + \frac{\pi - 2}{4\,\pi}\ln\frac{R}{R_o} \qquad (1.40)$$

Eqn. (1.39) has no mathematical basis and the results obtained will be doubtful. A better approximation can be obtained by adding the additional entrance resistance between plane and arched boundary conditions to the entrance resistance for the arched boundary case. This additional entrance resistance can be derived from the additional head loss given by ENGELUND (1953) and amounts to

$$\frac{\pi - 2}{2\,\pi\,m\,\delta_p} = \frac{\lambda_r(\pi - 2)}{2\,\pi\,N\,\delta_p}$$

in which m is the number of perforations per unit drain length. Adding this to eqn. (1.38), another solution for plane boundary conditions is obtained :

$$\alpha_{ep} = \frac{1}{\pi N}\left[2\sum_{n=1}^{\infty} K_o\left(\frac{n\,\pi\,\delta_p}{\lambda_r}\right) + 2\sum_{i=1}^{N-1}\left\{\sum_{n=1}^{\infty} K_o\left(\frac{4\,n\,\pi\,R_o}{\lambda_r}\sin\frac{\theta_i}{2}\right)\right\} + \ln\frac{2\,R_o}{N\,\delta_p} + \frac{\lambda_r(\pi-2)}{2\,\delta_p}\right] \qquad (1.41)$$

In a way analogous to that used for circumferential openings, ENGELUND (1953) derived, from the flow towards a plane surface with circular openings, the head loss for a cylindrical surface with the same perforation pattern. Thus, for a rectangular perforation pattern and arched boundary conditions, the entrance resistance derived is given by

$$\alpha_{ea} = \frac{1}{\pi\,m}\left\{\frac{1}{\delta_p} - \frac{1}{2\,\lambda_1}\left(3{,}91 - 2\ln\frac{\lambda_2}{\lambda_1}\right)\right\} \qquad (1.42)$$

in which λ_1 and λ_2 are the smallest and largest perforation spacings respectively. For plane boundary conditions the following formula holds :

$$\alpha_{ep} = \frac{1}{\pi\,m}\left\{\frac{\pi}{2\,\delta_p} - \frac{1}{2\,\lambda_1}\left(3{,}91 - 2\ln\frac{\lambda_2}{\lambda_1}\right)\right\} \qquad (1.43)$$

These equations are valid for $\delta_p \ll 2\,\lambda_1$. For a square perforation pattern $\lambda_2 = \lambda_1$ and eqns. (1.42) and (1.43) become respectively (CAVELAARS, 1967) :

$$\alpha_{ea} = \frac{1}{\pi\,m}\left(\frac{1}{\delta_p} - \frac{3{,}91}{2\,\lambda_s}\right) \qquad (1.44)$$

$$\alpha_{ep} = \frac{1}{\pi\,m}\left(\frac{\pi}{2\,\delta_p} - \frac{3{,}91}{2\,\lambda_s}\right) \qquad (1.45)$$

in which λ_s is the perforation spacing. An analytical check of the validity of eqn. (1.42) of ENGELUND (1953) and eqn. (1.44) of CAVELAARS (1967) gives the same results (Appendix III). The factor 3,91 equals $2\ln(4\,\pi) - 2\,\gamma$ where γ is EULER's constant (γ = 0,577 21...).

Since

$$\lambda_s = \sqrt{\frac{2\,\pi\,R_o}{m}} \qquad (1.46)$$

eqn. (1.44) can be rewritten as

$$\alpha_{ea} = \frac{1}{\pi\, m\, \delta_p} - \frac{0{,}248}{\sqrt{m\, R_o}} \qquad (1.47)$$

and eqn. (1.45) as

$$\alpha_{ep} = \frac{1}{2\, m\, \delta_p} - \frac{0{,}248}{\sqrt{m\, R_o}} \qquad (1.48)$$

From this, it can be concluded that the number and diameter of the perforations are the main influences on the entrance resistance, the drain diameter being less important.

2.1.3. Smooth drains with continuous longitudinal slits

The flow of water towards drains with continuous longitudinal slits (fig. 1.11) is a theoretical problem because such drains cannot exist in reality.

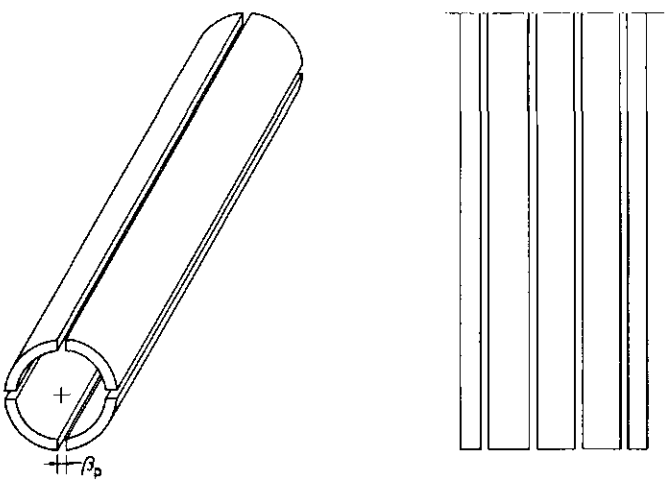

Fig. 1.11. Drain provided with continuous longitudinal slits.

The problem of radial flow towards a well screen provided with continuous longitudinal slits and plane boundary conditions, which was described by KIRKHAM & POWERS (1971), was solved by DODSON & CAROWELL (1945). From this, it may be deduced that

$$\alpha_{ep} = \frac{1}{\pi N} \ln \frac{2}{\pi A_{pp}} \tag{1.49}$$

in which N = number of continuous longitudinal slits

A_{pp} = percentage open area of the pipe.

Eq. (1.49) is accurate to within 1 percent error for $R/R_o \geqslant 5$ and $A_{pp} \leqslant 0,3$. If A_{pp} is expressed explicitly :

$$A_{pp} = \frac{N \beta_p}{2 \pi R_o} \tag{1.50}$$

with β_p the perforation width, eqn. (1.49) can be written as

$$\alpha_{ep} = \frac{1}{\pi N} \ln \frac{4 R_o}{N \beta_p} \tag{1.51}$$

ENGELUND (1953) derived, from the flow towards a plane surface provided with continuous longitudinal slits, an identical equation for a cylindrical surface.

For arched boundary conditions $\beta_p/2$ has to be replaced by β_p and hence

$$\alpha_{ea} = \frac{1}{\pi N} \ln \frac{2 R_o}{N \beta_p} \tag{1.52}$$

It is stated by ENGELUND (1953) that eqns. (1.51) and (1.52) are valid for $\beta_p \ll R_o$.

WIDMOSER (1966) arrived at identical equations for the entrance resistance of continuous longitudinal slits with arched and plane boundary conditions provided that $\beta_p N/R_o < 1,4$.

FUJIOKA & MARUYAMA (1970) also give a theoretical solution for continuous longitudinal slits with arched boundary conditions. This solution gives for α_{ea} :

$$\alpha_{ea} = \frac{R_o \left\{ \left(\frac{R}{R_o}\right)^N - \left(\frac{R}{R_o}\right)^{-N} \right\}}{2 \pi N R \left\{ \left(\frac{R}{R_o}\right)^{N-1} - \left(\frac{R}{R_o}\right)^{-N-1} \right\}} \left[\ln \left\{ \left(\frac{R}{R_o}\right)^N + \left(\frac{R}{R_o}\right)^{-N} \right\} \right.$$

$$\left. - \ln \left\{ \left(\frac{2 R_o + \beta_p}{2 R_o} \right)^N + \left(\frac{2 R_o + \beta_p}{2 R_o} \right)^{-N} - 2 \right\} \right] - \frac{1}{2 \pi} \ln \frac{R}{R_o} \tag{1.53}$$

If R is large, then $(R/R_o)^{-N}$ and $(R/R_o)^{-N-1}$ can be neglected against $(R/R_o)^N$ and $(R/R_o)^{N-1}$. Hence eqn. (1.53) can be simplified to give

$$\alpha_{ea} = \frac{1}{2\,\pi\,N} \ln \frac{\left\{2\,R_o\,(2\,R_o + \beta_p)\right\}^N}{\left\{(2\,R_o + \beta_p)^N - (2\,R_o)^N\right\}^2} \qquad (1.54)$$

Since, in het numerator, β_p can be neglected against $2\,R_o$ and when all terms of a higher degree in β_p are omitted in the denominator, eqn. (1.54) becomes identical with eqn. (1.52).

For well screens and plane boundary conditions, KRUIJTZER (1971) obtained the result given by eqn. (1.51).

From these theoretical solutions, it follows that the entrance resistance for continuous longitudinal slits is mainly determined by the number of slits and less by the perforation width and the drain diameter.

In fact, the solutions for continuous longitudinal slits and circumferential openings as given by ENGELUND (1953) are identical. Indeed, when c represents the spacing of continuous longitudinal slits, then

$$N = \frac{2\,\pi\,R_o}{c} \qquad (1.55)$$

and eqn. (1.52) ≡ eqn. (1.26), also eqn. (1.51) ≡ eqn. (1.27). Since ENGELUND (1953) considers the flow towards a plane surface, the pipe geometry is irrelevant and it does not influence the entrance resistance.

2.1.4. Smooth drains with discontinuous longitudinal slits

Plastic drain pipes can have discontinuous longitudinal slits. For a rectangular perforation pattern (fig. 1.12), MUSKAT (1942) gives a theoretical solution for a well screen and arched boundary conditions from which follows that :

$$\alpha_{ea} = \frac{1}{2\,\pi\,N}\left[2\sum_{n=1}^{\infty} K_o\left(\frac{n\,\pi\,\beta_p}{\lambda_r}\right)\frac{\sin(n\,\pi\,\gamma)}{n\,\pi\,\gamma} + 2\sum_{i=1}^{N-1}\left\{\sum_{n=1}^{\infty} K_o\left(\frac{4\,n\,\pi\,R_o}{\lambda_r}\sin\frac{\theta_i}{2}\right)\right.\right.$$

$$\left.\left.\frac{\sin(n\,\pi\,\gamma)}{n\,\pi\,\gamma}\right\} + \ln\frac{2\,R_o}{\beta_p} - \sum_{i=1}^{N-1}\ln\left(2\sin\frac{\theta_i}{2}\right)\right] \qquad (1.56)$$

in which λ_p = perforation length (m)

λ_r = perforation spacing within the row (m)

$\gamma = \lambda_p/\lambda_r$.

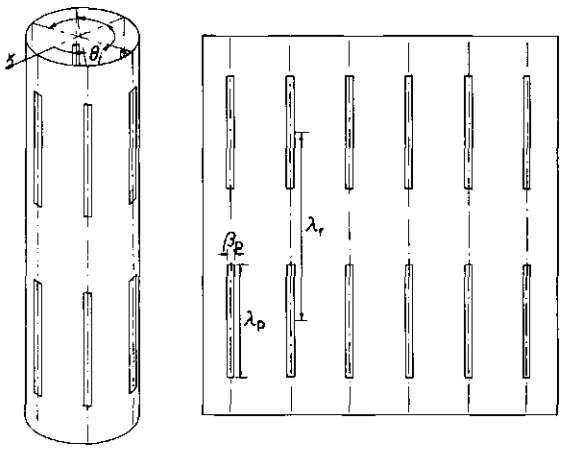

Fig. 1.12. Rectangular distribution of discontinuous longitudinal slits.

When $\lambda_r \to 0$ than $K_o \to 0$ and eqn. (1.34) is obtained in which δ_p is replaced by β_p. In principle, this solution is already obtained by putting $\lambda_r = \lambda_p$. Eqn. (1.56) gives also α_{ea}-values which are halved and a correction factor of 2 must be introduced. Taking into account eqn. (1.36), this results in

$$\alpha_{ea} = \frac{1}{\pi N}\left[2\sum_{n=1}^{\infty} K_o\left(\frac{n\,\pi\,\beta_p}{\lambda_r}\right)\frac{\sin(n\,\pi\,\gamma)}{n\,\pi\,\gamma} + 2\sum_{i=1}^{N-1}\left\{\sum_{n=1}^{\infty} K_o\left(\frac{4\,n\,\pi\,R_o}{\lambda_r}\sin\frac{\theta_i}{2}\right)\frac{\sin(n\,\pi\,\gamma)}{n\,\pi\,\gamma}\right\} + \ln\frac{2\,R_o}{N\,\beta_p}\right] \qquad (1.57)$$

Replacing the perforation width β_p in eqn. (1.57) by $\beta_p/2$ results in a solution for plane boundary conditions, namely

$$\alpha_{ep} = \frac{1}{\pi N}\left[2\sum_{n=1}^{\infty} K_o\left(\frac{n\,\pi\,\beta_p}{2\,\lambda_r}\right)\frac{\sin(n\,\pi\,\gamma)}{n\,\pi\,\gamma} + 2\sum_{i=1}^{N-1}\left\{\sum_{n=1}^{\infty} K_o\left(\frac{4\,n\,\pi\,R_o}{\lambda_r}\sin\frac{\theta_i}{2}\right)\frac{\sin(n\,\pi\,\gamma)}{n\,\pi\,\gamma}\right\} + \ln\frac{4\,R_o}{N\,\beta_p}\right] \qquad (1.58)$$

CAVELAARS (1970) applied the principles of a partially penetrating well in a confined aquifer (fig. 1.13) to discontinuous longitudinal slits. Compared to a fully penetrating well an additional head loss must be taken into account for a partially penetrating well having the same discharge. For the same diameter of the well the additional head loss depends on the length of the well and its place in the confined aquifer. The place is indicated by the eccentricity $\delta = \epsilon \lambda_r$ of the midpoint of the well to the midpoint of the confined aquifer and ϵ can be defined as the relative eccentricity of the well. Applying the formula for the additional head loss due to flow towards a partially penetrating well as given by the Hydrologisch Colloquium (1964) to discontinuous longitudinal slits and adding it to the head loss due to flow towards continuous longitudinal slits, with arched boundary conditions, CAVELAARS (1970) obtained the following solution for the entrance resistance :

$$\alpha_{ea} = \frac{1}{\pi N}\left[\ln \frac{2 R_o}{N \beta_p} + \frac{1-\gamma}{\gamma}\left\{\ln \frac{8 \lambda_r}{\beta_p} - F(\gamma,\epsilon)\right\}\right] \qquad (1.59)$$

in which $F(\gamma,\epsilon)$ is a function of γ and ϵ. The function $F(\gamma,\epsilon)$ has been tabulated in table 1.2.

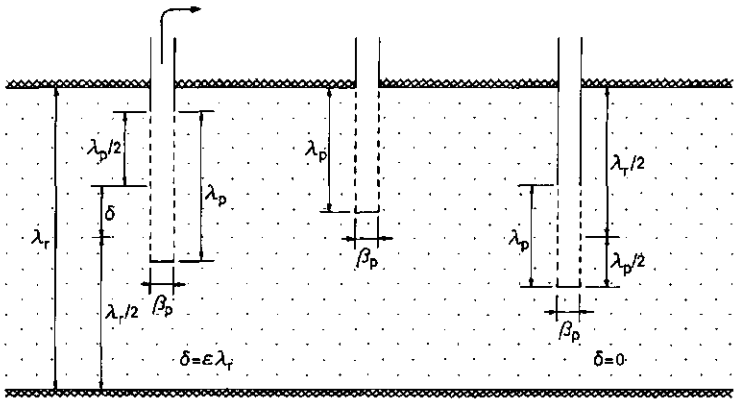

Fig. 1.13. Flow towards a partially penetrating well in a confined aquifer applied to discontinuous longitudinal slits at drains.

Similarly to CAVELAARS (1970), we applied the solution of MUSKAT (1946) for a partially penetrating well extending to the upper or lower boundary of the aquifer, after adapting it to a well situated symmetrically in the aquifer, and we obtained a solution similar to eqn. (1.57).
Eqns. (1.57) and (1.58) are based on the assumptions of a constant potential and a uniform flux density over the entire perforation length. Since these conditions are not satisfied, MUSKAT (1946) has modified his solution for partially penetrating wells on the basis of numerical calculations. He concluded that for a partially penetrating well extending to the upper or lower boundary of the aquifer, one may assume the flux density over the well to be uniform when for the potential an effective average is taken. This turns out to be that at a quarter from the free end of the well. For a well situated symmetrically in the aquifer, this means that the effective average potential is situated one-eight of the way from the free ends. Applying these considerations to discontinuous longitudinal perforations of a drain (Appendix IV) leads to the following modification of eqn. (1.57) :

$$\alpha_{ea} = \frac{1}{\pi N}\left[2\sum_{n=1}^{\infty} K_o\left(\frac{n\,\pi\,\beta_p}{\lambda_r}\right)\frac{\sin(n\,\pi\,\gamma)}{n\,\pi\,\gamma}\cos\left(\frac{3}{4}\,n\,\pi\,\gamma\right)\right.$$

$$\left. + 2\sum_{i=1}^{N-1}\left\{\sum_{n=1}^{\infty} K_o\left(\frac{4\,n\,\pi\,R_o}{\lambda_r}\sin\frac{\theta_i}{2}\right)\frac{\sin(n\,\pi\,\gamma)}{n\,\pi\,\gamma}\cos\left(\frac{3}{4}\,n\,\pi\,\gamma\right)\right\} + \ln\frac{2\,R_o}{N\,\beta_p}\right] \qquad (1.64)$$

Accordingly, eqn. (1.58) becomes :

$$\alpha_{ep} = \frac{1}{\pi N}\left[2\sum_{n=1}^{\infty} K_o\left(\frac{n\,\pi\,\beta_p}{2\,\lambda_r}\right)\frac{\sin(n\,\pi\,\gamma)}{n\,\pi\,\gamma}\cos\left(\frac{3}{4}\,n\,\pi\,\gamma\right)\right.$$

$$\left. + 2\sum_{i=1}^{N-1}\left\{\sum_{n=1}^{\infty} K_o\left(\frac{4\,n\,\pi\,R_o}{\lambda_r}\sin\frac{\theta_i}{2}\right)\frac{\sin(n\,\pi\,\gamma)}{n\,\pi\,\gamma}\cos\left(\frac{3}{4}\,n\,\pi\,\gamma\right)\right\} + \ln\frac{4\,R_o}{N\,\beta_p}\right] \qquad (1.65)$$

Since $\beta_p < \lambda_r$, K_o converges very slowly. Therefore another approximate solution, given by MUSKAT (1946) for flow towards partially penetrating wells in terms of Γ-functions, can be used. Taking into account the above-mentioned modifications (Appendix IV) it is found, for arched boundary conditions, that

$$\alpha_{ea} = \frac{1}{\pi N}\left[\ln \frac{2 R_o}{N \beta_p} + \frac{1-\gamma}{\gamma}\left\{\ln \frac{8 \lambda_r}{\beta_p} - \frac{1}{2(1-\gamma)} \ln \frac{\Gamma(\frac{1}{16}\gamma)\ \Gamma(\frac{7}{16}\gamma)\ \Gamma(\frac{1}{2}+\frac{7}{16}\gamma)\ \Gamma(\frac{1}{2}+\frac{1}{16}\gamma)}{\Gamma(1-\frac{1}{16}\gamma)\ \Gamma(1-\frac{7}{16}\gamma)\ \Gamma(\frac{1}{2}-\frac{7}{16}\gamma)\ \Gamma(\frac{1}{2}-\frac{1}{16}\gamma)}\right\}\right] \qquad (1.66)$$

and for plane boundary conditions that

$$\alpha_{ep} = \frac{1}{\pi N}\left[\ln \frac{4 R_o}{N \beta_p} + \frac{1-\gamma}{\gamma}\left\{\ln \frac{16 \lambda_r}{\beta_p} - \frac{1}{2(1-\gamma)} \ln \frac{\Gamma(\frac{1}{16}\gamma)\ \Gamma(\frac{7}{16}\gamma)\ \Gamma(\frac{1}{2}+\frac{7}{16}\gamma)\ \Gamma(\frac{1}{2}+\frac{1}{16}\gamma)}{\Gamma(1-\frac{1}{16}\gamma)\ \Gamma(1-\frac{7}{16}\gamma)\ \Gamma(\frac{1}{2}-\frac{7}{16}\gamma)\ \Gamma(\frac{1}{2}-\frac{1}{16}\gamma)}\right\}\right] \qquad (1.67)$$

Another approximation for flow towards partially penetrating wells was given by DE GLEE (1930). He replaced the curved surface of the cylindrical well by an equipotential ellipsoid of the same surface area. Applying his solution to discontinuous longitudinal slits leads to the following equation of the entrance resistance for arched boundary conditions :

$$\alpha_{ea} = \frac{1}{\pi N}\left\{\ln \frac{2 R_o}{N \beta_p} + \frac{1}{\gamma} \ln \frac{\pi \lambda_p}{2 \beta_p} - \ln \frac{4 \lambda_r}{\beta_p} + \frac{1}{2} f(\zeta)\right\} \qquad (1.68)$$

while for plane boundary conditions

$$\alpha_{ep} = \frac{1}{\pi N}\left\{\ln \frac{4 R_o}{N \beta_p} + \frac{1}{\gamma} \ln \frac{\pi \lambda_p}{\beta_p} - \ln \frac{8 \lambda_r}{\beta_p} + \frac{1}{2} f(\zeta)\right\} \qquad (1.69)$$

with

$$f(\zeta) = \frac{1}{2\zeta} - \frac{2}{\sqrt{4+\zeta^2}} + \sum_{n=1}^{\infty}\left\{\frac{1}{2(n-\zeta)} + \frac{2}{2n} + \frac{1}{2(n+\zeta)} - \frac{2}{\sqrt{4+(2n+\zeta)^2}} - \frac{2}{\sqrt{4+(2n-\zeta)^2}}\right\}$$

in which $\zeta = (\lambda_r + 2\delta)/2\lambda_r$. DE GLEE (1930) has tabulated the values of $f(\zeta)$ as a function of $1/\zeta$. Using this expression for $f(\zeta)$, his tabulated values differ from the values we obtained as can be seen in table 1.4.

Table 1.4. Values of $f(\zeta)$ according to DE GLEE (1930) and to our calculations.

$1/\zeta$	$f(\zeta)$	
	DE GLEE	corrected
1,1	5,40	5,282
1,15	3,72	3,626
1,2	2,90	2,806
1,3	2,05	2,005
1,4	1,66	1,626
1,5	1,46	1,418
1,6	1,36	1,296
1,7	1,30	1,223
1,8	1,26	1,181
1,9	1,24	1,161
2	1,23	1,154
3	1,46	1,414
4	1,91	1,845
5	2,40	2,315
6	2,90	2,799
7	3,40	3,290
8	3,90	3,784
9	4,40	4,280
10	4,90	4,777

For discontinuous longitudinal slits $\delta = 0$ and hence $1/\zeta = 2$. In calculating the entrance resistance we used 0,577 instead of 0,615 for $1/2\ f(\zeta)$. Eqns. (1.68) and (1.69) are valid on condition that $\lambda_r \geqslant 1{,}30\ \lambda_p$ and $\lambda_p \geqslant 10\ \beta_p$.

Other formulae, such as those of FORCHHEIMER (1898) based on experimental data and of ROTHER (1904) and KOOPER (1914) for which the supposed boundary conditions differ widely from reality, can hardly be applied.

All these solutions in fact consist of two parts of which one gives the entrance resistance for continuous longitudinal slits while the other takes into account the discontinuity of the slits.

KRUIJTZER (1971) proceeds from eqn. (1.49) and proposes that this equation is valid for discontinuous longitudinal slits with plane boundary con-

ditions provided that $1 - \gamma \ll 1$. Since he only gives a solution for plane boundary conditions, he takes into consideration the possible change of the percentage open area A_{pp} in course of time due to washing out of soil particles or to the formation of deposits in the perforations. Therefore A_{pp} has to be replaced by ωA_{pp} and

$$\alpha_e = \frac{1}{\pi N} \ln \frac{2}{\pi \omega A_{pp}} \qquad (1.70)$$

in which ω can take values between 0 and 2. For :

$\omega = 1$ no changes have occured, i.e. plane boundary conditions still apply;

$1 < \omega < 2$ soil particles are washed out;

$\omega = 2$ soil particles are washed out and arched boundaries are built up;

$0 < \omega < 1$ deposits are formed in the perforations.

Eqn. (1.70) gives α_{ep} when $\omega = 1$ and α_{ea} when $\omega = 2$.

KRUIJTZER (1971) gives a solution for the situation illustrated at fig. 1.15 where perforated sections alternate with unperforated ones.

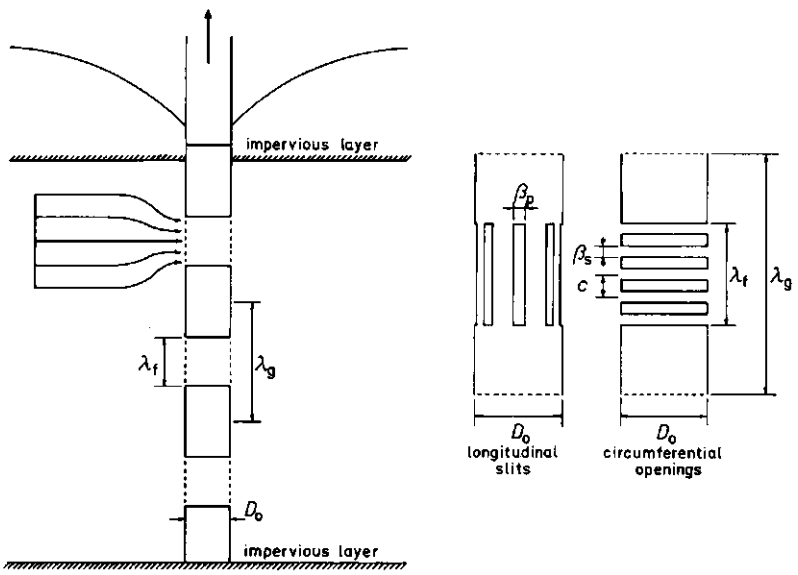

Fig. 1.15. Flow towards a well screen with perforated sections in a confined aquifer (KRUIJTZER, 1971).

Since the perforations in a drain are regularly distributed this is of no importance for drains unless certain sections of the drain are systematically clogged which is unlikely. In this case, the following expression for α_{ep} is obtained :

$$\alpha_{ep} = \frac{\lambda_g}{2\,\pi^2\,R_o}\left(-\ln \sin \frac{\pi\,\lambda_f}{2\,\lambda_g} + \frac{2\,\pi\,R_o}{\lambda_f\,N}\ln\frac{4\,R_o}{N\,\beta_p}\right) \tag{1.71}$$

with λ_f = length of the perforated section (m)

λ_g = spacing of the perforated sections (m).

Taking into account that the percentage open area of the perforated section A_{pz} is given by

$$A_{pz} = \frac{N\,\beta_p\,\lambda_f}{2\,\pi\,R_o\,\lambda_f} = \frac{N\,\beta_p}{2\,\pi\,R_o} \tag{1.72}$$

and considering a clogging factor ω, eqn. (1.71) can be rewritten as :

$$\alpha_e = \frac{\lambda_g}{2\,\pi^2\,R_o}\left(-\ln \sin \frac{\pi\,\lambda_f}{2\,\lambda_g} + \frac{2\,\pi\,R_o}{\lambda_f\,N}\ln\frac{2}{\pi\,\omega\,A_{pz}}\right) \tag{1.73}$$

In that way, eqn. (1.73) can be applied to discontinuous longitudinal slits for the fig. 1.15 case taking into account that A_{pz} is the ratio of the open to the total area of the perforated section and that the condition $1 - \gamma \ll 1$ is satisfied.

2.1.5. Smooth drains with discontinuous circumferential slits

In section 2.1.3., it was mentioned that the formulae for continuous longitudinal slits and circumferential openings are identical. The same can be said for discontinuous longitudinal and circumferential slits (fig. 1.16). Since $N = 2\,\pi\,R_o/c$, eqn. (1.59), for discontinuous circumferential slits and arched boundary conditions, becomes :

$$\alpha_{ea} = \frac{c}{2\,\pi^2\,R_o}\left[\ln\frac{c}{\pi\,\beta_s} + \frac{1-\gamma}{\gamma}\left\{\ln\frac{8\,\lambda_c}{\beta_s} - F(\gamma,\epsilon)\right\}\right] \tag{1.74}$$

and eqn. (1.61) :

$$\alpha_{ea} = \frac{c}{2\,\pi^2\,R_o}\left\{\ln\frac{c}{\pi\,\beta_s} + \frac{1-\gamma}{\gamma}\ln\frac{2\,\lambda_c\,f(\gamma,\epsilon)}{\beta_s}\right\} \tag{1.75}$$

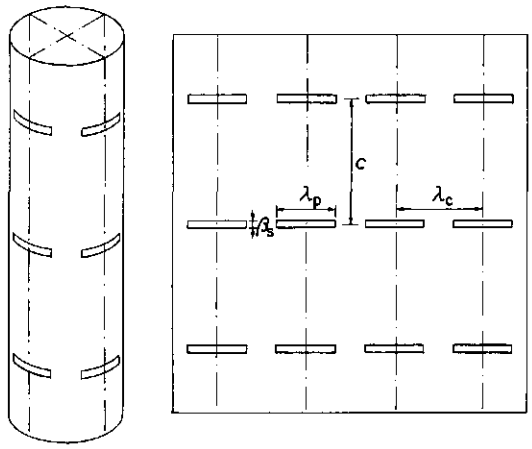

Fig. 1.16. Rectangular distribution of discontinuous circumferential slits.

For discontinuous circumferential slits and plane boundary conditions, eqn. (1.60) becomes :

$$\alpha_{ep} = \frac{c}{2\,\pi^2\,R_o}\left[\ln\frac{2\,c}{\pi\,\beta_s} + \frac{1-\gamma}{\gamma}\left\{\ln\frac{16\,\lambda_c}{\beta_s} - F(\gamma,\epsilon)\right\}\right] \qquad (1.76)$$

and eqn. (1.62) :

$$\alpha_{ep} = \frac{c}{2\,\pi^2\,R_o}\left\{\ln\frac{2\,c}{\pi\,\beta_s} + \frac{1-\gamma}{\gamma}\ln\frac{4\,\lambda_c\,f(\gamma,\epsilon)}{\beta_s}\right\} \qquad (1.77)$$

where $\gamma = \lambda_p/\lambda_c$. For the other symbols used, reference is made to fig. 1.16.

From the exact solution for circumferential openings with plane boundary conditions of SNEYD & HOSKING (1976), it may be argued, for discontinuous circumferential slits with plane boundary conditions, that

$$\alpha_{ep} = \frac{c}{2\,\pi^2\,R_o}\ln\frac{2\,c}{\pi\,\beta_s} - \frac{1}{2\,\pi}\left(\frac{c}{2\,\pi\,R_o}\right)^2$$

$$+ \frac{c}{2\,\pi\,R_o}\,g\left(\frac{2\,R_o}{c},\frac{2\,R}{c}\right) + \frac{c\,(1-\gamma)}{2\,\pi^2\,R_o\,\gamma}\left\{\ln\frac{16\,\lambda_c}{\beta_s} - F(\gamma,\epsilon)\right\} \qquad (1.78)$$

For circumferential openings with arched boundary conditions, SNEYD (1976) gives an exact solution. For discontinuous circumferential slits the following formula then holds :

$$\alpha_{ea} = \frac{c}{2\pi^2 R_o} \ln \frac{c}{\pi \beta_s} - \frac{1}{2\pi}\left(\frac{c}{2\pi R_o}\right)^2$$

$$+ \frac{c}{2\pi R_o} g\left(\frac{2R_o}{c}, \frac{2R}{c}\right) + \frac{c(1-\gamma)}{2\pi^2 R_o \gamma}\left\{\ln \frac{8\lambda_c}{\beta_s} - F(\gamma,\epsilon)\right\} \qquad (1.79)$$

These equations will give a better approximation than the solutions of CAVELAARS (1970) although it may be expected that

$$-\frac{1}{2\pi}\left(\frac{c}{2\pi R_o}\right)^2 + \frac{c}{2\pi R_o} g\left(\frac{2R_o}{c}, \frac{2R}{c}\right)$$

can be neglected and hence eqns. (1.74) and (1.76) can be applied to yield results which are sufficiently accurate for practical purposes.

The other formulae deduced in section 2.1.4. can be used after substituting $2\pi R_o/c$ for N, β_s for β_p and λ_c for λ_r. Hence eqn. (1.64) becomes :

$$\alpha_{ea} = \frac{c}{2\pi^2 R_o}\left[2\sum_{n=1}^{\infty} K_o\left(\frac{n\pi\beta_s}{\lambda_c}\right)\frac{\sin(n\pi\gamma)}{n\pi\gamma}\cos\left(\frac{3}{4}n\pi\gamma\right)\right.$$

$$\left. + 2\sum_{i=1}^{N-1}\left\{\sum_{n=1}^{\infty} K_o\left(\frac{4n\pi R_o}{\lambda_c}\sin\frac{\theta i}{2}\right)\frac{\sin(n\pi\gamma)}{n\pi\gamma}\cos\left(\frac{3}{4}n\pi\gamma\right)\right\} + \ln\frac{c}{\pi\beta_s}\right] \qquad (1.80)$$

while eqn. (1.65) reads :

$$\alpha_{ep} = \frac{c}{2\pi^2 R_o}\left[2\sum_{n=1}^{\infty} K_o\left(\frac{n\pi\beta_s}{2\lambda_c}\right)\frac{\sin(n\pi\gamma)}{n\pi\gamma}\cos\left(\frac{3}{4}n\pi\gamma\right)\right.$$

$$\left. + 2\sum_{i=1}^{N-1}\left\{\sum_{n=1}^{\infty} K_o\left(\frac{4n\pi R_o}{\lambda_c}\sin\frac{\theta i}{2}\right)\frac{\sin(n\pi\gamma)}{n\pi\gamma}\cos\left(\frac{3}{4}n\pi\gamma\right)\right\} + \ln\frac{2c}{\pi\beta_s}\right] \qquad (1.81)$$

Eqns. (1.66) and (1.67) respectively take the forms :

$$\alpha_{ea} = \frac{c}{2\,\pi^2\,R_o}\left[\ln\frac{c}{\pi\,\beta_s} + \frac{1-\gamma}{\gamma}\left\{\ln\frac{8\,\lambda_c}{\beta_s} - \frac{1}{2(1-\gamma)}\ln\frac{\Gamma(\frac{1}{16}\gamma)\;\Gamma(\frac{7}{16}\gamma)\;\Gamma(\frac{1}{2}+\frac{7}{16}\gamma)\;\Gamma(\frac{1}{2}+\frac{1}{16}\gamma)}{\Gamma(1-\frac{1}{16}\gamma)\;\Gamma(1-\frac{7}{16}\gamma)\;\Gamma(\frac{1}{2}-\frac{7}{16}\gamma)\;\Gamma(\frac{1}{2}-\frac{1}{16}\gamma)}\right\}\right] \tag{1.82}$$

$$\alpha_{ep} = \frac{c}{2\,\pi^2\,R_o}\left[\ln\frac{2\,c}{\pi\,\beta_s} + \frac{1-\gamma}{\gamma}\left\{\ln\frac{16\,\lambda_c}{\beta_s} - \frac{1}{2(1-\gamma)}\ln\frac{\Gamma(\frac{1}{16}\gamma)\;\Gamma(\frac{7}{16}\gamma)\;\Gamma(\frac{1}{2}+\frac{7}{16}\gamma)\;\Gamma(\frac{1}{2}+\frac{1}{16}\gamma)}{\Gamma(1-\frac{1}{16}\gamma)\;\Gamma(1-\frac{7}{16}\gamma)\;\Gamma(\frac{1}{2}-\frac{7}{16}\gamma)\;\Gamma(\frac{1}{2}-\frac{1}{16}\gamma)}\right\}\right] \tag{1.83}$$

The formulae of DE GLEE (1930) respectively take the forms :

$$\alpha_{ea} = \frac{c}{2\,\pi^2\,R_o}\left(\ln\frac{c}{\pi\,\beta_s} + \frac{1}{\gamma}\ln\frac{\pi\,\lambda_p}{2\,\beta_s} - \ln\frac{4\,\lambda_c}{\beta_s} + 0{,}577\right) \tag{1.84}$$

$$\alpha_{ep} = \frac{c}{2\,\pi^2\,R_o}\left(\ln\frac{2\,c}{\pi\,\beta_s} + \frac{1}{\gamma}\ln\frac{\pi\,\lambda_p}{\beta_s} - \ln\frac{8\,\lambda_c}{\beta_s} + 0{,}577\right) \tag{1.85}$$

Here, also, all these equations consist of two parts of which one represents the entrance resistance for circumferential openings, while the other takes into account the discontinuity.

According to KRUIJTZER (1971) it follows that

$$\alpha_e = \frac{c}{2\,\pi^2\,R_o}\ln\frac{2}{\pi\,\omega\,A_{pp}} \tag{1.86}$$

if $1-\gamma \ll 1$. For perforated sections with circumferential openings (see fig. 1.15) and plane boundary conditions, we obtained that

$$\alpha_{ep} = \frac{\lambda_g}{2\,\pi^2\,R_o}\left(-\ln\sin\frac{\pi\,\lambda_f}{2\,\lambda_g} + \frac{c}{\lambda_f}\ln\frac{2\,c}{\pi\,\beta_s}\right) \tag{1.87}$$

Taking into account that

$$A_{pz} = \frac{\beta_s}{c} \tag{1.88}$$

and considering a clogging factor ω, eqn. (1.87) can be rewritten as

$$\alpha_e = \frac{\lambda_g}{2\,\pi^2\,R_o}\left(-\ln \sin \frac{\pi\,\lambda_f}{2\,\lambda_g} + \frac{c}{\lambda_f} \ln \frac{2}{\pi\,\omega\,A_{pz}}\right) \qquad (1.89)$$

In that way, eqn. (1.89) can be applied to pipes consisting of perforated sections with discontinuous circumferential slits, taking into account that A_{pz} is the ratio of the open to the total area of the perforated section and provided that $1 - \gamma \ll 1$.

This literature review shows that a large number of theoretical solutions is available for the perforation shapes and distributions commonly applied to drains with a smooth outer surface. The following questions now arise :

- Which theoretical solutions correspond to the reality ?
- What are the limitations of the solutions ?
- Are the simple solutions as useful as the more complicated ones ?
- Can the solutions be applied to corrugated drain pipes ?

Once these questions being answered, the factors determining the entrance resistance, or the parameters which principally influence the entrance resistance, can be found.

2.2. *Analogue simulation*

The most ideal form of solution would be a complete mathematical description. Impressively elegant techniques have been developed for the analytical treatment of flow problems, but most solutions pertain to problems of very simple geometry. Despite that they often present the solution in the form of infinite series of higher mathematical functions which are frequently difficult to interpret. The analogue method can circumvent the shortcomings and, perhaps, the excessive educational requirements for a purely mathematical approach.

Analogue simulation can be defined as investigating a technical or physical phenomenon by studying another physical phenomenon which satisfies identical or analogous laws. The analogue simulation also called *model research* is an instrument in which continuous variables or physical quantities

behave analogously to :

- the variables or quantities of the problem under investigation;
- the variables or quantities in a mathematical equation.

As a rule, also here, the complex problem is schematized and often constant values of physical quantities are considered. Moreover, model research only gives an individual solution for the problem under investigation.

Two models are currently used to investigate the entrance resistance of drain pipes, namely the sand model and the electric analogue.

2.2.1. Sand model

Undoubtedly, the sand model is the analogue which comes closest to reality because it satisfies DARCY's law. From discharge measurements and potential readings in and close to the drain, the entrance resistance can be obtained.

As appeared from the investigations of WESSELING & HOMMA (1967), the sand model only lends itself with extreme difficulty to accurate study. The permeability of the porous medium that influences the flow resistance is liable to changes. The behaviour of drain pipes and envelope materials can only be compared when the investigations are carried out under equal circumstances. In spite of these disadvantages, the sand model has permitted the drawing of important conclusions on the performance of drain pipes and envelope materials.

At the introduction of plastic drain pipes, it was attempted to give them a total perforation area as the clay pipes used normally. However, the main difficulty was to find the exact inlet area of clay pipes because the gap width differs considerably. Practical recommendations regarding the gap width between clay pipes vary from a tight fit to as much as 6,4 mm (JUUSELA, 1958). With pipes having square smooth ends, the minimum gap width obtained in the field by DUTZ (1950) was 0,8 mm. In a sand model tank, DE JAGER (1960 a) observed gap widths of 0,7 to 1 mm which give a maximum inlet area of 7,1 cm^2 per metre length of drain for clay pipes with a 75 mm outer diameter. DE JAGER (1962) considered that, under field conditions, the gap width varies between 0 and 4 mm. BINSACK (1961) and WILLNER (1961) gave values of respectively 1,1 and 0,6 mm. Under normal conditions the gap width ranges from 0,8 to 3 mm (VAN DER BEKEN, 1962). KOWALD (1963) mentioned gap

widths of 0,33 to 0,82 mm which correspond to an inlet area ranging from 2,0 to 4,9 cm^2/m. For hand laid clay pipes, EGGELSMANN (1969) found gap widths of 1 to 5 mm. KOWALD (1963) and KUNTZE (1969) observed that the best quality drain pipes, after DIN 1180, can give gap widths smaller than 0,5 mm due to the exact square smooth ends and pipe expansion after wetting. MILLER & SNYDER (1944) and PILLSBURY *et al.* (1960) concluded that the expansion of clay drains on wetting is very small and does not significantly effect the drainage performance.

Plastic drains are provided with perforations in the form of circular holes and discontinuous longitudinal or circumferential slits. For smooth plastic drains, preference was given to discontinuous longitudinal slits as discontinuous circumferential slits lead to cracks during installation (WESSELING, 1961) while circular openings involve manufacturing problems and greater siltation risks (FEDDES, 1966).

WESSELING (1959) carried out comparative sand tank experiments with clay drains and 40 mm inner diameter polyethylene pipes with a 5 mm wall thickness provided with discontinuous circumferential slits of 0,5 mm x 12,5 mm at spacings of 12 and 40 mm. He stated that the entrance resistance is strongly influenced by the spacing of the slits. Also, with slits at the upper side of the drain, a higher entrance resistance was obtained than with slits at the lower side. This can be explained by the fact that the flow towards the drain mainly occurs from below. He found that the entrance resistance of a clay pipe with a 0,5 mm gap width is equal to the entrance resistance of a plastic drain with an open area of 4 cm^2/m for slits at the lower side of the drain and with an open area of 14 cm^2/m for slits at the upper side.

Experiments by DE JAGER (1960 a) indicated that the open area of smooth plastic drains has to be at least 15 cm^2/m to obtain the same drainage performance as clay pipes. The discontinuous longitudinal slits had a length of 25 and 50 mm, a width of 0,5 to 0,6 mm and were distributed over 4 rows for pipe diameters of 30, 40 and 50 mm. The clay drains were surrounded with glass fibre to prevent silting of the pipe, while the smooth plastic drains were not since no particular silting problem was expected. An increase in drainage performance could not be detected by increasing the gap width from 0,7 to 5 mm. VAN DER BEKEN (1962) obtained identical results from experiments in the same model tank with the same sand material. His experiments

confirmed that the favourable results of clay pipes had to be ascribed to the glass fibre envelope.

On the basis of the experiments of DE JAGER (1960 b) slit dimensions in the Netherlands were fixed on 0,6 mm x 25 mm as narrower and longer slits could easily be reduced by pipe deformation due to load. To obtain a satisfactory pipe strength, the inlet area should be limited to 9 cm^2/m.

The experiments of BINSACK (1961) showed that slit width does not significantly effect the drainage performance but that the number of slits per metre length of drain influences the uptake capacity. Increasing the inlet area from 5 to 10 cm^2/m improves the drainage performance considerably while only a slight effect was observed by increasing the area from 11 to 15 cm^2/m. He concluded that an inlet area of 7,5 cm^2/m should be enough for practical purposes. Experiments with clay pipes showed that the drainage performance increases with larger drain diameters. Comparing clay pipes with plastic pipes having the same perforation area it was found that the latter give better results in spite of their smaller diameter, although the differences were insignificant for practical purposes. Also LUTHIN & HAIG (1972) found that, with clay pipes, larger diameters and shorter pipe segments increase the flow rate.

BOUMANS (1963) concluded that the entrance resistance of a drain is mainly dependent on the relative slit length or the slit length per unit length of drain and the relative slit width or the ratio of slit width to the outer drain diameter. He ascribed different research results to different experimental circumstances since the influence of particle size and distribution on the entrance resistance is effected by the slit width. Washing out of fine soil particles decreases the entrance resistance. FEICHTINGER (1966) obtained much the same results as DE JAGER (1960 a) and BOUMANS (1963).

The investigations of WESSELING & HOMMA (1967) showed that the largest variation in entrance resistance is found between 1 and 4 perforation rows. More rows result in a relatively small change in entrance resistance. For the same perforation pattern, a larger diameter is more favourable due to the smaller radial resistance. For drains wrapped with glass fibre two perforation rows or a perforation area of 4,50 cm^2/m were found to be enough for most soils except for drains laid in a trench with very low permeability. Without an envelope a larger perforation area is recommended.

EGGELSMANN (1969) clearly established that the entrance resistance decreases with increasing gap or slit width. He arrived at an inlet area of at least 7 cm^2/m, regardless of the drain type, which means a gap width of 1,5 mm for clay drains. The perforation width of plastic drains should be 0,8 to 1,5 mm. HUSEMANN & PAHLKE (1969) found that slits of 0,4 mm width were soon clogged by iron deposits while only a few cases of clogging were observed with 0,8 mm wide slits. From laboratory investigations, KABINA (1969) concluded that an inlet area of 10 cm^2/m should be sufficient.

SCHWAB *et al.* (1969) found that the spacing of circular holes on the cylindrical surface of the drain has very little effect on the inflow when the ratio of the shortest to the longest spacing is greater than 0,2.

MEIJER (1969) found that corrugated plastic pipes improve the drainage performance as a result of the larger perforation area and the regular distribution of the perforations on the pipe surface. The entrance resistance, found by him, is only 60 to 70 % of the entrance resistance of smooth plastic pipes.

From the results of sand tank experiments VAN DER BEKEN (1962) deduced a semi-empirical formula for drains provided with discontinuous longitudinal slits. For arched boundary conditions he gives :

$$\alpha_{ea} = \frac{1}{\pi N \gamma} \ln \frac{2 R_o}{N \beta_p} \qquad (1.90)$$

and for plane boundary conditions :

$$\alpha_{ep} = \frac{1}{\pi N \gamma} \ln \frac{4 R_o}{N \beta_p} \qquad (1.91)$$

Based on laboratory experiments CROS (1973) also came to eqn. (1.90).

Proceeding from the theoretical analysis of VAN DEEMTER (1950), CHILDS & YOUNGS (1958) studied the influence of the drain on the position and shape of the water table at a given rainfall rate and came to the conclusion that a real drain can be replaced by an ideal drain of a smaller diameter.
If the impervious layer was at infinite depth below the drains, the required reduction of drain diameter has a marked effect on the height of the water table directly above the drain but does not seriously effect the water table height midway between the drains, especially when the maximum angle φ of the water table with the horizontal (fig. 1.17) is larger than 30°. This conclusion has also been extrapolated to drains on the impervious layer.

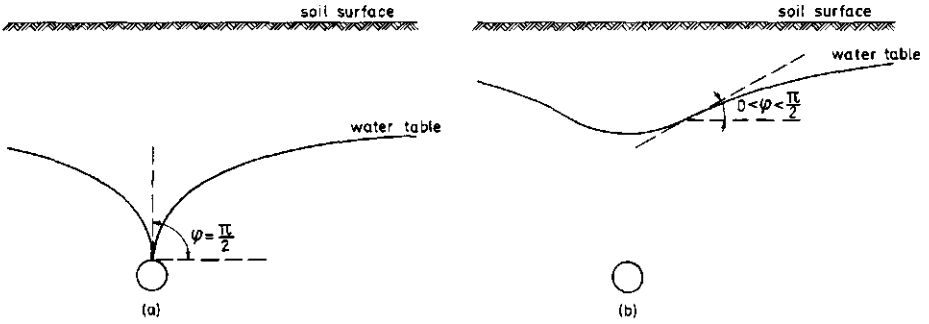

Fig. 1.17. Maximum angle φ of the water table with the horizontal.
a. The water table meets the drain and $\varphi = \pi/2$
b. The water table does not meet the drain and $0 < \varphi < \pi/2$.

The experimental study of CHILDS & YOUNGS (1958) showed an important rise in the water table midway between drains as a result of very small φ-values. Also, the existence of soil particles in the gaps between clay drains resulted in a considerable rise in the water table midway between the drains (YOUNGS, 1965). YOUNGS (1967) came to the conclusion that the effect of gaps on the water table height is not only dependent on the width and spacing of gaps but also on drain spacing. The conclusions of GUYK *et al.* (1973), for drains with the impervious layer at infinite depth, correspond with those of CHILDS & YOUNGS (1958) and YOUNGS (1967). Especially for small spacings, the effect of drain diameter on water table height midway between drains is noticeable.

SCHWAB *et al.* (1969) found that the theoretical effect of gap spacing can be applied to the drawdown case, provided that the water table midway between drains is at least 60 cm above drain centre. For a given drainage rate, depth and diameter of the drain, increasing joint spacing or the number of perforations increases the drawdown rate. The effect of gap spacing on drawdown rates increases as the drain spacing and soil porosity decrease.

2.2.2. Electric analogues

Electric analogues are based on the analogy between DARCY's law for flow of liquid through porous media and OHM's law for flow of electric current through conductors.

In studying the entrance resistance of drain pipes, thin metallic sheet and conductive paper models can only be used for the simulation of two-dimensional flow problems, e.g. drains with continuous longitudinal slits. Conductive liquid analogue systems or *electrolytic models* are particularly suitable for obtaining three-dimensional flow patterns. Detailed treatment of the use of electrolytic tanks is given by KARPLUS (1958).

The electrolytic model, in principle, consists of a shallow tank of non-conductive material filled with water containing a small amount of salts such as copper sulphate. The electrolytic conductivity is based on the movement of charge carriers, namely positive and negative ions, and is independent of the electric field, if not too high. The conductivity of a conductive liquid does not change in the same way as the concentration when a very weak solution of salt is replaced by a very strong solution. This phenomenon can be ascribed to the decrease of the dissociation degree, i.e. the relative amount of dissociated molecules in ions and to a decrease in ionic activities.

A model with the boundary configuration of the problem under study is immersed in the tank. Boundaries which are equipotential surfaces are made of metal while an insulating material is employed for streamline boundaries. An alternating current source is applied to the equipotential boundaries. The voltage distribution within the liquid can be measured with a sensing probe. For radial flow towards a drain, a cylindrical metallic wall forms one electrode of the system and a model of the drain is placed vertically in the centre forming the second electrode. The pipe wall consists of insulating material while a conductive metal is used for the perforations.

Radial flow towards an ideal conductor in a conductive liquid gives a straight line relationship between the voltage and the logarithm of the distance to the conductor. For a conductor with length L we have that

$$V_r = \frac{I \rho}{2 \pi L} \ln \frac{R}{R_o} \tag{1.92}$$

or

$$\frac{V_r}{\ln \frac{R}{R_o}} = \frac{I \rho}{2 \pi L} = \tan \alpha \tag{1.93}$$

On the other hand

$$V_r = I\ \Omega \tag{1.94}$$

or

$$V_r = \frac{I\ \rho\ \alpha_r}{L} \tag{1.95}$$

with

$$\alpha_r = \frac{1}{2\ \pi} \ln \frac{R}{R_o} \tag{1.96}$$

in which V_r = applied voltage between the two electrodes with radius R and R_o (V)

I = electric current (A)

ρ = resistivity of the electrolyte (Ω m)

L = conductor length (m)

Ω = electric resistance (Ω)

α_r = radial flow resistance (dimensionless).

The value of α_r is only dependent on the radius of the flow medium and of the conductor; moreover α_r is identical to eqn. (1.5). From eqn. (1.95) it follows that

$$\alpha_r = \frac{V_r\ L}{I\ \rho} \tag{1.97}$$

and considering eqn. (1.93), we obtain that

$$\alpha_r = \frac{V_r}{2\ \pi\ \tan\ \alpha} \tag{1.98}$$

Radial flow towards a model of a real drain gives :

$$V_t = V_r + V_e \tag{1.99}$$

The applied voltage V_t is the sum of the voltage V_r for radial flow and the additional voltage V_e to overcome the resistance of the model of a real drain. Analogously to eqn. (1.98), the entrance resistance can be derived from the electric voltage measurements, since

$$\alpha_e = \frac{V_e}{2\ \pi\ \tan\ \alpha} \tag{1.100}$$

and

$$\alpha_t = \alpha_r + \alpha_e = \frac{V_t}{2\,\pi\,\tan\,\alpha} \qquad (1.101)$$

For a model of an ideal drain, the electric potential distribution in relation to the logarithm of R/R_o is graphically represented by the straight line (a) in fig. 1.18. This straight line makes an angle α with the abscissa. From eqn. (1.93) it follows that tan α is a measure of the electric current because $\rho/2\,\pi\,L$ is a constant at a given temperature. For flow towards a model of a real drain the curves (b), (c) and (d) in fig. 1.18 are obtained depending on the position of the measuring place with respect to the perforations. CAVELAARS (1966) described how α_e can be derived. When the straight part of the curves (b), (c) and (d) has a slope angle α, then the electric current corresponds to the electric current for flow towards a model of an ideal drain. To maintain the same electric current as would be obtained for flow towards a model of a real drain, a higher voltage V_t has to be applied. The difference in voltage V_e (see fig. 1.18) represents the extra voltage to overcome the entrance resistance.

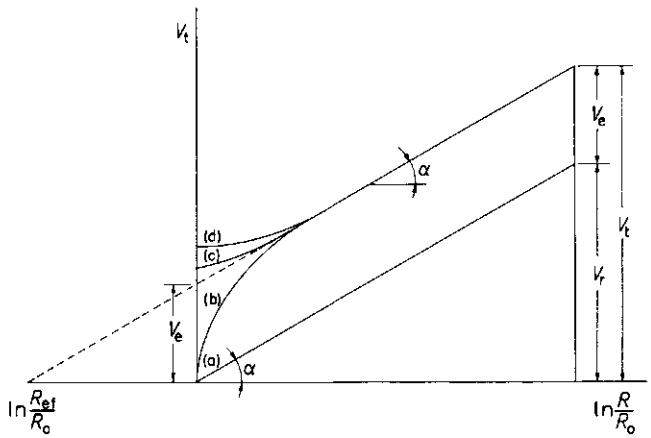

Fig. 1.18. Relationship between voltage and distance to the drain model (CAVELAARS, 1966).
(a) model of an ideal drain
(b), (c), (d) model of a real drain; the shape of the curves depends on the position of the measuring place with respect to the perforations.

This V_e-value can be found by extrapolating the straight part of the curves (b), (c) and (d) to its intersection with the ordinate. If the straight part of the curves is extrapolated to its intersection with the horizontal axis, the value of $\ln(R_{eff}/R_o)$ is found.

Another possibility which exists is that of deriving the entrance resistance from the ratio of electrical currents in the ideal and real drain model cases by applying equal voltages (SCHWAB & KIRKHAM, 1951). For flow towards a model of an ideal drain we have :

$$V_r = \frac{I_{id}\,\rho}{2\,\pi\,L} \ln \frac{R}{R_o} = \frac{I_{id}\,\rho}{L}\,\alpha_r \qquad (1.102)$$

and for flow towards a model of a real drain :

$$V_t = \frac{I_{rd}\,\rho}{L}\,(\alpha_e + \alpha_r) \qquad (1.103)$$

Combining eqns. (1.102) and (1.103) and considering eqn. (1.96) gives

$$\alpha_e = \frac{1}{2\,\pi}\left(\frac{I_{id}}{I_{rd}} - 1\right) \ln \frac{R}{R_o} \qquad (1.104)$$

in which I_{id} = electric current for flow towards the model of an ideal drain (A)

I_{rd} = electric current for flow towards the model of a real drain (A).

Apart from analytical solutions and sand tank experiments, present knowledge on the entrance resistance of drains has been obtained from investigations with electrolytic analogues.

SCHWAB & KIRKHAM (1951) checked the validity of their analytical solutions with electrolytic models and found a reasonable good agreement between theoretical and experimental values, although the theoretical uptake capacity seemed to be somewhat higher than the experimental one. These authors established that for the same number of circular perforations per unit length of drain much the same results were obtained, irrespective of the number of rows. The solution of KIRKHAM (1950) for circumferential openings was also checked and deviations not greater than 3 % were obtained.

From his investigations with an electrolytic analogue, CAVELAARS (1966) found that the relative perforation length is a good criterion for the per-

formance of drains. Both perforation width and drain diameter have less influence. Since the spacing of perforations determines the concentration of the flow lines, the spacing is of primary interest and the perforation area is not a useful parameter. Hence pipes with shorter perforations but the same perforation length per unit length of drain have a lower entrance resistance than pipes with longer perforations (CAVELAARS, 1967). Because of the perforation pattern, it may be expected that plastic pipes will have a better uptake capacity than clay pipes.

WIDMOSER (1966) also arrived, independently of CAVELAARS (1967), at analogous conclusions. WIDMOSER (1972) found a higher entrance resistance for circular holes than for slits having the same inlet area. For drains with two continuous longitudinal slits and identical geometrical conditions, an increase in diameter does not result in improvement of the drainage performance (WIDMOSER, 1967).

According to CAVELAARS (1970), doubling the perforation length reduces the entrance resistance to less than half. Doubling the perforation length and halving the width still halves the entrance resistance. Doubling the perforation width does not have much effect. A larger drain diameter with the same perforation pattern results in a higher entrance resistance because of increasing spacing between perforations. The inlet area of clay drains changes with increasing diameter and results in a lower entrance resistance.

BRAVO & SCHWAB (1977) investigated the effect of circumferential openings on smooth plastic pipes and discontinuous circumferential slits on both smooth and corrugated plastic pipes by means of an electrolytic analogue. It was found that the entrance resistance increased considerably when the valleys of the corrugations were filled with soil. If soil had entered the perforations the entrance resistance increased still further. According to these authors, a thin envelope material surrounding corrugated drains results in drains with circumferential openings which approximate to an ideal drain.

Higher permeability of the trench backfill can compensate for entrance resistance (CAVELAARS, 1970). In the case of clay and smooth plastic drains the permeability of the trench backfill should be 4 to 10 times the permeability of the undisturbed surrounding soil, while twice the permeability of the undisturbed soil suffices for corrugated plastic drains.

3. *Experimental Research*

3.1. *Electrolytic analogue and electric equipment*

The electrolytic analogue used in this study consisted of a square container (fig. 1.19) with inside dimensions of 810 mm, made of 15 mm thick plexiglass. A cylinder of brass copper with an inner diameter of 800 mm and a wall thickness of 1,5 mm was placed in the container. The height of the container and the copper cylinder was 330 mm. Drain models were placed at the centre of the cylinder. The brass copper cylinder and the drain model constituted the electrodes of the system.

A weak solution of copper sulphate ($CuSO_4$) in distilled water was employed as conductive liquid. To obtain full accuracy of the power supply, the concentration was adapted so that a load resistance greater than or equal to 300 Ω was reached.

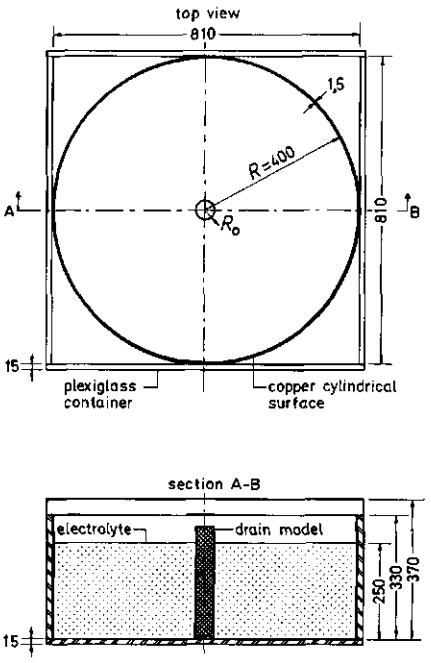

Fig. 1.19. Scheme of the electrolytic model (measurements in mm).

Rails were mounted over the plexiglass container on which a small carriage could move to and fro. The carriage carried the sensing probe which could be displaced both radially and vertically (fig. 1.20). Position and depth of the probe could be read very accurately in both the horizontal and vertical planes by means of a measuring staff with 0.05 mm divisions. By turning the drain model around its axis, it was possible to carry out measurements in several vertical radial planes.

The sensing probe was a platinum wire fused into a glass tube (fig. 1.21) connected via a mercury-contact to the measuring instrument.

A low-frequency generator, PHILIPS PM 5106, was used to supply sine-wave voltage in the frequency range 10 Hz to 100 kHz. A frequency could be selected in four overlapping subranges. In each range the frequency was continuously variable by means of a dial and the output voltage could be continuously adjusted from 0 to 10 V.

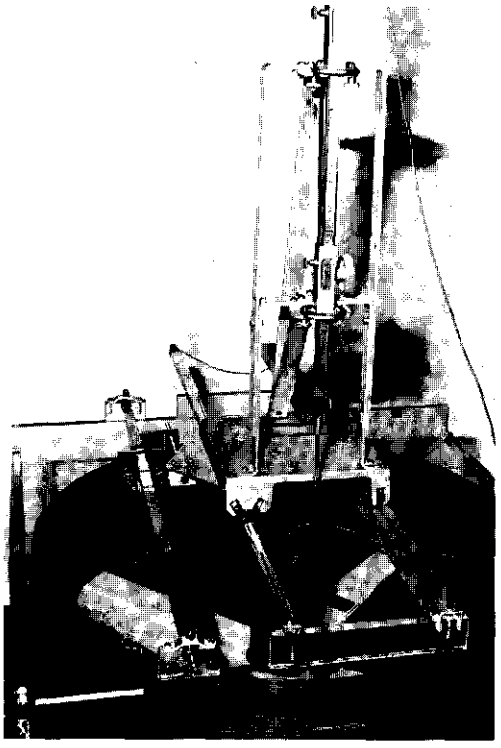

Fig. 1.20. Rails, travelling carriage and measuring staffs.

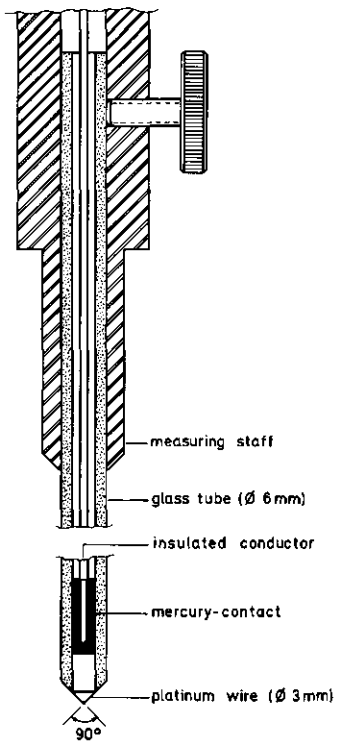

Fig. 1.21. The sensing probe.

The influence of the frequency on the measurements has been checked by carrying out measurements at 10 Hz, 1 kHz and 10 kHz. No appreciable effect on the entrance resistance has been noticed. In order to carry out the research under equal circumstances a frequency of 1 kHz has been applied throughout the experiments. The frequency dependence of the output voltage amounted to $\pm$ 2 % referring to 1 kHz while the mains voltage dependence was smaller than 1 %. Both effects were limited by a regular control of the output voltage. These requirements were met by using load resistances greater than or equal to 300 Ω.

To detect possible disturbing influences on the sine-wave output voltage of the generator, a portable oscilloscope, PHILIPS PM 3200, has been used. The instrument runs on mains voltage or on rechargeable batteries in a frequency range from 2 Hz to 10 MHz.

Measurements of the voltage distribution in, and the electric current through, the electric analogue were carried out with a digital multimeter, PHILIPS PM 2422 A. Alternating voltages from 0,1 mV to 600 V in 5 ranges : up to 200 mV, 2 V, 20 V, 200 V and 600 V could be measured. The accuracy was ± 0,2 % of the full range plus 0,2 % of the reading at frequencies of 1 kHz. The range used was 20 V since the maximum output voltage was 9 V; hence the accuracy of the measurements can be estimated at 0,06 V. The temperature coefficient amounts to about 1 digit per 5 °C. As such large temperature differences did not occur, the effect could be neglected.
Alternating current could be measured from 100 nA to 2 A in 5 ranges : up to 200 µA; 2 mA; 20 mA; 200 mA and 2 A. Accuracy of measurements amounted to 0,4 % of the full range plus 0,4 % of the reading. The temperature coefficient is ± 1 digit per 4 °C.
The maximum display on the instrument was 1999. It had to be connected to the mains voltage and a warming-up time of approximately 30 min had to be observed to obtain full accuracy.

3.2. *Drain models*

3.2.1. Smooth drains with circumferential openings

Clay drains with a 50 mm inner diameter, a 75 mm outer diameter and a unit length of 300 mm were simulated by lengths of plastic rods with the same outer diameter. A copper ring, having a thickness corresponding to the simulated gap width, was mounted between two pipe units (fig. 1.22a). The whole construction was held together by a screwed rod and fly-nut. The copper ring forms the zero potential electrode. This pipe has been coded S^1_{co} which means : Smooth outer surface with Circumferential Openings. The exponent refers to the drain diameter. The investigated gap widths are given in table 1.5. Fig. 1.22b shows the drain model and gap width simulations.

In order to check the general validity of the theoretical solutions drains with a 40 mm outer diameter and gap widths of 1 mm at different spacings have also been investigated. Table 1.6 gives the characteristics of the drain pipes investigated. These pipes have been coded $S^2_{co}(\beta_s)$.

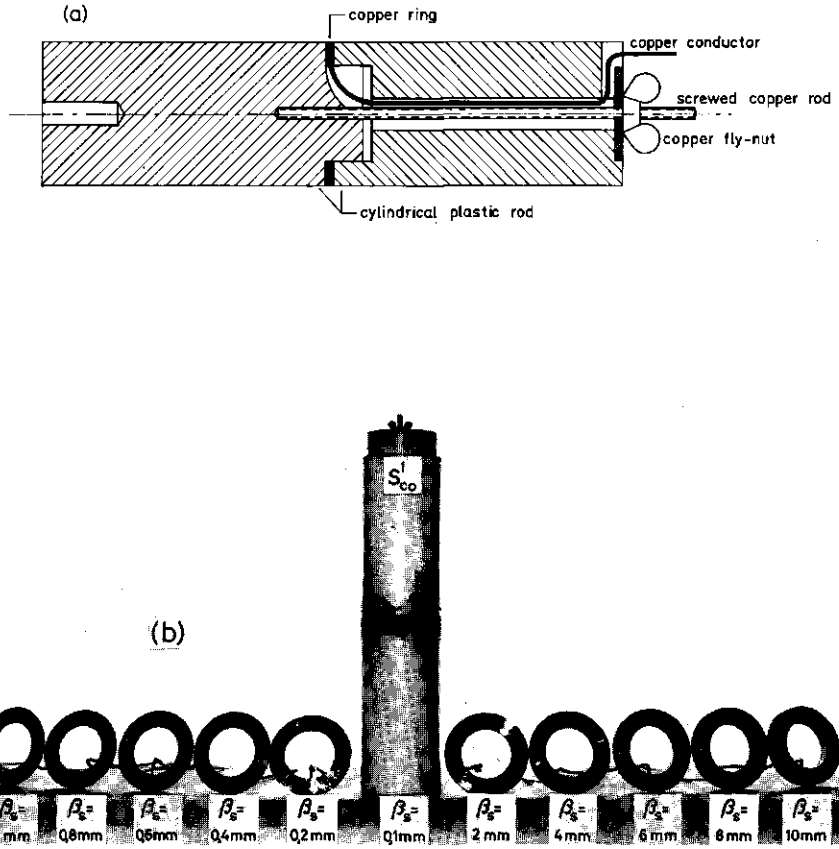

Fig. 1.22a. Scheme of the S^1_{co}-drain model
b. The S^1_{co}-drain model and the investigated gap widths.

The connection between the copper rings, forming together the zero potential electrode, has been completed by means of a strip of aluminium foil, as is shown schematically in fig. 1.23a. Conducting and insulating parts were kept together with a screwed rod and fly-nut. Fig. 1.23b. illustrates the $S^2_{co}(1)$-drain models.

3.2.2. Smooth drains with circular perforations

Drains with circular perforations were simulated by smooth plastic pipes fitting tight around a copper core in which holes were drilled and

Table 1.5. The simulated gaps for clay drains with a 75 mm outer diameter (S^1_{co}-drain).

gap spacing mm	gap width mm	inlet area cm^2/m	inlet circumference cm/m
300,1	0,10	0,8	157,0
300,2	0,20	1,6	157,0
300,4	0,40	3,1	156,9
300,6	0,60	4,7	156,8
300,8	0,80	6,3	156,7
301,0	1,00	7,8	156,6
302,0	2,00	15,6	156,0
304,0	4,00	31,0	155,0
306,0	6,0	46,2	154,0
308,0	8,0	61,2	153,0
310,0	10,0	76,0	152,0

Table 1.6. The simulated problems for a 40 mm drain with 1 mm wide circumferential openings $\left[S^2_{co}(1)\text{-drain}\right]$.

gap spacing mm	inlet area cm^2/m	inlet circumference cm/m
100,0	12,6	251
80,0	15,7	314
60,0	20,9	419
40,0	31,4	628
20,0	63	1257
10,0	126	2513
5,0	251	5027

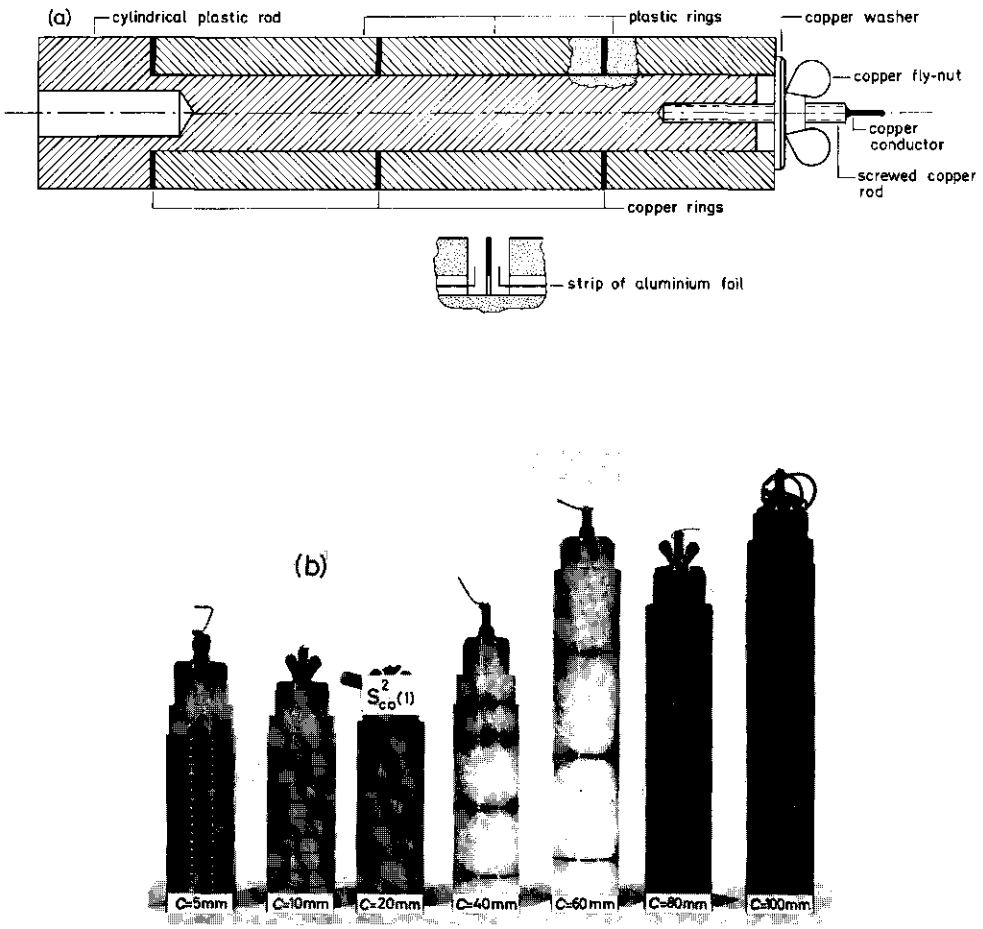

Fig. 1.23a. Scheme of the $S^2_{co}(1)$-drain model
b. The $S^2_{co}(1)$-drain models with different gap spacings.

cylindrical copper pins inserted. The copper pins were then fettled up in such a way that their ends were smooth with the outer surface of the plastic pipe. In this way a square perforation pattern could be obtained. The maximum number of perforations was provided and a smaller number was obtained by insulating the surplus perforations with adhesive tape. Table 1.7 gives the characteristics of the simulated drains, coded $S^1_{cp}(\delta_p)$, $S^2_{cp}(\delta_p)$, $S^3_{cp}(\delta_p)$ and $S^4_{cp}(\delta_p)$. The different drain models are shown in fig. 1.24.

Table 1.7. Simulated drains with circular perforations.

Type	Drain diameter mm	Perforation number m^{-1}	Perforation area cm^2/m	Perforation circumference cm/m
S^1_{cp}(2)	39,90	32; 64; 128; 256; 512; 1024; 1664;	1,01.....52,3	20,1.....1046
S^1_{cp}(3)	39,90	16; 32; 48; 64; 96; 128; 148; 192; 256; 296; 320; 384; 512; 592; 640; 768; 1024; 1760;	1,13..... 124,4	15,1..... 1659
S^1_{cp}(4)	39,90	16; 32; 64; 128; 256; 512; 592; 1184;	2,01..... 148,8	20,1..... 1488
S^1_{cp}(6)	39,90	8; 12; 16; 32; 48; 64; 96; 128; 192; 256; 320; 384; 448; 512; 640; 768; 1024;	2,3..... 290	15,1..... 1930
S^1_{cp}(8)	39,90	4; 8; 12; 16; 32; 48; 64; 96; 128; 192; 256; 320; 384; 448; 512; 640; 768;	2,0..... 386	10,1..... 1930
S^1_{cp}(10)	39,90	16; 32; 64; 128; 256;	12,6.....201	50,3.....804
S^2_{cp}(3)	50,00	16; 32; 64; 128; 256; 512; 1024;	1,13.....72,4	15,1.....965
S^3_{cp}(3)	63,50	16; 32; 64; 128; 256; 512; 1024;	1,13.....72,4	15,1.....965
S^4_{cp}(3)	70,00	16; 32; 64; 128; 256; 512; 1024;	1,13.....72,4	15,1.....965

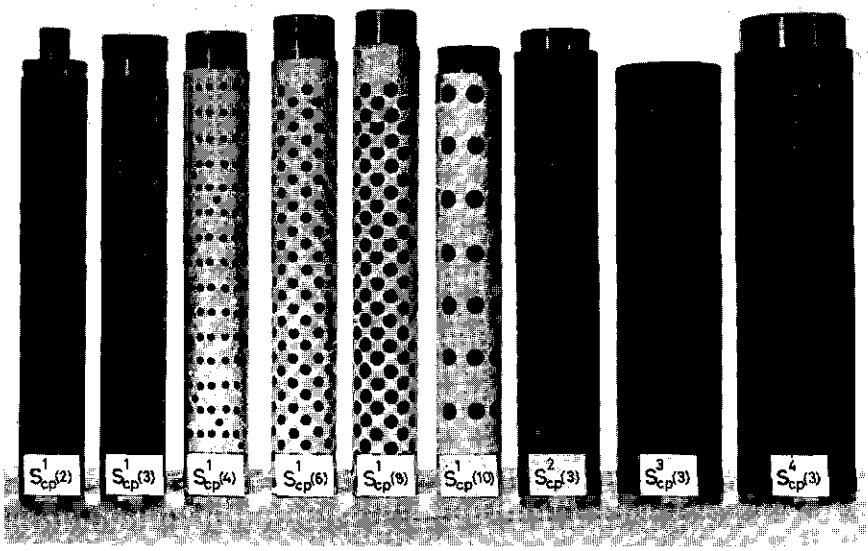

Fig. 1.24. The $S^1_{cp}(\delta_p)$ to $S^4_{cp}(\delta_p)$-drain models.

3.2.3. Smooth drains with continuous longitudinal slits

Drain models with continuous longitudinal slits were made by inserting 1 mm thick copper strips into a slotted copper core (fig. 1.25a). The core was then spun in paraffin wax, the paraffin wax, covering the copper strips, was carefully removed. The investigated types of drains (outer diameter of 40 mm and a perforation width of 1 mm) are given in table 1.8. The drains are coded $S^1_{cls}(\beta_p)$ and fig. 1.25b shows some investigated models.

3.2.4. Smooth drains with discontinuous longitudinal slits

For discontinuous longitudinal perforations the same technique has been applied. The copper strips had a step-shaped profile (fig. 1.26a). The drain models had an outer diameter of 40 mm provided with 2; 4; 6; 8 and 10 perforation rows. The perforations had a width of 1 mm, different lengths, (table 1.9) and formed a rectangular perforation pattern. These drains are coded $S^1_{dls}(\beta_p)$ and some simulated drains are shown in fig. 1.26b.

Table 1.8. Simulated drains with continuous longitudinal slits $\left[S^{1}_{cls}(1)\text{-drain}\right]$.

number of rows	inlet area cm^2/m	inlet perimeter cm/m
2	20,0	400,0
4	40,0	800
6	60,0	1200
8	80	1600
10	100	2000

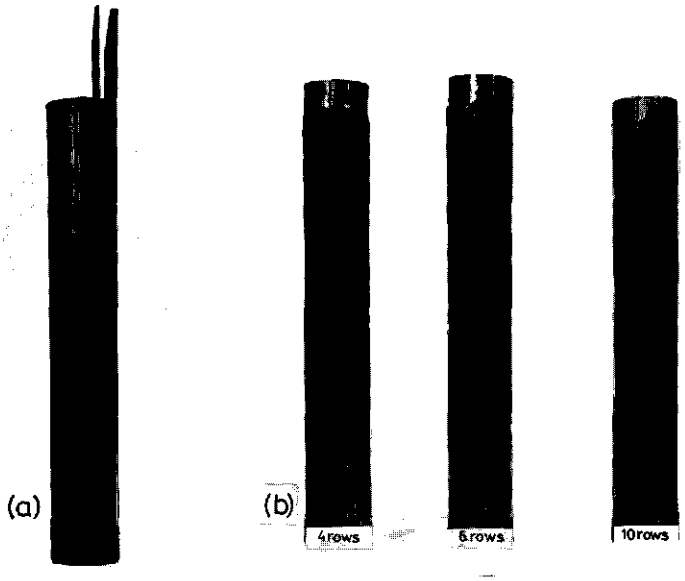

Fig. 1.25a. Slotted copper core with copper strips
b. Some $S^{1}_{cls}(1)$-drain models.

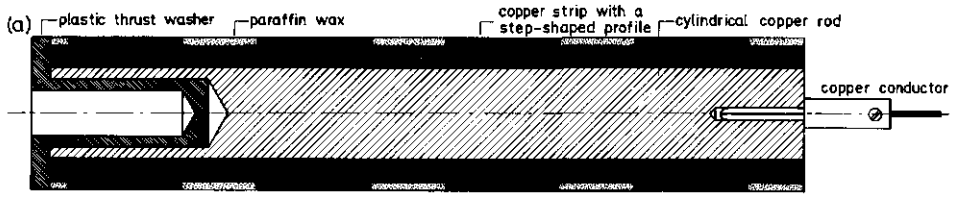

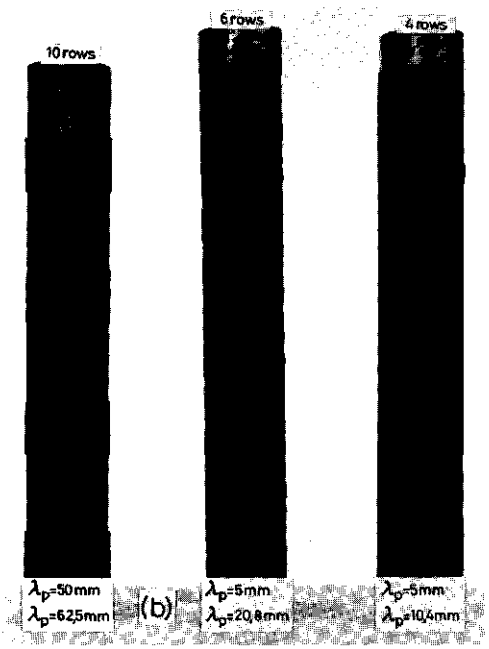

Fig. 1.26a. Scheme of the S^1_{dls}(1)-drain model

b. Some of the S^1_{dls}(1)-drain models.

Table 1.9. Simulated drains with discontinuous longitudinal slits [$S^1_{dls}(1)$- drain with 2; 4; 6; 8 and 10 perforation rows].

slit length	slit spacing	inlet area cm^2/m			inlet perimeter cm/m		
mm	mm	2 ← number of rows → 10			2 ← number of rows → 10		
50,0	62,5	16,0	.....	80	326,4	.....	1632
25,0	62,5	8,0	.....	40,0	166,4	.....	832
25,0	31,2	16,0	.....	80	333	.....	1664
12,5	62,5	4,0	.....	20,0	86,4	.....	432
12,5	31,2	8,0	.....	40,0	173	.....	864
12,5	20,8	12,0	.....	60	259	.....	1296
12,5	15,6	16,0	.....	80	346	.....	1728
5,0	62,5	1,60	.....	8,0	38,4	.....	192
5,0	31,2	3,2	.....	16,0	77	.....	384
5,0	20,8	4,8	.....	24,0	115	.....	576
5,0	15,6	6,4	.....	32	154	.....	768
5,0	10,4	9,6	.....	48	230	.....	1152

3.2.5. Smooth drains with discontinuous circumferential slits

Drains with discontinuous circumferential slits were simulated in a simular fashion to drains with circumferential openings. The circumferential openings were systematically insulated in the longitudinal direction with adhesive tape, dependent on the desired slit length, and a rectangular pattern was obtained. The measurements were carried out for a 40 mm diameter pipe with a slit width of 1 mm, a slit spacing in the row of 20 mm and different slit lengths (table 1.10) distributed over several rows. These drains are coded $S^1_{dcs}(\beta_p)$ and are illustrated in fig. 1.27.

Table 1.10. Simulated drains with discontinuous circumferential slits $\left[S^{1}_{dcs}(1)\text{-drain with } c = 20 \text{ mm}\right]$.

slit length	number of rows	inlet area cm^2/m	inlet perimeter cm/m
50,0	2	50,0	1020
25,0	2;4	25,0;50,0	520;1040
20,0	2;4;6	20,0 60,0	420 1260
15,0	2;4;6	15,0 45,0	320 960
10,0	2;4;6;8;10	10,0 50,0	220 1100
5,0	2;4;6;8;10	5,0 25,0	120 600

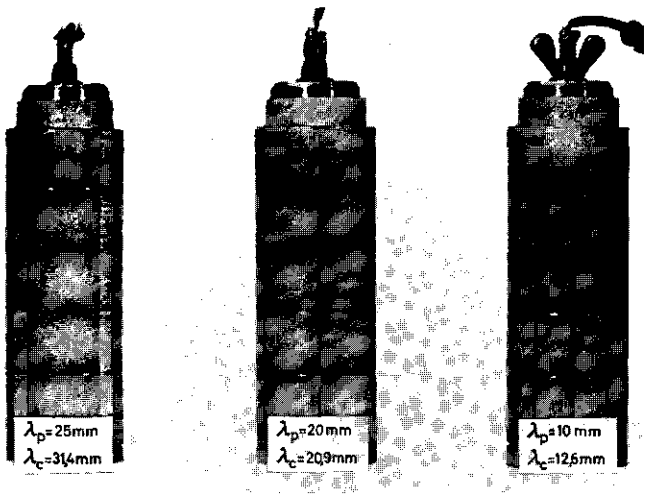

Fig. 1.27. Some $S^{1}_{dcs}(1)$-drain models.

3.2.6. Corrugated drains with circumferential openings

To study the effect of the corrugations on the entrance resistance, drains with block wave corrugations and circumferential openings in the valleys were simulated. It was assumed that the valleys of the corrugations were filled with soil having the same permeability as the surrounding soil. The largest outer radius R_o was 25 mm while the smallest outer radius R'_o was 23 mm, the corrugation height δ_r being 2 mm. Ridge and valley had a width β_v of 2,5 mm. Circumferential openings were provided every other valley and hence the spacing e was 10 mm. Fig. 1.28a shows a corrugated drain with circumferential openings having a width β_s of 2,5 mm equal to the valley width. Fig. 1.28b shows a corrugated drain with circumferential openings having a width β_s of 1 mm, which is smaller than the valley width. Corrugated drain models with circumferential openings were constructed in the same way as the $S^2_{co}(1)$-drain models after shaping plastic and copper rings in such a way that a block wave profile was obtained. These drains are coded C^1_{co} which signifies Corrugated outer surface with Circumferential Openings.

A drain with sine wave corrugations of 5 mm pitch length and 1 mm wide circumferential openings every other valley has also been constructed.

3.2.7. Corrugated drains with discontinuous circumferential slits

Normally, corrugated plastic drains are provided with discontinuous circumferential slits. One model, having a perforation width of 1 mm, was constructed using plastic rings with recesses in which small copper strips representing a perforation length of 5 mm were adhered and soldered to each other. For the other models, the discontinuous circumferential slits were obtained in an easier and simpler way by insulating the $C^1_{co}(1)$-drain model in longitudinal direction with adhesive tape. The drains are coded $C^1_{dcs}(\beta_s)$ and table 1.11 gives the simulated drains. Some corrugated drain models are shown in fig. 1.28c.

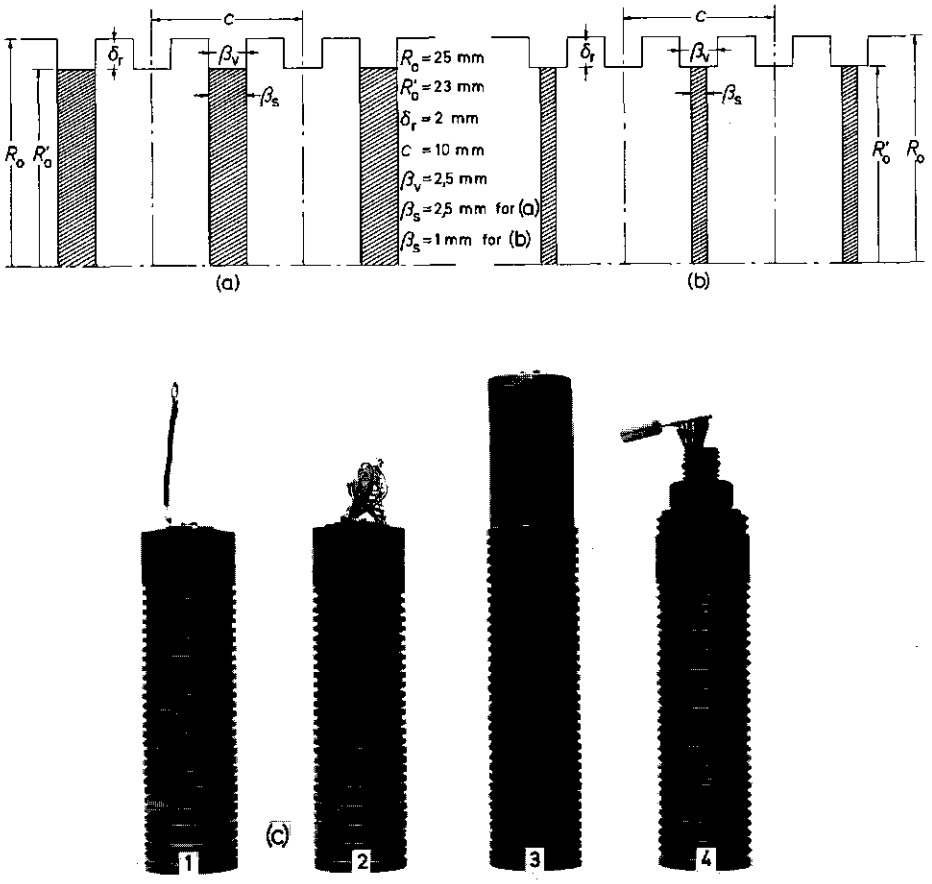

Fig. 1.28. Corrugated drains

a. Gap width equal to valley width

b. Gap width smaller than valley width

c. Some corrugated drain models

(1) $C^1_{co}(2,5)$-drain model with block wave corrugations

(2) $C^1_{co}(1)$-drain model with block wave corrugations

(3) $C^1_{dcs}(1)$-drain model with block wave corrugations

(4) $C_{co}(1)$-drain model with sine wave corrugations.

Table 1.11. Simulated corrugated drains with discontinuous longitudinal slits $\left[C^{1}_{dcs}(1)\text{-drain}\right]$.

slit length mm	slit spacing mm	perforation area cm^2/m	perforation perimeter cm/m
5,0	18,1	20,0	480
5,0	24,1	15,0	360
5,0	36,1	10,0	240
5,0	72,3	5,0	120
4,5	14,5	22,5	550
8,1	18,1	32,4	728
14,1	24,1	42,3	906
26,1	36,1	52,2	1084
62,3	72,3	62,3	1266
9,5	14,5	47,5	1050
13,1	18,1	52,4	1128
19,1	24,1	57,3	1206
31,1	36,1	62,2	1284
67,3	72,3	67,3	1366

3.3. *Measurement and calculation method*

A vertical radial plane was scanned by displacing the probe in radial and vertical direction. When measuring radial displacement, voltage readings were taken every 10 mm until 210 mm away from the drain centre. Hereafter readings were taken every 20 mm.

The liquid depth in the tank depended upon the plane of symmetry (fig. 1.29). Usually such planes were taken at spacings of 250 mm and the electrolytic tank was then filled to that height. The bottom of the tank and the liquid surface then formed the outside planes of symmetry. Measurements were carried out at 50; 100; 150 and 200 mm above the bottom of the tank depending on the length of the model. The liquid depth was adapted for pipes having no symmetry at spacings of 250 mm e.g. clay drain pipes. For pipes having planes of symmetry at larger spacings than the permissible liquid depth of

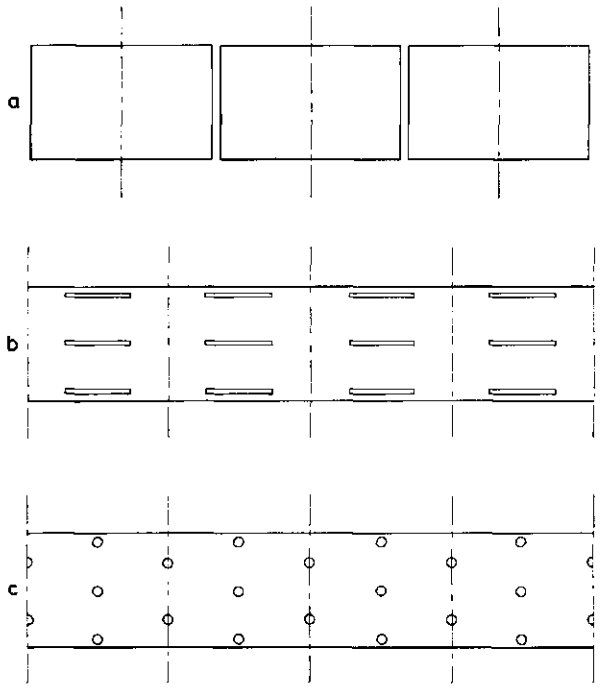

Fig. 1.29. Planes of symmetry define the flow zone towards perforations
a. circumferential openings
b. discontinuous longitudinal slits in a rectangular pattern
c. longitudinal rows with alternating circular perforations.

the tank, a liquid depth of 250 mm was maintained, since the perforation distribution was normally such that only a small error would result.

For scanning different vertical radial planes, the pipe was rotated around its axis. The first series of measurements were carried out opposite a perforation row, the second series between two perforation rows and the third series again opposite a perforation row. In this way 3 x 4 values of the entrance resistance of the investigated drain model could be calculated. For circumferential openings, only one vertical radial plane was scanned at four depths.

The measured voltage values were plotted against $\ln(R/R_o)$ and a regression line for the straight part was calculated by the method of least squares. A trial and error procedure was used in calculating the straight line taking

into account different numbers of points until the highest correlation was obtained. The intercept of this straight line on the vertical axis $R/R_o = 1$ gives the required voltage drop to overcome the extra resistance of the drain model as explained in § 2.2.2.

From the equation for a straight line

$$y = a + bx$$

we have

$$V_t = V_e + \tan \alpha \ln \frac{R}{R_o} \qquad (1.105)$$

The intercept V_e and tan α could be derived. The α_e-value then was calculated from eqn. (1.100). For continuous longitudinal and discontinuous slits the mean value of the 12 measurements was taken as being the entrance resistance of the drain. For circumferential openings, the mean value was based on 4 observations.

3.4. *Accuracy of measurements and calculations*

The outside diameter of the investigated drain models was measured with a sliding gauge as the mean value of 2 measurements on perpendicular axes with an accuracy of 0,05 mm. Centring the drain model in the tank can also cause a deviation of 0,05 mm. Hence the accuracy of the drain radius can be estimated at 0,075 mm. The relative error obtained in this way depends on R_o and is given in table 1.12.

Table 1.12. Relative error in R_o.

R_o (mm)	20	25	30	40	50
$\Delta R_o/R_o$ (%)	0,4	0,3	0,3	0,2	0,2

The position of the measuring point depends on the accuracy of measuring which was 0,05 mm, on the deviation of the midpoint of the tank which was 0,025 mm and on the accuracy with which the midpoint has been transfered to the measuring staff which was 0,05 mm. Hence the total error associated with locating the measuring point with respect to the tank midpoint is 0,125 mm.

The error in R/R_o depends on the position of measurement and the radius of the drain model. The error in $\ln(R/R_o)$ can be derived from

$$\Delta u = \frac{\partial u}{\partial x} \Delta x$$

or

$$\Delta(\ln \frac{R}{R_o}) = \frac{\Delta(R/R_o)}{R/R_o}$$

and is given in table 1.13.

Table 1.13. Relative error in $\ln(R/R_o)$

R_o (mm)→	20	25	30	40	50
R(mm) ↓	$\Delta[\ln(R/R_o)]/\ln(R/R_o)$ (%)				
100	0,4	0,4	0,4	0,4	0,5
200	0,2	0,2	0,2	0,2	0,2
300	0,2	0,2	0,2	0,2	0,2
400	0,2	0,2	0,2	0,2	0,2

Since the entrance resistance in a given vertical radial plane does not depend on the accuracy of the depth, no measuring error has been introduced. Also, the influence of the temperature on the specific conductivity has not been considered since the measurements were carried out at constant temperature.

Theoretically, tan α can be derived from

$$\tan \alpha = \frac{V_t - V_t'}{\ln(R/R')} \qquad (1.106)$$

in which V_t' is the potential at a distance R' from the drain centre provided that the linear relationship between V_t and $\ln(R/R_o)$ was established. For most cases R' had a value of 100 mm. The error in V_t is 0,7 %. The experimental error in tan α can be derived from the relative error in $V_t - V_t'$ and the relative error in $\ln(R/R')$ which is 0,2 %. Table 1.14 gives some relative errors in tan α as a function of V_t'.

Table 1.14. Relative error in tan α.

V_t' (V)	8	7	6	5	4	3	2	1
$\frac{\Delta(V_t - V_t')}{V_t - V_t'}$ (%)	11,9	6,0	3,9	2,9	2,3	1,9	1,6	1,4
$\frac{\Delta \tan \alpha}{\tan \alpha}$ (%)	12,1	6,2	4,1	3,1	2,5	2,1	1,8	1,6

From eqns. (1.105) and (1.106) it follows that

$$V_e = \frac{V_t'\left[\ln(R/R_o)\right] - V_t\left[\ln(R'/R_o)\right]}{\ln(R/R')} \qquad (1.107)$$

from which the relative error in V_e can be derived. The relative error in α_e is given by the sum of the relative errors in V_e and in tan α. Some relative errors in α_e are given in table 1.15.

Table 1.15. Relative errors in α_e as a function of V_e.

V_e	$\frac{\Delta \tan \alpha}{\tan \alpha}$	$\frac{\Delta V_e}{V_e}$	$\frac{\Delta \alpha_e}{\alpha_e}$
V	%	%	%
0,5	2,9	49,2	52,1
1,0	3,1	24,9	28,0
2,0	3,5	12,8	16,3
3,0	4,1	8,7	12,8
4,0	5,0	6,7	11,7
5,0	6,2	5,4	11,6
6,0	8,3	4,7	13,0
7,0	12,5	4,1	16,6
8,0	25,3	3,7	28,7
8,5	50,2	3,5	53,7

The real error differs from measurement to measurement and must be calculated separately. The mean relative error can be estimated at 15 %, although for extremely high and low entrance resistances the relative error amounts to 50 %. It suffices to accept a mean error to justify the number of significant figures with which the results are given. For an accuracy of 15 %, the values of the entrance resistance can be given in two significant figures.

In fact, V_e has been calculated according to eqn. (1.105) by the method of least squares, hence the standard deviations s_a and s_b are a better measure for the accuracy with which both quantities have been determined. For s_a, the variation coefficient obtained was never larger than 0,2 % whilst for s_b it varied between 0,2 % for low and 1,5 % for high values of b. It may be expected that the real accuracy will be much greater than the theoretical accuracy and may be estimated at about 5 %. But, even then, no more significant figures can be justified except for values of the entrance resistance between the significant figures 1 and 2. Only for values between 1 and 2 three significant figures have been given.

The accuracy further depends on the precision with which the drain model has been constructed, the cleanliness of the perforations before starting the experiment and any change during the experiment.

In order to distinguish clearly the different theoretical solutions, results have been calculated at three significant figures.

4. *Results and interpretation*

The most logical presentation of the experimental results is a double logarithmic diagram in which α_{ep} is plotted against the inlet area A_p. Since the inlet area is not a useful parameter for estimating the entrance resistance, the α_{ep}-values are also plotted against the inlet perimeter C_p. Because of the small differences, only some results obtained from analytical solutions are presented in the diagrams. They are completed by tables.

4.1. *Circumferential openings*

4.1.1. The S^1_{co}-drains

For plane boundary conditions, the results of the measurements on clay pipes with an outer diameter of 75 mm, a length of 300 mm and different gap widths are presented in fig. 1.30.

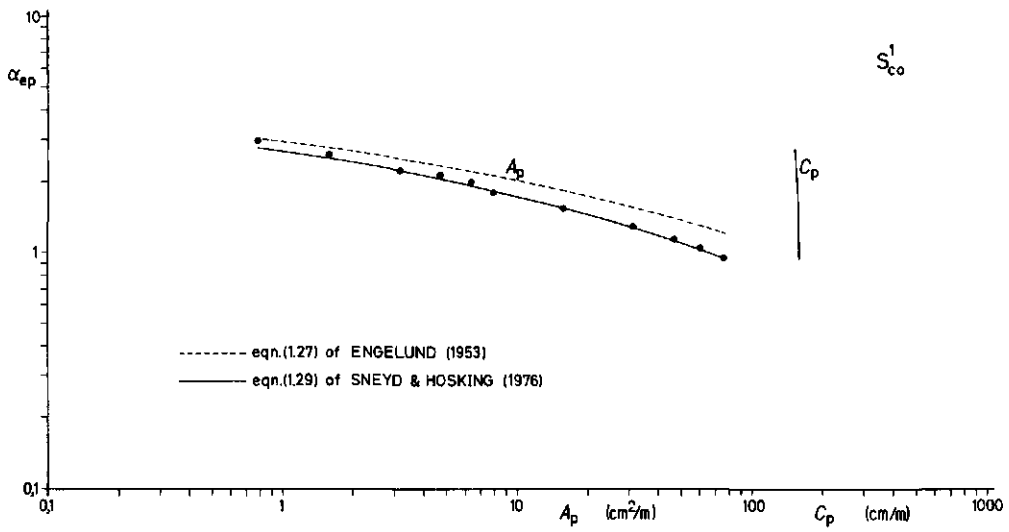

Fig. 1.30. The entrance resistance α_{ep} as a function of the inlet area A_p and the inlet circumference C_p for clay drains with R_o = 37,5 mm, l = 300 mm and different gap widths.

It can be seen that the variation of α_{ep} is small although the inlet area varies considerably due to the increasing gap width. The inlet circumference changes only slightly and, in this case, the variation of α_{ep} is mainly determined by that of the gap width.

Comparing experimental results with those obtained from the theory (table 1.16 and fig. 1.30) clearly shows rather good agreement. The rather simple eqn. (1.27) of ENGELUND (1953) gives results similar to those of eqn. (1.21) of KOZENY (1933), of eqn. (1.25) of KIRKHAM (1950) and of the approximate solution (1.28) of ERNST (1962). These α_{ep}-values are slightly greater than the experimental values. Eqn. (1.23) of Appendix I gives better agreement. As could be expected from theoretical considerations, eqn. (1.29) of SNEYD & HOSKING (1976) is a more exact solution. The results of eqn. (1.29) were obtained by interpolating the tabular values of $g(2\ R_o/c,\ 2\ R/c)$ given by SNEYD (1976). However, a reasonable good approximation is already obtained from eqn. (1.32) in which the term

$$\frac{c}{2\ \pi\ R_o}\ g\left(\frac{2\ R_o}{c}, \frac{2\ R}{c}\right)$$

in the solution of SNEYD & HOSKING (1976) has been omitted.

The results of the corresponding formulae for arched boundary conditions are given in table 1.17 and similar conclusions can be drawn.

From eqns. (1.31) and (1.32) it follows that the entrance resistance mainly depends on the gap spacing and the radius of the drain while the gap width is less important. For clay drains, the gap spacing is near constant and, for a given pipe diameter and length, the gap width only has a limited effect on the entrance resistance. This confirms the conclusions of OEHLERS (1932) and KOZENY (1933) that the drainage performance is only slightly influenced by gap width.

4.1.2. The $S^2_{co}(1)$-drains

For plane boundary conditions, the results for drains with 1 mm wide circumferential openings at different spacings are given in table 1.18 and fig. 1.31. Since the gap width is kept constant, the relationships between α_{ep}-A_p and α_{ep}-C_p show similar trends.

Table 1.16. Results of experimental and theoretical α_{ep}-values for clay drains with R_o = 37,5 mm, l = 300 mm and different gap widths (S^1_{co}-drains).

gap width	gap spacing	α_{ep}	α_{ep}-values according to eqns.						
mm	mm	Exp.	(1.21)	(1.23)	(1.25)	(1.27)	(1.28)	(1.29)	(1.32)
0,10	300,1	2,9	3,25	2,78	2,92	3,06	2,82	2,79	2,80
0,20	300,2	2,6	2,96	2,50	2,64	2,78	2,56	2,51	2,52
0,40	300,4	2,2	2,66	2,22	2,36	2,50	2,29	2,23	2,25
0,60	300,6	2,1	2,48	2,06	2,20	2,34	2,13	2,06	2,08
0,80	300,8	2,0	2,36	1,94	2,08	2,23	2,02	1,95	1,97
1,00	301,0	1,80	2,26	1,85	1,99	2,14	1,94	1,86	1,88
2,00	302,0	1,56	1,96	1,58	1,72	1,86	1,67	1,58	1,60
4,00	304,0	1,31	1,66	1,31	1,45	1,59	1,40	1,31	1,33
6,0	306,0	1,16	1,49	1,16	1,30	1,44	1,24	1,15	1,17
8,0	308,0	1,06	1,36	1,05	1,19	1,33	1,13	1,04	1,06
10,0	310,0	0,96	1,27	0,966	1,11	1,25	1,05	0,958	0,974

eqn. (1.21) of KOZENY (1933)
eqn. (1.23) of Appendix I
eqn. (1.25) of KIRKHAM (1950)
eqn. (1.27) of ENGELUND (1953)
eqn. (1.28) of ERNST (1962)
eqn. (1.29) of SNEYD & HOSKING (1976)
eqn. (1.32) of this contribution

Table 1.17. Results of theoretical α_{ea}-values for the S^1_{co}-drains.

gap width	gap spacing	α_{ea}-values according to eqns.					
mm	mm	(1.20)	(1.22)	(1.24)	(1.26)	(1.30)	(1.31)
0,10	300,1	2,99	2,50	2,64	2,78	2,51	2,52
0,20	300,2	2,70	2,22	2,36	2,50	2,23	2,24
0,40	300,4	2,40	1,94	2,08	2,22	1,95	1,96
0,60	300,6	2,23	1,78	1,92	2,06	1,78	1,80
0,80	300,8	2,11	1,66	1,80	1,94	1,67	1,69
1,00	301,0	2,01	1,57	1,71	1,86	1,58	1,60
2,00	302,0	1,71	1,30	1,44	1,58	1,30	1,32
4,00	304,0	1,42	1,03	1,17	1,31	1,03	1,04
6,0	306,0	1,25	0,879	1,02	1,15	0,867	0,884
8,0	308,0	1,13	0,773	0,916	1,04	0,775	0,771
10,0	310,0	1,04	0,693	0,837	0,959	0,667	0,683

eqn. (1.20) of KOZENY (1933)
eqn. (1.22) of Appendix I
eqn. (1.24) of KIRKHAM (1950)
eqn. (1.26) of ENGELUND (1953)
eqn. (1.30) of SNEYD (1976)
eqn. (1.31) of this contribution

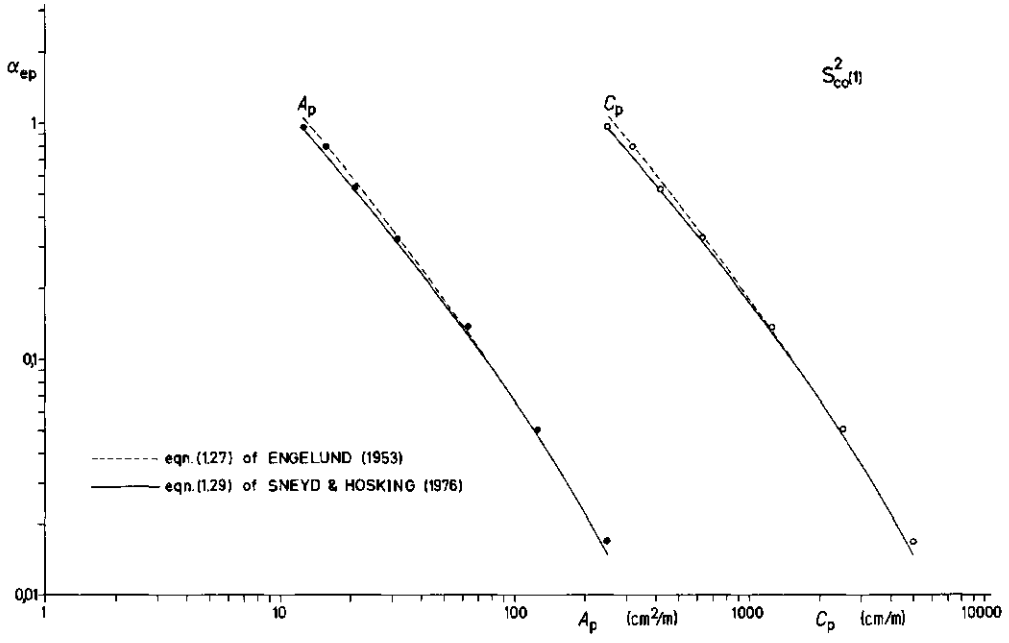

Fig. 1.31. The entrance resistance α_{ep} as a function of the inlet area A_p and the inlet circumference C_p for drains with R_o = 20 mm and 1 mm wide circumferential openings at different spacings.

It can be seen that the results of eqn. (1.21) of KOZENY (1933) differ widely from the experimental results. Also eqn. (1.23) of Appendix I and the approximate solution (1.28) of ERNST (1962) result in large deviations for small gap spacings. Hence, these formulae can only be applied under certain conditions. The results obtained from eqn. (1.27) of ENGELUND (1953), as well as those obtained from eqn. (1.29) of SNEYD & HOSKING (1976), show good agreement with the experimental values and are identical for small gap spacings. The simplified solution (1.32) can be applied with sufficient accuracy. Also eqn. (1.25) of KIRKHAM (1950) gives reasonably accurate results.

The results of the corresponding formulae for arched boundary conditions are given in table 1.19 and, here also, similar conclusions can be drawn.

Table 1.18. Results of experimental and theoretical α_{ep}-values for drains with R_o = 20 mm and 1 mm wide circumferential openings at different spacings $\left[S_{co}^2(1)\text{-drains}\right]$.

gap spacing	α_{ep}	α_{ep}-values according to eqns.						
mm	exp.	(1.21)	(1.23)	(1.25)	(1.27)	(1.28)	(1.29)	(1.32)
100,0	0,96	2,19	0,918	1,01	1,05	1,02	0,931	0,951
80,0	0,80	2,04	0,700	0,779	0,796	0,808	0,715	0,732
60,0	0,52	1,91	0,489	0,553	0,554	0,598	0,505	0,517
40,0	0,33	1,80	0,287	0,337	0,328	0,392	0,305	0,312
20,0	0,14	1,75	0,103	0,139	0,129	0,189	0,125	0,125
10,0	0,051	1,50	0,0245	0,0533	0,0469	0,0892	0,0459	0,0459
5,0	0,017	0,513	-0,00679	0,0183	0,0147	0,0396	0,0144	0,0144

eqn. (1.21) of KOZENY (1933)
eqn. (1.23) of Appendix I
eqn. (1.25) of KIRKHAM (1950)
eqn. (1.27) of ENGELUND (1953)
eqn. (1.28) of ERNST (1962)
eqn. (1.29) of SNEYD & HOSKING (1976)
eqn. (1.32) of this contribution

Table 1.19. Results of theoretical α_{ea}-values for the S^2_{co}(1)-drains.

gap spacing	α_{ea}-values according to eqns.					
mm	(1.20)	(1.22)	(1.24)	(1.26)	(1.30)	(1.31)
100,0	1,94	0,744	0,839	0,877	0,755	0,776
80,0	1,81	0,561	0,640	0,656	0,574	0,592
60,0	1,69	0,385	0,449	0,448	0,400	0,412
40,0	1,59	0,218	0,268	0,258	0,235	0,242
20,0	1,54	0,0681	0,104	0,0938	0,0897	0,0897
10,0	1,32	0,00718	0,0361	0,0293	0,0283	0,0283
5,0	0,419	-0,0155	0,00986	0,00589	0,00563	0,00563

eqn. (1.20) of KOZENY (1933) — eqn. (1.26) of ENGELUND (1953)
eqn. (1.22) of Appendix I — eqn. (1.30) of SNEYD (1976)
eqn. (1.24) of KIRKHAM (1950) — eqn. (1.31) of this contribution

The number of gaps, their width and the drain diameter determine the total inlet area. Per unit drain length we have :

$$A_p = \frac{2 \pi R_o \beta_s}{c} \tag{1.108}$$

and eqn. (1.32) can be rewritten as :

$$\alpha_{ep} = \frac{\beta_s}{\pi A_p}\left(\ln \frac{4 R_o}{A_p} - \frac{\beta_s}{2 A_p}\right) \tag{1.109}$$

For a given drain diameter and inlet area, the entrance resistance is mainly determined by the gap width. Doubling the gap width but maintaining the same inlet area results in about doubling the α_{ep}-value.

The number of openings also determines the inlet circumference. Per unit drain length we have :

$$C_p = \frac{4 \pi R_o}{c} \tag{1.110}$$

Substitution of eqn. (1.110) into (1.32) yields :

$$\alpha_{ep} = \frac{2}{\pi C_p}\left(\ln \frac{8 R_o}{C_p \beta_s} - \frac{1}{C_p}\right) \tag{1.111}$$

So, the entrance resistance is mainly determined by the inlet circumference. Both pipe diameter and gap width are less important. For the same inlet circumference, the α_{ep}-value slightly decreases as the gap width increases. For a larger diameter with the same inlet circumference and gap width, a slight increase in entrance resistance results.

4.1.3. Discussion

Comparison of experimental and theoretical results shows that eqn. (1.32) is generally adequate for the calculation of the entrance resistance of drains with continuous circumferential openings and plane boundary conditions.

Although no measurements with arched openings were carried out, comparison of the various theoretical results (tables 1.17 and 1.19) shows that eqn. (1.31) is valid for that case.

From eqn. (1.111), it further follows that the perforation circumference mainly determines the entrance resistance. The effect of pipe diameter and gap width are less important. This is illustrated in fig. 1.32 which gives the relationships, using eqn. (1.32), between α_{ep}-A_p and α_{ep}-C_p for a pipe diameter of 75 mm having different gap widths and spacings.

4.2. *Circular perforations*

4.2.1. The S^1_{cp}-drains

The experimental α_{ep}-values for several perforation diameters are presented in fig. 1.33 and compared with the results of the analytical solution (1.45), for square perforation patterns derived by CAVELAARS (1967). This solution was derived from the theoretical solution (1.43) of ENGELUND (1953) for rectangular patterns. The results are also given in table 1.20. It can be seen that there is good agreement between experimental and theoretical results. For rectangular patterns, the solution (1.43) of ENGELUND (1953) can also be accepted with sufficient accuracy as follows from tables 1.21 and 1.22 which give the α_e-values for a 40 mm drain with 120 and 12 perforations, of 2 mm and 10 mm diameter, per unit of drain length.

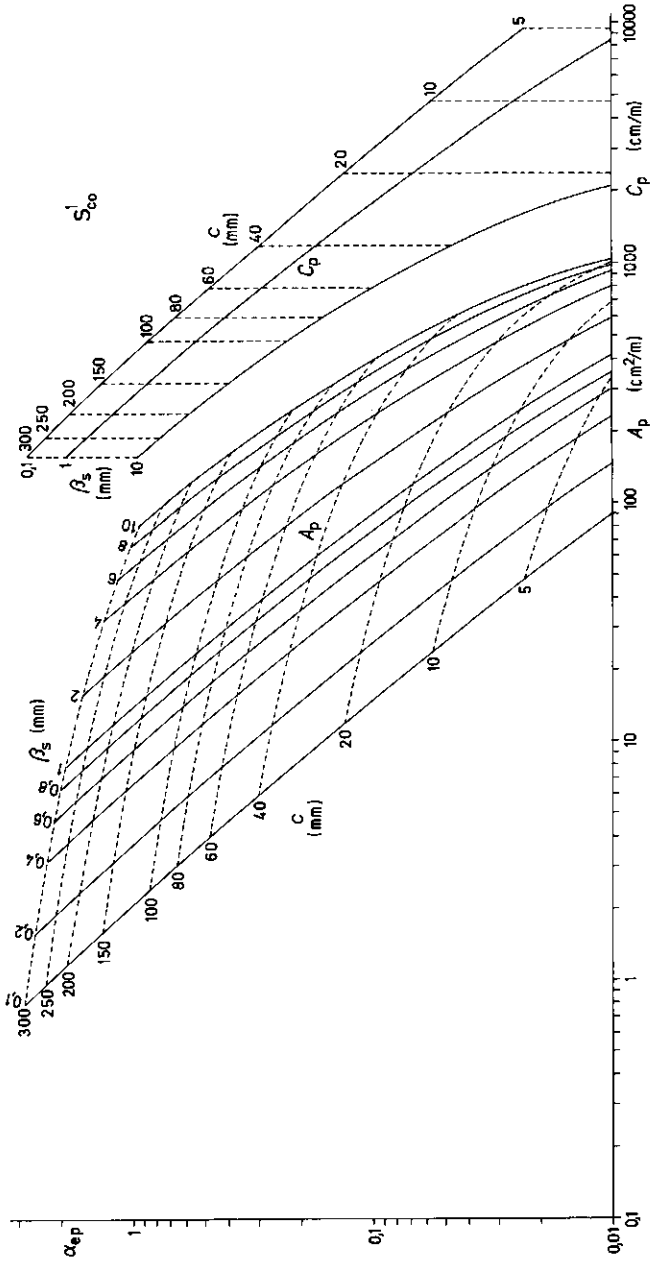

Fig. 1.32. The entrance resistance of 75 mm diameter clay pipes with plane boundary conditions as a function of the inlet area and circumference for different gap widths and spacings.

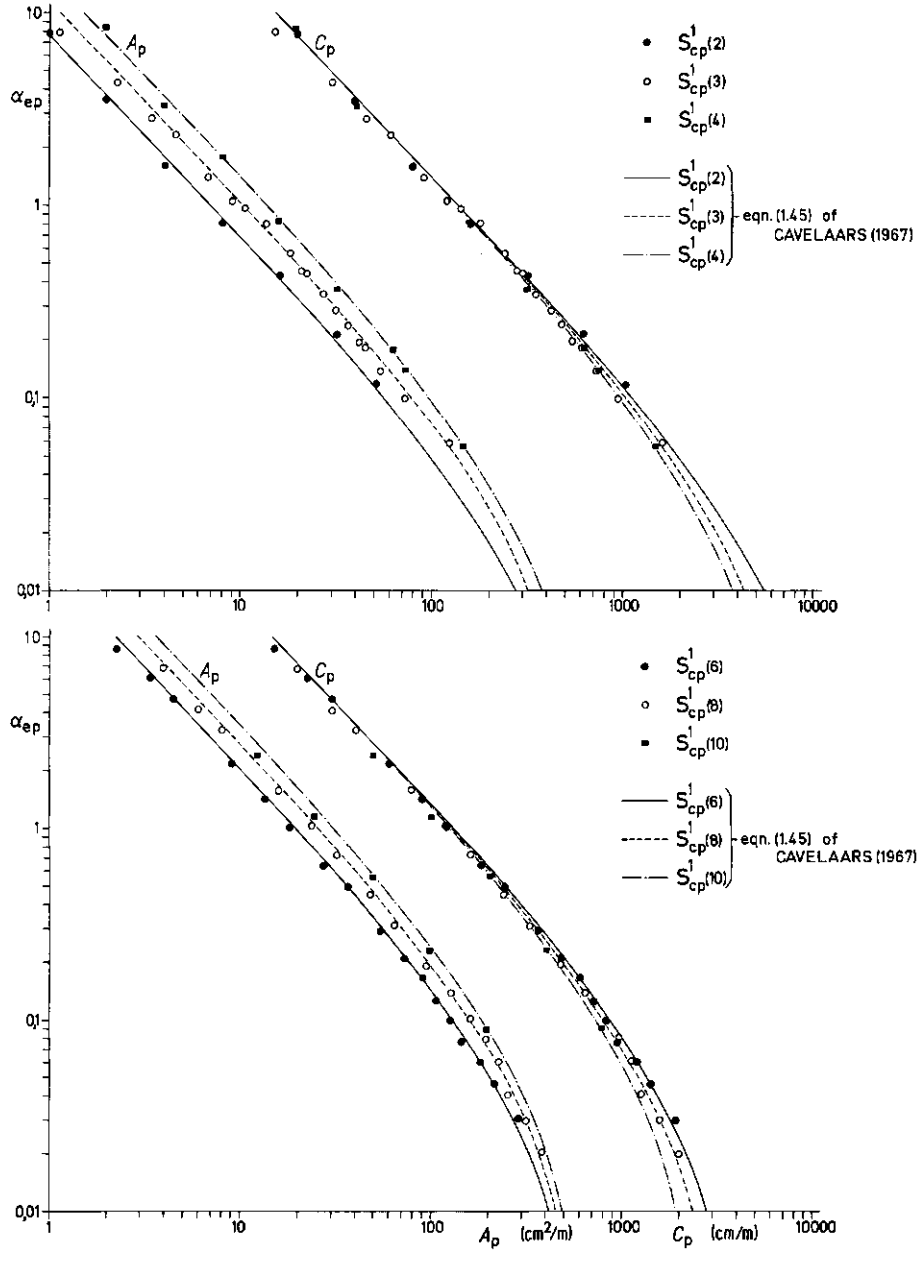

Fig. 1.33. Experimental and theoretical α_{ep}-values as a function of the perforation area A_p and the perforation circumference C_p for a square perforation pattern of circular perforations (R_o = 20 mm).

The α_{ea}-values of table 1.21 result from eqn. (1.44) for a square and from eqn. (1.42) for a rectangular perforation pattern, while the α_{ep}-values of table 1.22 were respectively calculated from eqns. (1.45) and (1.43). Moreover, if $\lambda_2/\lambda_1 \leqslant 2$, it appears that the formulae for a square pattern with the same number of perforations are already sufficiently accurate.

Additionally, the theoretical α_e-values obtained from eqns. (1.38) and (1.40) are presented. Eqns. (1.38) and (1.42) for arched boundary conditions give similar results, while, for plane boundary conditions, the results of eqn. (1.40) largely differ from those of eqn. (1.43). Better agreement is obtained using eqn. (1.41). These results explain why SCHWAB *et al.* (1969) found that the solution of ENGELUND (1953) resulted in a lower drainage performance than that of KIRKHAM & SCHWAB (1951).

MUSKAT (1942) also gives a solution for circular openings, spirally distributed on the drain wall. To find the effect of such a distribution, the results of eqn. (1.38) are compared with the results of the corrected eqn. (1.33) in table 1.23. As long as the perforation spacing in the row is not too large, the spiral and rectangular distribution give about the same results. At large spacings, the spiral distribution is more favourable, as could be expected.

Because of their simple form, eqns. (1.42) and (1.43) of ENGELUND (1953) for a rectangular perforation pattern and eqns. (1.44) and (1.45) of CAVELAARS (1967) for a square perforation pattern are to be preferred.

If eqn. (1.48) is expressed as a function of the perforation area

$$A_p = \frac{\pi \delta_p^2 m}{4} \qquad (1.112)$$

it becomes

$$\alpha_{ep} = \frac{\pi \delta_p}{8 A_p} - \frac{0{,}248}{\sqrt{m R_o}} = \frac{\pi \delta_p}{8 A_p} - \frac{0{,}220 \delta_p}{\sqrt{A_p R_o}} \qquad (1.113)$$

For the same perforation area the α_e-value mainly depends on δ_p; an increasing δ_p results in an increasing α_e-value. The radius of the drain is less important and the α_e-value is only slightly increased with increasing radius.

Table 1.20. Calculated and experimental α_{ep}-values for a square pattern of circular perforations with different diameters (R_o = 20 mm).

Type	Perforation number m^{-1}	Perforation area cm^2/m	Perforation circumference cm/m	α_{ep} exp.	α_{ep} (1.45)
$S^1_{cp}(2)$	32	1,01	20,1	8,9	7,50
	64	2,01	40,2	4,5	3,69
	128	4,02	80,4	2,1	1,80
	256	8,04	160,8	0,98	0,867
	512	16,1	322	0,42	0,411
	1024	32,2	643	0,21	0,189
	1664	52,3	1046	0,12	0,107
$S^1_{cp}(3)$	16	1,13	15,1	7,9	9,98
	32	2,26	30,2	4,3	4,90
	48	3,39	45,2	2,8	3,22
	64	4,52	60,3	2,3	2,38
	96	6,79	90,5	1,39	1,56
	128	9,05	120,8	1,05	1,15
	148	10,46	139,5	0,96	0,982
	192	13,57	181,0	0,80	0,741
	256	18,1	241,3	0,56	0,541
	296	20,9	279,0	0,46	0,461
	320	22,6	302	0,44	0,423
	384	27,1	362	0,35	0,344
	448	31,7	422	0,28	0,289
	512	36,2	483	0,24	0,248
	592	41,8	558	0,20	0,209
	640	45,2	603	0,18	0,191
	768	54,3	724	0,14	0,154
	1024	72,4	965	0,10	0,108
	1760	124,4	1659	0,058	0,0528
$S^1_{cp}(4)$	16	2,01	20,1	8,4	7,37
	32	4,02	40,2	3,3	3,60
	64	8,04	80,4	1,77	1,73
	128	16,08	160,8	0,82	0,821
	256	32,2	321,7	0,36	0,378
	512	64,3	643	0,18	0,166
	592	74,4	744	0,14	0,139
	1184	148,8	1488	0,057	0,0545

eqn. (1.45) of CAVELAARS (1967)

Type	Perforation number m^{-1}	Perforation area cm^2/m	Perforation circumference cm/m	α_{ep} exp.	α_{ep} (1.45)
$S^1_{cp}(6)$	8	2,3	15,1	8,7	9,80
	12	3,4	22,6	6,0	6,44
	16	4,5	30,2	4,7	4,77
	32	9,0	60	2,2	2,29
	48	13,6	90	1,42	1,48
	64	18,1	121	1,00	1,08
	96	27,1	181	0,65	0,689
	128	36	241	0,49	0,496
	192	54	362	0,30	0,307
	256	72	483	0,21	0,216
	320	90	603	0,17	0,162
	384	109	724	0,13	0,127
	448	127	844	0,10	0,103
	512	145	965	0,077	0,0851
	640	181	1208	0,060	0,0607
	768	217	1448	0,047	0,0451
	1024	290	1930	0,030	0,0265
$S^1_{cp}(8)$	4	2,0	10,1	7,4	14,7
	8	4,0	20,1	5,2	7,19
	12	6,0	30,2	3,6	4,70
	16	8,0	40,2	2,6	3,47
	32	16,1	80	1,31	1,64
	48	24,1	121	0,89	1,05
	64	32,2	161	0,72	0,757
	96	48	241	0,45	0,472
	128	64	322	0,31	0,333
	192	97	483	0,19	0,199
	256	129	643	0,14	0,134
	320	161	804	0,10	0,0971
	384	193	965	0,080	0,0731
	448	225	1126	0,060	0,0565
	512	257	1287	0,040	0,0444
	640	322	1608	0,030	0,0282
	768	386	1930	0,020	0,0180
$S^1_{cp}(10)$	16	12,6	50,3	2,4	2,68
	32	25,1	101	1,17	1,25
	64	50	201	0,56	0,562
	128	101	402	0,23	0,235
	256	201	804	0,090	0,0855

Table 1.21. α_{ea}-values for both a square and several rectangular patterns of circular perforations (R_o = 20 mm).

Perforation number m^{-1}	Perforation pattern	Perforation spacings λ_1 mm	λ_2 mm	α_{ea} for δ_p = 2 mm according to eqns. (1.42)	(1.37)	(1.38)	α_{ea} for δ_p = 10 mm according to eqns. (1.42)	(1.37)	(1.38)
120	square	32,4	32,4	1,17	-	-	0,105	-	-
120	2 rows of 60	16,7	62,8	1,23	0,61	1,23	0,165	0,0788	0,158
120	3 rows of 40	25,0	41,9	1,17	0,59	1,17	0,112	0,0551	0,110
120	4 rows of 30	31,4	33,3	1,17	0,58	1,17	0,105	0,0523	0,105
120	5 rows of 24	25,1	41,7	1,17	0,59	1,18	0,112	0,0568	0,114
120	6 rows of 20	20,9	50,0	1,19	0,60	1,19	0,128	0,0655	0,131
120	8 rows of 15	15,7	66,7	1,24	0,62	1,25	0,179	0,0938	0,188
120	10 rows of 12	12,6	83,3	1,31	0,66	1,33	0,252	0,133	0,266
120	12 rows of 10	10,5	100,0	1,40	0,71	1,42	0,342	0,181	0,363
120	20 rows of 6	6,3	166,7	1,88	0,96	1,93	-	-	-
120	40 rows of 3	3,1	333,3	3,61	1,81	3,61	-	-	-
120	60 rows of 2	2,1	500,0	5,78	2,78	5,57	-	-	-
12	square	102,3	102,3	12,8	-	-	2,14	-	-
12	2 rows of 6	62,8	166,7	12,8	6,44	12,9	2,24	1,13	2,27
12	3 rows of 4	41,9	250,0	13,2	6,59	13,2	2,55	1,29	2,58
12	4 rows of 3	31,4	333,3	13,6	6,80	13,6	3,00	1,49	2,99
12	6 rows of 2	20,9	500,0	14,8	7,31	14,6	4,19	2,01	4,01
12	12 rows of 1	10,5	1000,0	19,9	9,29	18,6	9,25	3,99	7,98

eqn. (1.42) of ENGELUND (1953) eqn. (1.37) of MUSKAT (1942)

eqn. (1.38) is eqn. (1.37) corrected by a factor of 2

Table 1.22. α_{ep}-values for both a square and several rectangular patterns of circular perforations (R_o = 20 mm and R = 400 mm).

Perforation number m^{-1}	Perforation pattern	Perforation spacings λ_1 mm	λ_2 mm	α_{ep} for δ_p = 2 mm according to eqns. (1.43)	(1.39)	(1.40)	(1.41)	α_{ep} for δ_p = 10 mm according to eqns. (1.43)	(1.39)	(1.40)	(1.41)
120	square	32,4	32,4	1,92	-	-	-	0,256	-	-	-
120	2 rows of 60	16,7	62,8	1,98	1,24	2,20	1,99	0,317	0,398	0,520	0,309
120	3 rows of 40	25,0	41,9	1,93	1,19	2,12	1,93	0,264	0,359	0,446	0,282
120	4 rows of 30	31,4	33,3	1,92	1,19	2,10	1,92	0,257	0,354	0,437	0,256
120	5 rows of 24	25,1	41,7	1,93	1,20	2,12	1,93	0,264	0,361	0,451	0,265
120	6 rows of 20	20,9	50,0	1,95	1,21	2,15	1,95	0,280	0,375	0,478	0,282
120	8 rows of 15	15,7	66,7	2,00	1,25	2,23	2,01	0,331	0,419	0,567	0,339
120	10 rows of 12	12,6	83,3	2,07	1,31	2,36	2,08	0,404	0,481	0,690	0,418
120	12 rows of 10	10,5	100,0	2,16	1,39	2,51	2,18	0,494	0,557	0,842	0,514
120	20 rows of 6	6,3	166,7	2,84	1,79	3,30	2,68	-	-	-	-
120	40 rows of 3	3,1	333,3	4,38	3,11	5,95	4,37	-	-	-	-
120	60 rows of 2	2,1	500,0	6,55	4,65	9,02	6,33	-	-	-	-
12	square	102,3	102,3	20,3	-	-	-	3,66	-	-	-
12	2 rows of 6	62,8	166,7	20,4	10,4	20,5	20,5	3,76	2,05	3,83	3,78
12	3 rows of 4	41,9	250,0	20,7	10,6	21,0	20,8	4,06	2,29	4,32	4,09
12	4 rows of 3	31,4	333,3	21,2	11,0	21,6	21,2	4,51	2,62	4,97	4,50
12	6 rows of 2	20,9	500,0	22,4	11,8	23,2	22,2	5,72	3,42	6,58	5,53
12	12 rows of 1	10,5	1000,0	27,4	14,9	29,5	26,2	10,8	6,54	12,8	9,49

eqn. (1.43) of ENGELUND (1953)
eqn. (1.39) of KIRKHAM & SCHWAB (1951)
eqn. (1.40) is eqn. (1.39) corrected by a factor of 2
eqn. (1.41) of this contribution, derived from eqn. (1.38)

Table 1.23. Comparison of α_{ea}-values for both rectangular and spiral distributions of the perforations (R_o = 20 mm).

Perforation number m^{-1}	Perforation pattern	Perforation spacing mm	α_{ea} for δ_p = 2 mm according to eqns.		α_{ea} for δ_p = 10 mm according to eqns.	
			(1.38)	(1.33) corrected	(1.38)	(1.33) corrected
120	2 rows of 60	16,7	1,23	1,23	0,158	0,158
120	3 rows of 40	25,0	1,17	1,17	0,110	0,110
120	4 rows of 30	33,3	1,17	1,16	0,105	0,104
120	5 rows of 24	41,7	1,18	1,17	0,114	0,109
120	6 rows of 20	50,0	1,19	1,18	0,131	0,120
120	8 rows of 15	66,7	1,25	1,21	0,188	0,151
120	10 rows of 12	83,3	1,33	1,25	0,266	0,186
120	12 rows of 10	100,0	1,42	1,28	0,363	0,221
120	20 rows of 6	166,7	1,93	1,39	-	-
120	40 rows of 3	333,3	3,61	1,50	-	-
120	60 rows of 2	500,0	5,57	1,52	-	-
12	2 rows of 6	166,7	12,9	12,7	2,27	2,13
12	3 rows of 4	250,0	13,2	12,7	2,58	2,13
12	4 rows of 3	333,3	13,6	12,7	2,99	2,14
12	6 rows of 1	500,0	14,6	12,8	4,01	2,15
12	12 rows of 1	1000,0	18,6	12,8	7,98	2,16

eqn. (1.38) is eqn. (1.37) of MUSKAT (1942) corrected by a factor of 2
eqn. (1.33) of MUSKAT (1942) after correction with a factor of 2

Expressing eqn. (1.48) in terms of the perforation circumference

$$C_p = \pi \delta_p m \tag{1.114}$$

results in

$$\alpha_{ep} = \frac{\pi}{2 C_p} - \frac{0,248}{\sqrt{m R_o}} = \frac{\pi}{2 C_p} - \frac{0,440 \sqrt{\delta_p}}{\sqrt{C_p R_o}} \tag{1.115}$$

From eqn. (1.115) it is clear that the α_e-value is mainly determined by the perforation circumference. For a given drain diameter and perforation cir-

cumference α_e depends only on the number of perforations or the perforation diameter; applying a larger number of perforations, thus a smaller perforation diameter, will increase α_e. This practically means that for a 40 mm diameter drain with 2 mm circular perforations and a perforation circumference of, for instance 300 cm/m, the perforation area amounts to 15 cm^2/m and an α_{ep}-value of 0,443 is obtained. Supposing the same drain with 1 mm circular openings and the same perforation circumference, a perforation area of 7,5 cm^2/m is obtained and an α_{ep}-value of 0,467. This is clearly illustrated in fig. 1.34 which gives α_{ep}-values for a 40 mm diameter drain provided with circular perforations of various diameters in a square pattern as a function of the perforation number m per unit drain length, the perforation area A_p and the perforation circumference C_p.

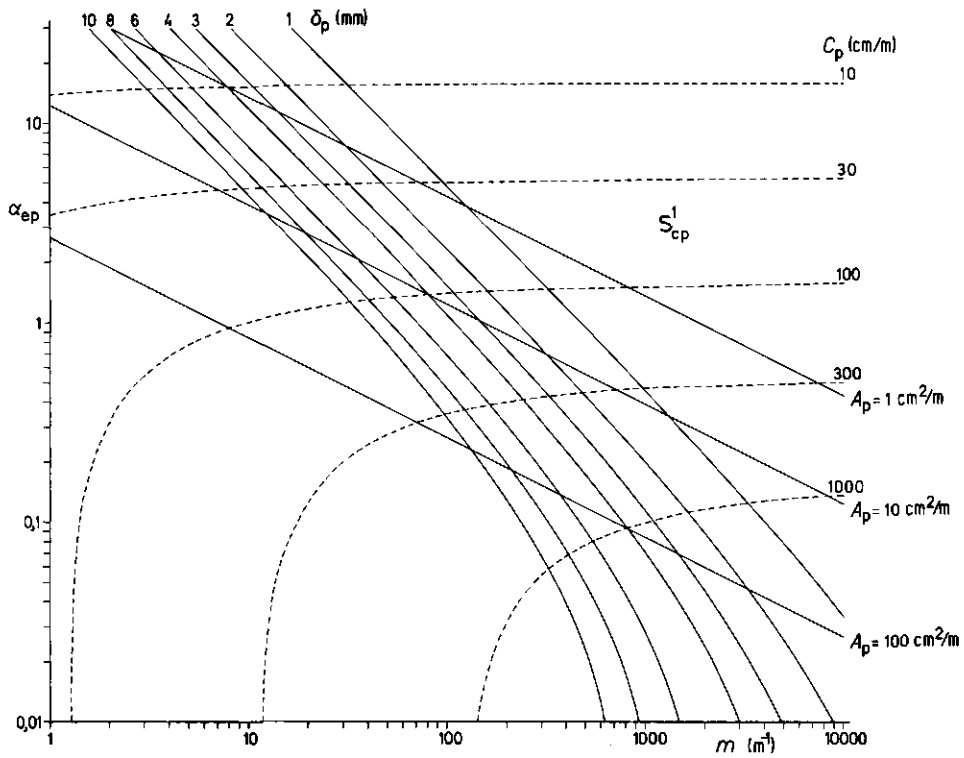

Fig. 1.34. α_{ep}-values for a 40 mm diameter drain with circular perforations of various diameters in a square pattern.

4.2.2. The $S^2_{cp}(3)$-; $S^3_{cp}(3)$-; $S^4_{cp}(3)$-drains

The influence of drain diameter is illustrated in fig. 1.35 and table 1.24. Measured and calculated values agree quite well. From the previously mentioned example in section 4.2.1., an α_{ep}-value of 0.443 was obtained for a 40 mm diameter drain provided with 2 mm diameter perforations in a square pattern and a perforation circumference of 300 cm/m. For the same perforation conditions, the α_{ep}-value is 0,473 for a 100 mm diameter pipe.

Table 1.24. Experimental and theoretical α_{ep}-values for the $S^2_{cp}(3)$; $S^3_{cp}(3)$ and $S^4_{cp}(3)$-drains.

Perforation number m^{-1}	Perforation area cm^2/m	Perforation circumference cm/m	α_{ep}					
			$S^2_{cp}(3)$		$S^3_{cp}(3)$		$S^4_{cp}(3)$	
			exp.	(1.45)	exp.	(1.45)	exp.	(1.45)
16	1,13	15,1	10	10,0	9,0	10,1	9,4	10,1
32	2,26	30,2	4,8	4,93	4,6	4,96	5,0	4,97
64	4,52	60,3	2,5	2,41	2,6	2,43	2,5	2,44
128	9,05	120,6	1,19	1,16	1,17	1,18	1,26	1,18
256	18,1	241,3	0,55	0,553	0,54	0,564	0,61	0,568
512	36,2	483	0,24	0,256	0,26	0,264	0,29	0,267
1024	72,4	965	0,11	0,114	0,12	0,119	0,13	0,121
eqn. (1.45) of CAVELAARS (1967)								

4.2.3. Discussion

For plane boundary conditions, eqns. (1.45) and (1.43), as derived by CAVELAARS (1967) and ENGELUND (1953) for square and rectangular perforation patterns respectively, can be applied with sufficient accuracy. Moreover, eqn. (1.45) can be used for a rectangular distribution provided that $\lambda_2/\lambda_1 \leqslant 2$ and the number of perforations per unit drain length remains constant. Results so obtained differ only slightly from the values which are obtained from the equations for rectangular patterns.

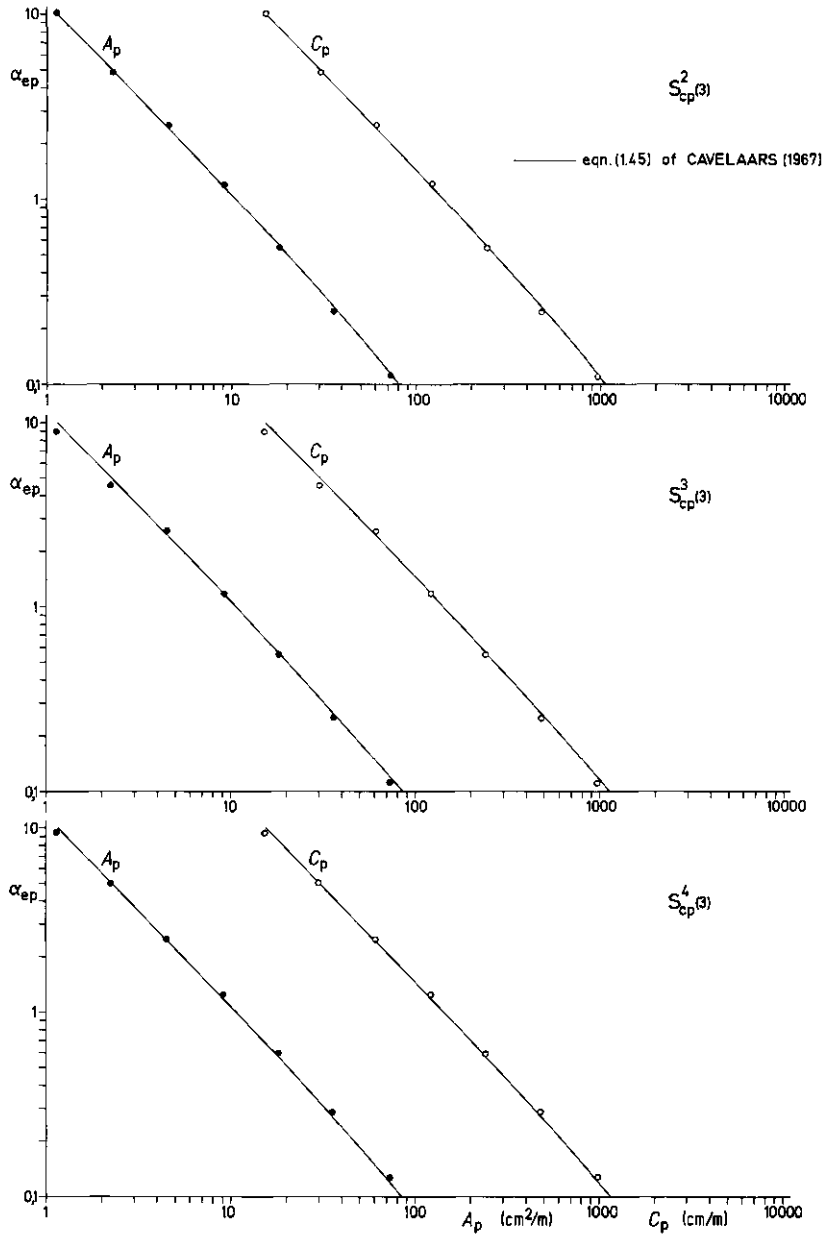

Fig. 1.35. Experimental and theoretical α_{ep}-values for various pipe diameters with circular perforations in a square pattern as a function of the perforation area A_p and the perforation circumference C_p.

From the results of experiments and theoretical equations it can be concluded that the perforation circumference is a better measure for the α_e-value than the perforation area. Both the perforation and drain diameters are less important.

For rectangular perforation patterns and arched boundary conditions eqn. (1.42) and for square perforation pattern eqn. (1.44) hold.

Eqn. (1.37) of MUSKAT (1942) or KIRKHAM & SCHWAB (1951) can also be applied, provided that the correction factor of 2 is employed to result in eqn. (1.38). Its use is likely to be restricted by the complicated mathematical form.

For plane boundary conditions, eqn. (1.39) of KIRKHAM & SCHWAB (1951) does not give good results. Eqn. (1.41) is a better approximation but its use is also likely to be restricted by the complicated mathematical form.

4.3. *Continuous longitudinal slits*

4.3.1. The $S^1_{cls}(1)$-drains

The results of experiments and eqn. (1.51) of ENGELUND (1953) for drain pipes with fictive continuous longitudinal slits and plane boundary conditions are presented in fig. 1.36 and table 1.25. They show that eqn. (1.51) is valid and that increasing the number of slits results in a decrease of the entrance resistance. Slit width and drain diameter only exert a slight influence.

Since the slit area is given by

$$A_p = N \beta_p \tag{1.116}$$

eqn. (1.51) can be rewritten as

$$\alpha_{ep} = \frac{\beta_p}{\pi A_p} \ln \frac{4 R_o}{A_p} \tag{1.117}$$

Hence, it appears that for a given inlet area the slit width exerts an important influence. Doubling β_p in this case results in double the α_{ep}-value because the number of slits is halved.

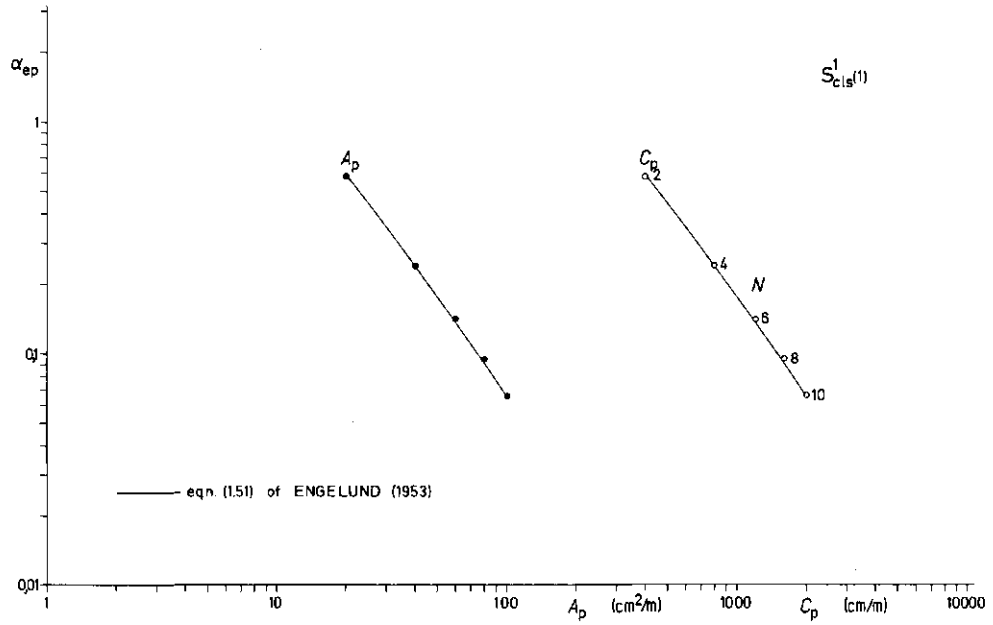

Fig. 1.36. Experimental and theoretical α_{ep}-values for a 40 mm diameter drain with continuous longitudinal slits as a function of the inlet area A_p and the inlet perimeter C_p.

Table 1.25. Experimental and theoretical α_{ep}-values for a 40 mm diameter drain with continuous longitudinal slits.

slit number	inlet area cm^2/m	inlet perimeter cm/m	α_{ep} exp.	α_{ep} (1.51)
2	20,0	400,0	0,57	0,587
4	40,0	800	0,24	0,238
6	60,0	1200	0,14	0,137
8	80	1600	0,095	0,0916
10	100	2000	0,066	0,0662

Eqn. (1.51) of ENGELUND (1953)

If eqn. (1.51) is expressed as a function of the inlet perimeter

$$C_p = 2\,N \tag{1.118}$$

then

$$\alpha_{ep} = \frac{2}{\pi\, C_p} \ln \frac{8\, R_o}{C_p\, \beta_p} \tag{1.119}$$

For a given inlet perimeter and pipe diameter, the slit width becomes less important.

Eqn. (1.119) can also be written as

$$\alpha_{ep} = \frac{2}{\pi\, C_p} \ln \frac{4\, R_o}{N\, \beta_p} \tag{1.120}$$

which indicates that the entrance resistance depends not only on C_p but in a lesser degree on both β_p and N. This conclusion does not have any meaning for continuous longitudinal slits since for a given inlet perimeter, N is fixed. However, it can be of significance for discontinuous longitudinal slits.

These considerations are illustrated in fig. 1.37 which gives α_{ep}-values as a function of the slit width, the inlet area and perimeter.

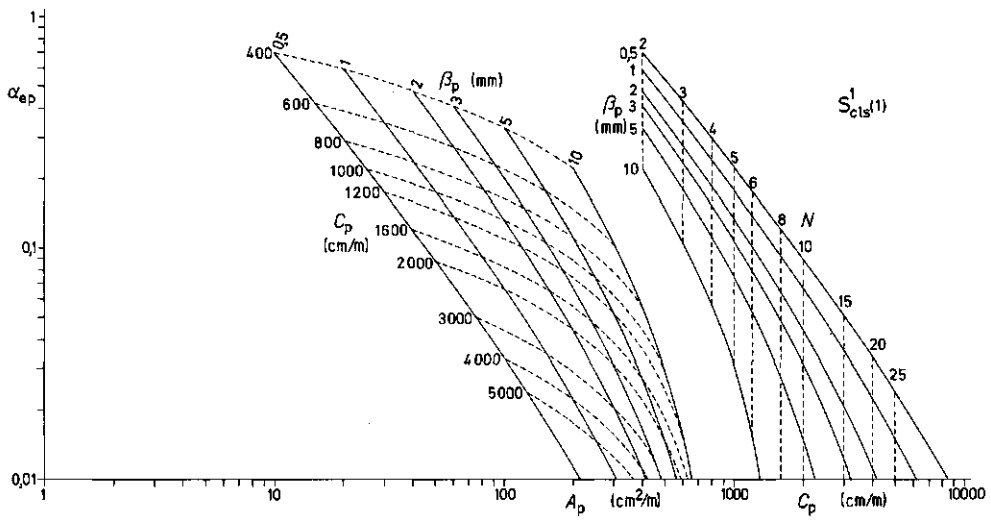

Fig. 1.37. Values of α_{ep} for a 40 mm diameter drain with continuous longitudinal slits as a function of the slit width, the inlet area A_p and the inlet perimeter C_p.

4.3.2. Discussion

For plane boundary conditions, eqn. (1.51) of ENGELUND (1953) can be accepted with sufficient accuracy to calculate the entrance resistance of continuous longitudinal slits. For arched boundary conditions, eqn. (1.52) is valid.

From eqn. (1.119) it follows that the inlet perimeter mainly determines the entrance resistance and renders perforation width and pipe diameter less important.

The solution (1.34) of MUSKAT (1942) for continuous longitudinal slits and arched boundary conditions is, except for a factor of 2, identical with the solution (1.52) of ENGELUND (1953). Since MUSKAT (1942) did not take into account the impervious wall of the pipe, the entrance resistance obtained will be half the correct value.

4.4. *Discontinuous longitudinal slits*

4.4.1. The $S^1_{dls}(1)$-drains

The experimental α_{ep}-values of the $S^1_{dls}(1)$-drains are presented in fig. 1.38a-d related to the inlet area A_p and the inlet perimeter C_p and compared with the theoretical results according to eqn. (1.60) of CAVELAARS (1970). These results are also presented at table 1.26. From the figures and table it may be seen that experimental and theoretical results conform quite well and eqn. (1.60) of CAVELAARS (1970) can be used for calculating the entrance resistance of drains with discontinuous longitudinal slits. A disadvantage of this solution is the rather complicated form of the function $F(\gamma,\epsilon)$. The use of tabular values (see table 1.2) or a graph (see fig. 1.14) simplifies the calculations considerably.

Although this equation is only valid for a rectangular perforation pattern, it can be applied with sufficient accuracy to any distribution pattern which approximates to this.

For arched boundary conditions, eqn. (1.59) can be applied. Table 1.27 gives some α_{ea}-values. In addition, the results obtained from eqn. (1.57) are mentioned. An only approximate agreement can be established.

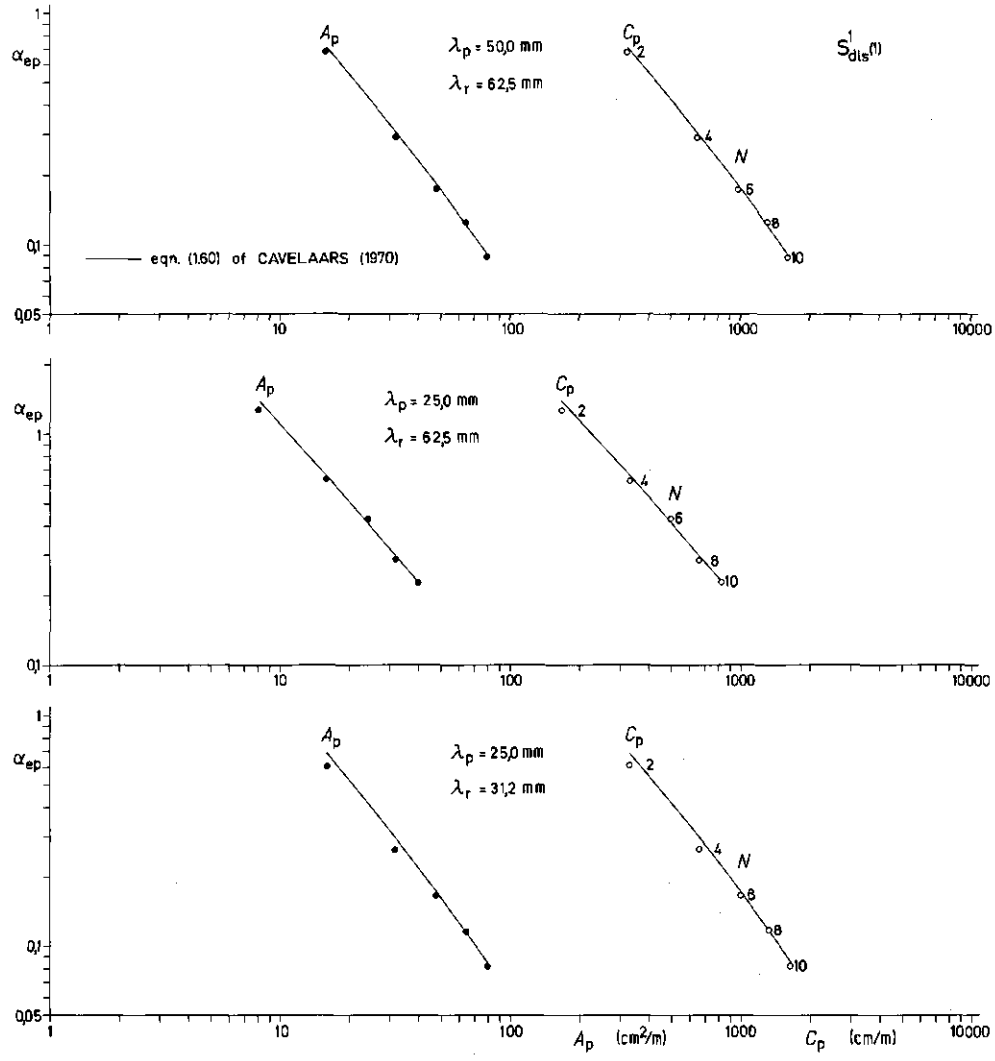

Fig. 1.38a. Experimental and theoretical α_{ep}-values for a 40 mm diameter drain provided with discontinuous longitudinal slits as a function of the inlet area A_p and the inlet perimeter C_p.

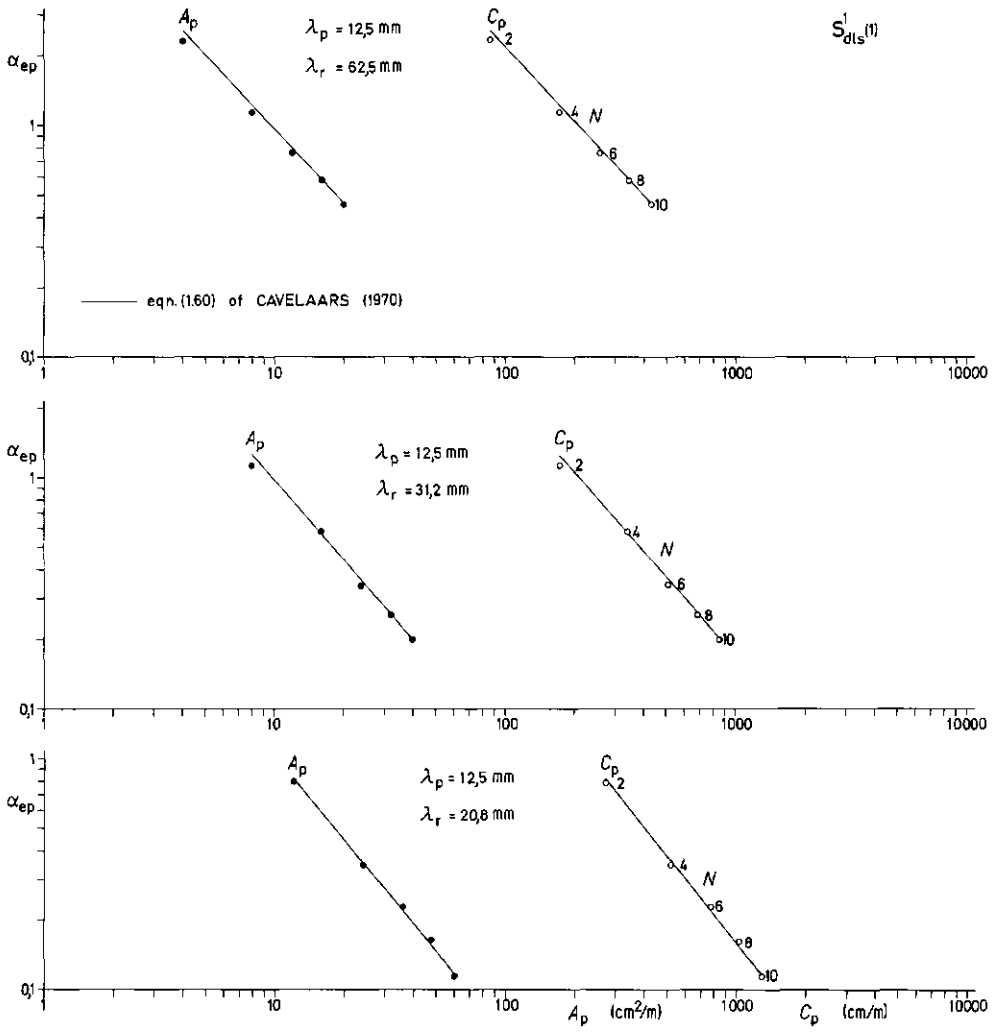
A_p
λ_p = 12,5 mm
λ_r = 62,5 mm
C_p
2
4
N
6
8
10
$S^1_{d(s}$(1)
α_{ep}
eqn. (1.60) of CAVELAARS (1970)
λ_p = 12,5 mm
λ_r = 31,2 mm
λ_p = 12,5 mm
λ_r = 20,8 mm
0,1
1
10
100
1000
10000
A_p (cm²/m)
C_p (cm/m)

Fig. 1.38b.

Table 1.27. Comparison of α_{ea}-values according to several theoretical solutions for $S^{1}_{dls}(1)$-drains.

slit length	slit spacing	α_{ea} for 2 rows					α_{ea} for 4 rows				
mm	mm	(1.59)	(1.57)	(1.64)	(1.66)	(1.68)	(1.59)	(1.57)	(1.64)	(1.66)	(1.68)
50,0	62,5	0,572	0,618	0,562	0,562	0,558	0,231	0,257	0,225	0,226	0,224
25,0	62,5	1,13	1,25	1,09	1,09	1,15	0,510	0,581	0,497	0,489	0,520
25,0	31,2	0,545	0,590	0,535	0,534	0,530	0,217	0,240	0,212	0,212	0,210
12,5	62,5	2,01	2,26	1,94	1,92	2,06	0,949	1,09	0,925	0,907	0,974
12,5	15,6	0,517	0,562	0,509	0,507	0,503	0,203	0,226	0,199	0,198	0,196
5,0	62,5	3,63	4,29	3,59	3,45	3,79	1,76	2,11	1,75	1,67	1,84
5,0	20,8	1,20	1,40	1,16	1,12	1,23	0,543	0,644	0,527	0,505	0,561
5,0	10,4	0,645	0,746	0,634	0,623	0,658	0,268	0,318	0,262	0,256	0,274

slit length	slit spacing	α_{ea} for 6 rows					α_{ea} for 8 rows				
mm	mm	(1.59)	(1.57)	(1.64)	(1.66)	(1.68)	(1.59)	(1.57)	(1.64)	(1.66)	(1.68)
50,0	62,5	0,133	0,154	0,127	0,128	0,128	0,0880	0,107	0,0832	0,0854	0,0843
25,0	62,5	0,318	0,381	0,318	0,305	0,325	0,227	0,290	0,236	0,217	0,232
25,0	31,2	0,123	0,139	0,120	0,120	0,119	0,0811	0,0935	0,0782	0,0785	0,0774
12,5	62,5	0,611	0,722	0,612	0,583	0,628	0,447	0,552	0,466	0,426	0,460
12,5	15,6	0,114	0,129	0,111	0,111	0,109	0,0742	0,0855	0,0721	0,0716	0,0705
5,0	62,5	1,15	1,40	1,17	1,09	1,21	0,853	1,07	0,887	0,807	0,892
5,0	20,8	0,340	0,408	0,330	0,315	0,352	0,244	0,295	0,237	0,225	0,253
5,0	10,4	0,157	0,190	0,153	0,149	0,161	0,108	0,131	0,103	0,100	0,109

slit length	slit spacing	α_{ea} for 10 rows				
mm	mm	(1.59)	(1.57)	(1.64)	(1.66)	(1.68)
50,0	62,5	0,0633	0,0832	0,0589	0,0612	0,0604
25,0	62,5	0,175	0,241	0,190	0,167	0,179
25,0	31,2	0,0578	0,0687	0,0552	0,0557	0,0548
12,5	62,5	0,350	0,457	0,384	0,334	0,361
12,5	15,6	0,0522	0,0614	0,0506	0,0501	0,0493
5,0	62,5	0,675	0,870	0,727	0,741	0,707
5,0	20,8	0,188	0,230	0,183	0,173	0,195
5,0	10,4	0,0778	0,0979	0,0757	0,0733	0,0804

eqn. (1.59) of CAVELAARS (1970)

eqn. (1.57) is eqn. (1.56) of MUSKAT (1942) corrected by a factor of 2

eqn. (1.64) of this contribution, derived from the solution of MUSKAT (1946)

eqn. (1.66) of this contribution, derived from the solution of MUSKAT (1946)

eqn. (1.68) of this contribution, derived from the solution of DE GLEE (1930)

Table 1.28. Comparison of α_{ep}-values according to several theoretical solutions for S^1_{dls}(1)-drains.

slit length	slit spacing	α_{ep} for 2 rows					α_{ep} for 4 rows				
mm	mm	(1.60)	(1.58)	(1.65)	(1.67)	(1.69)	(1.60)	(1.58)	(1.65)	(1.67)	(1.69)
50,0	62,5	0,710	0,756	0,700	0,700	0,696	0,300	0,326	0,294	0,295	0,293
25,0	62,5	1,41	1,53	1,37	1,37	1,43	0,648	0,719	0,634	0,627	0,658
25,0	31,2	0,683	0,728	0,673	0,672	0,668	0,286	0,309	0,281	0,281	0,279
12,5	62,5	2,56	2,81	2,48	2,48	2,61	1,22	1,36	1,20	1,18	1,25
12,5	15,6	0,655	0,700	0,645	0,645	0,641	0,272	0,295	0,268	0,267	0,265
5,0	62,5	5,01	5,66	4,87	4,83	5,17	2,45	2,79	2,39	2,36	2,53
5,0	20,8	1,66	1,85	1,59	1,58	1,69	0,772	0,872	0,741	0,735	0,790
5,0	10,4	0,875	0,973	0,849	0,852	0,888	0,382	0,431	0,369	0,371	0,389

slit length	slit spacing	α_{ep} for 6 rows					α_{ep} for 8 rows				
mm	mm	(1.60)	(1.58)	(1.65)	(1.67)	(1.69)	(1.60)	(1.58)	(1.65)	(1.67)	(1.69)
50,0	62,5	0,178	0,200	0,173	0,175	0,174	0,122	0,143	0,118	0,120	0,119
25,0	62,5	0,410	0,473	0,410	0,397	0,417	0,296	0,359	0,305	0,286	0,301
25,0	31,2	0,169	0,185	0,166	0,166	0,164	0,116	0,128	0,113	0,113	0,112
12,5	62,5	0,795	0,906	0,793	0,767	0,812	0,585	0,690	0,602	0,564	0,598
12,5	15,6	0,160	0,175	0,157	0,157	0,155	0,109	0,120	0,108	0,108	0,105
5,0	62,5	1,61	1,86	1,59	1,55	1,66	1,20	1,41	1,21	1,15	1,24
5,0	20,8	0,493	0,560	0,473	0,468	0,505	0,359	0,409	0,343	0,340	0,368
5,0	10,4	0,233	0,266	0,225	0,226	0,238	0,164	0,188	0,157	0,158	0,167

slit length	slit spacing	α_{ep} for 10 rows				
mm	mm	(1.60)	(1.58)	(1.65)	(1.67)	(1.69)
50,0	62,5	0,0908	0,111	0,0865	0,0888	0,0879
25,0	62,5	0,230	0,296	0,245	0,222	0,234
25,0	31,2	0,0853	0,0963	0,0827	0,0832	0,0824
12,5	62,5	0,461	0,587	0,493	0,444	0,471
12,5	15,6	0,0798	0,0889	0,0778	0,0777	0,0769
5,0	62,5	0,951	1,14	0,984	0,914	0,983
5,0	20,8	0,280	0,321	0,269	0,265	0,287
5,0	10,4	0,124	0,143	0,118	0,119	0,126

eqn. (1.60) of CAVELAARS (1970)
eqn. (1.58) of this contribution, derived from the solution of MUSKAT (1942)
eqn. (1.65) of this contribution, derived from the solution of MUSKAT (1946)
eqn. (1.67) of this contribution, derived from the solution of MUSKAT (1946)
eqn. (1.69) of this contribution, derived from the solution of DE GLEE (1930)

Table 1.29. Comparison of α_{ep}-values for S^{1}_{dis}(1)-drains when $\gamma \rightarrow 1$.

slit length mm	slit spacing mm	slit length / slit spacing	α_{ep}-values for rows of slits according to eqns.													
			2			4			6			8			10		
			(1.60)	(1.70)	(1.120)	(1.60)	(1.70)	(1.120)	(1.60)	(1.70)	(1.120)	(1.60)	(1.70)	(1.120)	(1.60)	(1.70)	(1.120)
50,0	62,5	0,80	0,710	0,623	0,719	0,300	0,256	0,292	0,179	0,149	0,168	0,122	0,100	0,112	0,0908	0,0733	0,0811
25,0	62,5	0,40	1,41	0,733	1,41	0,648	0,311	0,573	0,410	0,186	0,330	0,296	0,128	0,220	0,230	0,0954	0,159
25,0	31,2	0,80	0,683	0,623	0,706	0,286	0,256	0,287	0,169	0,149	0,165	0,116	0,100	0,110	0,0853	0,0733	0,0796
12,5	62,5	0,20	2,56	0,843	2,72	1,22	0,386	1,10	0,795	0,223	0,636	0,585	0,156	0,424	0,461	0,117	0,306
12,5	15,6	0,80	0,655	0,623	0,680	0,272	0,256	0,276	0,160	0,149	0,159	0,109	0,100	0,106	0,0798	0,0733	0,0766
5,0	62,5	0,08	5,01	0,989	6,12	2,45	0,439	2,48	1,61	0,271	1,43	1,20	0,192	0,954	0,951	0,147	0,689
5,0	20,8	0,24	1,66	0,814	2,04	0,772	0,352	0,828	0,493	0,213	0,477	0,359	0,148	0,318	0,280	0,112	0,230
5,0	10,4	0,48	0,875	0,704	1,02	0,382	0,297	0,414	0,233	0,176	0,239	0,164	0,121	0,159	0,124	0,0896	0,115

eqn. (1.60) of CAVELAARS (1970) eqn. (1.70) of KRUIJTZER (1971) eqn. (1.120) of this contribution

Also, the α_e-values increase only slightly when the slit width is doubled. This indicates that the inlet perimeter is more important than the inlet area (fig. 1.39). However, it is evident that the entrance resistance cannot be characterized by the inlet perimeter alone because width, length and spacing of the slits also exert an influence on the entrance resistance.

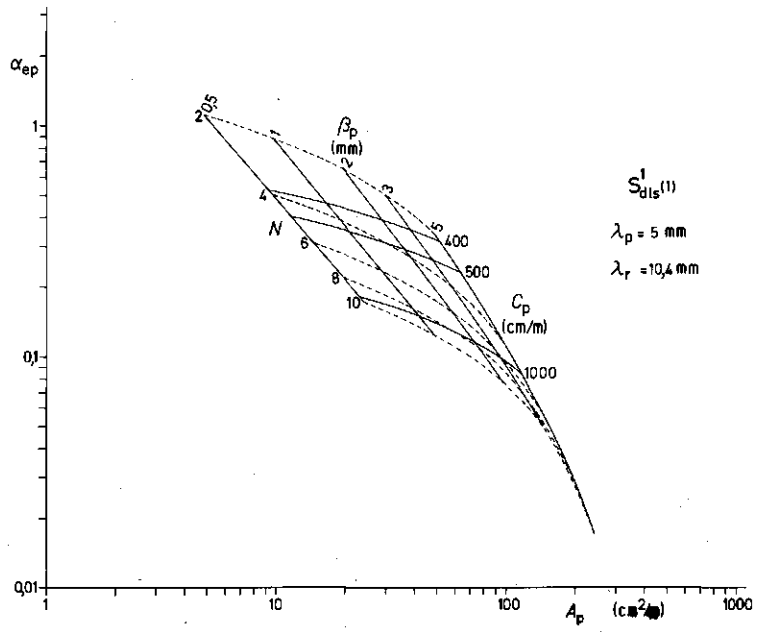

Fig. 1.39. Values of α_{ep} for a drain 40 mm diameter drain provided with discontinuous longitudinal slits as a function of the number of rows N, the slit width β_p, the inlet area A_p and the inlet perimeter C_p.

4.5. *Discontinuous circumferential slits*

4.5.1. The $S^1_{dcs}(1)$-drains

The experimental α_{ep}-values for the $S^1_{dcs}(1)$-drains are shown in fig. 1.40 as a function of A_p and C_p, as are the theoretical results obtained from eqn. (1.76). These results are also given in table 1.30.

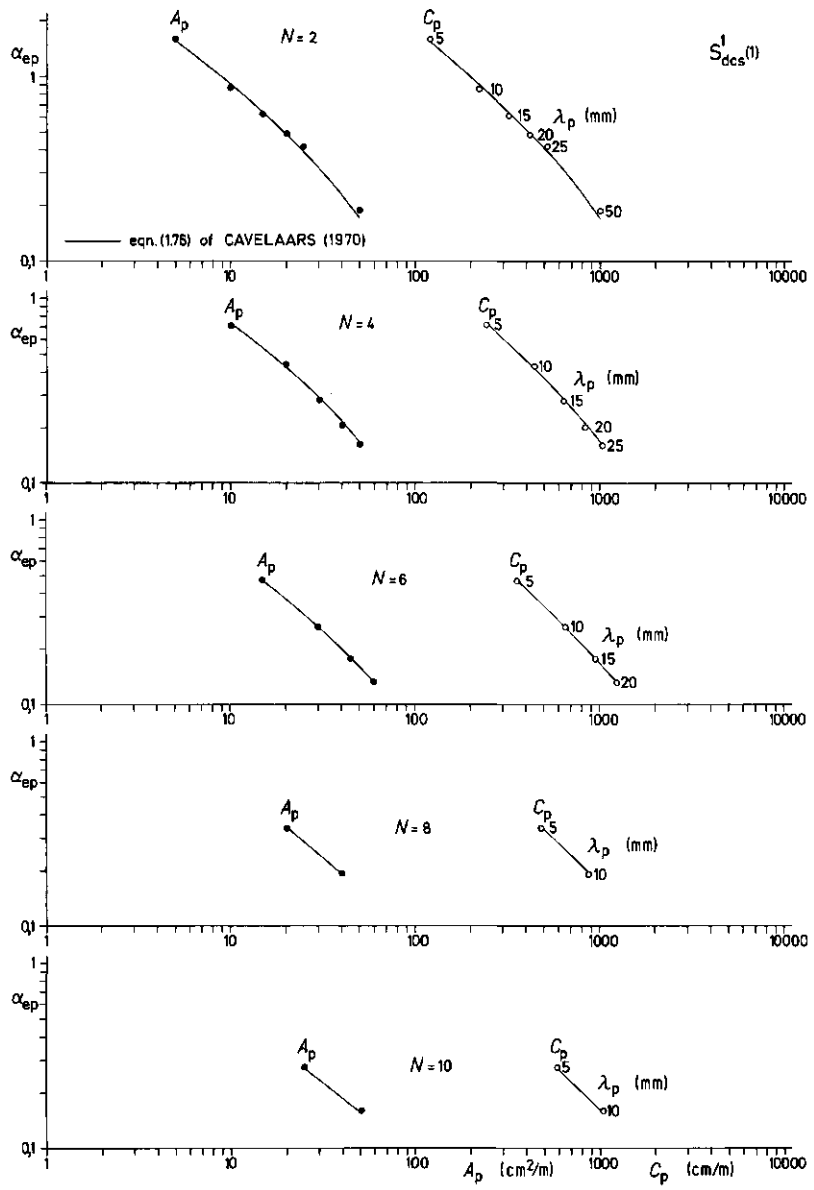

Fig. 1.40. Experimental and theoretical α_{ep}-values for $S^1_{dcs}(1)$-drains as a function of the inlet area A_p and the inlet perimeter C_p.

Table 1.30. Comparison of experimental and theoretical α_{ep}-values for $S^1_{dcs}(1)$-drains.

slit length mm	slit spacing mm	slit length / slit spacing	α_{ep} exp.	α_{ep} according to eqns. (1.76)	(1.81)	(1.83)	(1.85)	(1.86)	(1.121)
5,0	62,8	0,08	1,61	1,55	1,50	1,49	1,60	0,257	1,35
10,0	62,8	0,16	0,87	0,922	0,889	0,886	0,940	0,222	0,736
15,0	62,8	0,24	0,63	0,650	0,626	0,625	0,661	0,201	0,506
20,0	62,8	0,32	0,50	0,493	0,477	0,476	0,502	0,187	0,386
25,0	62,8	0,40	0,42	0,392	0,380	0,376	0,399	0,176	0,311
50,0	62,8	0,80	0,19	0,169	0,166	0,166	0,165	0,140	0,159
5,0	31,4	0,16	0,70	0,736	0,707	0,700	0,755	0,222	0,675
10,0	31,4	0,32	0,44	0,417	0,402	0,401	0,427	0,187	0,368
15,0	31,4	0,48	0,28	0,283	0,272	0,272	0,287	0,166	0,253
20,0	31,4	0,64	0,21	0,207	0,201	0,201	0,208	0,152	0,193
25,0	31,4	0,80	0,16	0,160	0,157	0,157	0,156	0,140	0,156
5,0	20,9	0,24	0,47	0,472	0,452	0,447	0,483	0,201	0,450
10,0	20,9	0,48	0,26	0,260	0,250	0,250	0,264	0,166	0,245
15,0	20,9	0,72	0,18	0,173	0,168	0,168	0,171	0,146	0,169
20,0	20,9	0,96	0,13	0,130	0,131	0,131	0,118	0,131	0,129
5,0	15,7	0,32	0,39	0,342	0,329	0,326	0,352	0,187	0,337
10,0	15,7	0,64	0,19	0,187	0,181	0,181	0,188	0,152	0,184
5,0	12,6	0,40	0,28	0,269	0,258	0,253	0,275	0,176	0,270
10,0	12,6	0,80	0,16	0,148	0,145	0,145	0,144	0,140	0,147

eqn. (1.76) of CAVELAARS (1970)

eqn. (1.81) of this contribution, derived from the solution of MUSKAT (1946)

eqn. (1.83) of this contribution, derived from the solution of MUSKAT (1946)

eqn. (1.85) of this contribution, derived from the solution of DE GLEE (1930)

eqn. (1.86) of KRUIJTZER (1971)

eqn. (1.121) of this contribution.

The results show good agreement and hence eqn. (1.76) can be accepted with sufficient accuracy to calculate the α_{ep}-value for practical purposes. Here, also, the function $F(\gamma,\epsilon)$ can be read from table 1.2 or fig. 1.14 to simplify the calculations.

Although the theoretical solution is only valid for a rectangular perforation pattern, it may be expected that it can be applied with sufficient accuracy to any pattern which approximates to this.

Eqn. (1.74) holds for arched boundary conditions and some calculated results are given in table 1.31.

The results obtained from the other solutions mentioned in section 2.1.5 are also given in table 1.30 for plane and in table 1.31 for arched boundary conditions. Table 1.30 also contains the results obtained from eqn. (1.86) of KRUIJTZER (1971) which is an approximate solution with the condition that $\gamma \to 1$. For this condition, a better approximation is obtained by taking into account the inlet perimeter in eqn. (1.27):

$$\alpha_{ep} = \frac{2}{\pi\, C_p} \ln \frac{2\, e}{\pi\, \beta_s} \qquad (1.121)$$

These results are also given in table 1.30 and better agreement is observeable provided that λ_p and λ_c differ only slightly so that the concentration of streamlines directed to the drain circumference can be omitted. For smaller γ-values, the convergence of the streamlines to the drain circumference becomes important and hence these approximate solutions are no longer valid.

4.5.2. Discussion

Conclusions identical to those drawn for discontinuous longitudinal slits may be made. Eqns. (1.74) and (1.76) are sufficiently accurate, for practical purposes, to determine the entrance resistance of drains with discontinuous circumferential slits. The use of tabular values or a graph to obtain $F(\gamma,\epsilon)$ makes their use quite simple. Additionally, eqns. (1.80) and (1.81) and eqns. (1.82) and (1.83) are also sufficiently accurate but of a rather complicated mathematical form.

Finally, the entrance resistance can also be obtained in a rather simple but sufficiently accurate way, by means of eqns. (1.84) and (1.85).

Table 1.31. Comparison of theoretical α_{ea}-values for S^1_{dcs}(1)-drains.

slit lenght mm	slit spacing mm	α_{ea} according to eqns. (1.74)	(1.80)	(1.82)	(1.84)
5,0	62,8	1,11	1,09	1,05	1,16
10,0	62,8	0,701	0,673	0,665	0,720
15,0	62,8	0,502	0,481	0,478	0,514
20,0	62,8	0,382	0,367	0,366	0,392
25,0	62,8	0,304	0,292	0,288	0,310
50,0	62,8	0,125	0,122	0,122	0,121
5,0	31,4	0,516	0,502	0,480	0,534
10,0	31,4	0,307	0,294	0,291	0,316
15,0	31,4	0,209	0,200	0,199	0,213
20,0	31,4	0,152	0,146	0,145	0,152
25,0	31,4	0,116	0,113	0,113	0,112
5,0	20,9	0,325	0,314	0,300	0,336
10,0	20,9	0,187	0,178	0,176	0,191
15,0	20,9	0,124	0,119	0,119	0,122
20,0	20,9	0,0933	0,0944	0,0944	0,0816
5,0	15,7	0,232	0,226	0,215	0,241
10,0	15,7	0,132	0,127	0,125	0,132
5,0	12,6	0,181	0,176	0,165	0,187
10,0	12,6	0,104	0,102	0,101	0,0999

eqn. (1.74) of CAVELAARS (1970)

eqn. (1.80) of this contribution, derived from the solution of MUSKAT (1946)

eqn. (1.82) of this contribution, derived from the solution of MUSKAT (1946)

eqn. (1.84) of this contribution, derived from the solution of DE GLEE (1930)

4.6. *Corrugated drains*

The theoretical solutions for the entrance resistance only hold for drains with a smooth outside surface. The question arises of whether these solutions can also be applied to corrugated drains for which the corrugations are filled with soil; in other words, has the profile of a corrugated drain a significant effect on the entrance resistance ?

In cases where the corrugated drains have perforations on the top of the corrugations the effect of the corrugations can be neglected and the entrance resistance can be calculated by means of the theoretical equations for drains with a smooth outside surface. However, since corrugated drains usually have perforations in the valleys of the corrugations, it cannot be concluded that the pipe profile does not have any influence.

4.6.1. The C^1_{co}-drain

The influence of the corrugations on the entrance resistance can easily be shown for a corrugated drain with a block wave profile and continuous circumferential openings with a perforation width β_s equal to the valley width β_v, the larger outer radius R_o being 25 mm and the smaller outer radius R'_o being 23 mm.

Eqn. (1.32) holds for S_{co}-drains and plane boundary conditions. For c = 10 mm; β_s = 2,5 mm and $R_o = R'_o$ = 23 mm, an α_{ep}-value of 0,0198 may be calculated. The values obtained with the electrolytic model were 0,060 and 0,056 or as average 0,058. Hence, it is evident that the corrugations exert an influence on the entrance resistance. This entrance resistance results from the concentration of the streamlines towards the corrugations provided with the perforation and in addition the flow resistance of the corrugation filled with soil (fig. 1.41).

Mathematically, it can be written as :

$$\alpha_{ep} = \frac{c}{2\,\pi^2\,R_o}\left(\ln\frac{2\,c}{\pi\,\beta_s} - \frac{c}{4\,\pi\,R_o}\right) + \frac{c}{2\,\pi\,\beta_s}\ln\frac{R_o}{R'_o} - \frac{1}{2\,\pi}\ln\frac{R_o}{R'_o} \qquad (1.122)$$

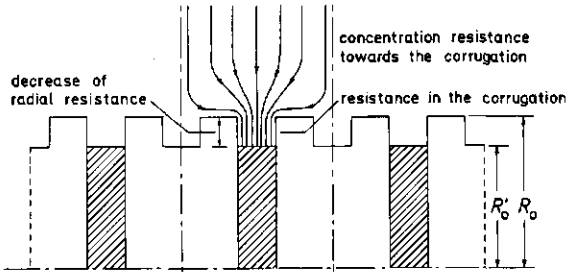

Fig. 1.41. The partial resistances for flow towards a corrugated drain with circumferential openings for which the width equals the corrugation width.

The last term is a correction for the radial flow resistance over the distance $R_o - R_o'$ which does not appear and has to be replaced by the resistance in the corrugation. The α_{ep}-value calculated from eqn. (1.122) amounts to 0,0581 and agrees with the measurements.

For perforation widths smaller than the valley width, the α_{ep}-value is the result of the convergence of the streamlines towards the corrugations with perforations and, in addition, of the convergence of the streamlines in the corrugations towards the perforations (fig. 1.42a). Here also a correction for the radial resistance must be considered. The influence of the convergence of the streamlines, in the corrugation towards the perforation, can be derived from the flow towards a plane plate (fig. 1.42b) with continuous slits and plane boundary conditions (ENGELUND, 1953) for which it holds that

$$h_A - h_C = \frac{q}{\pi k} \ln \frac{2 \sinh \frac{\pi \delta_r}{\beta_s}}{\sin \frac{\pi \beta_s}{2 \beta_v}} \qquad (1.123)$$

$$h_B - h_C = \frac{q}{\pi k} \ln \frac{2 \cosh \frac{\pi \delta_r}{\beta_s}}{\sin \frac{\pi \beta_s}{2 \beta_v}} \qquad (1.124)$$

in which δ_r = corrugation depth
β_v = valley width
β_s = perforation width.

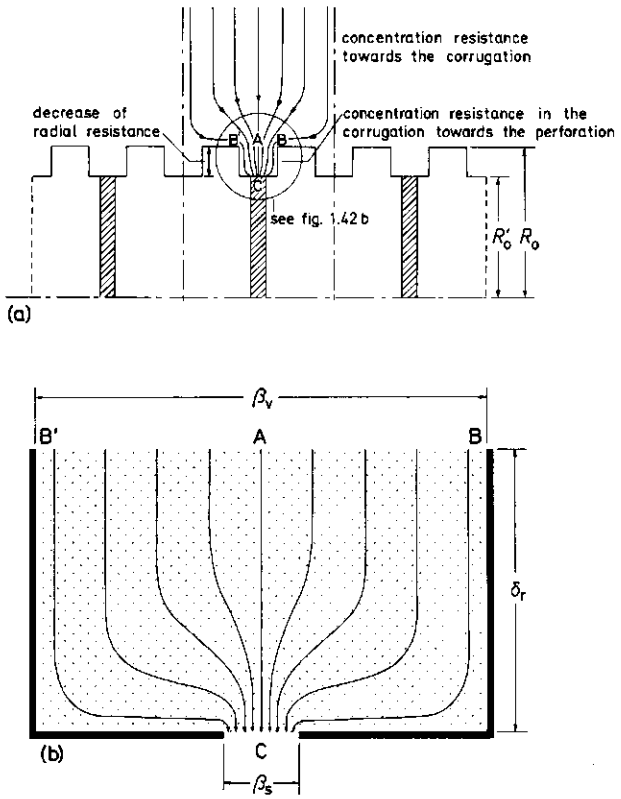

Fig. 1.42a. Corrugated drain with continuous circumferential openings, having a width smaller than the valley width.
b. Convergence of the streamlines towards circumferential openings in the valleys of a corrugated drain.

As h_A and h_B differ only slightly, the mean value can be accepted as an approximation to the hydraulic head at the top BB' between two corrugations, and hence

$$h_{AB} - h_C = \frac{q}{2\,\pi\,k} \ln \frac{4 \sinh \frac{\pi\,\delta_r}{\beta_v} \cosh \frac{\pi\,\delta_r}{\beta_v}}{\sin^2 \frac{\pi\,\beta_s}{2\,\beta_v}} \qquad (1.125)$$

The perforation length per unit drain length is $c/2\,\pi\,R'_o$ and the additional entrance resistance is given by

$$\frac{c}{4\,\pi^2\,R'_o} \ln \frac{4 \sinh \frac{\pi\,\delta_r}{\beta_v} \cosh \frac{\pi\,\delta_r}{\beta_v}}{\sin^2 \frac{\pi\,\beta_s}{2\,\beta_v}} = \frac{c}{4\,\pi^2\,R'_o} \ln \frac{2 \sinh \frac{2\,\pi\,\delta_r}{\beta_v}}{\sin^2 \frac{\pi\,\beta_s}{2\,\beta_v}}$$

The α_{ep}-value for corrugated drains with a rectangular block wave profile and continuous circumferential openings of a width less than the valley width, is given by

$$\alpha_{ep} = \frac{c}{2\,\pi^2\,R_o}\left(\ln \frac{2\,c}{\pi\,\beta_v} - \frac{c}{4\,\pi\,R_o}\right)$$

$$+ \frac{c}{4\,\pi^2\,R'_o} \ln \frac{2 \sinh \frac{2\,\pi\,\delta_r}{\beta_v}}{\sin^2 \frac{\pi\,\beta_s}{2\,\beta_v}} - \frac{1}{2\,\pi} \ln \frac{R_o}{R'_o} \qquad (1.126)$$

The α_{ep}-value so calculated for c = 10 mm; β_s = 1 mm; β_v = 2,5 mm; R_o = 25 mm and R'_o = 23 mm is 0,0721. The experimental values were 0,078 and 0,074 or a mean value of 0,076. Eqn. (1.32), valid for S_{co}-drains, gives a value of 0,0400.

4.6.2. The C^1_{dcs}-drains

No exact solution could be found for discontinuous circumferential slits in the valleys of the corrugations. An approximate solution may be obtained by introducing the perforation length in the expression for the additional entrance resistance, hence we have :

$$\alpha_{ep} = \frac{c}{2\,\pi^2\,R_o}\left(\ln\frac{2\,c}{\pi\,\beta_v} - \frac{c}{4\,\pi\,R_o}\right)$$

$$+ \frac{c}{2\,\pi\,N\,\lambda_p}\ln\frac{2\,\sinh\frac{2\,\pi\,\delta_r}{\beta_v}}{\sin^2\frac{\pi\,\beta_s}{2\,\beta_v}} - \frac{1}{2\,\pi}\ln\frac{R_o}{R_o'} \qquad (1.127)$$

When $2\,\pi\,\delta_r/\beta_v \gg 1$ then $\ln\left\{2\,\sinh(2\,\pi\,\delta_r/\beta_v)\right\} \approx 2\,\pi\,\delta_r$ and eqn. (1.127) becomes :

$$\alpha_{ep} = \frac{c}{2\,\pi^2\,R_o}\left(\ln\frac{2\,c}{\pi\,\beta_v} - \frac{c}{4\,\pi\,R_o}\right)$$

$$+ \frac{c\,\delta_r}{N\,\lambda_p\,\beta_v} - \frac{c}{\pi\,N\,\lambda_p}\ln\sin\frac{\pi\,\beta_s}{2\,\beta_v} - \frac{1}{2\,\pi}\ln\frac{R_o}{R_o'} \qquad (1.128)$$

The α_{ep}-values obtained from eqn. (1.127), the experimental results and the theoretical α_{ep}-values for S_{dcs}-drains calculated by means of eqn. (1.76) are presented in table 1.32. The results obtained for a perforation length of 5 mm and various perforation rows are also presented in fig. 1.43.

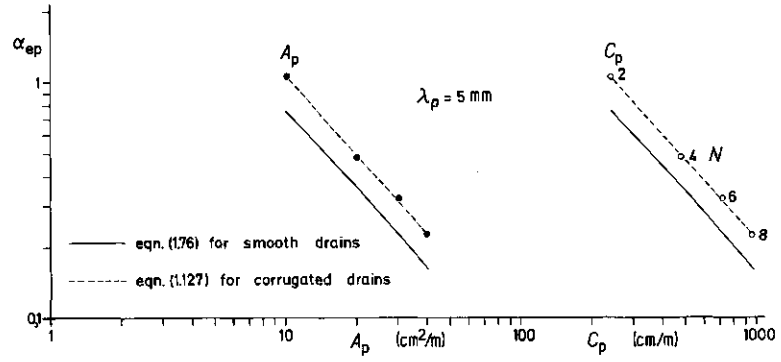

Fig. 1.43. Theoretical and experimental α_{ep}-values for C^1_{dcs}-drains as a function of the inlet area A_p and the inlet perimeter C_p.

Table 1.32. Theoretical and experimental α_{ep}-values for the $C^{1}_{dcs}(1)$-drains.

valley width mm	perforation length mm	row number	α_{ep} exp.	α_{ep} according to eqns. (1.76)	(1.127)
2,50	5,0	8	0,22	0,159	0,247
2,50	5,0	6	0,32	0,223	0,328
2,50	5,0	4	0,48	0,358	0,490
2,50	5,0	2	1,06	0,763	0,974
2,30	4,5	10	0,24	0,133	0,233
2,30	8,1	8	0,17	0,101	0,164
2,30	14,1	6	0,14	0,0796	0,127
2,30	26,1	4	0,11	0,0638	0,104
2,30	62,3	2	0,097	0,0513	0,0883
2,30	9,5	10	0,11	0,0628	0,114
2,30	13,1	8	0,10	0,0580	0,104
2,30	19,1	6	0,10	0,0533	0,0954
2,30	31,1	4	0,091	0,0489	0,0884
2,30	67,3	2	0,082	0,0447	0,0822

eqn. (1.76) of CAVELAARS (1970) for smooth drains
eqn. (1.127) of this contribution for corrugated drains

4.6.3. Discussion

From these considerations it can be concluded that for drain pipes with a rectangular block wave profile a theoretical solution can be obtained for some simple situations like continuous circumferential slits. Such pipes do not have any practical meaning and therefore an approximate solution is given for discontinuous circumferential slits. Moreover, the results clearly show that a rectangular block wave profile exerts an unfavourable influence on the flow towards the drain. Hence, for a given perforation pattern the entrance resistance of corrugated drains will be larger than for drains with a smooth outside surface, provided that the corrugations are filled with soil but, in practice, corrugated drains have far more perforations than smooth ones.

In the case of corrugated drains with a sine wave profile, it may reasonably be suggested that the unfavourable effect will be smaller. Indeed for continuous circumferential openings with β_s = 1 mm and a sine wave profile with a pitch length of 5 mm, a mean α_{ep}-value of 0,069 was obtained from the experiment, this is significantly less than the experimental value of 0,076 for a rectangular block wave profile.

The same can be concluded from the results of BRAVO & SCHWAB (1977). For corrugated drains with a sine wave profile, a pitch length of 12 mm, a radial flow radius R = 381 mm and the following characteristics of the drain: c = 35 mm; β_s = 3 mm; λ_p = 36 mm; N = 5; R_o = 57 mm and R_o' = 51 mm, an α_{ep}-value of 0,201 was obtained. For β_s = 1,6 mm; λ_p = 27 mm but otherwise identical circumstances, α_{ep} = 0,341. Applying eqn. (1.127) for a rectangular block wave profile, for which β_v = 6 mm, results respectively in 0,237 and 0,355.

It can be stated that generally the theoretical formulae to determine the entrance resistance of drains with a smooth outside surface may not be applied to drains with a corrugated outside surface. For a given perforation pattern, corrugated drains possess a higher entrance resistance than smooth drains. For the most unfavourable case of a block wave profile, eqn. (1.127) may be used as an approximation.

5. *Conclusion*

The comparison of theoretical and experimental results confirms that rather simple, and for practical purposes sufficiently accurate, theoretical solutions exist for

- circumferential openings [eqns. (1.31), (1.32)]
- circular perforations [eqns. (1.42), (1.43)]
- continuous longitudinal slits [eqns. (1.51), (1.52)]
- discontinuous longitudinal slits [eqns. (1.59), (1.60) and eqns. (1.68), (1.69)]
- discontinuous circumferential slits [eqns. (1.74), (1.76) and eqns. (1.84), (1.85)].

These theoretical solutions only hold for drains with a smooth outer surface and they may not be applied to drains with a corrugated one. If it is assumed that the corrugations are filled with soil, the entrance resistance depends on the corrugation profile, and for the same perforation pattern it will be larger than for smooth drains. For the most unfavourable case of a block wave profile and plane boundary conditions eqn. (1.127) can be used to obtain an estimate of the entrance resistance.

However the important question is, which perforation shape results in the lowest entrance resistance for a given perforation width or diameter and a given inlet area or perimeter. This is illustrated in figs. 1.44 and 1.45 which give the entrance resistance as a function of the inlet area and perimeter respectively for different perforation shapes. For continuous and discontinuous longitudinal slits, the increase of inlet area and perimeter has been obtained by increasing the number of slit rows; for circular openings, a square perforation pattern has been assumed and the increase was obtained by increasing the perforation number, while for continuous and discontinuous circumferential slits the spacing in the longitudinal direction was varied. For the same inlet area or perimeter and $\delta_p = \beta_p = \beta_s = 1$ mm, it follows that the perforation shape with the smallest area or perimeter and as a consequence the one which is present in the greatest number, is the most favourable. This is the case for both circular and discontinuous longitudinal perforations with the smallest length. This conclusion also holds for discontinuous circumferential slits since the same equations are valid.

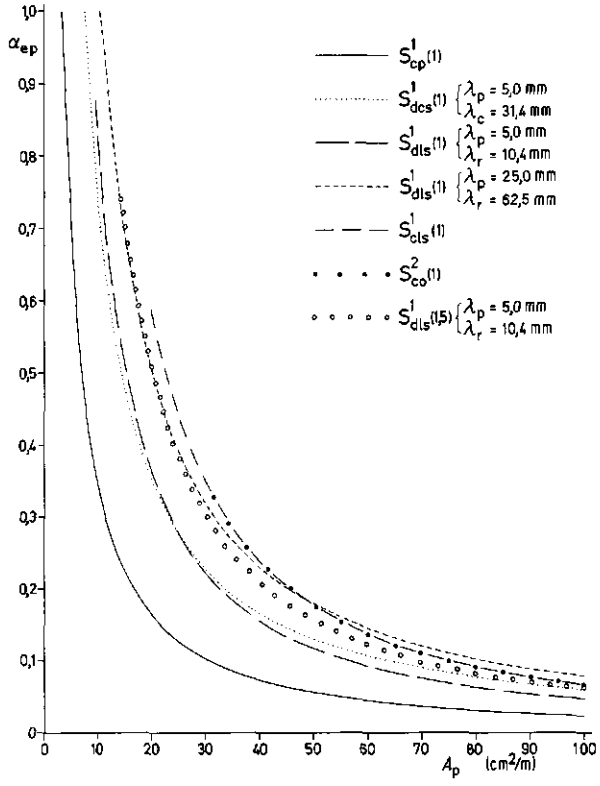

Fig. 1.44. The entrance resistance α_{ep} as a function of the inlet area A_p for different shapes of inlet openings.

The main parameter determining the entrance resistance is the perforation distribution, both the inlet area and perimeter are only of secondary importance. However, the inlet perimeter is more significant than the inlet area since, considering the perforation shape, the difference in entrance resistance is less for a given inlet perimeter than for a given inlet area. This becomes clear by comparing the curves on figs. 1.44 and 1.45 with the same slit length but width of 1 mm and 1.5 mm.

From fig. 1.44 it can be seen that for all perforation shapes, the entrance resistance decreases considerably until a perforation area of about 50 cm^2/m is reached. Increasing the perforation area with about 20 to

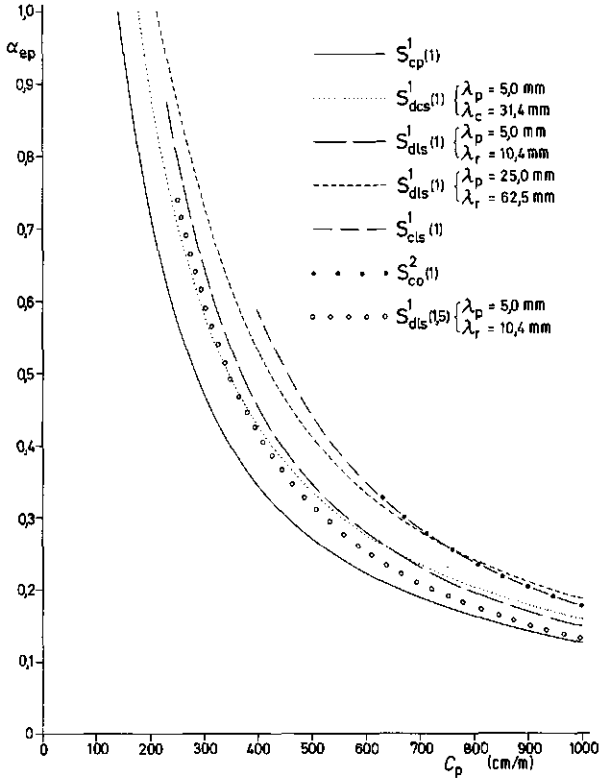

Fig. 1.45. The entrance resistance α_{ep} as a function of the inlet perimeter C_p for different shapes of inlet openings.

25 cm^2/m should result in a lower entrance resistance, except for circular perforations which have a fairly low resistance for all areas greater than about 20 cm^2/m.

In general it may be concluded that the differences in entrance resistance are smaller for a given inlet perimeter than for a given inlet area, regardless of the perforation shape. This conclusion certainly holds for inlet areas smaller than 50 cm^2/m. When the ratio of the perforation width to the perforation length approaches unity, or the greater the subdivision of a given inlet area or perimeter, the smaller the entrance resistance will be.

CHAPTER II

THE ENTRANCE RESISTANCE OF DRAINS SURROUNDED BY PERMEABLE ENVELOPES

---

1. *Theoretical background*

1.1. *Proposition*

Envelope materials are often used as surrounds to drain pipes. The purposes of such envelopes may be to provide adequate bedding for the pipe - in order to increase its crushing strength - or to prevent damage when filling the drain trench. More usually, however, an envelope will be applied to prevent significant soil invasion of the drain and to avoid clogging of the pipe inlets. A further function of envelope materials is to decrease the entrance resistance of drain pipes.

From the investigation performed, it is clear that the entrance resistance of drain pipes depends on the pipe diameter, the perforation shape and the perforation distribution. The total perforation area of commercial drains is only 0,5 to 1 % of the total wall area and in this way entrance resistances of the same order of those due to the whole soil mass can arise (WIDMOSER, 1968). Flow towards the drain pipe mainly depends upon the geometrical relationships in the immediate vicinity of the pipe. Each change in this zone will markedly influence drainage performance.

Granular, organic or synthetic envelopes, having a higher permeability than the surrounding soil, are applied to increase the uptake capacity of drain pipes. The permeability and the thickness of the envelope influences the entrance resistance. In studying these factors, it is supposed that each zone around the drain is homogeneous and isotropic.

1.2. *Effect of envelopes on an ideal drain*

In the case of radial flow towards an ideal drain $\alpha_e = 0$ and $k_e = k$ which means that no envelope surrounds the pipe and only soil is involved.

The total head loss is due only to the radial flow through the porous medium, i.e. soil, and the radial resistance is given by :

$$\alpha_r = \frac{1}{2\pi} \ln \frac{R}{R_o} \qquad (2.1)$$

If an envelope with a thickness $d_e = R_e - R_o$ and a permeability $k_e > k$ surrounds this ideal drain (fig. 2.1), then the radial flow resistance α_{rs} of the soil is given by

$$\alpha_{rs} = \frac{1}{2\pi} \ln \frac{R}{R_e} \qquad (2.2)$$

in which it naturally holds that $R > R_e$. Further, the radial flow resistance α_{re} of the envelope material with a permeability k_e yields :

$$\alpha_{re} = \frac{1}{2\pi} \ln \frac{R_e}{R_o} \qquad (2.3)$$

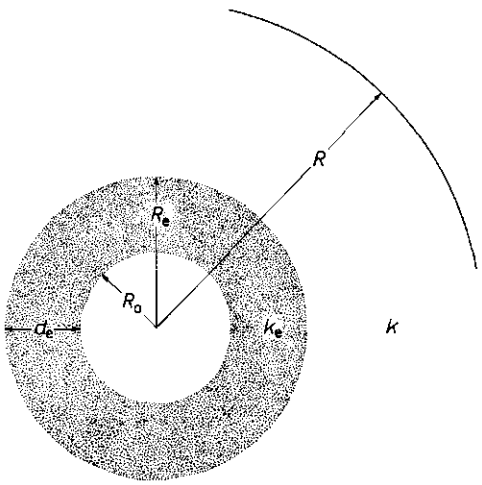

Fig. 2.1. Flow towards an ideal drain surrounded by an envelope.

This α_{re}-value is related to the permeability of the envelope material itself. When the radial resistance is expressed as a function of the permeability of the soil, we get that

$$\alpha'_{re} = \frac{1}{2\pi\kappa_e} \ln \frac{R_e}{R_o} \qquad (2.4)$$

soil and envelope is not exactly an equipotential, but, at a short distance away from the envelope, it may readily be accepted that in the all-round flow case, the equipotentials in the soil form concentric circles (fig. 2.3). It can thus be accepted, as an approximation, that the streamlines are perpendicular to the circumference of the envelope and in the envelope further concentrate towards the perforations in the drain. In the second case the envelope is less thick and does not have a particularly high permeability, consequently the streamlines will start to concentrate towards the perforations while still in the surrounding soil. Because of the difference in permeability, the streamlines are refracted at the soil-envelope interface and further concentrate towards the perforations in the drain pipe.

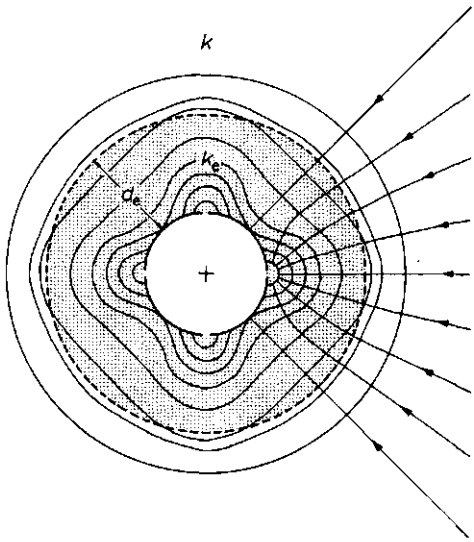

Fig. 2.3. Flow towards a real drain surrounded by a voluminous envelope.

Thus, using a voluminous and high permeable envelope, the circumference of the envelope approximates to an equipotential and the entrance resistance can easily be determined, with the premise that the entrance resistance of the drain surrounded by an homogeneous and isotropic soil is known. This entrance resistance can be calculated from certain formulae or can be determined with the aid of an electrolytic model. When the drain is surrounded by an envelope of permeability k_e, the entrance resistance α'_e related to the

permeability k of the soil is expressed as :

$$\alpha'_e = \frac{\alpha_e}{\kappa_e} \tag{2.8}$$

For drains with continuous longitudinal slits and plane boundary conditions eqn. (1.51) holds and taking into account eqn. (2.8) we thus obtain :

$$\alpha'_e = \frac{1}{\pi N \kappa_e} \ln \frac{4 R_o}{\beta_p N} \tag{2.9}$$

This expression gives the entrance resistance of a drain surrounded by a voluminous envelope of permeability k_e.

In considering the entrance resistance of pipe and envelope, the α_{ee}-value is given by

$$\alpha_{ee} = \alpha'_e + \alpha'_{re} = \frac{1}{\kappa_e}\left(\alpha_e + \frac{1}{2\pi} \ln \frac{R_e}{R_o}\right) \tag{2.10}$$

For an ideal drain $\alpha_e = 0$ and eqn. (2.10) changes into eqn. (2.4). Drains with continuous longitudinal slits and plane boundary conditions yield :

$$\alpha_{ee} = \frac{1}{\kappa_e}\left(\frac{1}{\pi N} \ln \frac{4 R_o}{\beta_p N} + \frac{1}{2\pi} \ln \frac{R_e}{R_o}\right) \tag{2.11}$$

This equation gives the entrance resistance of drain and envelope for the case of drain pipes with continuous longitudinal perforations, the drain being surrounded by a voluminous envelope which forms a plane boundary with the perforations.

The entrance resistance as defined by WIDMOSER (1968) yields :

$$(\alpha_{ee})_W = \frac{1}{\kappa_e}\left(\frac{1}{\pi N} \ln \frac{4 R_o}{\beta_p N} + \frac{1}{2\pi} \ln \frac{R_e}{R_o}\right) - \frac{1}{2\pi} \ln \frac{R_e}{R_o} \tag{2.12}$$

1.4. Discussion

In the case of drain pipes without envelopes, the definition of entrance resistance does not give any particular difficulty. However, when an envelope is used, it must be stated what entrance resistance is desired.

The drain and the envelope can also be considered as a whole and the entrance resistance related to drain and envelope. Indeed, it is that value which is determined in many laboratory investigations and field experiments.

2. *Methods to determine the effect of envelopes*

2.1. *Analytical solutions*

The effect of envelope materials can only be determined theoretically for the case of voluminous envelopes having a sufficient permeability in relation to that of the soil to ensure that the streamlines reach the soil-envelope interface almost perpendicularly. Only in such a case can the entrance resistance be represented analytically, see eqn. (2.8).

No analytical solution exists for thin envelopes and the results of the drainage performance of such materials can only be obtained by numerical solutions and model research.

2.2. *Numerical solutions*

The numerical solution to a given flow problem is obtained by putting the differential equation into finite difference form and finding the potential value at various points throughout the flow region according to the relaxation procedure. Once the potential distribution is known, the discharge can be calculated and from this the entrance resistance can be derived.

This method was applied by WIDMOSER (1968) and NIEUWENHUIS (1976) for the case of a two-dimensional flow towards a drain provided with continuous longitudinal slits surrounded by envelope material. For that purpose, the radial flow has been transformed into parallel flow by means of conformal mapping.

In that way WIDMOSER (1968) found that the streamlines are almost perpendicular and the flux uniformly distributed when $\kappa_e = 10$ and $d_e = 0{,}2\ R_o$. The radial nature of the flux is still small when the drain is provided with only 4 continuous longitudinal slits but it can be improved by applying a larger number of such slits and a thicker envelope, rather than by using a higher permeability of the envelope or by increasing the perforation width. At an envelope thickness $d_e = 0{,}2\ R_o$, a $\kappa_e > 20$ does not appreciably influence the radial flow.

By extrapolating the results for thick envelopes surrounding a drain with discontinuous longitudinal slits in accordance with the results for thin envelopes and continuous longitudinal slits, WIDMOSER (1968) deduced

the effect of drains with discontinuous longitudinal slits surrounded by thin envelopes. He concluded that the effect of the discontinuity of the perforations can be neglected for envelopes with a thickness $d_e = 0{,}2\ R_o$ and $\kappa_e > 100$. A small increase of the uptake capacity is still possible at $\kappa_e > 100$. Voluminous envelopes at thicknesses $d_e = 4\ R_o$ do not give a significant increase of the uptake capacity at $\kappa_e > 100$. For drains with a low entrance resistance (many and favourably distributed perforations) and thin envelopes, κ_e-values larger than 40 and possibly larger than 20 have not much influence on the radial flow pattern. However, a larger κ_e-value is preferred for drains having large entrance resistances surrounded by thin envelopes. The effect of the entrance resistance of commercial drains becomes insignificant for voluminous envelopes at κ_e-values larger than 40. As pointed out by WIDMOSER (1968), envelopes can compensate for entrance resistance and increase uptake capacity to such an extent that it equals that of an ideal drain of larger diameter.

NIEUWENHUIS (1976) arrives at the conclusions that a $\kappa_e > 20$ gives rise to only a very small increase of the R_{ef} of the drain. At constant κ_e-values, an envelope thickness $d_e > 1$ cm gives no further decrease of the true entrance resistance of the pipe. However, the radial resistance will decrease which causes an increase of the effective radius of the drain.

Due to the differences in definition of the entrance resistance, the results of WIDMOSER (1968) and NIEUWENHUIS (1976) differ. However, taking these differences into account, both investigations finally result in analogous conclusions.

2.3. *Sand model*

Sand models have been extensively used to determine and to compare the drainage performance of different drain pipes; also to study the influence of envelope materials on drainage performance.

All those investigations carried out in a sand model confirm that the use of envelope materials results in a considerable reduction of the entrance resistance. After WESSELING & VAN SOMEREN (1972), a thin layer of envelope material can considerably reduce the entrance resistance and, as a consequence, increase the effective radius of the drain. The number, shape and magnitude of the perforations influences the entrance resistance less strongly than does an envelope material. The need for perforation area can be reduced

additional difficulties arising from the different permeabilities which have to be simulated. However, this does not cause insuperable difficulties for thin metallic sheet or conductive paper models; only two-dimensional flow problems can be studied with such analogues.

The use of an electrolytic analogue is difficult since two electrolytes with different conductivities have to be kept separate. The separation can only be achieved by means of a solid wall which is made in such a way that the potential distribution at the interface is transmitted across the wall from one electrolytic liquid to the other. To date, no direct determinations of the entrance resistance of drains surrounded by envelopes have been carried out by means of such a model. RIBBENS (1971) and MANTEI & WINGER (1973) used an electrolytic model to determine the convergence loss (entrance resistance) of drain pipes. For voluminous envelope materials, the permeability of the envelope is determined for certain conditions of uptake capacity and head loss over the envelope (WINGER & RYAN, 1971). Eqn. (2.8) can also be applied to this situation and hence no new information is obtained. Both methods allow the calculation of the permeability (or thickness) of an envelope material which is required with drains of different perforation patterns in order to obtain a given uptake capacity.

3. Experimental research

3.1. Electrolytic analogue and electric equipment

Research on the effect of envelope materials on drainage performance has been carried out with the same equipment used to study the different perforation shapes. The apparatus is detailed in chapter I § 3.1. The only difference that need be noted is the replacement of copper sulphate solution by zinc chloride ($ZnCl_2$), the former resulted in deposits on the separating wall between the two electrolytes which caused concentration changes. This was largely prevented by using zinc chloride.

3.2. Separation of the electrolytes

In simulating radial flow across a soil mass towards a drain surrounded by an envelope, two electrolytes of different specific conductivity, depending on the permeability ratio of envelope to soil, were used. The separation of the electrolytes was achieved by means of a pipe wall consisting of isolated contact points so that the prevailing potentials at the outside were transmitted to the inside of the separating wall.

The separating wall has been formed from textile carding sheet (fig. 2.4) which consists of indiarubber into which short steel wires are inserted. The sheet was mounted between two pipes of appropriate diameters and filled up with a thin liquid epoxy resin which had good adhesive and insulating properties. Once hardened, both pipes were removed and the card-cloth pipe formed was ground off to a thin-walled pipe of which the steel wires formed the isolated contact points (fig. 2.5). One end of the tube was closed in order that the pipe might be filled with electrolytic liquid and to provide a mount for the simulated drain. The whole was put into the electrolytic tank (fig. 2.6) and this filled with an electrolytic liquid of a specific conductivity different to that used for filling the tube.

3.3. Determination of the conductivity ratio of the electrolytes

The ratio of the electrical conductivities of the electrolytes should be the same as the ratio of soil conductivity to envelope conductivity.

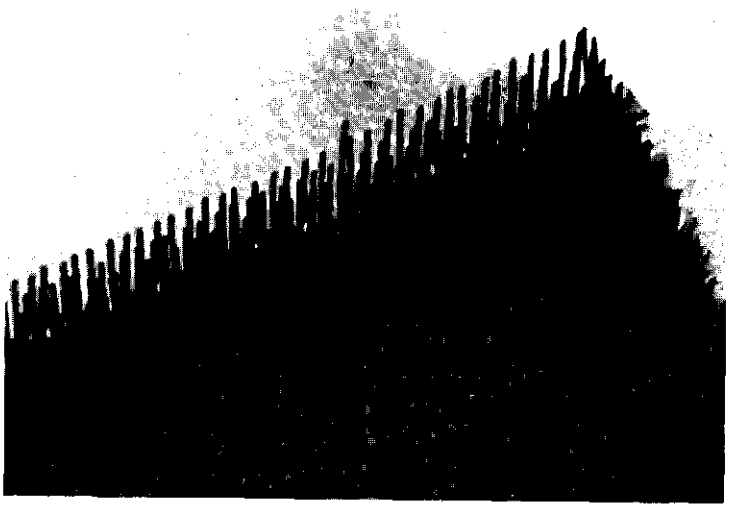

Fig. 2.4. Textile carding sheet consisting of indiarubber into which short steel wires are inserted.

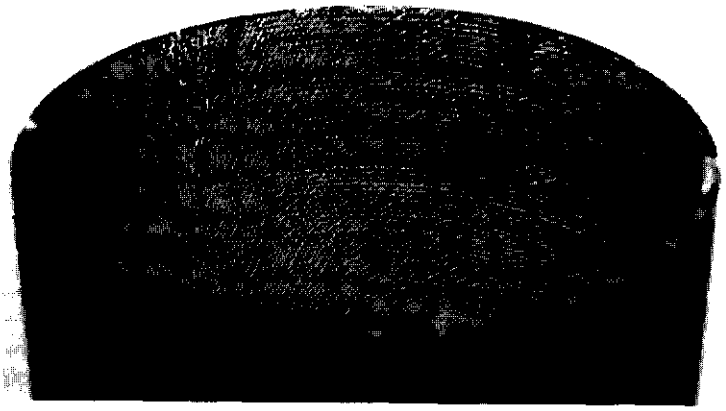

Fig. 2.5. Thin-walled pipe with isolated contact points.

Measurements were made by means of a meter RADIOMETER type COM2 with which the conductivity can be measured from 0 to 500 mS in ranges up to 1,5-5-15-50-150-500 µS and 1,5-5-15-50-150-500 mS. The accuracy amounts to 1 % of the range for 0-50 µS and 0-150 mS and to 2 % for the other ranges. The instrument has to be connected to the mains voltage.

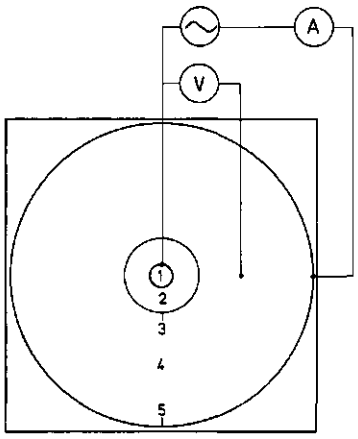

1. Inner electrode, formed by a simulated drain
2. Electrolytic liquid representing the permeability of the envelope material
3. Wall separating the electrolytes
4. Electrolytic liquid representing the permeability of the soil
5. Outer electrode representing a cylindrical equipotential

Fig. 2.6. Schematic representation of the simulation of drain pipes surrounded by envelope materials.

Since temperature exerts an important influence on the conductivity of the electrolytic solutions, the measurements on both liquids were carried out in a room at constant temperature.

3.4. *Simulated problems*

3.4.1. Permeability and thickness of envelopes

The influence of the permeability and thickness of envelopes has been studied for a two-dimensional flow problem. For that purpose the $S^1_{cls}(1)$-drain with 4 continuous longitudinal slits was used.

To study the influence of permeability and thickness of envelopes with three-dimensional flow, the $S^1_{dls}(1)$-drain provided with 4 rows of discontinuous longitudinal slits, each row having 16 slits per meter of drain length, was used. The length of individual slits λ_p was 25 mm.

The permeability ratios κ_e of the envelope to soil were : 1-2-5-10-20-50-100, while various thicknesses d_e of the envelope were simulated by using

a number of separating pipes with isolated contact points (fig. 2.7). The characteristics of these pipes are given in table 2.1.

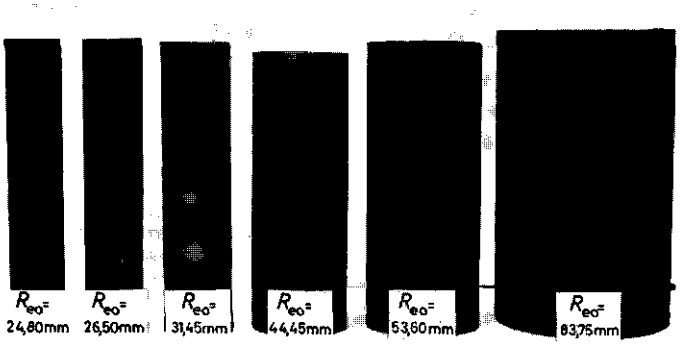

Fig. 2.7. Separating pipes with isolated contact points, used in the simulation of envelope materials.

Table 2.1. Characteristics of pipes acting as a separating wall between two electrolytes of different conductivity.

Inner radius R_{ei} (mm)	Outer radius R_{eo} (mm)	Envelope thickness d_e (mm)
22,85	24,80	2,85
25,30	26,50	5,30
29,95	31,45	9,95
41,15	44,45	21,15
50,60	53,60	30,60
80,55	83,75	60,55

The thickness d_e of the envelope has been determined as the difference between R_{ei} and R_o since the electrolytic liquid representing the envelope is kept in between.

3.4.2. Row number of drains surrounded by envelopes

Besides the $S^{1}_{cls}(1)$-drain with $N = 4$, drains with 2; 6; 8 and 10 continuous longitudinal slits were investigated. There were surrounded by an envelope for which $\kappa_e = 10$, at different thicknesses, as given in table 2.1.

3.4.3. Diameter of drains surrounded by envelopes

Drains with a radius of 25; 30; 40 and 50 mm (fig. 2.8) surrounded by different envelope thicknesses (table 2.2), at a permeability ratio $\kappa_e = 10$, have also been investigated.

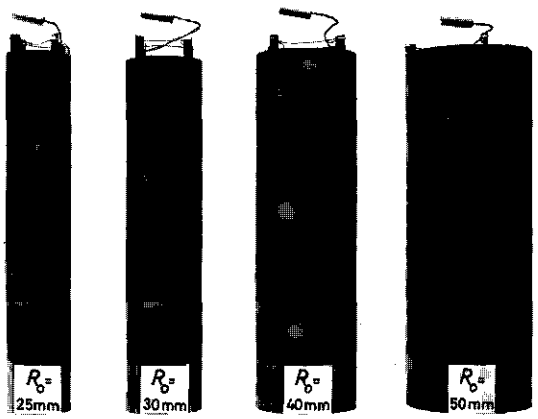

Fig. 2.8. Drains of different diameters provided with 4 continuous longitudinal slits.

3.5. Measurement and calculation method

The measuring technique is identical to the one applied to determine the influence of the perforation shape and distribution (Chapter I, § 3.3).

After mounting the drain model into the separating pipe with isolated contact points, the pipe was filled with the appropriate electrolyte to the same level as the liquid level in the tank. A liquid depth of 250 mm was maintained. Also here 3 x 4 values of the entrance resistance of each simulated situation were determined.

Table 2.2. Details of simulated drains of differing diameters provided with 4 continuous longitudinal slits and surrounded by different envelope thicknesses.

Drain radius R_o (mm)	Radius of the separating pipe R_{ei} (mm)
20	22,85 - 25,30 - 29,95 - 41,15 - 50,60 - 80,55
25	29,95 - 41,15 - 50,60 - 80,55
30	41,15 - 50,60 - 80,55
40	50,60 - 80,55
50	80,55

The potential measurements were carried out between the outside radius R_{eo} of the separating pipe with isolated contact points and the radius R of the cylindrical copper plate representing an equipotential surface. These measured values were graphically plotted against $\ln(R/R_{eo})$. The line of best fit was calculated for the points of the straight section, this being analogous to the method described in Chapter I, § 3.3. The intercept of this straight line on the vertical axis $R/R_{eo} = 1$ gives the required potential V_{ee} to overcome both the extra resistance of the drain model and the electrolytic liquid representing the envelope material (fig. 2.9). The thus obtained entrance resistance α_{ee} is related to drain and envelope. In subtracting the radial flow resistance α'_{re} of the envelope, according to eqn. (2.4), the true entrance resistance α'_e of the drain is obtained.

It may be accepted that the potential is transmitted without appreciable resistance by the isolated contact points. However, the pipe with the isolated contact points introduces an additional entrance and exit resistance (fig. 2.10) which cause deviations of the obtained α_{ee} and α'_e-values. Taking into account these additional resistances and introducing the model thicknesses of the considered soil and envelope layer, eqn. (2.15) changes into

$$\alpha_t = \frac{1}{2\pi} \ln \frac{R}{R_{eo}} + \frac{1}{2\pi\kappa_e} \ln \frac{R_{ei}}{R_o} + \alpha'_e + \beta_{en} + \frac{\beta_{ex}}{\kappa_e} \qquad (2.20)$$

in which β_{en} = the entrance resistance of the separating pipe with isolated contact points

β_{ex} = the exit resistance of the separating pipe with isolated

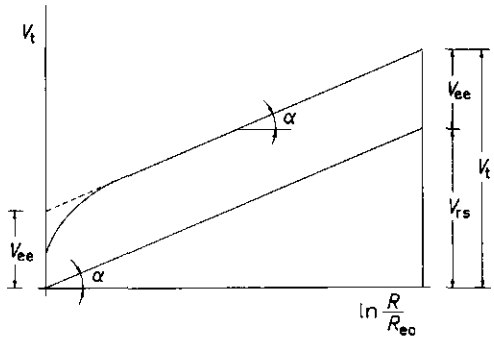

Fig. 2.9. The potential V_{ee} required to overcome both the extra resistance of the drain model and the electrolyte representing the envelope material.

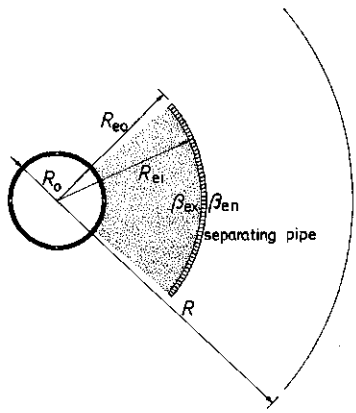

Fig. 2.10. The separating pipe with isolated contact points introduces an additional entrance resistance β_{en} and exit resistance β_{ex}.

The additional entrance and exit resistance are equal and can be calculated from the characteristics of the pipe with isolated contact points by means of eqn. (1.45). The contact points have a circular section with a diameter of 0,25 mm, squarely distributed at 1 mm spacings. The thus calculated β_{en} depends on the pipe diameter and table 2.3 gives the additional resistances of the used pipes. The number of contact points has been calculated by means of the mean radius R_m of the pipe. This table clearly illustrates that the greatest deviations will occur at thin envelope thicknesses with low κ_e-values. Although the influence seems to be small, it is necessary to make corrections in order to reduce the experimental error as the α'_e-values are usually very small when drains are surrounded by an envelope that is more permeable than the soil.

Table 2.3. Additional entrance and exit resistances due to the separating wall with isolated contact points.

R_{ei} mm	R_{eo} mm	R_m mm	m m^{-1}	$\beta_{en} = \beta_{ex}$
22,85	24,80	23,82	149865	0,00921
25,30	26,50	25,90	162734	0,00847
29,95	31,45	30,70	192898	0,00714
41,15	44,45	42,80	268920	0,00512
50,60	53,60	52,10	327354	0,00421
80,55	83,75	82,15	516164	0,00267

3.6. Accuracy of measurements and calculations

The inner and outer diameters of the pipe with isolated contact points were determined by means of a vernier caliber gauge as the mean of 2 measurements on perpendicular axes, to an accuracy of 0,05 mm. Hence, the accuracy of the radius R_{eo} is 0,025 mm. Placing this pipe into the electrolytic tank and placing the drain model into this pipe can cause a deviation of 2 times 0,05 mm or 0,10 mm. Thus, the accuracy of the radius R_{eo} can be estimated at 0,125 mm. Table 2.4. gives the relative errors in R_{eo}.

Table 2.4. Relative error in R_{eo}.

R_{eo} (mm)	24,80	26,50	31,45	44,45	53,60	83,75
$\Delta R_{eo}/R_{eo}$ (%)	0,6	0,5	0,4	0,3	0,3	0,2

The error associated with cylindrical equipotentials was treated in Chapter I, § 3.4. Table 2.5 gives the relative errors in $\ln(R/R_{eo})$.

Table 2.5. Relative error in $\ln(R/R_{eo})$.

R_{eo} (mm)→	24,80	26,50	31,45	44,45	53,60	83,75
R(mm) ↓	$\Delta\left[\ln(R/R_{eo})\right]/\ln(R/R_{eo})$ (%)					
100	0,6	0,5	0,5	0,6	0,7	1,9
200	0,4	0,3	0,3	0,3	0,3	0,4
300	0,3	0,3	0,2	0,2	0,3	0,2
400	0,3	0,2	0,2	0,2	0,2	0,2

Since the output voltage V_t was determined by the characteristics of the L.F. generator used (see Chapter I, § 3.1), an output voltage of 7 V was applied in simulating envelope materials. The accuracy of V_t can be estimated at 0,8 %.

The experimental error in tan α can be derived, according to eqn. (1.106), from the relative error in $V_t - V_t'$ and the relative error in $\ln(R/R')$ which is also 0,2 %.

As V_{ee} is given by

$$V_{ee} = \frac{V_t' \ln(R/R_{eo}) - V_t \ln(R'/R_{eo})}{\ln(R/R')} \qquad (2.21)$$

the relative error in V_{ee} can be derived and, further, the relative error in α_{ee}. Table 2.6 contains some relative errors in α_{ee} depending on the value of V_{ee}.

Table 2.6. Relative errors in α_{ee} as a function of V_{ee}.

V_{ee}	tan α	V'_t	$\frac{\Delta \tan \alpha}{\tan \alpha}$	$\frac{\Delta V_{ee}}{V_{ee}}$	$\frac{\Delta \alpha_{ee}}{\alpha_{ee}}$
V		V	%	%	%
6,0	0,36	6,50	22	4,0	26
5,0	0,72	6,00	11	4,8	16
4,0	1,08	5,50	7,3	6,0	14
3,0	1,44	5,00	5,5	7,5	13
2,0	1,80	4,51	4,4	11	16
1,0	2,16	4,01	3,7	22	26
0,8	2,23	3,91	3,5	28	32
0,6	2,30	3,81	3,4	36	40
0,4	2,37	3,71	3,3	53	57
0,2	2,44	3,61	3,2	104	108

The presence of a highly conductive liquid surrounding the drain model can, in certain situations, result in very low V_{ee}-values for which the relative error in V_{ee} becomes large. Small V_{ee}-values result in small α_{ee}-values and hence the relative error in α_{ee} and also in α'_e will be large as α'_e is given by

$$\alpha'_e = \alpha_{ee} - \frac{1}{2 \pi \kappa_e} \ln \frac{R_{ei}}{R_o} - \beta_{en} - \frac{\beta_{ex}}{\kappa_e} \qquad (2.22)$$

In spite of these theoretically large relative errors, no larger coefficients of variation in relation to the standard deviation s_a and s_b have been noticed and therefore the results were also rounded off to two significant figures.

Besides the factors mentioned in Chapter I, § 3.4, the accuracy further depends on the pipes with isolated contact points and the conductivity stability of the electrolytes during the experiments. These factors are inherent to the experimental research and difficult to take into account. In order to minimize these errors as much as possible, the pipes with isolated contact points were tested before each measurement in a homogeneous electrolyte and the results obtained were compared with the measured α_e-value of the drain model alone. The conductivity stability of the electrolytes was checked by measuring the conductivity before and after each experimental run.

4. *Results and interpretation*

Since it is intended to study the influence of envelope materials on the entrance resistance of the drain, preference was given to the representation of α_e'-values. In order to forestall objections to the use of entrance resistance, the results were also converted to effective radii R_{ef} which allows direct comparison of the real radius with the effective one.

4.1. *Influence of permeability and thickness of envelopes*

The results of the $S^1_{cls}(1)$-drain provided with 4 continuous longitudinal slits are presented at fig. 2.11 as a function of the thickness and the permeability of the envelope material.

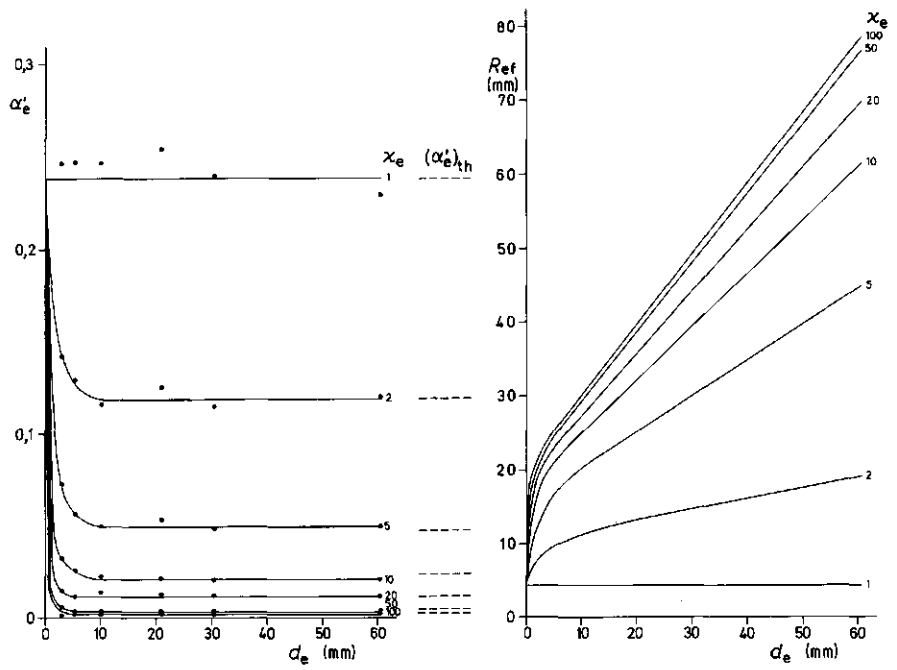

Fig. 2.11. Entrance resistances and effective radii for the $S^1_{cls}(1)$-drain with 4 continuous longitudinal slits as a function of the envelope thickness and its permeability.

4.2. *Influence of row number on drains surrounded by envelopes*

The influence of the number of continuous longitudinal slits for $\kappa_e = 10$ is shown at fig. 2.14. Here also the envelope reduces the absolute differences between the number of continuous longitudinal slits, the relative differences remaining constant.

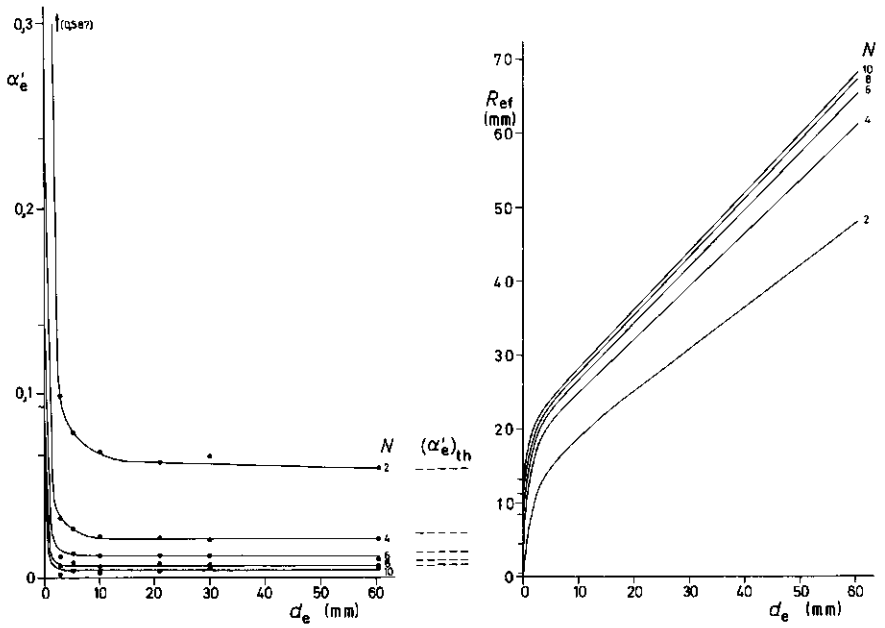

Fig. 2.14. Entrance resistances and effective radii, for the $S^1_{cls}(1)$-drain, as a function of the envelope thickness and the number of continuous longitudinal slits, for $\kappa_e = 10$.

The influence of the number of perforation rows is markedly reduced by applying a sufficiently permeable envelope ($\kappa_e \geqslant 10$) at a thickness $d_e \geqslant 5$ mm (fig. 2.15). At $\kappa_e = 10$, however, there is still a relatively large decrease of the α'_e-value until 4 - 6 perforation rows (fig. 2.16).

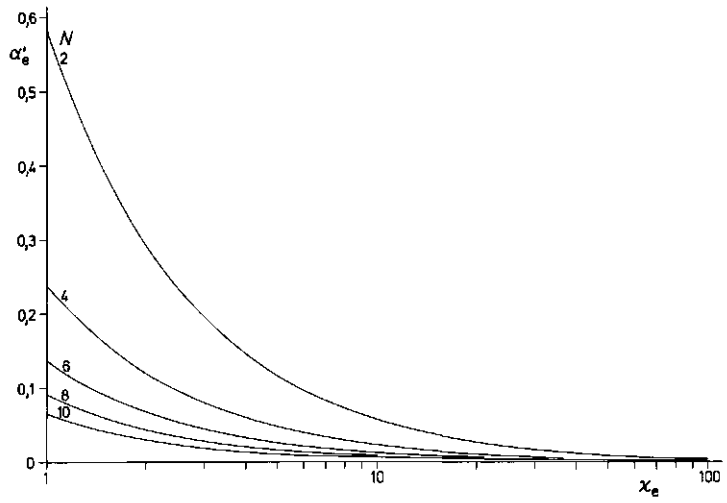

Fig. 2.15. Theoretical α'_e-values as a function of the envelope permeability and the number of continuous longitudinal slits for a $S_{cls}(1)$-drain at an envelope thickness d_e > 10 mm.

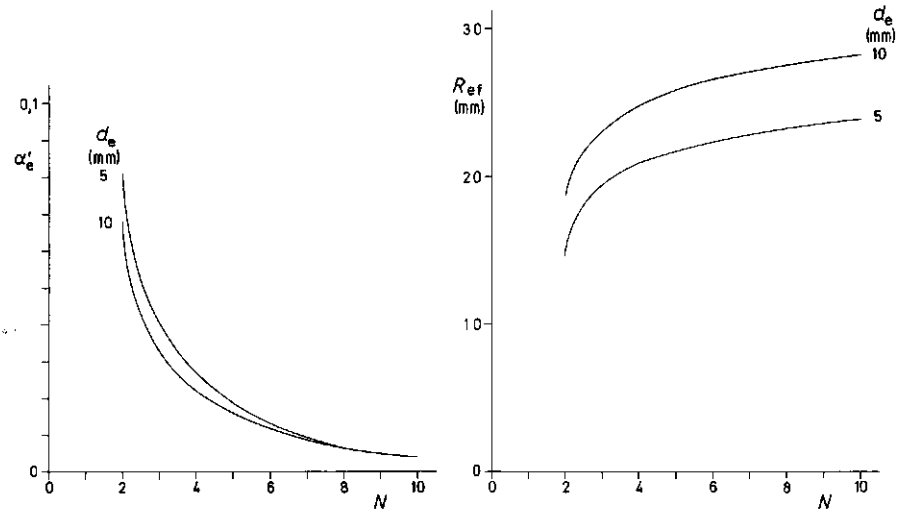

Fig. 2.16. The influence of the number of rows of continuous longitudinal slits on the entrance resistance and the effective radius at κ_e = 10, and for d_e = 5 and 10 mm.

4.3. *Influence of diameter on drains surrounded by envelopes*

From fig. 2.17, it follows that the diameter of a drain pipe which is surrounded by an envelope material does not markedly influence the entrance resistance. The effective radius will differ as well if a same envelope thickness is applied. A constant value of drain radius plus envelope thickness will result in very similar effective radii provided that d_e is at least 5 mm.

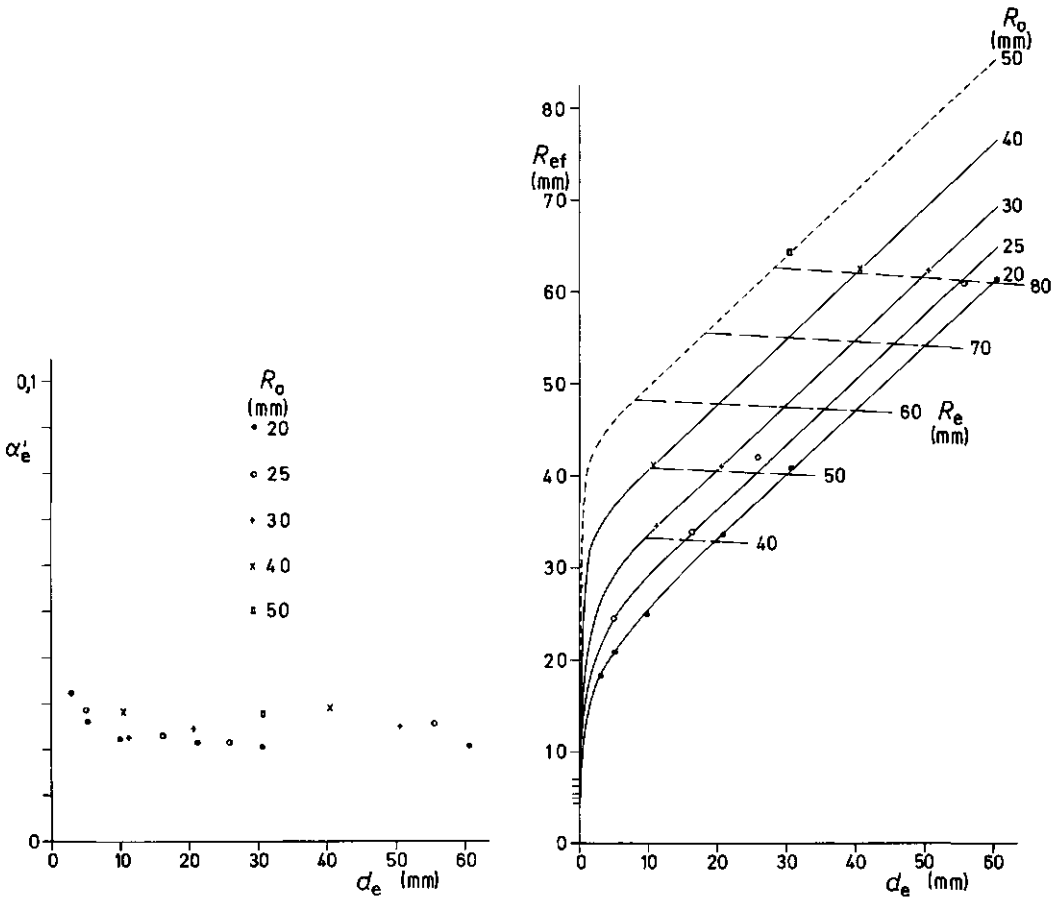

Fig. 2.17. Entrance resistances and effective radii for different pipe diameters provided with 4 continuous longitudinal slits as a function of the envelope thickness d_e at $\kappa_e = 10$.

5. Conclusion

A thin envelope with a permeability which is at least 20 times that of the surrounding soil considerably reduces the entrance resistance; the maximum reduction of the entrance resistance being obtained at a thickness of about 5 mm. A further increase of the thickness does not result in a worthwhile decrease of the entrance resistance. The effective radius, however, continues to increase due to the decrease in radial resistance.

The streamlines approach the envelope almost perpendicularly when $d_e \geq 10$ mm and the drain is provided with 4 perforation rows. It may be accepted for all practical purposes that radial flow occurs when $\kappa_e \geq 10$ and $d_e \geq 5$ mm. Based on these considerations it may be concluded that eqn. (2.8) holds for the case of at least 4 perforation rows with $d_e \geq 10$ mm and that it may be applied with acceptable accuracy when $\kappa_e \geq 10$ and $d_e \geq 5$ mm.

The use of a sufficiently permeable envelope ($\kappa_e \geq 10$) which is adequately thick ($d_e \geq 5$ mm) markedly reduces the influence of both the discontinuity of the perforations and the number of perforation rows.

At constant R_e, the effect of drain diameter is very small as long as d_e is at least 5 mm. To increase the effective radius of a drain, it will be more economical to use a smaller drain diameter with a thicker envelope than a larger diameter with a thinner envelope.

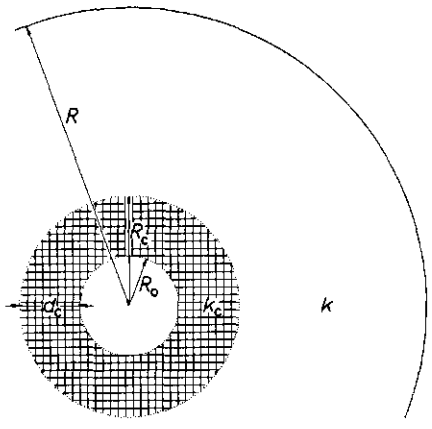

Fig. 3.1. Flow towards an ideal drain surrounded by a layer with a lesser permeability than that of the soil.

Fig. 3.2. illustrates this difference for an ideal drain of 40 mm diameter as a function of the thickness d_c for different permeability ratios κ_c.

1.3. *Influence of partially blocked envelopes on an ideal drain*

The total resistance for the case of radial flow towards an ideal drain surrounded by an envelope with permeability k_e that is partially blocked (fig. 3.3), the blocked part having a permeability k_b, is given by the sum of the radial resistances of the unblocked portion of the envelope, that of the partially blocked portion and that of the surrounding soil :

$$\alpha_t = \frac{1}{2\pi\kappa_e} \ln \frac{R_e}{R_o} + \frac{1}{2\pi\kappa_b} \ln \frac{R_b}{R_e} + \frac{1}{2\pi} \ln \frac{R}{R_b} \qquad (3.7)$$

in which $\kappa_b = k_b/k$ or the ratio between the permeability k_b of the blocked portion of the envelope and the permeability k of the surrounding soil. The difference in radial resistance $\Delta\alpha_r$ between that situation and the situation of radial flow towards an ideal drain in a homogeneous soil, with permeability k, is given by

$$\Delta\alpha_r = \frac{1}{2\pi\kappa_e} \ln \frac{R_e}{R_o} + \frac{1}{2\pi\kappa_b} \ln \frac{R_b}{R_e} - \frac{1}{2\pi} \ln \frac{R_b}{R_o} \qquad (3.8)$$

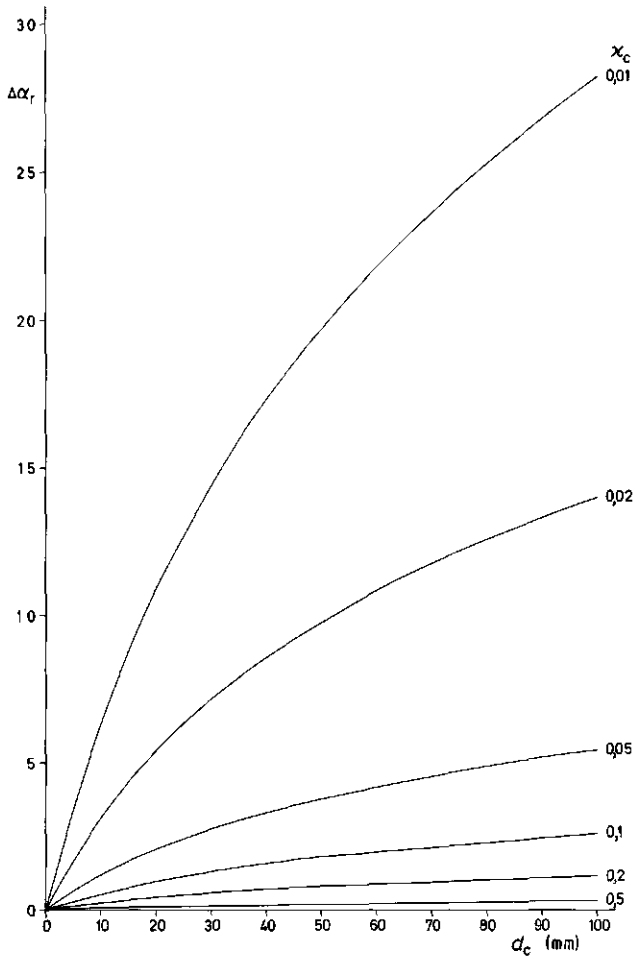

Fig. 3.2. Increase of radial resistance due to a less permeable layer of thickness d_c around an ideal drain of 40 mm diameter.

Fig. 3.4 and fig. 3.5 illustrate these differences for an ideal drain of 40 mm diameter surrounded by envelopes with κ_e = 10 which are partly blocked over respectively 25 and 50 % of the original thickness, the blocked part taking various κ_b-values.

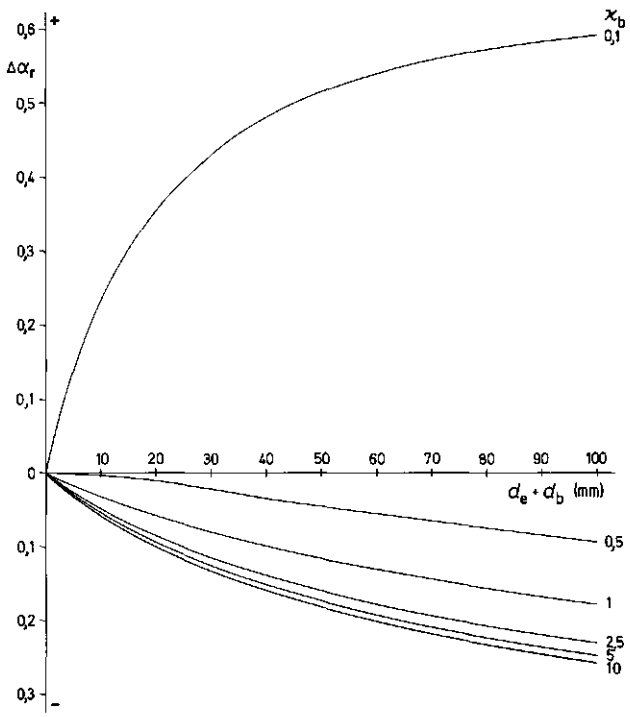

Fig. 3.5. Change in radial resistance of an ideal drain of 40 mm diameter due to an envelope with κ_c = 10 that is blocked over 50 % of its original thickness.

2. *Methods to determine the effect of less permeable surrounds*

2.1. *Analytical solutions*

The effect of a less permeable surround can only be determined theoretically for a thick layer where the streamlines reach the interface of soil and less permeable surround perpendicularly. Due to the refraction of the streamlines into a layer of higher resistance, a slight deviation of the radial approach flow results in an increase of the entrance resistance α'_e.

This also holds for the three-layer problem; a theoretical solution is only possible for very thick envelopes and very thin layers of reduced permeability. If the condition of fully radial approach flow towards the interfaces of the different layers is satisfied, eqn. (2.8) may be used.

2.2. *Numerical solutions*

For the two-dimensional flow problem numerical solutions for drains surrounded by a less permeable layer are given by WIDMOSER (1968) and for drains surrounded by a partially blocked envelope by WIDMOSER (1968) and NIEUWENHUIS & WESSELING (1979).

After the findings of WIDMOSER (1968), a fully radial approach to the interface between soil and a less permeable surround is not reached as quickly as a fully radial approach to the interface between soil and a more permeable surround. A less permeable surround reduces the flux more than a permeable envelope increases it. WIDMOSER (1968) also established that invasion of soil particles into the envelope has less influence on the entrance resistance the more voluminous the envelope is. The effect of soil particle invasion at envelope thicknesses $d_e \geq 4\ R_o$ is negligibly small for thin layers ($d_b \leq 0{,}08\ R_o$) with a reduced permeability $\kappa_b = 0{,}1$.

NIEUWENHUIS (1976) concludes that thin envelopes which are partially blocked give rise to a considerable increase of the entrance resistance at low permeability values of the blocked portion. The influence of envelope blocking on the entrance resistance, as long as approximately 10 mm of the envelope around the pipe remains unchanged, is small compared to the increase in radial resistance, as the effect of such blocking is mainly concentrating on the radial resistance.

2.3. *Sand model*

Although the sand model offers the possibility of building in a less permeable drain surround, few investigations have been carried out, in contrast to the more permeable envelope case. The reason must probably be sought in the fact that less permeable drain surrounds cannot be so easily placed as more permeable ones.

Based on sand model experiments, FEICHTINGER (1966) ascertains that the uptake capacity of drain pipes largely depends on the permeability of the immediate drain surround and, therefore, decreases when the drain is surrounded by a compacted layer.

Model experiments, carried out by CAVELAARS (1962) demonstrated that the installation of drain pipes under wet conditions gives rise to a very marked increase in entrance resistance.

HOMMA (1973) investigated the influence of the conditions in which drains are laid using a vertical model. These experiments clearly demonstrated the importance of this aspects. Drainage under wet conditions can reduce the permeability of the surrounding soil by a factor of 100 which explains how drainage can fail completely under such circumstances. These investigations confirmed that less permeable drain surrounds do exist; but such surrounds are generally not concentric since they consist of consolidated trench backfill.

2.4. *Electric analogue*

For the reason explained in Chapter II, § 2.4, an electric analogue study of less permeable drain surrounds or partially blocked envelopes has not yet been carried out so far.

3. *Experimental research*

3.1. *Electric equipment and separation of the electrolytes*

For this part of the experimental research reference is made to Chapter I, § 3.1. and Chapter II, § 3 since there is no essential difference between simulating a less permeable drain surround or a more permeable envelope.

For the simulation of a partly blocked envelope, two pipes with isolated contact points are concentrically placed around the drain model (fig. 3.6).

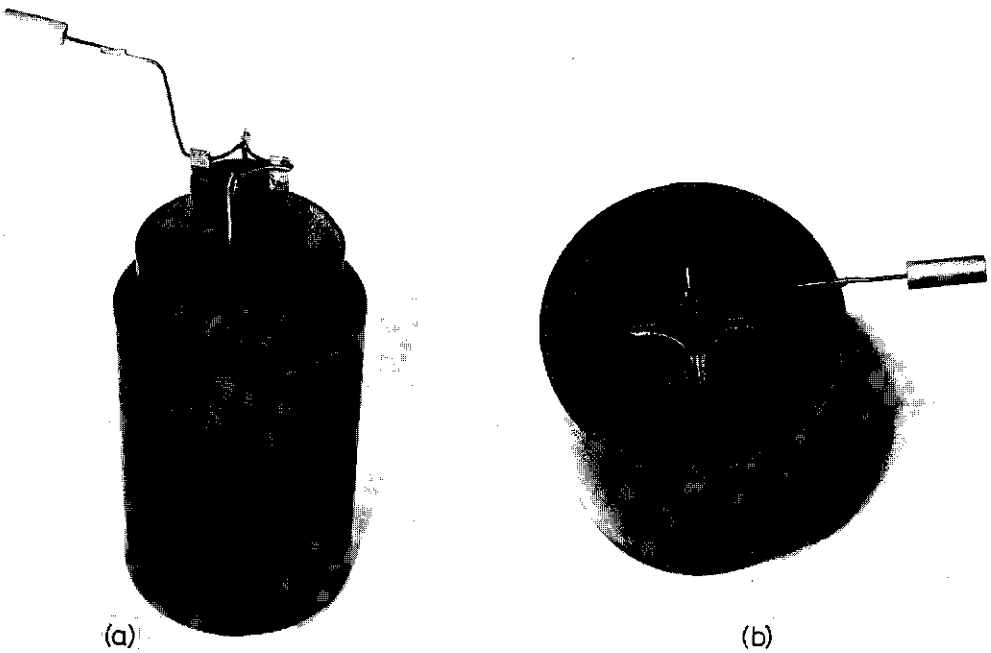

Fig. 3.6. Model to simulate a drain pipe surrounded by partially blocked envelope material.
a. the constituent parts
b. model in use

In that way three electrolytes may be used with the drain model :

- an electrolyte, between the drain model and the inner pipe with isolated contact points, which has a specific conductivity representing

the permeability of the more permeable envelope;

- an electrolyte, between the two pipes with isolated contact points, which has a specific conductivity representing the permeability of the blocked envelope;
- an electrolyte, between the outer pipe with isolated contact points and the cylindrical outer electrode, which has a specific conductivity representing the permeability of the soil.

3.2. *Simulated problems*

3.2.1. Permeability and thickness of less permeable surrounds

These simulated problems are analogous to those for a more permeable envelope. The influence of less permeable drain surrounds with various thicknesses and different permeabilities has been studied at the $S^1_{cls}(1)$-drain with 4 continuous longitudinal slits. The permeability ratios κ_c studied were 0,5; 0,2; 0,1; 0,05; 0,02 and 0,01 while the thicknesses investigated correspond to those of table 2.1. The only difference is that the index e is changed into c. Here, also, the difference between R_{ci} and R_o is the thickness d_c of the less permeable drain surround.

The influence of the number of perforation rows was also investigated for drains surrounded by a less permeable layer. The $S^1_{cls}(1)$-drain provided with 2; 4; 6; 8 and 10 continuous longitudinal slits at various thicknesses of the less permeable drain surround, as given in table 2.1, was used.

Further, the influence of the diameter of drains surrounded by a less permeable layer, has been studied. The situations simulated correspond to those of the more permeable envelopes and are given in table 2.2.

3.2.2. Partially blocked envelopes

The simulation of partially blocked envelopes has been carried out for blockage of a quarter (25 %) and a half (50 %) of the original envelope thickness. The original permeability κ_e of the envelope was 10 while the permeability ratios κ_b of the partially blocked envelope took values of 10; 5; 2; 1; 0,5 and 0,1. The value $\kappa_b = 10$ was included in the measuring programm in order to investigate the influence of the two concentric pipes with isolated contact points. Indeed, the results obtained should correspond with

the results given in Chapter II, § 4.1. Here also, the model drain is the S^1_{cls}(1)-drain with 4 continuous longitudinal slits. The characteristics of the pipes with isolated contact points are given in table 3.1. Only the electrolytes, which are associated with a thickness d_e of original permeability and a thickness d_b of reduced permeability, are considered since pipes with isolated contact points do not have a significant resistance.

In simulating a partially blocked envelope, a filling height of only 125 mm was maintained in the electrolytic tank.

Table 3.1. Characteristics of the pipes with isolated contact points used in the simulation of a partially blocked envelope; for the symbols used, see fig. 3.7.

R_{ei}/R_{eo}	R_{bi}/R_{bo}	d_e	d_b	$d_e + d_b$	d_b
mm	mm	mm	mm	mm	%
22,50/24,50	25,30/26,50	2,25	0,75	3,00	25,0
25,95/27,95	29,95/31,45	5,95	2,00	7,95	25,2
29,30/31,30	34,40/36,40	9,30	3,10	12,40	25,0
34,35/36,35	41,15/44,15	14,35	4,80	19,15	25,1
41,45/43,45	50,50/53,60	21,45	7,10	28,55	24,9
21,65/23,65	25,30/26,50	1,65	1,65	3,30	50,0
24,00/26,00	29,95/31,45	4,00	3,95	7,95	49,7
26,20/28,20	34,40/36,40	6,20	6,20	12,40	50,0
29,60/31,60	41,15/44,15	9,60	9,55	19,15	49,9
34,30/36,30	50,60/53,60	14,30	14,30	28,60	50,0

3.3. Measurement and calculation method

For the less permeable drain surrounds, reference should be made to Chapter II, § 3.5. For partially blocked envelopes, the potential measurements are carried out from the outer pipe with isolated contact points to the cylindrical outer electrode. The values obtained were then plotted as a function of $\ln(R/R_{bo})$. The intercept of the straight line through the measured points on the vertical axis $R/R_{bo} = 1$ gives the potential required to overcome the resistance of the electrolyte representing the blocked part of the envelope, the resistance of the electrolyte representing the envelope,

the soil already causes a large increase in entrance resistance. A further decrease of κ_c leads to a considerable increase of the entrance resistance and to extremely small effective radii.

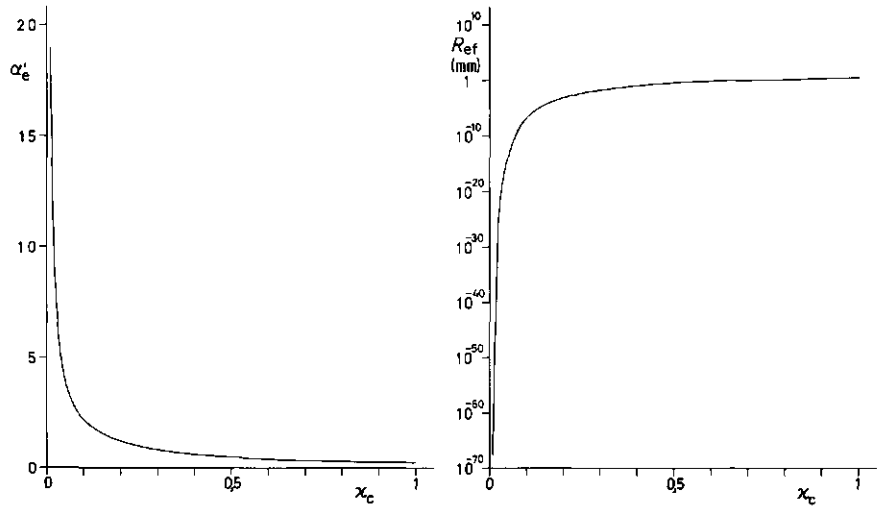

Fig. 3.9. The influence of the permeability κ_c on the entrance resistance and effective radius at a thickness d_c = 10 mm.

4.2. Influence of row number for drains surrounded by a less permeable layer

The influence of row number on drains surrounded by a layer with κ_c = 0,1 is shown in fig. 3.10. This influence is strongly accentuated if the less permeable drain surrounds have values of $\kappa_c \leq 0{,}1$ at thicknesses $d_c \geq 10$ mm (fig. 3.11). However, the increase of the entrance resistance is limited if the drain is provided with at least 4 to 6 perforation rows (fig. 3.12).

4.3. Influence of diameter for drains surrounded by a less permeable layer

As with the more permeable envelopes, pipe diameter does not influence the entrance resistance to any great extent (fig. 3.13). Nevertheless, this does result in small effective radii for the $S^1_{cls}(1)$-drain with 4 continuous longitudinal slits at κ_c = 0,1. Contrary to the more permeable envelopes, a larger diameter pipe surrounded by a thin, less permeable, layer is somewhat more favorable than a smaller diameter pipe surrounded by a thick layer.

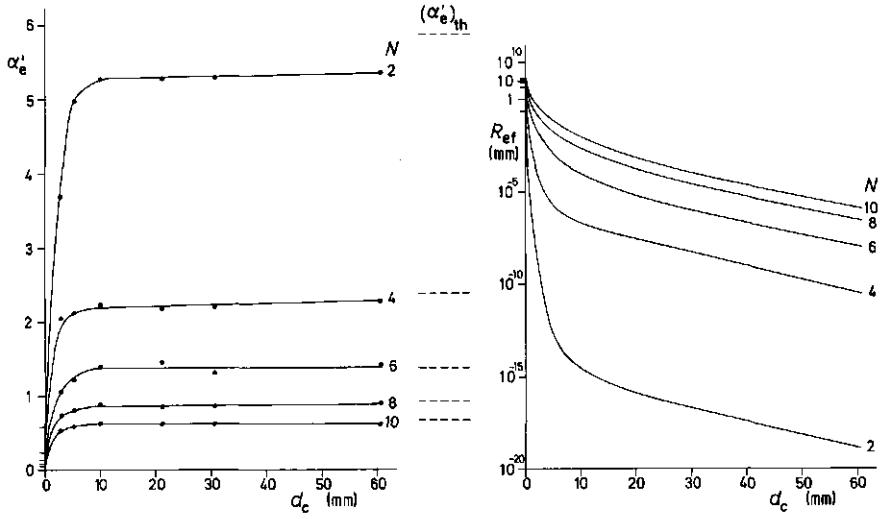

Fig. 3.10. Entrance resistances and effective radii as a function of the thickness of the less permeable drain surround at $\kappa_c = 0{,}1$ for $S^1_{cls}(1)$-drains with different numbers of continuous longitudinal slits.

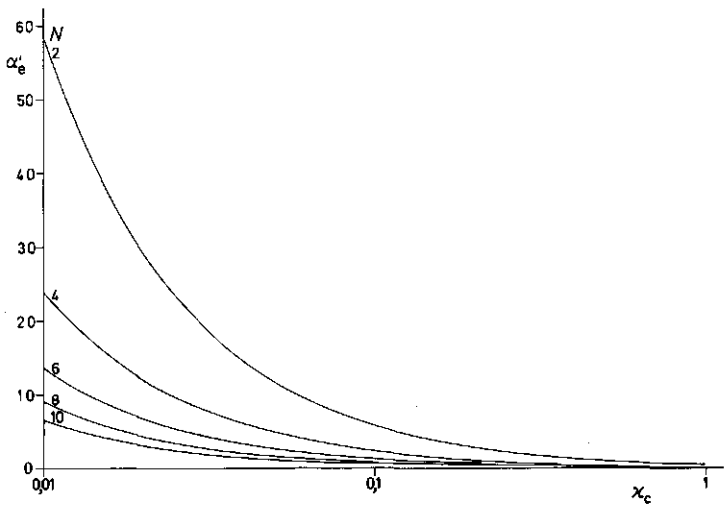

Fig. 3.11. Theoretical α'_e-values as a function of the permeability κ_c at a thickness $d_c \geqslant 10$ mm for different numbers of continuous longitudinal slits.

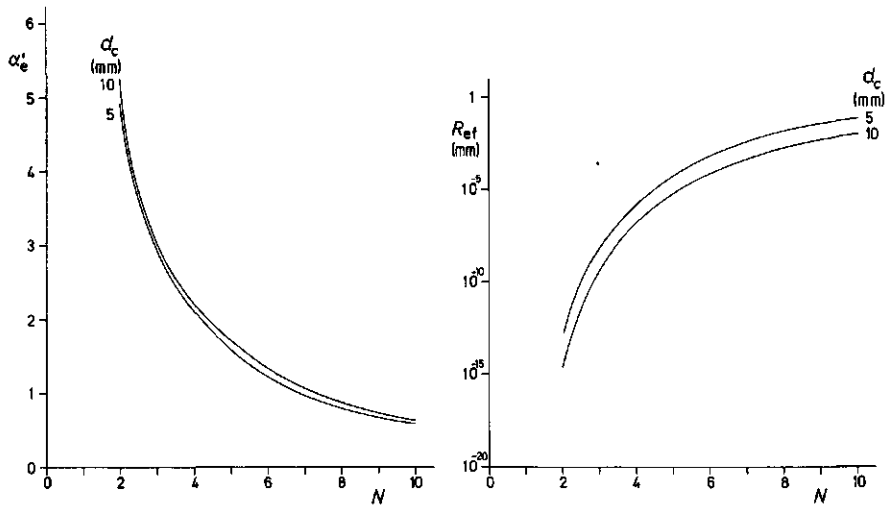

Fig. 3.12. The influence of the number of continuous longitudinal slits on the entrance resistance and the effective radius at κ_c = 0,1 and d_c = 5 and 10 mm.

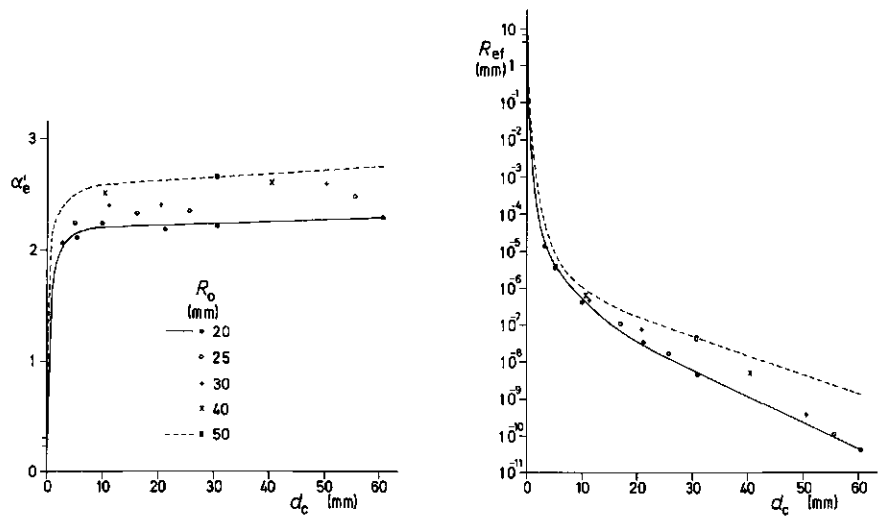

Fig. 3.13. Entrance resistances and effective radii for different diameter pipes provided with 4 continuous longitudinal slits, as a function of the thickness of the less permeable drain surround (κ_c = 0,1).

4.4. Influence of a partially blocked envelope

The results of the $S^1_{cls}(1)$-drain provided with 4 continuous longitudinal slits surrounded by a more permeable envelope with $\kappa_e = 10$, of which respectively 25 % and 50 % of the thickness has a reduced permeability κ_b, are presented in fig. 3.14 and fig. 3.15. These figures clearly demonstrate that the α'_e-value is only slightly influenced by the blocked portion. Nevertheless, the entrance resistance increases with increasing thickness of the blocked part. Owing to this blocked part, the radial resistance will increase, causing a decrease of the effective radius. The reduction becomes important only when the blocked part of the envelope has permeability values which are smaller than the permeability of the surrounding soil.

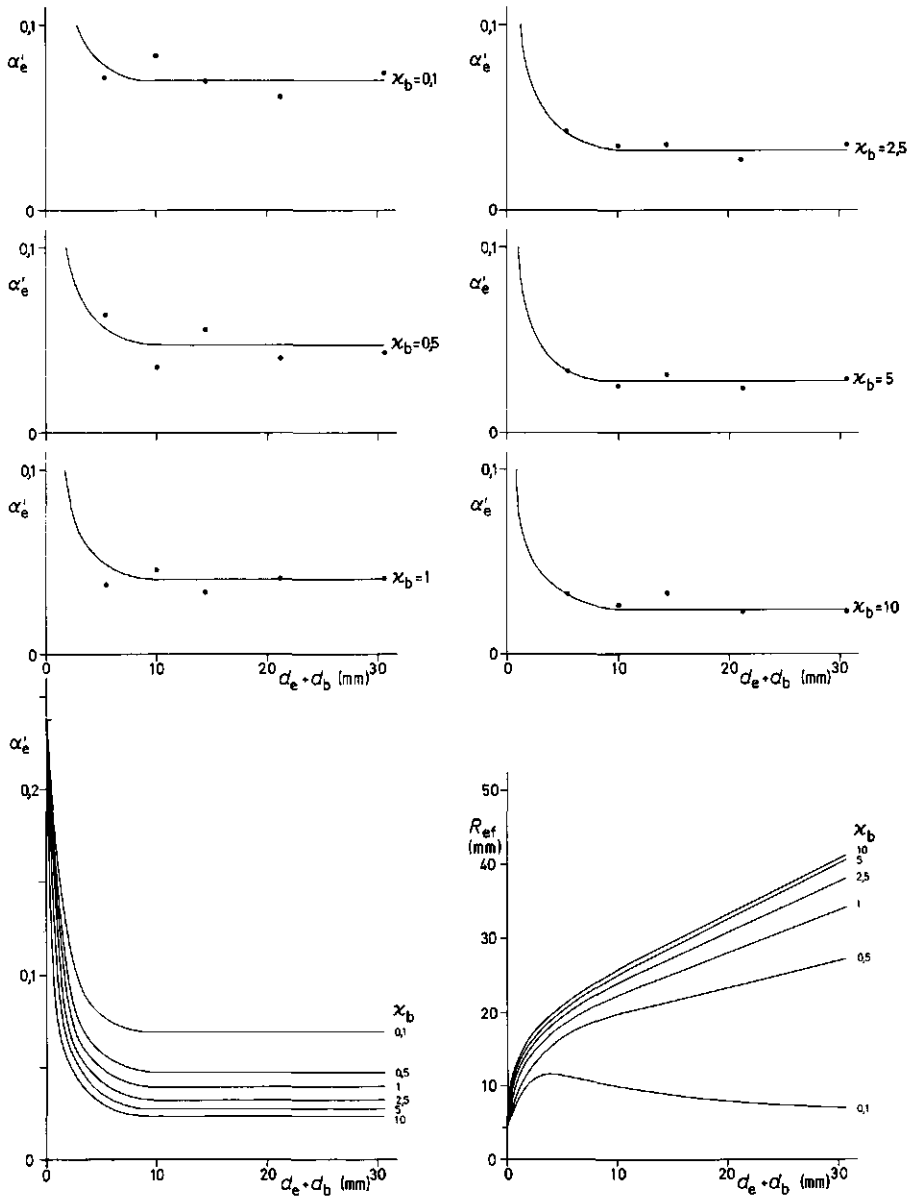

Fig. 3.14. Entrance resistances and effective radii of the $S^{1}_{cls}(1)$-drain with 4 continuous longitudinal slits as a function of the more permeable (κ_e = 10) envelope thickness with a reduced permeability (κ_b) over 25 % of its original thickness.

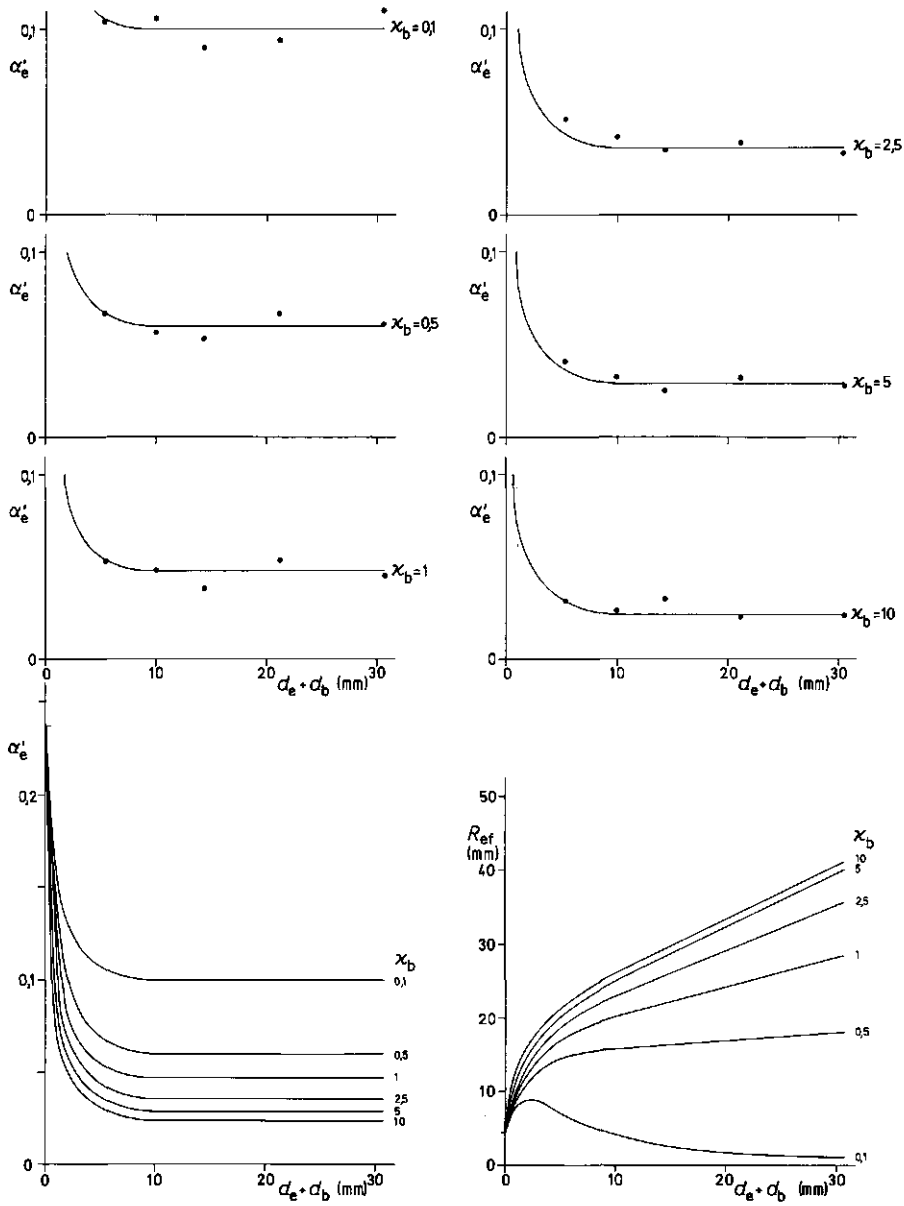

Fig. 3.15. Entrance resistances and effective radii of the $S^1_{cls}(1)$-drain with 4 continuous longitudinal slits as a function of the more permeable (κ_e = 10) envelope thickness with a reduced permeability (κ_b) over 50 % of its original thickness.

5. *Conclusion*

A less permeable drain surround results in an increase of entrance resistance and a decrease of the effective radius. Especially at thicknesses $d_c \geq$ 5 mm and $\kappa_c \leq 0{,}1$ the entrance resistance increases markedly and the effective radius is reduced to extremely small values.

Increasing the number of perforation rows decreases the entrance resistance to some extent, but there are definite practical limits to this approach.

Using a larger pipe diameter does not result in a substantial improvement when the drain is surrounded by a less permeable layer.

If the drain pipe is surrounded by a more permeable envelope which is partially blocked, the entrance resistance will only be influenced to a limited extent. Nevertheless, the radial resistance will increase, which results in a reduction of the effective radius. This reduction never results in the extremely small effective radii obtained when the drain is directly surrounded by a less permeable layer.

CHAPTER IV

FURTHER CONSIDERATIONS ON THE SIGNIFICANCE OF ENTRANCE RESISTANCE

---

1. *Entrance resistance and flow pattern in asymmetric flow*

For radial flow towards an ideal full flowing drain in a homogeneous medium, the head loss is adequately defined by eqn. (1.2), while head loss for radial flow towards a real drain is given by eqn. (1.13).

For unsymmetrical radial flow towards a full flowing ideal drain, from eccentric circular equipotentials (fig. 4.1), the head loss is given by MUSKAT (1946) as

$$\Delta h_u = \frac{q}{2 \pi k} \ln \frac{R^2 - X^2}{R R_o} \qquad (4.1)$$

in which Δh_u : total head loss (m)

q : discharge per unit drain length (m^2/d)

k : hydraulic conductivity (m/d)

R : circular equipotential radius (m)

R_o : outer drain radius (m)

X : midpoint eccentricity of the equipotential and drain pipe (m).

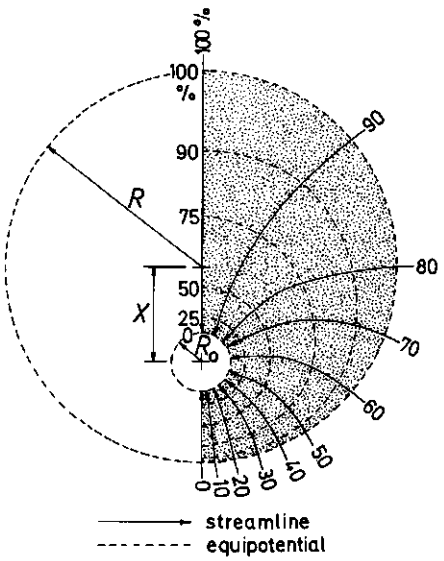

Fig. 4.1. Flow between eccentric circular equipotentials.

The head loss Δh_u can also be written as

$$\Delta h_u = q\, W_u = \frac{q}{k}\,\alpha_u \qquad (4.2)$$

in which W_u : the flow resistance due to eccentric circular equipotentials (d/m)

α_u : the corresponding dimensionless flow resistance.

The head loss for such flow towards a real drain can be written, according to eqns. (1.11) and (1.13) :

$$\Delta h_t = \Delta h_u + \Delta h_e = q(W_u + W_e) = q\, W_t \qquad (4.3)$$

or

$$\Delta h_t = \frac{q}{k}\,(\alpha_u + \alpha_e) = \frac{q}{k}\,\alpha_t \qquad (4.4)$$

As in the case of symmetrical radial flow, the flow pattern for unsymmetrical flow towards a real drain is only influenced in the immediate vicinity of the drain. The real drain has no further effect on the general flow path.

In simulating an eccentrically placed ideal drain and a $S^1_{cls}(1)$-drain with 4 continuous longitudinal slits, the entrance resistance can be derived from the electric current measurements. After adapting eqn. (1.104) for this flow situation, α_e is given by :

$$\alpha_e = \frac{1}{2\pi}\left(\frac{I_{id}}{I_{rd}} - 1\right) \ln \frac{R^2 - X^2}{R\, R_o} \qquad (4.5)$$

The results of table 4.1 clearly illustrate that the eccentricity does not influence the α_{ep}-value.

Table 4.1. α_{ep}-values at a given eccentricity X of the drain midpoint (R_o = 20 mm), with respect to the circular equipotential midpoint (R = 400 mm).

X	I_{id}	I_{rd}	α_{ep}	α_{ep}
mm	mA	mA	measured	theor.
0	35,09	23,67	0,230	0,238
180	37,55	24,77	0,227	0,238
330	55,78	31,50	0,227	0,238

Another way of looking at the matter is to suppose that there is a radial flow component α_r, upon which is superimposed a flow resistance α_{su} which can be thought of as an additional entrance resistance due to the unsymmetrical radial flow conditions. Hence

$$\alpha_t = \alpha_r + \alpha_{su} + \alpha_{ep} \qquad (4.6)$$

For an ideal drain $\alpha_{ep} = 0$ and α_{su} can be calculated from the electric current values obtaining at an eccentricity $X = 0$ and a given eccentricity X. For a real drain, the sum of α_{su} and α_{ep} can be determined at a given eccentricity X from which follows α_{ep}. The results of table 4.1 have been reworked in that way to give table 4.2.

Table 4.2. α_{su}, $\alpha_{su} + \alpha_{ep}$ and α_{ep}-values for a given eccentricity X of the drain midpoint (R_o = 20 mm) and the circular equipotential midpoint (R = 400 mm).

X	I_{id}	I_{rd}	α_{su}		$\alpha_{su} + \alpha_{ep}$	α_{ep}
mm	mA	mA	theoret.	measured		
0	35,09	23,67	0	0	0,230	0,230
180	37,55	24,77	- 0,036	- 0,031	0,199	0,230
330	55,78	31,50	- 0,182	- 0,177	0,054	0,231

Symmetrical radial flow towards the $S^1_{cls}(1)$-drain with 4 continuous longitudinal slits of which one slit is sealed for one reason or another will result in an α_{ep}-value which is approximately that of a drain pipe with 3 uniformly distributed continuous longitudinal slits. This also holds for 2 and 3 sealed slits (table 4.3). In effect, these situations are nothing else but symmetrical radial flows towards slits which are unsymmetrically distributed on the drain circumference.

For symmetrical radial flow towards a full flowing ideal drain which is partially sealed, there is some distortion of the flow paths in the region of the drain (fig. 4.2). The flow pattern can be attributed to the fact that the drain pipe is no longer ideal and, as a consequence, the additional flow resistance can be considered as an entrance resistance.

This situation can also be considered as flow towards an ideal drain such that the flow only occurs through the open part of the pipe.

Table 4.3. α_{ep}-values for the $S^{1}_{cls}(1)$-drain with 4 continuous longitudinal slits of which a number of slits are sealed.

Number of slits N		I_{id}	I_{rd}	α_{ep}	$(\alpha_{ep})^{\star}_{th}$
open	sealed	mA	mA		
4	0	35,09	23,67	0,230	0,238
3	1	35,09	20,46	0,341	0,348
2	2	35,09	15,37	0,612	0,587
1	3	35,09	8,98	1,386	1,395

★ Theoretical values for uniformly distributed continuous longitudinal slits.

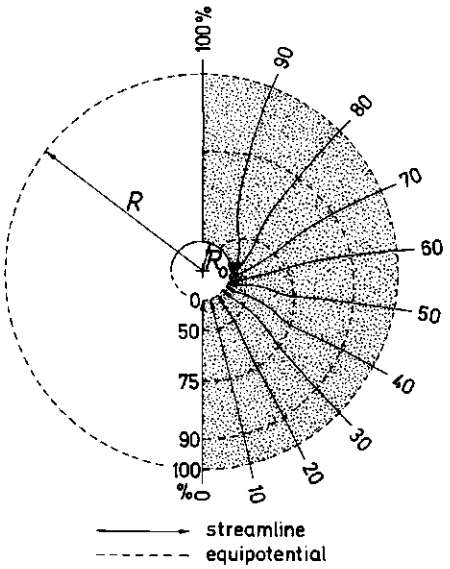

Fig. 4.2. Radial flow towards an ideal drain with sealed upper half.

The additional resistance consequent upon distortion of the flow paths can be assigned an α_{su}-value, the magnitude of which is determined by the open part of the circumference of the ideal drain. In both cases the resistance is just the same, and is given in column 4 of table 4.4.

The same argument can be applied to a real drain pipe. Thus, if this pipe is partially sealed, then - besides the radial flow resistance α_r and

and the entrance resistance α_{ep} - there is also an identical flow resistance α_{su} towards the open part of the drain, the sum of α_{ep} plus α_{su} (column 6 of table 4.4) being the α_{ep}-value of table 4.3.

Table 4.4. α_{su} and α_{ep}-values of a drain pipe with a partially sealed circumference.

(1) Open part	(2) I_{id} mA	(3) I_{rd} mA	(4) α_{su}	(5) α_{ep}	(6) $\alpha_{ep} + \alpha_{su}$
4/4	35,09	23,67	0	0,230	0,230
3/4	33,91	20,46	0,017	0,325	0,341
2/4	30,50	15,37	0,072	0,540	0,612
1/4	25,80	8,98	0,172	1,215	1,386

Thus, we may accept that the entrance resistance of a drain flowing full does not undergo any change as a result of unsymmetrical radial inflow. If such a drain is partly blocked, the entrance resistance will increase as the active part decreases.

CAVELAARS (1967) introduced the concept of *approach flow resistance* α_{ap} as the sum of α_r plus α_e. Since this definition includes α_{su} the concept refers to the whole flow pattern in the vicinity of the drain.

Thus far, only drain pipes flowing full have been considered. However, similar reasoning can be applied to a partially full drain under conditions of radial flow. The drain surface below the water level is an equipotential, while the drain surface above the water level is a surface of seepage and, therefore, has a potential greater than that below the water surface, depending on the elevation. Nevertheless, water will enter the drain at the seepage surface or perforations above water level. A partially full drain results in a decrease in the amount of water entering the drain for a given head difference*. The measured loss of discharge is attributed to the higher potentials that exist on the drain surface above the water level in the drain. These higher potentials reduce the energy available to move water into the drain (WILLARDSON, 1967).

* When a drain is flowing partially full, there is some question as to what the reference potential should be. In his study, WILLARDSON (1967) took the surface of the water in the drain as reference potential.

MONKE (1959) and BURGHARDT (1977 a, 1977 b, 1977 c and 1978) describe the flow pattern in the immediate vicinity of the drain for both the completely and partially full cases. After BURGHARDT (1977 b), it appears that water predominantly enters the drain where it has contact with the water in the drain. Depending on the depth of flow, water moves into the drain from below and the sides. For a drain without envelope material, the streamlines will be concentrated towards the full part of the drain (fig. 4.3a) and a head loss additional to that for a drain flowing full will occur. Envelopes can, under certain conditions, even with a partially full drain, take up soil water over the whole circumference and release it to the drain without significant head losses (fig. 4.3b). Compared to a drain flowing full, the available head will be greater and, under certain circumstances, an increase of the uptake capacity will be possible. The position of the groundwater table is not important since it does not form the boundary of the flow zone. Water flow occurs in the saturated zone both below and above the water table and also in the unsaturated zone. Hence, in soils of uniform permeability, the equipotentials approach the circular shape (fig. 4.4) in addition to which the midpoints of drain and equipotential are eccentric to each other.

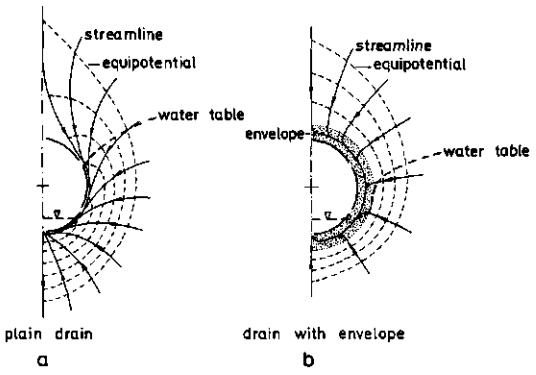

Fig. 4.3. Although the orthogonality of streamlines and equipotentials is not respected, these drawings after BURGHARDT (1977 b), illustrate the deflection of streamlines for a partially full drain with and without envelope.

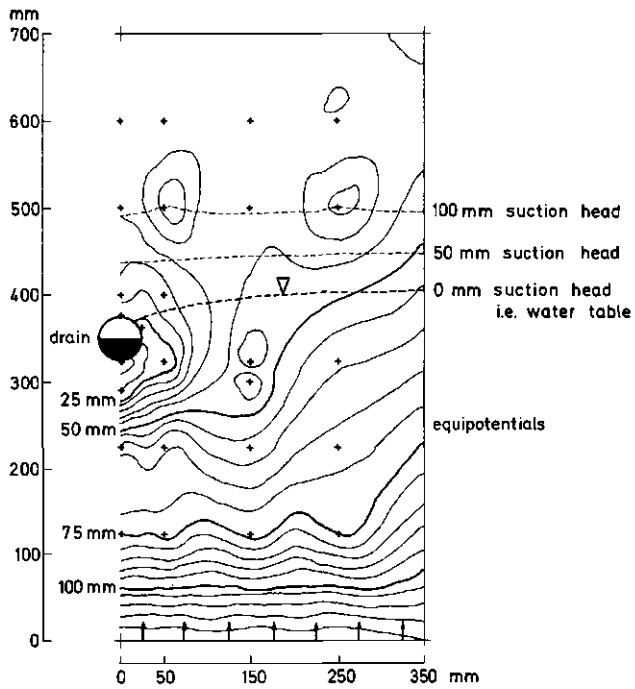

Fig. 4.4. Equipotentials for upwards flow towards a partially full drain as measured in a sand tank model (BURGHARDT, 1977 a).

BURGHARDT (1977 a, 1977 c) questions the definition of *entrance resistance*. His investigations clearly demonstrate that, besides the entrance resistance of the drain, there are other factors influencing the total head loss, such as :

- the eccentricity of equipotential to drain midpoint
- the depth of flow within the drain.

The concept of *entrance resistance* only relates to radial flow towards a drain flowing full. For a partially full drain, the active perforations must be taken into account in determining the entrance resistance. The additional flow resistance α_{su} - which can be negative - and the radial flow resistance α_r, together with the entrance resistance, compose the *approach flow resistance* α_{ap} in the vicinity of the drain pipe. This approach flow resistance can markedly deviate from the theoretical total radial resistance $\alpha_e + \alpha_r$.

For the case of radial flow towards a partially full drain, the entrance resistance does not undergo any change. The differences in outflow must be attributed to the head differences at the drain circumference. When the available head is too small to overcome the surface tension at the soil-air interface, the streamlines are deflected around the drain towards the water level in the drain and additional entrance and flow resistances must be considered. When the midpoints of drain and circular equipotentials do not coincide, the total flow resistance will decrease.

Envelope materials considerably decrease the entrance resistance and, in addition, they will reduce the additional resistances.

2. *Entrance resistance and soil particle invasion*

Differential movement of soil particles or erosion depends on the shearing resistance which opposes a possible relative movement of the soil particles. The shearing resistance of a soil is given by COULOMB's equation :

$$\tau_f = c_o + \sigma_e \tan \phi \qquad (4.7)$$

in which τ_f : shearing resistance per unit area (N/m^2)
c_o : cohesion (N/m^2)
σ_e : effective stress of the soil particles or intergranular stress (N/m^2)
ϕ : angle of internal friction or shearing resistance.

The intergranular stress is determined by soil loadings and water pressure.

Water, flowing through a porous medium, exerts a pressure on the soil particles in the direction of movement. This pressure is called *flow pressure*. If this flow pressure is larger than the shearing resistance, erosion will occur as the soil loses its structural strength. Since the flow pressure is proportional to the acting hydraulic gradient, erosion will appear as soon as the hydraulic gradient i reaches a given critical value i_c (TERZAGHI & PECK, 1965) :

$$i \geq i_c \qquad (4.8)$$

For cohesionless soil $c_o = 0$ and the corresponding equation is :

$$\tau_f = \sigma_e \tan \phi \qquad (4.9)$$

which means that the shearing resistance only depends on the intergranular stress and the angle of internal friction.

For a saturated sandy soil, the critical hydraulic gradient is obtained as soon as

$$i_c = \frac{\rho_s - \rho_w}{\rho_w} \qquad (4.10)$$

in which ρ_w : specific mass of water (kg/m^3)
ρ_s : specific mass of saturated soil (kg/m^3).

Taking $\rho_s = 2000$ kg/m^3 and $\rho_w = 1000$ kg/m^3 , the critical hydraulic gradient i_c takes the value of 1.

Considering flow downwards through a saturated sandy soil, supported by such a screen that arching of soil particles cannot occur, the sand simply flows through the screen meshes. When the supporting screen is such as to make arching possible, the flow exerts a downward pressure on the sand particles and as a consequence, increases the intergranular stress. Taking the contrary case, flow upwards tends to lift up the sand particles due to the friction between the flowing water and the void walls. Arching is less probably and sand particles will pass the screen as soon as i_c is reached. This condition of instability resulting from upwards flow of water is called *quicksand*. The soil acts as though it were weightless and becomes highly unstable.

The same phenomenon arises in the vicinity of the drain. MONKE (1959) concludes that with radial flow towards a drain, a large number of soil particles enter the drain pipe through the lower half; the argument being that the flow pressure tends to stabilize the upper half of the drain while the lifting action of the flow pressure on the lower half of the drain promotes the invasion of soil particles. It should be noted that the gradient at which the soil around a drain will fail is higher than that for the same soil in an unconfined state due to the overburden effects (WILLARDSON & WALKER, 1978). The hydraulic gradient for failure which arises under field conditions is beyond the scope of this study. However, the investigations performed allow us to deduce, for certain circumstances, the hydraulic gradients.

The head loss for radial flow towards an ideal drain flowing full is given by eqn. (1.2), from which the hydraulic gradient can be derived

$$i = \frac{dh}{dR} = \frac{q}{2 \pi k R} \qquad (4.11)$$

As can be seen from eqn. (4.11), the hydraulic gradient will be largest at the drain circumference (VAN DER BEKEN, 1968). For an ideal drain with R_o = 20 mm, $i = 8\ q/k$. Accepting a q/k ratio of 0,188 m (drain spacing E = 12 m, hydraulic conductivity k = 0,45 m/d, precipitation N = 7 mm/d), the hydraulic gradient at the drain circumference is 1,5 (fig. 4.5).

Radial flow towards a real drain flowing full with R_o = 20 mm, provided with 4 continuous longitudinal slits of width β_s = 1 mm is equivalent to an ideal drain with an effective radius R_{ef}, given by eqn. (1.19).

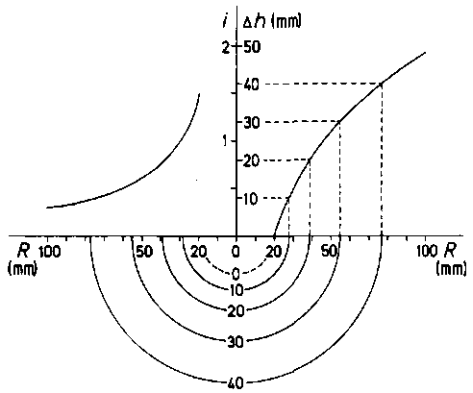

Fig. 4.5. Head loss Δh and hydraulic gradient i for radial flow towards an ideal drain flowing full with R_o = 20 mm at q/k = 0,188 m.

According to eqn. (1.51) for plane boundary conditions, α_{ep} takes the value of 0,238 and R_{ef} = 4,5 mm. In the circumstances given, the hydraulic gradient reaches a value of 6,6 and danger of erosion is considerably increased. Increasing the diameter only results in a slight decrease of the gradient. With the aforementioned conditions, it takes the value of 4,2 for a drain with R_o = 50 mm.

These hydraulic gradients are still too small since a real drain was replaced by an ideal drain with truly radial flow. In reality, the streamlines converge towards the perforations so that still higher hydraulic gradients occur. This result can be derived from the electrical potential measurements. After converting the electrical potentials into hydraulic potentials, the hydraulic gradients at the perforations can be derived. Fig. 4.6 gives the head losses as a function of the distance to the drain circumference for a pipe with R_o = 20 mm provided with 2; 4; 6; 8 and 10 continuous longitudinal slits. By linear extrapolation from the first measuring point, a value of 10,2 is obtained for 4 continuous longitudinal slits. As can be seen from fig. 4.6, a deflection is already observable so that the real gradient will be slightly larger. The hydraulic gradient for 10 continuous longitudinal slits, determined in the same way, is 5,2. A larger diameter will not result in significant improvement; a drain pipe with R_o = 50 mm, provided with 4 continuous longitudinal perforations, results in a

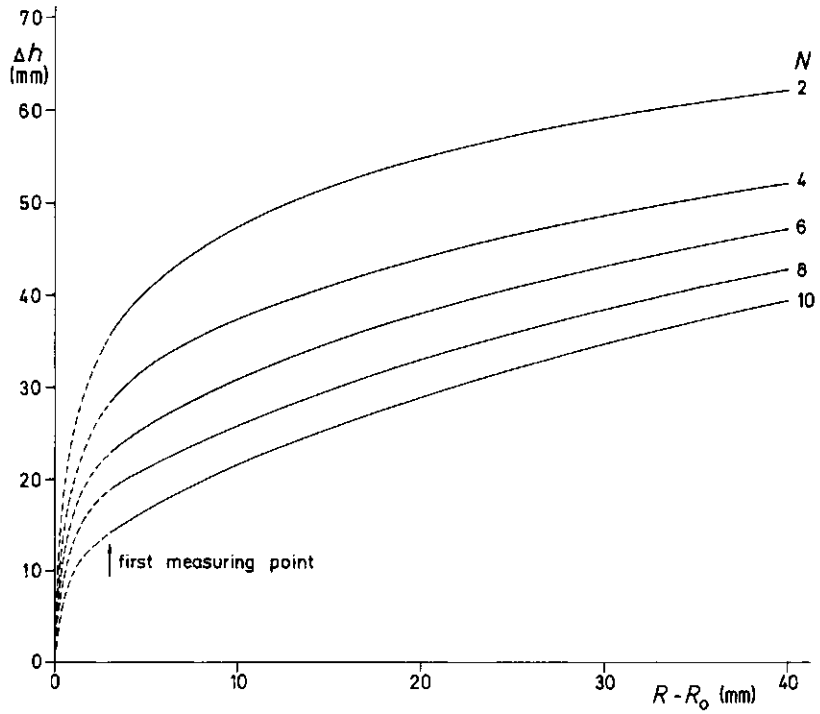

Fig. 4.6. Head loss as a function of the distance to the drain circumference for a drain with R_o = 20 mm and provided with N rows of continuous longitudinal slits.

hydraulic gradient of 7,4 when calculated by linear extrapolation from the first measuring point (fig. 4.7).

An ideal drain surrounded by a more permeable envelope having a thickness d_e = 10 mm and κ_e = 10 results in a hydraulic gradient of 1 at the soil-envelope interface (fig. 4.8). The hydraulic gradient is greatly reduced in the envelope and at the drain circumference. The same hydraulic gradient is obtained in the case of an ideal drain with R_o = 30 mm.

A real drain with R_o = 20 mm provided with 4 continuous longitudinal slits, surrounded by an envelope with d_e = 10 mm and κ_e = 10 results, according to eqn. [2.17], in a R_{ef} = 24 mm and a hydraulic gradient at the soil-envelope interface of 1,2. The hydraulic gradient is 1 for a drain with R_o = 25 mm, and 0,9 for a drain with R_o = 30 mm. The hydraulic gradient resulting from the measurements is 1,2 for R_o = 20 mm, d_e = 10 mm and κ_e = 10 (fig. 4.9).

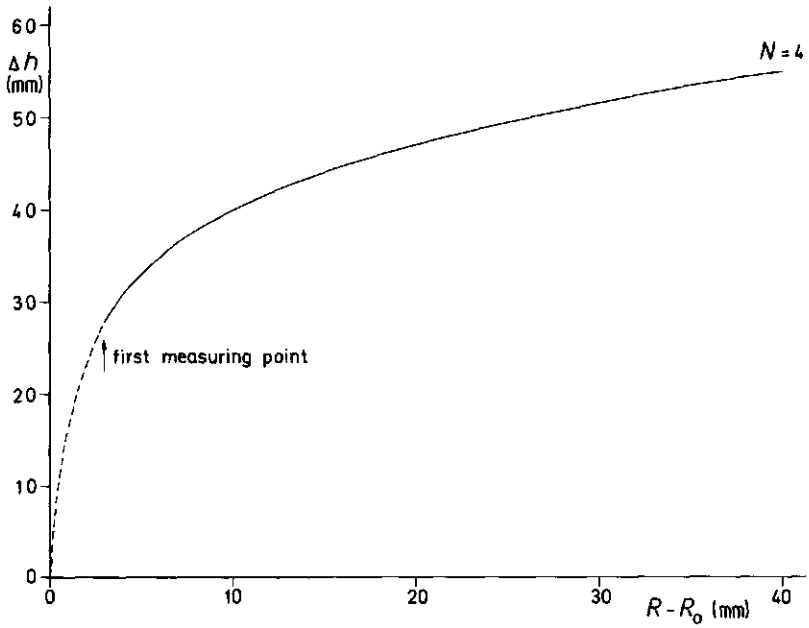

Fig. 4.7. Head loss as a function of the distance to the drain circumference for a drain with R_o = 50 mm, provided with 4 continuous longitudinal slits.

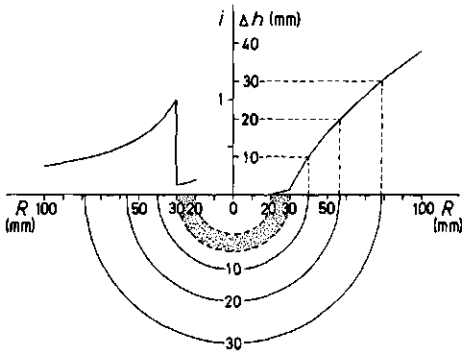

Fig. 4.8. The influence of an envelope with a thickness d_e = 10 mm and κ_e = 10, surrounding an ideal drain with R_o = 20 mm, on the head loss Δh and the hydraulic gradient i for q/k = 0,188 m.

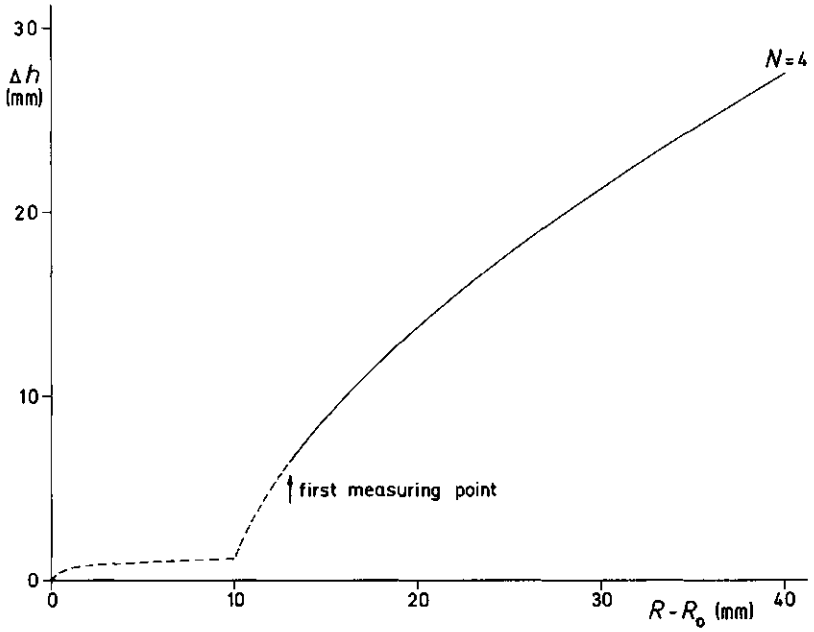

Fig. 4.9. Head loss as a function of the distance to the drain circumference for a drain with R_o = 20 mm provided with 4 continuous longitudinal slits and surrounded by an envelope with a thickness d_e = 10 mm and κ_e = 10.

Thus far, only symmetrical radial flow towards drains flowing full has been considered. Unsymmetrical radial flow towards partially full drains increases the danger of soil particle invasion because of the additional flow resistance and midpoint eccentricity. Under such circumstances soil particle invasion will start from below the drain and move upwards as the water level in the drain increases. This conclusion is confirmed by the experimental research of JONES (1960) and SISSON & JONES (1962).

3. *Entrance resistance and design criteria*

Drainage formulae have been derived for ideal drains. In reality drainage materials have an entrance resistance which reduces the effective radius of the drain. Applying the existing drainage formulae (HOOGHOUDT, 1940; KIRKHAM, 1958), after introducing the effective radius of a real pipe, will unavoidably result in a reduced drain spacing. Using the hodograph analysis of VAN DEEMTER (1950), and introducing the values of the effective radius, DENNIS & TRAFFORD (1975) pointed out that for clay drains in a deep soil, a partial gravel surround, either above or below the drain, would allow an increase in drain spacing of some 100 % compared with the plain drain. For a complete gravel surround, the equivalent figure is 120 %.

Deriving the drain spacing for use in actual drainage schemes from considerations of the ideal drain implies that water is standing above the drain. WESSELING (1964) established that submerged drains result in more favorable flow conditions than those for which the drainage formulae have been derived. On the other hand, VAN DEEMTER (1950) and CHILDS & YOUNGS (1958) concluded that a rise in the groundwater table immediately above drains results in a smaller rise midway between drains. Also, the theoretical solutions of KIRKHAM (1958), ERNST (1962) and DAGAN (1964) lead to similar results as shown by WESSELING (1979). Under these circumstances, the question arises of whether the drain spacing needs to be reduced.

For the following design criteria : N = 0,007 m/d; k = 0,5 m/d; depth of the impervious layer H = 2 m; drain depth d = 1 m; water table height midway between drains h_m = 0,5 m and drain spacing E = 18 m a drain diameter of 47 mm has been calculated by WESSELING (1979) using the approximate solution of LIST (1964) for the drainage problem with an impervious layer at finite depth. Since the effective radii of plain drains can take smaller values, water will stand above the drain with these design criteria. The use of more permeable envelopes considerably increases the effective radii, and there will be less chance of water standing above the drain.

Using the theory of ERNST (1962), based on flow resistance, WESSELING (1979) found that the entrance resistance values effected the water table midway between drains to a negligible or, at worst, entirely acceptable extent.

According to ERNST (1962), the difference in water table height midway between drains and above the drain is given by

$$\Delta h = h_m - h_o = N\,E(W_h + W_r) = \frac{N\,E}{k}(\alpha_h + \alpha_r) \qquad (4.12)$$

in which h_m : water table height midway between drains (m)

h_o : water table height immediately above the drain (m)

N : flow rate per unit surface area (m/d)

E : drain spacing (m)

k : hydraulic conductivity (m/d)

W_h : horizontal flow resistance (d/m)

W_r : radial flow resistance (d/m)

α_h : horizontal flow resistance at k = 1 m/d

α_r : radial flow resistance at k = 1 m/d.

For optimal drainage, i.e. no water standing above the drain centre, the horizontal resistance is given by

$$\alpha_h = \frac{E}{8\,H} \qquad (4.13)$$

and the radial resistance by

$$\alpha_r = \frac{1}{\pi} \ln \frac{H}{\pi\,R_o} \qquad (4.14)$$

For submerged drains (fig. 4.10)

$$\alpha_h = \frac{E}{8(H + h_o)} \qquad (4.15)$$

and

$$\alpha_r = \frac{1}{2\,\pi}\left(\ln \frac{H + h_o}{2\,\pi\,R_o} - \ln \sin \frac{\pi\,h_o}{H + h_o}\right) \qquad (4.16)$$

With increasing submergence, the radial resistance decreases quite rapidly whilst the horizontal resistance decrease is negligible. This is clearly illustrated in table 4.5 from WESSELING (1979).

Considering α_h to be near constant, WESSELING (1979) concludes that the entrance resistance has a value given by the difference in radial resistance between h_o = 0 and a h_o-value which does not cause a worthwhile rise of the water table midway between drains, thus

$$\alpha_e = (\alpha_r)_0 - (\alpha_r)_{h_o} \qquad (4.17)$$

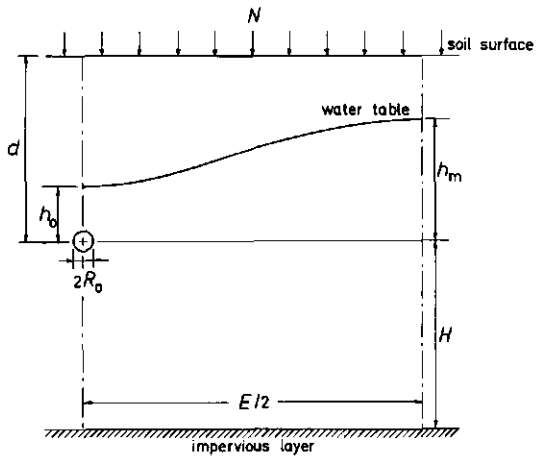

Fig. 4.10. Submerged drain.

Table 4.5. Values of h_o, α_r, α_h and h_m for N = 0,007 m/d; k = 0,5 m/d; H = 2 m; d = 1 m; R_o = 0,0325 m and E = 18 m.

h_o m	α_r	α_h	h_m m
0,00	0,95	1,13	0,52
0,0325	0,84	1,11	0,52
0,05	0,78	1,10	0,52
0,06	0,75	1,09	0,52
0,07	0,73	1,09	0,53
0,10	0,67	1,07	0,54
0,15	0,62	1,05	0,57
0,20	0,58	1,02	0,60
0,25	0,55	1,00	0,64
0,30	0,53	0,98	0,68

Accepting eqn. (4.17), the permissible h_o-values result in corresponding α_e-values from which effective radii R_{ef} can be obtained and the calculations reworked - resulting in table 4.6.

the additional resistance due to unsymmetrical flow and the radial flow component can be defined as the *approach flow resistance*. The entrance resistance for the case of unsymmetrical radial flow towards a drain running only part full is only changed when a suction head exists above the drain; in which situation the streamlines are deflected around the drain and the number of functioning perforation rows has to be taken into account in determining the entrance resistance.

When a drain running only part full is surrounded by a more permeable envelope, flow also occurs through the envelope towards the water filled section.

Due to entrance resistance, the hydraulic gradient in the vicinity of the perforations can reach high values and massive invasion of soil particles may occur especially on the underside. These gradients are markedly reduced when the drain is surrounded by a more permeable envelope.

The entrance resistance must be taken into account when determing drain spacing. Although the approach flow conditions are more favourable if water is standing above the drain, the entrance resistance which causes a certain water level above the drain will raise the water table midway between drains more than an ideal drain operating with the same head.

These aspects of entrance resistance need to be further investigated in order to reach a deeper understanding and to obtain more definitive rulings.

SAMENVATTING EN BESLUITEN

ONDERZOEK MET BEHULP VAN EEN ELEKTROLYTMODEL NAAR DE INVLOED VAN INLAATOPENINGEN EN LAGEN MET VERSCHILLENDE DOORLATENDHEDEN OP DE WERKING VAN DRAINEERBUIZEN

Voor het bepalen van de drainafstand wordt vrijwel in alle formules een ideale drain verondersteld. Nochtans bestaat een reële draineerbuis uit een ondoorlatende wand voorzien van inlaatopeningen. De stroomlijnen konvergeren naar deze openingen en geven aanleiding tot een intreeweerstand waardoor de effektieve straal van de reële drain gereduceerd wordt.

HOOFDSTUK I

Naast de buiskarakteristieken is de intreeweerstand afhankelijk van de begrenzing van de bodemdeeltjes met de openingen. Voor vlakke en gewelfvormige begrenzingen kan de intreeweerstand van gladde buizen, voorzien van bepaalde perforatievormen en -verdelingen, met behulp van analytische oplossingen berekend worden. Dit is het geval voor :

- stootvoegen of kontinue dwarsspleten (KOZENY, 1933; KIRKHAM, 1950; ENGELUND, 1953; ERNST, 1962; SNEYD & HOSKING, 1976)
- cirkelvormige perforaties (MUSKAT, 1942; KIRKHAM & SCHWAB, 1951; ENGELUND, 1953)
- kontinue langsspleten (MUSKAT, 1942; ENGELUND, 1953)
- diskontinue langs- en dwarsspleten of rechthoekige perforaties (MUSKAT, 1942; CAVELAARS, 1970).

Enkel SCHWAB & KIRKHAM (1951) toetsten de resultaten van de theoretische oplossingen van KIRKHAM & SCHWAB (1951) en van KIRKHAM (1950) aan de resultaten, bekomen met behulp van een elektrolytmodel. Daarenboven werden, door talrijke onderzoekers, proeven uitgevoerd in zandmodellen om de drainerende werking van gladde plastieken draineerbuizen te vergelijken met de klassieke gebakken buizen. Deze zandmodellen werden verder ook aangewend om de invloed van de perforatievorm en -verdeling op de drainerende werking, van zowel gladde als geribbelde plastieken draineerbuizen, te bestuderen en te optima-

Deze oplossingen worden, voor gewelfvormige begrenzing, gegeven door de vergelijkingen (1.64) en (1.66) en voor vlakke begrenzing door de vergelijkingen (1.65) en (1.67). Ook uit de door de DE GLEE (1930) gegeven oplossing voor een onvolkomen put in een gespannen grondwaterlaag werden de vergelijkingen (1.68) voor gewelfvormige en (1.69) voor vlakke begrenzingen van diskontinue langsperforaties afgeleid. Al deze oplossingen geven aanleiding tot vrij goed overeenstemmende resultaten. De oplossing van CAVELAARS (1970) is, met behulp van een tabel of grafiek, vrij eenvoudig. Ook de vergelijkingen (1.66) en (1.67) kunnen, met tabellen die de gamma-funktie geven, nog betrekkelijk eenvoudig doorgerekend worden. De eenvoudigste oplossing, met een voldoende juiste benadering, wordt gegeven door de vergelijkingen (1.68) en (1.69).

Voor gladde buizen met diskontinue dwarsperforaties kunnen de analoge korresponderende formules worden toegepast. De eenvoudigste oplossingen worden gegeven door de vergelijkingen (1.74) en (1.76) van CAVELAARS (1970), en de vergelijkingen (1.84) en (1.85), afgeleid uit de oplossing van DE GLEE (1930) voor putstroming. De vergelijkingen (1.82) en (1.83), afgeleid uit de door MUSKAT (1946) gegeven oplossing voor putstroming, kunnen met tabellen van de gamma-funktie nog betrekkelijk eenvoudig opgelost worden terwijl de vergelijkingen (1.80) en (1.81) vrij ingewikkelde berekeningen vergen.

Deze theoretische oplossingen voor gladde buizen gelden niet voor geribbelde draineerbuizen met perforaties in het dal van de ribbels, wanneer aangenomen wordt dat de ribbels met grond gevuld zijn. Voor een gegeven perforatiepatroon bezitten geribbelde draineerbuizen, van een bepaalde diameter, een hogere intreeweerstand dan gladde buizen. Om praktische redenen zijn gladde draineerbuizen minder intensief geperforeerd dan geribbelde draineerbuizen zodat de intreeweerstand, door de intensievere perforering, in het voordeel van de geribbelde draineerbuizen uitvalt. Voor geribbelde draineerbuizen zijn geen theoretische oplossingen voorhanden. Vergelijking (1.122) geeft een theoretische oplossing voor geribbelde draineerbuizen met blokvormige ribbels, voorzien van kontinue dwarsperforaties met een perforatiebreedte gelijk aan de dalbreedte. De perforaties zijn in het dal van de ribbel gelegen en vormen een vlakke begrenzing met de bodemdeeltjes. Vergelijking (1.126) is een theoretische oplossing voor kontinue dwarsperforaties met een breedte kleiner dan de dalbreedte. Voor diskontinue dwars-

perforaties geeft vergelijking (1.127) een benaderende oplossing. Bij geribbelde draineerbuizen met sinusvormig profiel mag redelijkerwijze aangenomen worden dat de ongunstige invloed geringer is door de ietwat gunstiger toestromingsvoorwaarden.

Wanneer de perforaties op de kop van de ribbels aangebracht zijn, kunnen de formules voor gladde buizen toegepast worden. Dit betekent niet ipso facto dat de perforaties op de kop van de ribbels aangebracht moeten worden. De ribbels kunnen namelijk een gunstige invloed uitoefenen door gewelfvorming van de bodem over de ribbels of door een grotere doorlatendheid van de grond in de ribbels.

Algemeen kan besloten worden dat vrij eenvoudige en voldoende nauwkeurige oplossingen bestaan voor het bepalen van de intreeweerstand van gladde buizen. De vorm van de ribbels en de begrenzing van de bodem met de ribbels vormen bijkomende moeilijkheden voor een exact theoretische oplossing van geribbelde draineerbuizen.

Uit het doorgevoerde onderzoek volgt verder dat noch de totale perforatie-oppervlakte, noch de totale perforatie-omtrek per drainlengte, maar wel de perforatieverdeling bepalend is voor de intreeweerstand. Nochtans kan gesteld worden dat de perforatie-omtrek meer bepalend is dan de perforatie-oppervlakte omdat, onafhankelijk van de perforatievorm, het verschil in intreeweerstand kleiner is voor eenzelfde perforatie-omtrek dan voor eenzelfde perforatie-oppervlakte, vooral bij perforatie-oppervlakten kleiner dan 50 cm^2/m (fig. 1.44 en 1.45). Hoe groter de onderverdeling van een gegeven perforatie-oppervlak is, hoe geringer de intreeweerstand zal zijn; de gunstigste perforaties zijn deze met de kleinste oppervlakte of omtrek, zoals de cirkelvormige perforaties en rechthoekige perforaties met de kleinste lengte.

Met uitzondering van cirkelvormige perforaties zal een toename van de huidige perforatie-oppervlakte (20 tot 25 cm^2/m) naar ongeveer 50 cm^2/m, de intreeweerstand nog aanzienlijk verminderen.

HOOFDSTUK II

Uit het onderzoek met zandmodellen bleek dat de drainerende werking van draineerbuizen aanzienlijk verbeterde door het gebruik van omhullingsmaterialen, die een grotere doorlatendheid bezitten dan de doorlatendheid van de omringende grond. De dikte en de graad van de doorlatendheid zijn hierbij bepalend.

Alhoewel de intreeweerstand van omhulde draineerbuizen op verschillende manieren kan gedefinieerd worden, heeft het begrip intreeweerstand, strikt genomen, alleen betrekking op de buis zelf. De verschillende definities kunnen echter ondervangen worden door de effektieve straal te bepalen. Het probleem van omhullingsmaterialen die een grotere doorlatendheid bezitten dan deze van de omringende grond kan alleen analytisch opgelost worden voor volumineuze omhullingen. De intreeweerstand wordt dan gegeven door vergelijking (2.8). Voor dunne omhullingsmaterialen en tweedimensionale stroming werd het probleem numeriek opgelost door WIDMOSER (1968) en NIEUWENHUIS (1976); hierdoor werd meer informatie bekomen over de invloed van de dikte en de graad van doorlatendheid van omhullingsmaterialen.

De invloed van omhullingsmaterialen op de intreeweerstand werd, voor het eerst, bestudeerd met behulp van het elektrolytmodel. Omhullingsmateriaal en bodem werden gesimuleerd door twee elektrolytische vloeistoffen met een geleidbaarheidsverhouding overeenstemmend met de doorlatendheidsverhouding van omhulling en grond. De scheiding van de electrolyten werd verwezenlijkt door een buis met onderling geïsoleerde kontaktpunten, vervaardigd uit een kaardbeslag. De invloed van de dikte en de graad van doorlatendheid van omhullingsmaterialen werden bestudeerd voor een twee- en driedimensionaal stromingsprobleem. De invloed van het aantal perforatierijen en de buisdiameter van draineerbuizen, voorzien van een omhulling, werden bestudeerd voor het tweedimensionaal stromingsprobleem.

Uit het doorgevoerde onderzoek volgt dat de intreeweerstand tot een dikte van het omhullingsmateriaal van ongeveer 5 mm sterk afneemt waarna een konstante waarde bekomen wordt (fig. 2.11 en 2.12). De effektieve straal blijft echter toenemen, bij toenemende dikte, wegens de afname van de radiale weerstand. Bij toenemende relatieve doorlatendheid tot een waarde van ongeveer 20 neemt de intreeweerstand sterk af, en de effektieve straal sterk toe (fig. 2.13). Verdere toename van deze relatieve doorlatendheid heeft weinig betekenis.

Omhullingsmaterialen nivelleren sterk het absolute verschil tussen de intreeweerstanden van verschillende draineerbuizen vanaf een relatieve doorlatendheid van ongeveer 10 (fig. 2.13 en 2.15).

Algemeen kan gesteld worden dat het omhullingsmateriaal radiaal aangestroomd wordt bij een dikte begrepen tussen 5 en 10 mm. De buisdiameter heeft weinig invloed op de intreeweerstand van draineerbuizen voorzien van een omhulling; de effektieve stralen zullen nochtans verschillen, afhankelijk

van de straal van het scheidingsoppervlak tussen omhullingsmateriaal en omringende bodem. Bij een konstante waarde van deze straal wordt ongeveer dezelfde effektieve straal bekomen wanneer de omhullingslaag minstens 5 mm dik is. Om de effektieve straal van een draineerbuis te vergroten zal een draineerbuis met een kleinere diameter en een volumineus omhullingsmateriaal economischer zijn dan een draineerbuis met een grotere diameter en een dunnere omhullingslaag.

HOOFDSTUK III

De drainage-omstandigheden bepalen in belangrijke mate de drainerende werking van drainagematerialen. In bepaalde omstandigheden kan zich rondom de draineerbuis, al dan niet voorzien van een omhullingsmateriaal, een minder doorlatende laag vormen. Ook kan de doorlatendheid van het omhullingsmateriaal door inspoeling van gronddeeltjes, over een bepaalde laagdikte, een verminderde doorlatendheid vertonen in vergelijking met de oorspronkelijke doorlatendheid van de omhulling.

Vergeleken met omhullingsmaterialen met een grotere relatieve doorlatendheid werd het probleem van een laag met geringere relatieve doorlatendheid rondom de drain minder intensief bestudeerd. Een aantal laboratoriumproeven bevestigen dat een laag met een geringere relatieve doorlatendheid rond de drain kan leiden tot het falen van de drainage.

Het probleem is analytisch slechts op te lossen wanneer de laag met geringere relatieve doorlatendheid voldoende dik is. Voor dunnere lagen werd het tweedimensionale stromingsprobleem numeriek benaderd door WIDMOSER (1968). Met behulp van het elektrolyt model werd dit probleem op analoge wijze gesimuleerd als het probleem van omhullingsmaterialen met een grotere relatieve doorlatendheid. De invloed van de dikte en de graad van de geringere relatieve doorlatendheid werden bestudeerd evenals de invloed van het aantal perforatierijen en de buisdiameter. Uit het onderzoek volgt dat een laag met een geringere relatieve doorlatendheid rondom de drain de intreeweerstand sterk doet toenemen waarbij vrij vlug ontoelaatbare waarden bereikt worden. Vanaf een dikte van ongeveer 10 mm wordt een konstante intreeweerstand bekomen (fig. 3.8). De effektieve straal blijft echter afnemen en als gevolg van de toename van de radiale weerstand kunnen uitzonderlijk kleine waarden bekomen worden. De toename van de intreeweerstand en de afname van de

effektieve straal worden sterk geaccentueerd vanaf een relatieve doorlatendheid van 0,2 (fig. 3.9). Ook het verschil in intreeweerstand van verschillende draineerbuizen komt sterker tot uiting vanaf een relatieve doorlatendheid van 0,1 (fig. 3.11).

Voor draineerbuizen, voorzien van een omhullingsmateriaal met gedeeltelijk een verminderde doorlatendheid, werden lagen met een verminderde doorlatendheid over 25 en 50 % van de oorspronkelijke dikte van het omhullingsmateriaal gesimuleerd. Hiervoor werden twee buizen met geïsoleerde kontaktpunten concentrisch in elkaar geplaatst waardoor drie elektrolyten konden gescheiden worden.

Het doorgevoerde onderzoek toont aan dat de intreeweerstand slechts in beperkte mate beïnvloed wordt door een omhullingsmateriaal dat gedeeltelijk een verminderde doorlatendheid vertoont. Nochtans zullen, ten gevolge van de radiale weerstand, de effektieve stralen afnemen naarmate de doorlatendheid van de minder doorlatende laag afneemt en naarmate de dikte ervan toeneemt (fig. 3.14 en 3.15). De effektieve straal neemt echter nooit de extreem kleine waarden aan die bekomen werden voor een drain die direkt omgeven is met een laag met geringere relatieve doorlatendheid. Hieruit volgt dat bij niet ideale uitvoeringsomstandigheden de drainerende werking van een draineerbuis voorzien van een omhullingsmateriaal toch merkelijk beter zal zijn dan deze van een draineerbuis zonder omhullingsmateriaal. Alleen, wanneer de verminderde doorlatendheid zijn oorsprong vindt in het verstoppen van het omhullingsmateriaal, kan dit aanleiding geven tot een minder goede drainerende werking. Dit zal zich pas voordoen wanneer de doorlatendheid van de minder doorlatende laag beduidend kleiner wordt dan de doorlatendheid van de omringende grond.

HOOFDSTUK IV

Bij een alzijdige stroming naar een vollopende drain is de intreeweerstand een konstante die alleen bepaald wordt door de geometrische karakteristieken van de buis zelf. Van belang is dat het stromingsbeeld op een juiste wijze gekarakteriseerd wordt, zoniet kunnen hieruit verkeerde konklusies nopens de intreeweerstand afgeleid worden. Kan het stromingsbeeld niet op een exacte wijze beschreven worden, dan kan de intreeweerstand, de bijkomende weerstand ten gevolge van een niet radiale stroming en de fiktieve radiale

weerstand gedefinieerd worden als een *toestromingsweerstand*. Bij een alzijdige stroming naar een niet vollopende drain wordt de intreeweerstand niet gewijzigd; alleen, wanneer onderdruk heerst boven de drain zullen de stroomlijnen afgebogen worden rond de draineerbuis en moet bij het bepalen van de intreeweerstand rekening gehouden worden met de werkzame perforatierijen.

Is de niet vollopende drain voorzien van een omhullingsmateriaal, dan kan de stroming ook via de omhulling naar het met water gevulde gedeelte van de draineerbuis stromen.

Ten gevolge van de intreeweerstand kan de hydraulische gradiënt in de nabijheid van de perforaties zeer hoog oplopen waardoor bodemdeeltjes, vooral via de onderzijde, massaal in de buis kunnen spoelen. Deze hydraulische gradiënten worden sterk gereduceerd wanneer rondom de drain een omhullingsmateriaal met een grotere relatieve doorlatendheid is aangebracht.

Bij het bepalen van de drainafstand moet rekening gehouden worden met de intreeweerstand. Alhoewel de toestromingsvoorwaarden gunstiger worden wanneer zich boven de drain water bevindt, zal de intreeweerstand, die een bepaalde waterstand boven de drain veroorzaakt, de grondwatertafel midden tussen de drains meer doen toenemen dan de op dezelfde diepte onder water uitmondende ideale drain.

Verder onderzoek, aangaande deze aspekten van de intreeweerstand, is echter noodzakelijk om tot duidelijker inzichten en meer definitieve uitspraken te komen.

RESUME ET CONCLUSIONS

ETUDE A L'AIDE DU MODELE ELECTROLYTIQUE DE L'INFLUENCE EXERCEE SUR L'EFFET DE DRAINAGE PAR LES ORIFICES DES TUYAUX ET PAR DES COUCHES DE PERMEABILITE DIFFERENTE ENTOURANT LES TUYAUX

Presque toutes les formules utilisées pour déterminer la distance entre les drains supposent un drain idéal. Le drain réel consiste en une paroi imperméable percée d'orifices d'entrée. Les filets liquides convergent vers ces orifices et engendrent une résistance d'entrée qui réduit le rayon effectif du drain réel.

CHAPITRE I

La résistance d'entrée dépend à la fois des caractéristiques du tuyau et de la surface de contact ou interface entre les particules de sol et les orifices. Si l'interface est plane ou bombée on peut calculer, par des méthodes analytiques, la résistance d'entrée de tuyaux lisses dont la forme et la distribution des perforations sont connues. C'est le cas pour :

- les interstices ou les fentes annulaires (KOZENY, 1933; KIRKHAM, 1950; ENGELUND, 1953; ERNST, 1962; SNEYD & HOSKING, 1976)
- les perforation circulaires (MUSKAT, 1942; KIRKHAM & SCHWAB, 1951; ENGELUND, 1953)
- les fentes longitudinales continues (MUSKAT, 1942; ENGELUND, 1953)
- les fentes discontinues longitudinales et transversales ou les perforations rectangulaires (MUSKAT, 1942; CAVELAARS, 1970).

Seuls SCHWAB & KIRKHAM (1951) ont comparé les résultats des solutions théoriques de KIRKHAM & SCHWAB (1951) et de KIRKHAM (1950) à ceux obtenus à l'aide d'un modèle électrolytique. En outre, de nombreux chercheurs ont effectué des essais dans les modèles en sable pour comparer l'effet de drainage de tuyaux lisses en matière plastique avec celui des tuyaux en terre cuite classiques. Ces modèles en sable ont également été utilisés pour étudier et optimiser l'influence de la forme et de la distribution des orifices

sur l'effet de drainage de tuyaux en matière plastique lisses ou annelés. Le modèle électrolytique a aussi été utilisé à ces fins. Des modèles en sable ont également servi à déterminer l'influence d'un drain réel sur le niveau et la forme de la surface libre de la nappe.

Le modèle en sable se prêtant moins bien à une étude approfondie, le choix s'est porté sur le modèle électrolytique pour vérifier la validité des solutions théoriques et pour fixer les facteurs déterminants de la résistance d'entrée.

Le modèle électrolytique construit pour simuler un écoulement radial vers un tuyau de drainage était entre autre pourvu d'un pont de mesure mobile, sur lequel était monté une sonde de mesure. La distribution de potential entre les deux électrodes, constituées par une surface équipotentielle cylindrique et un modèle du tuyau de drainage à simuler, a pu être déterminée dans n'importe quel plan radial à différentes profondeurs. Les tuyaux de drainage simulés étaient :

- des tuyaux lisses d'un diamètre extérieur de 75 mm, d'une longueur de 300 mm et à fentes annulaires de largeur variable (drains S^1_{co});
- des tuyaux lisses d'un diamètre extérieur de 40 mm, munis de fentes annulaires larges de 1 mm à espacements variables [drains $S^2_{co}(1)$];
- des tuyaux lisses d'un diamètre extérieur de 39,9 mm; les tuyaux étaient munis de perforations circulaires de diamètre variable, disposées en carré [drains $S^1_{cp}(2)$; drains $S^1_{cp}(3)$; drains $S^1_{cp}(4)$; drains $S^1_{cp}(6)$; drains $S^1_{cp}(8)$ et drains $S^1_{cp}(10)$];
- des tuyaux lisses à perforations circulaires d'un diamètre de 3 mm, disposées en carré; les tuyaux avaient un diamètre de 50 mm [drains $S^2_{cp}(3)$] de 63,5 mm [drains $S^3_{cp}(3)$] et de 70 mm [drains $S^4_{cp}(3)$];
- des tuyaux lisses d'un diamètre extérieur de 40 mm, munis de fentes longitudinales continues, larges de 1 mm [drains $S^1_{cls}(1)$];
- des tuyaux lisses d'un diamètre extérieur de 40 mm, munis de fentes discontinues longitudinales [drains $S^1_{dls}(1)$] ou transversales [drains $S^1_{dcs}(1)$] de 1 mm de largeur disposées en rectangle;
- des tuyaux annelés d'un diamètre extérieur de 50 mm, munis de fentes annulaires (drains C_{co}) ou transversales discontinues de 1 mm de largeur et disposées en rectangle [drains $C^1_{dcs}(1)$].

En ce qui concerne les tuyaux de drainage en terre cuite, ou plus généralement les tuyaux lisses à fentes annulaires, les solutions de KIRKHAM (1950) et d'ENGELUND (1953) donnent des valeurs de résistance d'entrée légèrement surestimées. Les solutions de SNEYD & HOSKING (1976) pour une interface plane et de SNEYD (1976) pour une interface bombée donnent une tres bonne approximation. Les calculs de ces solutions peuvent être simplifiés à l'aide d'un tableau. Pourtant équations (1.31) et (1.32), qui en sont dérivées, peuvent également être appliquées avec une précision suffisante. Ces solutions apportent en outre une correction à la solution très simple d'ENGELUND (1953). La solution de KOZENY (1933), la solution modifiée de l'Appendix I et la solution d'ERNST (1962) donnent des valeurs approximatives pour une longueur de tuyau de 300 mm. D'importants écarts étant constatés pour de moins grandes longueurs de tuyau, ces solutions ne sont pas généralement valables.

En ce qui concerne les tuyaux lisses à perforations circulaires et interface bombée, la solution de KIRKHAM et SCHWAB (1951), qui est du reste identique à celle de MUSKAT (1942), donne des valeurs de résistance d'entrée deux fois trop faibles, parce que l'imperméabilité du paroi de tuyau était négligée. En cas d'interface plane, la solution de KIRKHAM et SCHWAB (1951) donne encore lieu, après correction par un facteur 2, à d'importants écarts; une deuxième correction a abouti à l'équation (1.41). Ces solutions modifiées ainsi que la solution d'ENGELUND (1953) pour une disposition rectangulaire et celle de CAVELAARS (1967) pour une disposition carrée des perforations peuvent être appliquées avec une précision suffisante. La préférence va aux solutions d'ENGELUND (1953) et de CAVELAARS (1967), pour leur simplicité.

La solution de MUSKAT (1942) pour tuyaux lisses à perforations longitudinales continues est, après correction par un facteur 2, identique à la solution simple d'ENGELUND (1953), qui peut être appliquée avec une précision suffisante.

Pour les tuyaux lisses à perforations longitudinales discontinues, MUSKAT (1942) propose une solution qui, après correction par un facteur 2, donne des valeurs de résistance d'entrée d'une exactitude plutôt suffisante. La solution de CAVELAARS (1970), dérivée de l'écoulement vers un puits pénétrant partiellement dans une nappe captive, peut aussi être considérée comme généralement valable. Des solutions pour les fentes longitudinales discontinues ont été dérivées, de façon analogue des solutions

données par MUSKAT (1946) pour l'écoulement vers un puits pénétrant partiellement dans une nappe captive. Ces solutions sont données par les équations (1.64) et (1.66) pour une interface bombée et par les équations (1.65) et (1.67) pour une interface plane. D'autres équations pour interface bombée (1.68) ou plane (1.69) ont été dérivées de la solution donnée par DE GLEE (1930) pour un puits pénétrant partiellement dans une nappe captive. Toutes ces solutions aboutissent à des résultats bien concordants. La solution de CAVELAARS (1970) peut être simplifiée avec l'aide d'un tableau ou d'un graphique. Le calcul des équations (1.66) et (1.67) est aussi encore relativement simple si l'on s'aide de tableaux donnant la fonction gamma. La solution la plus simple est toutefois fournie par les équations (1.68) et (1.69) avec une approximation suffisante.

Dans le cas des tuyaux lisses à perforations transversales discontinues, on peut appliquer les formules analogues correspondantes. Les solutions les plus simples sont fournies par les équations (1.74) et (1.76) de CAVELAARS (1970). Les équations (1.84) et (1.85), dérivées de la solution de DE GLEE (1930) pour l'écoulement vers les puits peuvent, elles aussi, être calculées de façon assez simple. Les équations (1.82) et (1.83), dérivées de la solution donnée par MUSKAT (1946) pour l'écoulement vers les puits, peuvent encore être résolues de façon relativement simple à l'aide de tableau de la fonction gamma, tandis que les équations (1.80) et (1.81) demandent des calculs relativement compliqués.

Ces solutions théoriques pour tuyaux lisses ne peuvent pas être appliquées à des tuyaux de drainage annelés à perforations dans le creux de l'ondulation si l'on admet que les ondulations sont remplies de terre. Pour une disposition donnée des perforations, des tuyaux de drainage annelés d'un certain diamètre ont une résistance d'entrée plus élevée que les tuyaux lisses. Pour des raisons pratiques, les tuyaux de drainage lisses sont moins abondamment perforés que les tuyaux annelés, de sorte que la résistance d'entrée de ces derniers est plus favorable. On ne dispose pas de solutions théoriques pour les tuyaux de drainage annelés. L'équation (1.122) donne une solution théorique pour des tuyaux de drainage annelés à profil crénelé munis de perforations annulaires avec une largeur de perforation égale à la largeur de creux. Les perforations sont situées dans le creux et constituent une interface plane avec les particules de sol. L'équation (1.126) est une solution théorique pour les perforations annulaires dont la largeur est

moindre que celle du creux. L'équation (1.127) donne une solution approximative pour les perforations transversales discontinues. Pour les tuyaux de drainage annelés à profil sinusoidal, on peut admettre raisonnablement que l'influence défavorable sera moins grande du fait des conditions de flux un peu plus favorable.

Si les perforations sont pratiquées au sommet de l'ondulation, on peut appliquer les formules relatives aux tuyaux lisses, ce qui ne signifie pas ipso facto que les perforations doivent être pratiquées en cette position. Les ondulations peuvent, en effet, exercer une influence favorable du fait de la disposition en voûte du sol au-dessus des ondulations ou du fait d'une plus grande perméabilité du sol dans les ondulations.

On peut conclure, d'une manière générale, qu'il existe des solutions assez simples et suffisamment précises pour la pratique, pour déterminer la résistance d'entrée des tuyaux de drainage lisses. En ce qui concerne les tuyaux annelés, la forme des ondulations et l'interface entre le sol et les ondulations rendent plus difficile l'obtention d'une solution théorique exacte.

En outre, il ressort des recherches que ni la superficie totale des perforations ni le périmètre de perforation par unité de longueur de drain, mais bien la distribution des perforations est déterminante pour le résistance d'entrée. On peut néanmoins poser que le périmètre de perforation est plus déterminant que la superficie de perforation parce que, indépendamment de la forme des perforations, la différence en résistance d'entrée est plus petite pour un même périmètre de perforation que pour une même superficie de perforation, surtout si celle-ci est inférieure à 50 cm^2/m (fig. 1.44 et fig. 1.45). Plus une superficie de perforation donnée est subdivisée, plus petite sera la résistance d'entrée; les perforations les plus favorables sont celles qui présentent la plus petite superficie ou le plus petit périmètre. Ce sont, en l'occurrence, les perforations circulaires et, pour les perforations rectangulaires, celles qui présentent la plus petite longueur.

Exception faite des perforations circulaires, une augmentation jusqu'à environ 50 cm^2/m de la superficie de perforation actuelle (20 à 25 cm^2/m) fera diminuer encore considérablement la résistance d'entrée.

CHAPITRE II

Les recherches dans des modèles en sable ont établi que la fonction drainante des tuyaux de drainage est considérablement améliorée par l'emploi de matériaux d'enrobage plus perméables que le sol avoisinant. L'épaisseur et le degré de perméabilité sont déterminants sous ce rapport.

Quoique la résistance d'entrée des tuyaux de drainage enrobés puisse être définie de différentes façons, la notion de résistance d'entrée ne se rapporte, à strictement parler, qu'au tuyau même. Les différentes définitions peuvent toutefois être ramenées à la détermination du rayon effectif. Le problème des matériaux d'enrobage d'une perméabilité relative plus grande ne peut être résolu que par la méthode analytique pour des enrobages volumineux et la valeur de résistance d'entrée est obtenue ainsi par l'équation (2.8). WIDMOSER (1968) et NIEUWENHUIS (1976) ont résolu, par la méthode numérique, le problème concernant les enrobages minces en écoulement bidimensionnel, ce qui a permis d'obtenir plus d'informations sur l'influence de l'épaisseur et de la perméabilité des matériaux d'enrobage.

L'influence des matériaux d'enrobage sur la résistance d'entrée a été étudiée, pour la première fois, à l'aide du modèle électrolytique. Le matériau d'enrobage et le sol ont été simulés par deux liquides électrolytiques dont le rapport de conductivités correspondait au rapport de perméabilité entre l'enrobage et le sol. Pour séparer les électrolytes, on a utilisé un tuyau à points de contact isolés les uns des autres, réalisé à partir d'un élement de carde. L'influence de l'épaisseur et celle du degré de perméabilité des matériaux d'enrobage ont été étudiées dans le contexte d'un problème d'écoulement bi- et tridimensionnel. L'influence du nombre de rangées de perforations et celle du diamètre de tuyau dans le cas de tuyau de drainage enrobés ont été étudiées dans le contexte du problème d'écoulement bidimensionnel.

Il ressort des recherches que la résistance d'entrée diminue considérablement jusqu'à une épaisseur du matériau d'enrobage d'environ 5 mm et qu'on obtient ensuite une valeur constante (fig. 2.11 et fig. 2.12). Par contre, le rayon effectif continue à augmenter quand l'épaisseur augmente, cela du fait de la diminution de la résistance radiale. Quand la perméabilité du matériau d'enrobage augmente, la résistance d'entrée diminue considérablement et le rayon effectif augmente considérablement jusqu'à une

perméabilité relative de 20 (fig. 2.13). Un accroissement ultérieur de la perméabilité relative n'a que peu d'influence.

Les matériaux d'enrobage nivellent considérablement la différence absolue en résistance d'entrée de tuyaux de drainage différents, à partir d'une perméabilité relative d'environ 10 (fig. 2.13 et fig. 2.15).

D'une façon générale, on peut poser que le matériau d'enrobage reçoit un flux radial à une épaisseur comprise entre 5 et 10 mm. Le diamètre du tuyau influe peu sur la résistance d'entrée de drains pourvus d'un enrobage; les rayons effectifs différeront pourtant en fonction du rayon de l'interface entre l'enrobage et le sol. Pour une valeur constante de ce rayon on obtient environ le même rayon effectif si l'épaisseur de l'enrobage est au moins 5 mm. Pour augmenter le rayon effectif du tuyau de drainage, il sera donc plus économique de choisir un tuyau plus petit à enrobage volumineux qu'un tuyau plus grand à enrobage plus mince.

CHAPITRE III

Les conditions de drainage déterminent dans une importante mesure l'efficacité des matériaux de drainage. Dans certaines circonstances il peut se former autour du tuyau de drainage, qu'il soit pourvu ou dépourvu d'un matériau d'enrobage, une couche moins perméable. Il peut aussi arriver que la perméabilité originelle d'une certaine couche du matériau d'enrobage diminue du fait de l'envasement par des particules de sol.

Le problème d'une couche, moins perméable que le sol, autour d'un drain, a été étudié de façon moins approfondie que celui des enrobage de perméabilité relative plus grande. Un certain nombre d'expériences en laboratoire ont confirmé que la présence d'une telle couche peut rendre le drainage inefficace.

Le problème ne peut être résolu par la méthode analytique que si la couche à perméabilité relative plus faible est suffisamment épaisse. En ce qui concerne les couches plus minces, le problème d'écoulement bidimensionnel a été abordé par la méthode numérique par WIDMOSER (1968). Il a aussi été simulé au moyen du modèle éléctrolytique par une méthode analogue à celle utilisée pour les enrobages à perméabilité relative plus grande. L'influence de l'épaisseur et celle du degré de perméabilité relative reduite ont été étudiées ainsi l'influence du nombre de rangées de perforations et celle du diamètre du drain. Il ressort de ces recherches qu'une couche à perméabili-

té relative reduite autour du drain fait augmenter considérablement la résistance d'entrée, qui atteint très rapidement des valeurs inacceptables. Une résistance d'entrée constante est obtenue à partir d'une épaisseur d'environ 10 mm (fig. 3.8). Le rayon effectif diminue et l'augmentation de la résistance radiale aboutit à l'obtention de valeurs exceptionnellement basses. L'augmentation de la résistance d'entrée et la diminution du rayon effectif sont fortement accentuées à partir d'une perméabilité relative de 0,2 (fig. 3.9). La différence en résistance d'entrée entre tuyaux de drainage différents devient aussi plus prononcée à partir d'une perméabilité relative de 0,1 (fig. 3.11).

En ce qui concerne les tuyaux de drainage pourvus d'un enrobage présentant partiellement une perméabilité diminuée, on a simulé des couches à perméabilité diminuée sur 25 % et 50 % de l'épaisseur initiale d'enrobage. A cette fin, deux tuyaux à points de contact isolés ont été placés concentriquement l'un dans l'autre afin de séparer 3 électrolytes.

Les expériences ont démontré que la résistance d'entrée du tuyau n'est influencée que dans une mesure très limitée par cet agencement. Les rayons effectifs diminueront néanmoins, du fait de la résistance radiale, à mesure que la perméabilité relative de la couche moins perméable diminue et à mesure que l'épaisseur de cette couche augmente (fig. 3.14 et 3.15). Le rayon effectif ne se réduit toutefois jamais aux valeurs extrêmement faibles que l'on obtient pour un drain enrobé directement d'une couche à perméabilité relative plus faible. Lorsque les conditions d'exécution du drainage ne sont pas idéales, l'effet drainant d'un tuyau de drainage pourvu d'un enrobage sera sensiblement meilleur que celui d'un tuyau sans enrobage. Il ne peut en résulter un moins bon effet de drainage que si la diminution de perméabilité a son origine dans un colmatage de l'enrobage. Ceci ne se produira que si la perméabilité de la couche moins perméable devient notablement inférieure à celle du sol environnant.

CHAPITRE IV

Lorsque l'eau afflue de toutes les directions vers un drain entièrement plein, la résistance d'entrée est une constante qui n'est déterminée que par les caractéristiques du tuyau même. Il est important de caractériser exactement la distribution de ce flux sous peine d'en tirer des conclusions

erronées quant à la résistance d'entrée. Si cette caractérisation exacte n'est pas possible, la résistance d'entrée, la résistance additionnelle résultant d'un écoulement non radial et la résistance radiale fictive peuvent être définies comme *une résistance de flux*. Lorsque l'eau afflue de toutes les directions vers un drain qui ne se remplit pas entièrement, la résistance d'entrée n'est pas modifiée et ce n'est qu'en cas de sous-pression régnant au-dessus du drain que les filets liquides seront déviés autour du drain et qu'il faut tenir compte des rangées de perforations agissantes pour déterminer la résistance d'entrée.

Si le drain qui ne se remplit pas entièrement est pourvu d'un matériau d'enrobage, le flux peut se diriger également via l'enrobage vers la partie remplie d'eau du tuyau de drainage.

Du fait de la résistance d'entrée, le gradient hydraulique au voisinage des perforations peut atteindre des valeurs très élevées, avec la conséquence que des particules de sol peuvent pénétrer en masse dans le tuyau, surtout par en dessous. Ces gradients hydrauliques sont fortement réduits quand un matériau d'enrobage relativement plus perméable est appliqué autour du drain.

Quand on détermine la distance entre drains, il faut tenir compte de la résistance d'entrée. Quoique les conditions de flux deviennent plus favorables s'il y a de l'eau au-dessus du drain, la résistance d'entrée qui détermine l'existence d'un certain niveau d'eau au-dessus du drain, provoquera une plus grande élévation de la nappe d'eau entre les drains que le drain idéal débouchant sous eau à la même profondeur.

Des recherches supplémentaires sur ces aspects de la résistance d'entrée sont toutefois nécessaires pour en acquérir des notions plus précises et pour permettre des jugements plus définitifs.

ZUSAMMENFASSUNG UND SCHLUSSFOLGERUNGEN

UNTERSUCHUNGEN MITTELS EINES ELEKTROLYTMODELLES ÜBER DEN EINFLUSS DER WASSEREINTRITTSÖFFNUNGEN UND ANGRENZENDEN SCHICHTEN AUF DIE ENTWÄSSERUNGSWIRKUNG VON DRÄNROHREN

In fast allen Formeln zur Bestimmung des Dränabstandes wird ein ideales Dränrohr angenommen. Das reelle Dränrohr besteht aus einer mit Eintrittsöffnungen versehenen undurchlässigen Wand. Die Strömungslinien konvergieren nach den Öffnungen und verursachen einen Eintrittswiderstand, der den tatsächlichen Radius des reellen Dränrohres reduziert.

ABSCHNITT I

Der Eintrittswiderstand ist, neben den Charakteristiken des Rohres, auch abhängig von der Beschaffenheit der Grenzflächen zwischen den Bodenteilchen und den Öffnungen. Wenn flache und gewölbte Grenzflächen vorliegen, kann der Eintrittswiderstand glatter Rohre, die mit bestimmten Perforationsformen und Perforationsverteilungen ausgestattet sind, analytisch wiedergegeben werden. Dies ist der Fall bei :

- Stossfugen oder ununterbrochenen Querspalten (KOZENY, 1933; KIRKHAM, 1950; ENGELUND, 1953; ERNST, 1962; SNEYD & HOSKING, 1976);
- Kreisförmigen Perforationen (MUSKAT, 1942; KIRKHAM & SCHWAB, 1951; ENGELUND, 1953);
- ununterbrochenen Längsspalten (MUSKAT, 1942; ENGELUND, 1953);
- unterbrochenen Längs- und Querspalten oder rechteckigen Perforationen (MUSKAT, 1942; CAVELAARS, 1970).

Nur SCHWAB & KIRKHAM (1951) haben die theoretischen Lösungen von KIRKHAM & SCHWAB (1951) und von KIRKHAM (1950) mit den anhand eines Electrolytmodelles erzielten Ergebnissen verglichen. Ausserdem ist die entwässernde Wirkung glatter Kunststoffdränrohre und die der üblichen Tonrohre anhand von Sandmodellen häufig untersucht worden. Letztere sind auch verwendet worden, um den Einfluss der Perforationsform und der Perforationsverteilung auf die

entwässernde Wirkung von sowohl glatten als auch gewellten Kunststoffdränrohren zu studieren sowie zu optimieren. Auch das Electrolytmodell wurde zu diesem Zwecke verwendet. Der Einfluss eines reellen Rohres auf den Stand und die Form des Grundwasserspiegels ist ebenfalls mit Hilfe von Sandmodellen untersucht worden.

Da sich das Sandmodell für einen genauen Versuch weniger gut eignet, wurde das Electrolytmodell gewählt. Mit diesem wurden verschiedene theoretischen Lösungen auf ihre Gültigkeit untersucht und die Faktoren, die den Eintrittswiderstand bestimmen, festgelegt.

Das Elektrolytmodell, das zur Simulation einer Radialströmung zum Dränrohr gefertigt wurde, war mit einer verstellbaren Messbrücke ausgestattet, die mit einem Messfühler verbunden war. Die Spannungsverteilung zwischen den beiden durch eine zylindrische Äquipotentialfläche und ein Modell des zu simulierenden Dränrohres gebildeten Elektroden konnte an jeder beliebigen Radialfläche in verschiedenen Tiefen bestimmt werden. Die folgende Dränrohre wurden simuliert :

- glatte Rohre mit einem Aussendurchmesser von 75 mm; Rohrlänge 300 mm; Breite der ununterbrochenen Querspalten schwankend (S^1_{co}-Dränrohre);
- glatte Rohre mit einem Aussendurchmesser von 40 mm; 1 mm breite ununterbrochene Querspalten mit wechselndem Abstand [S^2_{co}(1)-Dränrohre];
- glatte Rohre mit einem Aussendurchmesser von 39,9 mm; kreisförmige quadratisch angeordnete Perforationen verschiedenen Durchmessers [S^1_{cp}(2)-Dränrohre; S^1_{cp}(3)-Dränrohre; S^1_{cp}(4)-Dränrohre; S^1_{cp}(6)-Dränrohre; S^1_{cp}(8)-Dränrohre; S^1_{cp}(10)-Dränrohre];
- glatte Rohre mit kreisförmigen, quadratisch angeordneten Perforationen (Durchmesser 3 mm), mit einem Durchmesser von 50 mm [S^2_{cp}(3)-Dränrohre]; 63,5 mm [S^3_{cp}(3)-Dränrohre] und 70 mm [S^4_{cp}(3)-Dränrohre];
- glatte Rohre mit einem Aussendurchmesser von 40 mm; 1 mm breite ununterbrochene Längsspalten [S^1_{cls}(1)-Dränrohre];
- glatte Rohre mit einem Aussendurchmesser von 40 mm; rechteckig angeordnete, 1 mm breite unterbrochene Längsspalten [S^1_{dls}(1)-Dränrohre] bzw. unterbrochene Querspalten [S^1_{dcs}(1)-Dränrohre];
- Wellrohre mit einem Aussendurchmesser von 50 mm; ununterbrochene Querspalten (C_{co}-Dränrohre) bzw. rechteckig angeordnete 1 mm breite unterbrochene Querspalten [C^1_{dcs}(1)-Dränrohren].

Die Lösungen für Tonrohre mit Stossfugen oder, allgemeiner formuliert, für glatte Rohre mit ununterbrochenen Querspalten von KIRKHAM (1950) und ENGELUND (1953) ergeben etwas zu grosse Werte des Eintrittswiderstandes. Die Lösungen von SNEYD & HOSKING (1976) für flache Begrenzung und von SNEYD (1976) für gewölbte Begrenzung geben sehr gute Annäherungswerte. Mit hilfe einer Tabelle werden die Berechnungen nach diesen Lösungen stark vereinfacht. Die davon abgeleiteten Gleichungen (1.31) und (1.32) können ebenfalls mit ausreichender Genauigkeit angewandt werden. Diese Lösungen verbessern ausserdem die ziemlich einfache Lösung von ENGELUND (1953). Die Lösung von KOZENY (1933), die modifizierte Lösung in Appendix I und die Lösung von ERNST (1962) geben nur annähernde Werte für eine Rohrlänge von 300 mm. An kürzeren Rohrlängen wurden erhebliche Abweichungen festgestellt, so dass diese Lösungen nicht allgemein gültig sind.

Für gewölbte Grenzflächen von glatten Rohren mit kreisförmiger Perforation gibt die Lösung von KIRKHAM & SCHWAB (1951), die übrigens der von MUSKAT (1942) entspricht, Eintrittswiderstandswerte an die um 50 % zu niedrig sind weil die Undurchlässigkeit der Rohrwand ausser Betracht gelassen wurde. Bei flacher Begrenzung zeigt die Lösung von KIRKHAM & SCHWAB (1951) auch nach Verbesserung mit einem Faktor 2 noch erhebliche Abweichungen; eine zweite Korrektion ergibt die Gleichung (1.41). Diese abgeänderten Lösungen können, wie auch die Lösung von ENGELUND (1953) für eine rechteckige und die von CAVELAARS (1967) für eine quadratische Perforationsausführung mit genügender Genauigkeit angewendt werden. Der einfachen Form wegen werden die Lösungen von ENGELUND (1953) und CAVELAARS (1967) bevorzugt.

Die Lösung von MUSKAT (1942) für glatte Rohre mit ununterbrochenen Längsspalten entspricht, nach Verbesserung mit einem Faktor 2, der einfachen Lösung von ENGELUND (1953). Diese Lösung kann mit genügender Genauigkeit angewandt werden.

Für glatte Rohre mit unterbrochenen Längsspalten bietet MUSKAT (1942) eine Lösung, die nach Verbesserung mit einem Faktor 2, ziemlich genaue Eintrittswiderstände gibt. Auch die Lösung von CAVELAARS (1970), die von der Strömung nach einem nur unvollständig durchlässigen Brunnen in einer gespannten Grundwasserschicht abgeleitet ist, kann als allgemein gültig betrachtet werden. Es wurden ebenso Lösungen für unterbrochene Längsspalten aus den von MUSKAT (1946) gegebenen Lösungen für Strömungen nach einem unvollständig durchlässigen Brunnen in einer gespannten Grundwasserschicht abgeleitet.

Diese Lösungen findet man für eine gewölbte Grenzfläche in Gleichung (1.64) sowie (1.66) und für eine flache Grenzfläche in Gleichung (1.65) sowie (1.67). Auch von der von DE GLEE (1930) vorgeschlagenen Lösung für Brunnenströmungen wurden die Gleichung (1.68) für eine gewölbte und die Gleichung (1.69) für eine flache Grenzfläche, die für unterbrochene Längsspalten gelten, abgeleitet. Alle diese Lösungen erzielen Ergebnisse, die ziemlich gut übereinstimmen. Die Lösung von CAVELAARS (1970) ist mit Hilfe einer Tabelle oder Graphik ziemlich einfach. Auch die Gleichungen (1.66) und (1.67) können mit Tabellen, die die Gammafunktion anzeigen, noch relativ einfach durchgerechnet werden. Mit den Gleichungen (1.68) und (1.69) wird jedoch die einfachste Lösung mit einer für die praktische Anwendung ausreichenden Genauigkeit erzielt.

An glatten Rohren mit unterbrochenen Querspalten können die gleichen Formeln angewandt werden. Die einfachsten Lösungen erzielen die Gleichungen (1.74) und (1.76) von CAVELAARS (1970). Auch die Gleichungen (1.84) und (1.85), die von der Lösung von DE GLEE (1930) für Brunnenströmung abgeleitet sind, können ziemlich einfach durchgerechnet werden. Die Gleichungen (1.82) und (1.83), die von der von MUSKAT (1946) gegebenen Lösung für Brunnenströmung abgeleitet sind, können mit Tabellen der Gammafunktion noch relativ einfach gelöst werden, während die Gleichungen (1.80) und (1.81) ziemlich verwickelten Berechnungen erfordern.

Diese theoretischen Lösungen für glatte Rohre können nicht ohne weiteres an Wellrohren mit Perforationen in den Wellentälern angewandt werden, sofern angenommen wird, dass die Wellentäler mit Erde gefüllt sind. Für eine gegebene Perforationsausführung haben Wellrohre eines bestimmten Durchmesser einen höheren Eintrittswiderstand als glatte Rohre. Aus praktischen Gründen sind glatte Rohre weniger perforiert als Wellrohre, so dass der Eintrittswiderstand an Wellrohren der grösseren Perforierung wegen allgemein geringer ist. Theoretische Lösungen für Wellrohre sind nicht vorhanden. Die Gleichung (1.122) gibt eine theoretische Lösung für Rohre mit blockförmigen Wellen, die mit ununterbrochenen Querspalten versehen sind und deren Breite der des Wellentals entspricht. Die Spalten befinden sich im Wellental und bilden mit den Bodenteilchen eine flache Grenzfläche. Die Gleichung (1.126) gibt eine theoretische Lösung für ununterbrochene Querspalten mit einer Breite kleiner als die des Wellentals. Für unterbrochene Querperforationen gibt die Gleichung (1.127) eine annähernde Lösung. In Falle von Wellrohren mit sinusförmigem Profil darf angenommen werden, dass der ungünstige Einfluss der et-

was günstigeren Zuströmungsverhältnisse wegen kleiner ist.

Wenn die Perforationen auf dem Wellenkamm angebracht sind, so können die Formeln für glatte Rohre angewandt werden, was nicht heisst, dass die Perforationen unbedingt auf dem Wellenkamm angebracht werden müssen. Ausserdem ist die Anwesenheit von Wellen als günstig zu betrachten, und zwar durch die Gewölbebildung des Bodens über den Wellen oder die grössere Durchlässigkeit des Bodens in den Wellentälern.

Es kann allgemein geschlossen werden, dass es ziemlich einfache und ausreichend genaue Lösungen für die Bestimmung des Eintrittswiderstandes glatter Rohre gibt. Die Wellenform und die Grenzflächenbildung des Bodens mit den Wellen erschweren jedoch die exakt theoretische Lösung für Wellrohre.

Aus der durchgeführten Untersuchung geht ausserdem noch hervor dass weder die gesamte Perforationsfläche noch der Perforationsumfang pro Einheitslänge des Dräns, sondern die Perforationsverteilung den Eintrittswiderstand bestimmen. Es kann jedoch angenommen werden, dass der Einfluss der Perforationsumfanges grösser ist als der der Perforationsfläche. Der Unterschied im Eintrittswiderstand ist, unabhängig von der Perforationsform, im Falle eines gleichen Perforationsumfanges kleiner als im Falle einer gleichen Perforationsfläche, besonders dann wenn die Perforationsflächen kleiner sind als 50 cm^2/m (fig. 1.44 und 1.45). Je grösser die Gliederung einer gegebenen Perforationsfläche wird, um so kleiner wird der Eintrittswiderstand. Die günstigsten Perforationen sind die mit der kleinsten Fläche oder mit dem kleinsten Umfang, wie die Kreisförmigen; unter den rechteckigen sind die mit der kleinsten Länge am günstigsten.

Eine Erhöhung der heutigen Perforationsfläche von 20 - 25 cm^2/m auf etwa 50 cm^2/m wird, ausser im Falle von kreisförmigen Perforationen, den Eintrittswiderstand erheblich vermindern.

ABSCHNITT II

Aus den Untersuchungen an Sandmodellen ergibt sich, dass die entwässernde Wirkung von Dränrohren durch die Anwendung von Umhüllungsmaterialien die eine grössere Durchlässigkeit besitzen als der umgebende Boden, erheblich verbessert wird. Dabei sind sowohl die Dicke als auch der Grad der Durchlässigkeit des Umhüllungsmaterials bestimmend.

Obwohl der Eintrittswiderstand umhüllter Dräne in verschiedener Weise definiert werden kann, bezieht sich dieser Begriff im strengsten Sinne nur auf das Rohr. Die verschiedenen Definitionen können jedoch durch Bestimmung des effektiven Radius in Übereinstimmung gebracht werden. Die Frage der Umhüllungsmaterialien, die eine grössere Durchlässigkeit besitzen als die des ungebenden Bodens, ist analytisch nur für voluminöse Umhüllungen zu lösen, wobei sich der Eintrittswiderstand des Rohres aus der Gleichung (2.8) ergibt. Die Frage der dünnen Umhüllungsmaterialien und der zweidimensionalen Strömung wurde numerisch von WIDMOSER (1968) und NIEUWENHUIS (1976) gelöst, so dass über den Einfluss der Dicke und des Grades der Durchlässigkeit von Umhüllungsmaterialien mehr Informationen erhalten wurden.

Der Einfluss der Umhüllungsmaterialien auf den Eintrittswiderstand wurde zum ersten Male mit Hilfe eines Electrolytmodells untersucht. Das Umhüllungsmaterial und der Boden wurden dabei durch zwei elektrolytische Flüssigkeiten, deren Leitfähigkeitsverhältnis mit dem Durchlässigkeitsverhältnis von Umhüllung und Boden übereinstimmte, simuliert. Die Trennung der Elektrolyte wurde durch eine aus Kardenbeschlag gefertigte und mit gegenseitig isolierten Kontaktpunten versehenem Rohr erzielt. Der Einfluss der Dicke und des Grades der Durchlässigkeit von Umhüllungsmaterialien wurde im Rahmen der zwei- und dreidimensionalen Strömungsfrage untersucht. Der Einfluss der Perforationsreihenzahl und des Durchmessers umhüllter Dräne wurde im Rahmen der zweidimensionalen Strömungsfrage studiert.

Aus den Versuchen geht hervor, dass der Eintrittswiderstand bis zu einer Dicke von etwa 5 mm des Umhüllungsmaterials stark abnimmt und alsdann konstant bleibt (fig. 2.11 und 2.12). Der Verminderung des Radialwiderstandes wegen erhöht sich der effektive Radius bei zunehmender Dicke jedoch weiter. Bei zunehmender relativer Durchlässigkeit des Umhüllungsmaterials bis auf das Zwanzigfache nimmt der Eintrittswiderstand stark ab und erhöht sich der effektive Radius erheblich (fig. 2.13). Weitere Erhöhung des Durchlässigkeitsverhältnisses hat nur geringen Einfluss.

Umhüllungsmaterialien gleichen die absolute Differenz zwischen dem Eintrittswiderstand verschiedener Dräne erheblich aus, sobald die relative Durchlässigkeit etwa 10 beträgt (fig. 2.13 und 2.15).

Es kann allgemein angenommen werden, dass das Umhüllungsmaterial bei einer Dicke zwischen 5 und 10 mm radial angeströmt wird. Der Rohrdurchmesser hat nur wenig Einfluss auf den Eintrittswiderstand von Dränen, die mit einer Umhüllung versehen sind; die effektiven Radien werden jedoch in Abhängigkeit

des Rohrradius und der Dicke des Umhüllungsmaterials differieren. Ist der Rohrradius plus die Dicke des Umhüllungsmaterials konstant, so wird etwa der gleiche effektive Radius beobachtet wenn die Dicke des Umhüllungsmaterials mindestens 5 mm beträgt. Zur Erhöhung des effektiven Radius ist es deshalb ökonomischer einen Drän mit kleinem Durchmesser und umfangreicherem Umhüllungsmaterial als einen Drän mit grösserem Durchmesser und dünnerer Umhüllungsschicht zu verwenden.

ABSCHNITT III

Die Umstände bei der Dränung bestimmen in hohem Masse die entwässernde Wirkung von Entwässerungsmaterialien. Unter bestimmten Umstände kann sich um den Drän, unabhängig davon, ob er mit Umhüllungsmaterial versehen ist, eine Schicht mit verminderter relativer Durchlässigkeit bilden, oder kann die ursprüngliche Durchlässigkeit des Umhüllungsmaterials durch Einspülung von Bodenteilchen beeinträchtigt werden.

Im Vergleich zu den Umhüllungsmaterialien mit grösserer relativer Durchlässigkeit wurde die Frage einer Schicht mit verminderter relativer Durchlässigkeit um den Drän weiniger intensiv studiert. Aus einer Anzahl Laboratoriumversuche geht hervor, dass eine Schicht mit verminderter relativer Durchlässigkeit um den Drän das Scheitern der Entwässerung veranlassen kann.

Analytisch ist die Frage erst zu lösen, wenn die Schicht mit verminderter relativer Durchlässigkeit genügend dick ist. Die zweidimensionale Strömungsfrage für dünnere Schichten ist numerisch von WIDMOSER (1968) untersucht worden. Diese Frage wurde in derselben Weise wie die der Umhüllungsmaterialien mit einer grösseren relativen Durchlässigkeit anhand des Elektrolytmodells simuliert. Besonders der Einfluss der Dicke und des Grades der verminderten relativen Durchlässigkeit sowie der Einfluss der Perforationsreihenanzahl und des Rohrdurchmessers werden untersucht. Aus den Versuchen geht hervor, dass eine Schicht mit verminderter relativer Durchlässigkeit um den Drän den Eintrittswiderstand stark erhöht, wobei ziemlich schnell umzulässige Werte beobachtet werden. Von einer Dicke von etwa 10 mm an wird ein konstanter Eintrittswiderstand erlangt (Fig. 3.8). Der effektive Radius nimmt weiter infolge der Erhöhung des Radialwiderstandes ab. Es werden ausserordentlich kleine Werten beobachtet. Die Erhöhung des Eintrittswiderstandes und die Verminderung des Effektiven Radius treten deutlich hervor, sobald das Durchlässigkeitsverhältnis 0,2 beträgt (fig. 3.9). Von einem Durchlässigkeits-

verhältnis von 0,1 an wird auch die Differenz zwischen den Eintrittswiderständen verschiedener Dräne erheblich deutlicher (Fig. 3.11).

Zur Untersuchung von Dränen, die mit einem Umhüllungsmaterial mit z.T. verminderter Durchlässigkeit versehen sind, wurden Schichten mit einer verminderten Durchlässigkeit um 25 und 50 % der ursprünglichen Dicke des Umhüllungsmaterials simuliert. Zu diesem Zwecke wurden zwei Rohre mit isolierten Kontaktpunkten zur Trennung von drei Elektrolyten konzentrisch ineinandergeschoben.

Aus dem durchgeführten Versuch ergibt sich, dass der Eintrittswiderstand des Rohres nur in sehr beschränkten Mass durch ein Umhüllungsmaterial mit z.T. verminderter Durchlässigkeit beeinflusst wird. Dem Radialwiderstand zufolge vermindern sich die effektiven Radien mit abnehmender Durchlässigkeit bzw. grösser werdender Dicke der Schicht mit verminderter relativer Durchlässigkeit (Fig. 3.14 und 3.15). Die extrem kleinen Werte des effektiven Radius, die an einem mit einer gering durchlässigen Schicht umgebenen Drän beobachtet wurden, konnten hier jedoch nicht ermittelt werden. Wenn die Bedingungen für die Verlegung der Dräne nicht ideal sind, ist die entwässernde Wirkung eines mit einem Umhüllungsmaterial versehenen Dräns erheblich besser, als die eines Dräns ohne Umhüllungsmaterial. Nur wenn die Durchlässigkeit durch Verstopfung des Umhüllungsmaterials kleiner wird, kann die entwässernde Wirkung beeinträchtigt werden. Dies ist jedoch nur der Fall, wenn die Durchlässigkeit der weniger durchlässigen Schicht erheblich kleiner wird als die des umgebenden Bodens.

ABSCHNITT IV

Bei einer allseitigen Strömung nach einem vollaufden Drän ist der Eintrittswiderstand eine Konstante, die nur durch die geometrischen Charakteristiken des Rohres selbst bestimmt wird. Wichtig ist, dass das Strömungsbild genau bezeichnet wird; ist dies nicht der Fall, so kann der Eintrittswiderstand falsch interpretiert werden. Kann das Strömungsbild nicht genau bezeichnet werden, so sind der Eintrittswiderstand, der zusätzliche Widerstand infolge einer nichtradialen Strömung und der fiktive Radialwiderstand als *Zuströmungswiderstand* zu deuten. Bei einer allseitigen Strömung nach einem nicht vollaufden Drän ändert sich der Eintrittswiderstand nicht; nur wenn über dem Drän Unterdruck herrscht, biegen die Strömungslinien um den

Drän ab, so dass bei der Bestimmung des Eintrittswiderstandes die wirksamen Perforationsreihen berücksichtigt werden sollten.

Ist der nicht vollaufende Drän mit einem Umhüllungsmaterial versehen, so kann die Strömung über die Umhüllung nach dem mit Wasser gefüllten Teil des Dräns stattfinden.

Dem Eintrittswiderstand zufolge kann der hydraulischen Gradient in der Nähe der Perforationen sehr stark ansteigen, wodurch Bodenteilchen besonders über die Unterseite in grosser Menge in den Drän dringen können. Die hydraulischen Gradiente können stark reduziert werden, wenn der Drän mit einem durchlässigeren Umhüllungsmaterial versehen wird.

Bei der Bestimmung des Dränabstandes soll der Eintrittswiderstand berücksichtigt werden. Obwohl die Zuströmungsverhältnisse günstiger werden, wenn sich über dem Drän Wasser befindet, erhöht der Eintrittswiderstand, der einem bestimmten Wasserstand über dem Drän bedingt, den Grundwasserspiegel zwischen den Dränen in stärkerem Masse als der in derselben Tiefe unter Wasser ausmündende ideale Drän.

Die verschiedenen Aspekte des Eintrittswiderstandes sind jedoch näher zu untersuchen, bevor endgültige Schlüsse gezogen werden können.

APPENDIX I : Modified solution of KOZENY (1933)

Considering radial flow towards one gap between clay drain pipes (fig. I.1), the torus ABC DEF is an equipotential plane of which the area can be determined in the following way :

$$dA = 2 \pi R^{*} \, dp$$

where $dp = r \, d\varphi$ (φ in radians)

$R^{*} = R_o + r \cos \varphi$

or

$$dA = 2 \pi (R_o + r \cos \varphi) \, r \, d\varphi = 2 \pi R_o \, r \, d\varphi + 2 \pi r^2 \cos \varphi \, d\varphi$$

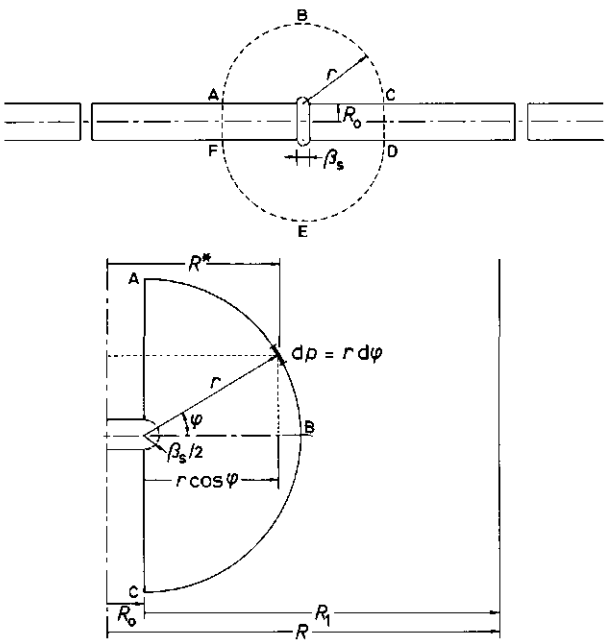

Fig. I.1

Integration with respect to φ between the limits $\varphi = -\pi/2$ to $\varphi = +\pi/2$ gives :

$$A = 2\,\pi\,R_o\,r\int_{-\pi/2}^{+\pi/2} d\varphi + 2\,\pi\,r^2\int_{-\pi/2}^{+\pi/2}\cos\varphi\,d\varphi$$

or

$$A = 2\,\pi\,r(\pi\,R_o + 2\,r)$$

According to DARCY's law, we can write that

$$dh = \frac{Q_g}{k}\frac{dr}{A} = \frac{Q_g}{2\,\pi\,k}\frac{dr}{r(\pi\,R_o + 2\,r)}$$

and integration with respect to r between the limits $r = \beta_s/2$ to $r = R_1$ yields :

$$\Delta h = \frac{Q_g}{2\,\pi\,k}\int_{\beta_s/2}^{R_1}\frac{dr}{r(\pi\,R_o + 2\,r)}$$

or

$$\Delta h = \frac{Q_g}{2\,\pi^2\,k\,R_o}\ln\frac{2\,R_1(\pi\,R_o + \beta_s)}{\beta_s(\pi\,R_o + 2\,R_1)}$$

where Δh : head loss between the equipotentials with radii R_1 and $\beta_s/2$ (m)

Q_g : flow rate towards one gap (m^3/d)

k : hydraulic conductivity (m/d)

R_o : drain radius (m)

β_s : gap width (m).

This equation corresponds to eqn. (16) of KOZENY (1933).

For radial flow towards a series of gaps at spacings c, the other gaps influence the hydraulic head in P and Q (fig. I.2). The additional head loss between P and Q due to a series of gaps must be added to the head loss for one gap. For the n^{th} gap N at a distance $r_n = \sqrt{(n\,c)^2 + R_1^2}$ from P and a distance $r_n^\star = n\,c$ from Q, the head losses are :

$$\Delta h_{PN} = \frac{Q_g}{2\,\pi^2\,k\,R_o}\ln\frac{2\,r_n(\pi\,R_o + \beta_s)}{\beta_s(\pi\,R_o + 2\,r_n)}$$

$$\Delta h_{QN} = \frac{Q_g}{2\,\pi^2\,k\,R_o}\ln\frac{2\,r_n^\star(\pi\,R_o + \beta_s)}{\beta_s(\pi\,R_o + 2\,r_n^\star)}$$

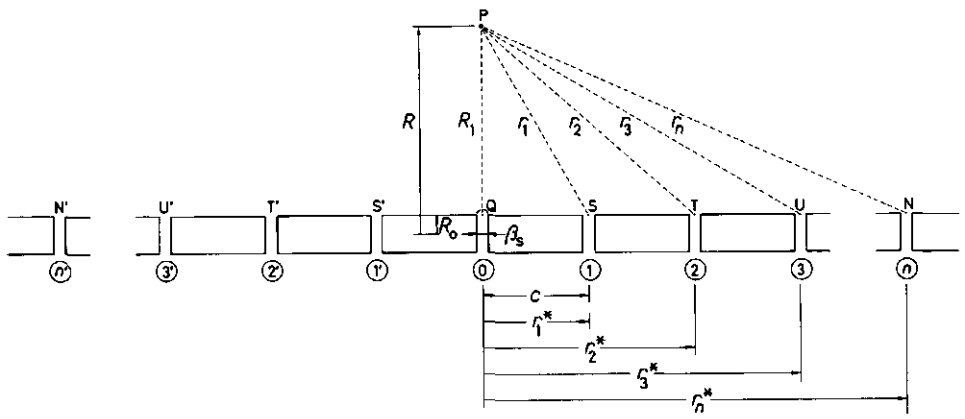

Fig. I.2

and

$$\Delta h_{PQ} = \frac{Q_g}{2\,\pi^2\,k\,R_o}\,\ln\frac{r_n(\pi\,R_o + 2\,r_n^*)}{r_n^*(\pi\,R_o + 2\,r_n)} = \frac{Q_g}{2\,\pi^2\,k\,R_o}\,\ln\frac{2 + \dfrac{\pi\,R_o}{n\,c}}{2 + \dfrac{\pi\,R_o}{\sqrt{(n\,c)^2 + R_1^2}}}$$

Since there are two gaps in the n^{th} position (N and N'), the total influence will be twice as large and

$$\Delta h_{PQ} = \frac{Q_g}{2\,\pi^2\,k\,R_o}\,2\,\ln\frac{2 + \dfrac{\pi\,R_o}{n\,c}}{2 + \dfrac{\pi\,R_o}{\sqrt{(n\,c)^2 + R_1^2}}}$$

Finally, for all gaps, the total head loss Δh_t is given by :

$$\Delta h_t = \frac{Q_g}{2\,\pi^2\,k\,R_o}\left\{\ln\frac{2\,R_1(\pi\,R_o + \beta_s)}{\beta_s(\pi\,R_o + 2\,R_1)} + 2\sum_{n=1}^{\infty}\ln\frac{2 + \dfrac{\pi\,R_o}{n\,c}}{2 + \dfrac{\pi\,R_o}{\sqrt{(n\,c)^2 + R_1^2}}}\right\}$$

Since $Q_g = q\,c$ with q the discharge per unit drain length and the head loss for radial flow $\Delta h_r = (q/2\,\pi\,k)\,\ln(R/R_o)$ with $R = R_o + R_1$, the additional

head loss due to the gaps is given by

$$\Delta h_t - \Delta h_r = \frac{q\,c}{2\,\pi^2\,k\,R_o}\left\{\ln\frac{2\,R_1(\pi\,R_o+\beta_s)}{\beta_s(\pi\,R_o+2\,R_1)} + 2\sum_{n=1}^{\infty}\ln\frac{2+\frac{\pi\,R_o}{n\,c}}{2+\frac{\pi\,R_o}{\sqrt{(n\,c)^2+R_1^2}}}\right\} - \frac{q}{2\,\pi\,k}\ln\frac{R}{R_o}$$

Since

$$\Delta h_t = \frac{q}{k}(\alpha_r+\alpha_e) \quad \text{or} \quad \alpha_e = \frac{\Delta h_t\,k}{q} - \alpha_r$$

the entrance resistance α_{ea} for arched boundary conditions is given by :

$$\alpha_{ea} = \frac{c}{2\,\pi^2\,R_o}\ln\frac{2\,R_1(\pi\,R_o+\beta_s)}{\beta_s(2\,R_1+\pi\,R_o)} + \frac{c}{\pi^2\,R_o}\sum_{n=1}^{\infty}\ln\frac{2+\frac{\pi\,R_o}{n\,c}}{2+\frac{\pi\,R_o}{\sqrt{(n\,c)^2+R_1^2}}} - \frac{1}{2\,\pi}\ln\frac{R}{R_o}$$

which is eqn. (1.22) for arched boundary conditions. Similar to other equations for circumferential and continuous longitudinal slits, the entrance resistance α_{ep} for plane boundary conditions has been obtained by substituting $\beta_s/2$ for β_s, resulting in

$$\alpha_{ep} = \frac{c}{2\,\pi^2\,R_o}\ln\frac{2\,R_1(2\,\pi\,R_o+\beta_s)}{\beta_s(2\,R_1+\pi\,R_o)} + \frac{c}{\pi^2\,R_o}\sum_{n=1}^{\infty}\ln\frac{2+\frac{\pi\,R_o}{n\,c}}{2+\frac{\pi\,R_o}{\sqrt{(n\,c)^2+R_1^2}}} - \frac{1}{2\,\pi}\ln\frac{R}{R_o}$$

which is eqn. (1.23) for plane boundary conditions.

APPENDIX II : Mathematical proof that $\sum_{i=1}^{N-1} \ln(2 \sin \frac{\theta_i}{2}) = \ln N$

Since $\theta_i = \frac{2\pi i}{N}$ or $\frac{\theta_i}{2} = \frac{\pi i}{N}$, $i = 1, 2, \ldots\ldots N-1$, we may write that

$$\sum_{i=1}^{N-1} \ln(2 \sin \frac{\theta_i}{2}) = \sum_{i=1}^{N-1} \ln(2 \sin \frac{\pi i}{N})$$

or

$$\ln \prod_{i=1}^{N-1} (2 \sin \frac{\theta_i}{2}) = \ln \prod_{i=1}^{N-1} (2 \sin \frac{\pi i}{N})$$

In the product, we have $N-1$ factors of 2, hence

$$\prod_{i=1}^{N-1} (2 \sin \frac{\pi i}{N}) = 2^{N-1} \prod_{i=1}^{N-1} \sin(\frac{\pi i}{N})$$

According to § 1.392 of GRADSHTEYN & RYZHIK (1965) on p. 33 we may write

$$\sin(N x) = 2^{N-1} \prod_{i=0}^{N-1} \sin(x + \frac{\pi i}{N})$$

or

$$\sin(N x) = 2^{N-1} \sin x \prod_{i=1}^{N-1} \sin(x + \frac{\pi i}{N})$$

or

$$\frac{\sin(N x)}{\sin x} = 2^{N-1} \prod_{i=1}^{N-1} \sin(x + \frac{\pi i}{N})$$

Since $x = 0$, we have that

$$2^{N-1} \prod_{i=1}^{N-1} \sin \frac{\pi i}{N} = \lim_{x \to 0} \left\{ 2^{N-1} \prod_{i=1}^{N-1} \sin(x + \frac{\pi i}{N}) \right\} = \lim_{x \to 0} \frac{\sin(N x)}{\sin x}$$

Applying L'HOSPITAL's rule, we finally obtained

$$\lim_{x \to 0} \frac{\sin(N x)}{\sin x} = \lim_{x \to 0} \frac{N \cos(N x)}{\cos x} = N$$

Hence

$$\sum_{i=1}^{N-1} \ln(2 \sin \frac{\theta_i}{2}) \equiv \ln N$$

APPENDIX III : Determination of the coefficient of 3,91 in the formulae of ENGELUND (1953)

Proceeding on eqn. (1.38) which is the corrected solution of MUSKAT (1942) for arched boundary conditions :

$$\alpha_{ea} = \frac{1}{\pi N}\left[2 \sum_{n=1}^{\infty} K_o\left(\frac{n \pi \delta_p}{\lambda_r}\right) + 2 \sum_{i=1}^{N=1} \left\{ \sum_{n=1}^{\infty} K_o\left(\frac{4 n \pi R_o}{\lambda_r} \sin \frac{\theta i}{2}\right)\right\} + \ln \frac{2 R_o}{N \delta_p}\right]$$

we may write that

$$\alpha_{ea} = \frac{1}{\pi N}\left\{2 \sum_{n=1}^{\infty} K_o\left(\frac{n \pi \delta_p}{\lambda_r}\right) + \ln \frac{2 R_o}{N \delta_p}\right\}$$

if $R_o \gg \lambda_r$ because then $K_o \to 0$ so that the second term can be neglected. According to § 8.526 of GRADSHTEYN & RYZHIK (1965) on p. 978 we have that

$$\sum_{n=1}^{\infty} K_o(n x) = \frac{1}{2}(\gamma + \ln \frac{x}{4 \pi}) + \frac{\pi}{2 x} + \frac{1}{2} \sum_{n=1}^{\infty} \left\{ \frac{1}{\sqrt{(\frac{x}{2 \pi})^2 + n^2}} - \frac{1}{n}\right\}$$

or

$$2 \sum_{n=1}^{\infty} K_o\left(\frac{n \pi \delta_p}{\lambda_r}\right) = \gamma + \ln \frac{\delta_p}{4 \lambda_r} + \frac{\lambda_r}{\delta_p} + \sum_{n=1}^{\infty} \left\{ \frac{1}{\sqrt{\left(\frac{\delta_p}{2 \lambda_r}\right)^2 + n^2}} - \frac{1}{n}\right\}$$

In which γ is EULER's constant (γ = 0,577 21....). If $\delta_p \ll 2 \lambda_r$, the summation can be neglected and hence

$$2 \sum_{n=1}^{\infty} K_o\left(\frac{n \pi \delta_p}{\lambda_r}\right) = \gamma + \ln \frac{\delta_p}{4 \lambda_r} + \frac{\lambda_r}{\delta_p}$$

and

$$\alpha_{ea} = \frac{1}{\pi N}\left(\gamma + \ln \frac{\delta_p}{4 \lambda_r} + \frac{\lambda_r}{\delta_p} + \ln \frac{2 R_o}{N \delta_p}\right)$$

According to ENGELUND (1953), we may write that

$$\alpha_{ea} = \frac{1}{\pi m}\left(\frac{1}{\delta_p} - \frac{3,91}{2 \lambda_1} + \frac{1}{\lambda_1} \ln \frac{\lambda_2}{\lambda_1}\right)$$

with $\lambda_1 < \lambda_2$. If $\lambda_2 = \lambda_c$ and $\lambda_1 = \lambda_r$, with λ_c the circumferential and λ_r the longitudinal perforation spacing, we can write that

$$\alpha_{ea} = \frac{1}{\pi m}\left(\frac{1}{\delta_p} - \frac{3,91}{2\,\lambda_r} + \frac{1}{\lambda_r}\ln\frac{\lambda_c}{\lambda_r}\right)$$

or, since

$$m = \frac{2\,\pi\,R_o}{\lambda_c\,\lambda_r} \quad \text{and} \quad N = \frac{2\,\pi\,R_o}{\lambda_c}$$

we have that

$$\alpha_{ea} = \frac{1}{\pi N}\left(\frac{\lambda_r}{\delta_p} - \frac{3,91}{2} + \ln\frac{2\,\pi\,R_o}{N\,\lambda_r}\right)$$

Hence it follows that

$$\frac{\lambda_r}{\delta_p} - \frac{3,91}{2} + \ln\frac{2\,\pi\,R_o}{N\,\lambda_r} = \gamma + \ln\frac{\delta_p}{4\,\lambda_r} + \frac{\lambda_r}{\delta_p} + \ln\frac{2\,R_o}{N\,\delta_p}$$

or

$$3,91 \equiv 2\,\ln(4\,\pi) - 2\,\gamma$$

APPENDIX IV : Derivation of eqns. (1.64) and (1.66) from the solution of MUSKAT (1946) for a partially penetrating well.

Derivation of eqn. (1.64)

From the solution of MADELUNG (1918) for the electrical potential of a straight line of point charges, MUSKAT (1942) derived a solution for the hydraulic potential at wells with circular perforations, continuous or discontinuous longitudinal slits. It has been assumed that no significant error is introduced by not taking into account explicitly the presence of the impervious wall in which the perforations are embedded.

The entrance resistances obtained from that theoretical solution are halved compared to experimental results.

The problem can theoretically be solved by introducing a central source of strength $q/2$ besides the sinks of total strength q (see fig. 1.10). In that way the impervious wall of the pipe is a streamline and the boundary conditions are satisfied. This results in a somewhat different equation for the head loss Δh_t due to radial flow for a system of N slits per pitch than that which can be derived from MUSKAT (1942) :

$$\Delta h_t = \frac{q}{\pi N k \gamma}\left[2 \sum_{n=1}^{\infty} K_o(2 n \pi \rho_p) \int_{-\alpha_1}^{+\alpha_1} \cos(2 n \pi w - 2 n \pi \alpha)\, d\alpha \right.$$

$$+ 2 \sum_{i=1}^{N-1} \left\{ \sum_{n=1}^{\infty} K_o(4 n \pi \rho_d \sin \frac{\theta_i}{2}) \int_{-\alpha_1}^{+\alpha_1} \cos(2 n \pi w - 2 n \pi \alpha)\, d\alpha \right\} + \gamma \ln \frac{\rho_d}{\rho_p}$$

$$\left. - \gamma \ln N + \frac{N \gamma}{2} \ln \frac{\rho}{\rho_d} \right]$$

in which q is the discharge per unit pipe length and

$$\gamma = \frac{\lambda_p}{\lambda_r} \; ; \; \rho_p = \frac{\beta_p}{2 \lambda_r} \; ; \; \rho_d = \frac{R_o}{\lambda_r} \; ; \; \alpha_1 = \frac{\lambda_p}{2 \lambda_r} \; ; \; w = \frac{z}{\lambda_r} \; ; \; \rho = \frac{R}{\lambda_r} \; ;$$

z is the ordinate of a point of the perforation with the origin in the middle of the perforation.

Since

$$\int_{-\alpha_1}^{+\alpha_1} \cos(2\,n\,\pi\,w - 2\,n\,\pi\,\alpha)\,d\alpha = \frac{1}{\pi\,n}\cos(2\,n\,\pi\,w)\,\sin(n\,\pi\,\gamma)$$

and $z = 0$ in the middle of the perforation or $\cos(2\,n\,\pi\,w) = 1$, it follows that

$$\Delta h_t = \frac{q}{\pi\,N\,k}\left[2\sum_{n=1}^{\infty} K_o(2\,n\,\pi\,\rho_p)\,\frac{\sin(n\,\pi\,\gamma)}{n\,\pi\,\gamma}\right.$$

$$\left. + 2\sum_{i=1}^{N-1}\left\{\sum_{n=1}^{\infty} K_o(4\,n\,\pi\,\rho_d \sin\frac{\theta\,i}{2})\,\frac{\sin(n\,\pi\,\gamma)}{n\,\pi\,\gamma}\right\} + \ln\frac{\rho_d}{N\,\rho_p} + \frac{N}{2}\ln\frac{\rho}{\rho_d}\right]$$

After subtracting the radial flow resistance, we finally obtain for the entrance resistance of discontinuous longitudinal slits with arched boundary conditions :

$$\alpha_{ea} = \frac{1}{\pi\,N}\left[2\sum_{n=1}^{\infty} K_o\left(\frac{n\,\pi\,\beta_p}{\lambda_r}\right)\,\frac{\sin(n\,\pi\,\gamma)}{n\,\pi\,\gamma}\right.$$

$$\left. + 2\sum_{i=1}^{N-1}\left\{\sum_{n=1}^{\infty} K_o\left(\frac{4\,n\,\pi\,R_o}{\lambda_r}\sin\frac{\theta\,i}{2}\right)\,\frac{\sin(n\,\pi\,\gamma)}{n\,\pi\,\gamma}\right\} + \ln\frac{2\,R_o}{N\,\beta_p}\right]$$

This is eqn. (1.57). Since this equation is based on the assumptions of a constant potential and a uniform flux density over the entire length of the perforations, MUSKAT (1946) has modified his solution for flow towards a partially penetrating well on the bases of numerical calculations. He concluded that for a partially penetrating well extending to the upper or lower boundary of the aquifer, one may assume the flux density over the well to be uniform if z is taken at a quarter from the free end of the well. For a well situated symmetrically in the aquifer, this means that

$$z = \frac{3}{4}\,\frac{\lambda_p}{2} = \frac{3}{8}\,\lambda_p$$

or the effective average potential is situated one-eight of the way from the free ends. Introducing this value of z, we obtain for α_{ea} :

$$\alpha_{ea} = \frac{1}{\pi N}\left[2 \sum_{n=1}^{\infty} K_o\left(\frac{n \pi \beta_p}{\lambda_r}\right) \frac{\sin(n \pi \gamma)}{n \pi \gamma} \cos\left(\frac{3}{4} n \pi \gamma\right)\right.$$

$$\left. + 2 \sum_{i=1}^{N-1} \left\{ \sum_{n=1}^{\infty} K_o\left(\frac{4 n \pi R_o}{\lambda_r} \sin \frac{\theta_i}{2}\right) \frac{\sin(n \pi \gamma)}{n \pi \gamma} \cos\left(\frac{3}{4} n \pi \gamma\right) \right\} + \ln \frac{2 R_o}{N \beta_p}\right]$$

which is eqn. (1.64) for arched boundary conditions. Replacing β_p by $\beta_p/2$ results in eqn. (1.65) for plane boundary conditions.

Derivation of eqn. (1.66)

Eqn. (6) of MUSKAT (1946) on p. 274 gives the head loss for a partially penetrating well extending to the upper or lower boundary of a confined aquifer (fig. IV.1a) for which a uniform flux density has been assumed by taking the potential at a quarter from the free end of the well.

For a well situated symmetrically in the confined aquifer, using eqn. (6) of MUSKAT (1946) on p. 267, we may write, after integration with respect to α from $\alpha = x$ to $\alpha = y$, for the additional head loss Δh compared to a fully penetrating well [Hydrologisch Colloquium, 1964 : eqn. (7) on p. 81] :

$$\Delta h = \frac{Q}{2 \pi k \lambda_r}\left(\frac{1 - \gamma}{\gamma} \ln \frac{8 \lambda_r}{\beta_p} - \frac{1}{2 \gamma} \ln A\right)$$

in which

$$A = \frac{\Gamma(\omega - x)\ \Gamma(y - \omega)\ \Gamma(1 - \omega - x)\ \Gamma(y + \omega)}{\Gamma(1 - \omega + x)\ \Gamma(1 - y + \omega)\ \Gamma(\omega + x)\ \Gamma(1 - y - \omega)}$$

and

$$\omega = \frac{z}{2 \lambda_r} \; ; \; x = \frac{a}{2 \lambda_r} \; ; \; y = \frac{b}{2 \lambda_r} \; ; \; \gamma = \frac{\lambda_p}{\lambda_r}$$

Q is the well discharge and for the other symbols used reference is made to fig. IV,1b.

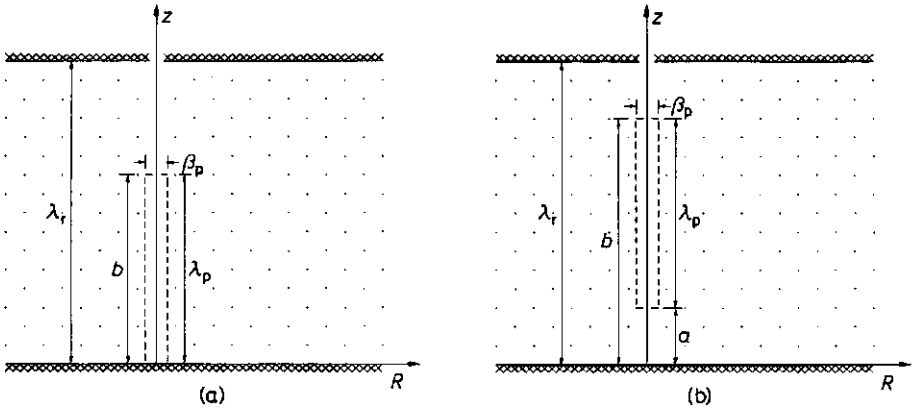

Fig. IV.1

Assuming a uniform flux density and taking the potential one-eight of the way from the free ends of the well, we may write that

$$w = \frac{1}{4} - \frac{3}{16}\gamma \; ; \; x = \frac{1-\gamma}{4} \text{ and } y = \frac{1+\gamma}{4}$$

Hence

$$A = \frac{\Gamma(\frac{1}{16}\gamma)\;\Gamma(\frac{7}{16}\gamma)\;\Gamma(\frac{1}{2}+\frac{7}{16}\gamma)\;\Gamma(\frac{1}{2}+\frac{1}{16}\gamma)}{\Gamma(1-\frac{1}{16}\gamma)\;\Gamma(1-\frac{7}{16}\gamma)\;\Gamma(\frac{1}{2}-\frac{7}{16}\gamma)\;\Gamma(\frac{1}{2}-\frac{1}{16}\gamma)}$$

Applying the reasoning of CAVELAARS (1970), we obtain for the additional head loss of half a cylindrical well and N such wells :

$$\Delta h = \frac{Q}{\pi\, N\, k\, \lambda_r}\left(\frac{1-\gamma}{\gamma}\ln\frac{8\,\lambda_r}{\beta_p} - \frac{1}{2\,\gamma}\ln A\right)$$

This is also the additional head loss due to the discontinuity of slits, and has to be added to the head loss for continuous longitudinal slits. Since $Q/\lambda_r = q$, the discharge per unit drain length, the entrance resistance for discontinuous longitudinal slits with arched boundary conditions can be derived :

$$\alpha_{ea} = \frac{1}{\pi N}\left[\ln \frac{2 R_o}{N \beta_p} + \frac{1-\gamma}{\gamma}\left\{\ln \frac{8 \lambda_r}{\beta_p} - \frac{1}{2(1-\gamma)} \ln \frac{\Gamma(\frac{1}{16}\gamma)\ \Gamma(\frac{7}{16}\gamma)\ \Gamma(\frac{1}{2}+\frac{7}{16}\gamma)\ \Gamma(\frac{1}{2}+\frac{1}{16}\gamma)}{\Gamma(1-\frac{1}{16}\gamma)\ \Gamma(1-\frac{7}{16}\gamma)\ \Gamma(\frac{1}{2}-\frac{7}{16}\gamma)\ \Gamma(\frac{1}{2}-\frac{1}{16}\gamma)}\right\}\right]$$

which is eqn. (1.66). Replacing β_p by $\beta_p/2$ results in eqn. (1.67) for discontinuous longitudinal slits with plane boundary conditions.

LITERATURE

BINSACK, R. 1961. Untersuchungen über die Eignung von Kunststoffrohren als Dränstränge. Das Kunststoffrohr 7 : 6-9. Hauszeitschr. des Kunststoffwerkes Gebr. Anger GMBH & CO. München.

BOUMANS, J.H. 1963. Over instroming en aanstroming bij draineerbuizen zonder en met afdekking. Cult. Tijdschr. 2 : 218-229.

BRAVO, N.J. & SCHWAB, G.O. 1977. Effect of openings on inflow into corrugated drains. Trans. A.S.A.E. 20, 1 : 100-104.

BURGHARDT, W. 1977 a. Zur technik, Durchführung und Auswertung von Modellversuchen im Dränkasten. Z.f. Kult. und Flurber. 18 : 83-91.

BURGHARDT, W. 1977 b. Zur Theorie und Methodik der Untersuchung der Dränfilterwirkung. C.R. Coll. Int. Sols Textiles. Paris, Volume II : 183-188.

BURGHARDT, W. 1977 c. Wasserbewegung am Dränrohr. Z.f. Kult. und Flurber. 18 : 166-177.

BURGHARDT, W. 1978. Die Wasserbewegung zum Dränrohr in Abhängigkeit von Richtung und Stärke der Anströmung, Rohrfüllung, Rohrdurchmesser und Vollfilterung. Z.f. Kult. und Flurber. 19 : 17-25.

CAVELAARS, J.C. 1962. Stroming van water naar drains. Tijdschr. Kon. Ned. Heidem. 73, 12 : 1-8.

CAVELAARS, J.C. 1966. Hydrological Aspects of the application of plastic drain pipes and filter materials. Hydrological and technical problems of land drainage. Discussions. Czechoslovak Nat. Commitee C.I.G.R., Prague : 71-88.

CAVELAARS, J.C. 1967. Problems of water entry into plastic and other drain tubes. Proc. Agr. Eng. Symp. A.E.S. Paper No. 5/E/46 : 13 p.

CAVELAARS, J.C. 1970. Toestromingsweerstanden bij buisdrainage. Kon. Ned. Heidem. Afdeling Onderzoek, Arnhem : 38 p.

CHEESEMAN, P.C.; HOSKING, R.J. & SNEYD, A.D. 1974. Effect of drain depth and gap width on potential flow in homogeneous porous soil. J. of Hydrology 21 : 219-229.

CHILDS, E.C. & YOUNGS, E.G. 1958. The nature of the drain channel as a factor in the design of a land-drainage system. Journ. Soil Sci. 9, 2 : 316-331.

CROS, Ph. 1973. Les essais des tuyaux de drainage effectués par le "Centre Technique du Génie Rural des Eaux et des Forets". Rapport particulier. Journées d'études Nationales à Orleans. Antony : 18 p.

DAGAN, G. 1964. Spacing of drains by an approximate method. J. Irr. Drain. Div. A.S.C.E. 90, IR1 : 41-66.

DE GLEE, G.J. 1930. Over grondwaterstromingen bij wateronttrekking door middel van putten. Techn. Boekhandel en Drukkerij J. Waltman, Delft : 175 p. (p. 79-93).

DE JAGER, A.W. 1960 a. Diameter en perforatie van plastic draineerbuizen. De Ingenieur 72, 46 : 167-172.

DE JAGER, A.W. 1960 b. Plastic draineerbuizen. Nieuwe mogelijkheden voor de mechanische uitvoering. Tijdschrift Ned. Heidem. 71, 7/8 : 194-200.

DE JAGER, A.W. 1960 c. Over het verstoppen van drainreeksen. Glasvlies als nieuw afdekkingsmateriaal. Waterschapsbelangen 24 : 198-201.

DE JAGER, A.W. 1962. Eintrittsöffnungen von Kunststoff-Dränrohren. Z.f. Kulturtechnik 1, 3 : 47-48.

DENNIS, C.W. & TRAFFORD, B.D. 1975. The effect of permeable surrounds on the performance of clay field drainage pipes. J. of Hydrology 24 : 239-249.

DIN 1180 Dränrohre. Abmessungen - Gütebestimmungen - Prüfung. Deutscher Normenausschuss. Beuth-Vertrieb GmbH. Berlin und Köln.

DODSON, C.R. & CARDWELL, W.T. Jr. 1945. Flow into slotted liners and an application of the theory to core analysis. Trans. Am. Inst. of Mining and Metallurgical Eng., Petroleum Division 160 : 53-63.

DUTZ, H.G. 1950. Flow of ponded water into tile drains as affected by space between individual tiles. Unpublished Master's Thesis. Iowa State College, Ames : 97 p.

EGGELSMANN, R. 1969. Akute Dränprobleme. Wasser und Boden 21 : 1-8.

ENGELUND, F. 1953. On the laminar and turbulent flows of ground water through homogeneous sand. Trans. Danish Acad. Techn. Sci., A.T.S. 3 : 1-105.

ERNST, L.F. 1954. Het berekenen van stationaire grondwaterstromingen, welke in een vertikaal vlak afgebeeld kunnen worden. Rapport IV. Landbouwproefstation en Bodemk. Inst. T.N.O. Groningen : 55 p.

ERNST, L.F. 1962. Grondwaterstromingen in de verzadigde zone en hun berekening bij de aanwezigheid van horizontale evenwijdige open leidingen. Versl. Land. Onderz. 67. 15. Pudoc. Wageningen : 189 p.

FEDDES, R.A. 1966. Recente ontwikkelingen in plastiek drainage.I.C.W. : 48 p.

FEICHTINGER, F. 1966. Die Wasseraufnahmefähigkeit der Dränrohre. Ein Vergleich von Ton- und Kunststoffrohrdränen. Österreichische Wasserwirtschaft 18, 11/12 : 247-255.

FORCHHEIMER, P. 1898. Grundwasserspiegel bei Brunnenanlagen. Z. des Oesterr. Ing.- und Arch. Vereines 50 : 629-635, 645-648.

FUJIOKA, Y. & MARUYAMA, T. 1970. Investigation on plastic pipe and its filter for underdrainage system. (In Japanese with English abstract) Trans. J.S.I.D.R.E. : 498-505 (From correspondence with TAJINO, N., Kagawa University, Japan).

GRADSHTEYN, I.S. & RYZHIK, I.M. 1965. Tables of integrals, series and products. Academic Press, London : 1086 p.

GUYK, I.; SORIANO, A. & KARADI, G.M. 1973. Flow towards periodic tile drains. Journ. of Hydrology 19 : 113-129.

HOMMA, F. 1973. Invloed van de doorlatendheid van de drainsleuf op de werking van een drainagesysteem. Cult. Tijdschr. 12, 5 : 207-218.

HOOGHOUDT, S.B. 1940. Bijdragen tot de kennis van eenige natuurkundige grootheden van de grond. 7. Algemeene beschouwing van het probleem van de detailontwatering en de infiltratie door middel van parallel loopende drains, greppels, slooten en kanalen. Versl. Land. Onderz. 46. 14 : 515-707.

HUISMAN, L. 1972. Groundwater recovery. Mac Millan London : 336 p. (p. 126-136).

HUSEMANN, C. & PAHLKE, K. 1969. Der Einfluss des Rohrmaterials auf den Erfolg der Dränung eines Brackmarschbodens. Z.f. Kult. und Flurber. 10 : 339-350.

Hydrologisch Colloquium. 1964. Steady flow of ground water towards wells. Versl. Med. Comm. Hydrol. Onderz. TNO No. 10 Den Haag : 179 p. (p. 67-97).

JONES, B.A. Jr. 1960. Effect of crack width at tile joints on soil movement into draintile lines. Transactions of the A.S.A.E. 3, 1 : 33-35, 41, 54.

JUUSELA, T. 1958. On the methods of protecting drain pipes and on the use of gravel as a protective material. Acta Agriculturae Scandinavica 8 : 62-87.

KABINA, P. 1969. Určenie optimálnej vel'kosti celkovej plochy vsakovacich otvorov na drénoch z plastických hmôt. (Determination of the optimum size of seeping openings on drains of plastics). Meliorace, Praha 5, 1 : 33-38.

KARPLUS, W.J. 1958. Analog Simulation. Solution of field problems. McGraw-Hill Book Company, Inc., London : 434 p. (p. 149-169).

KIRKHAM, D. 1950. Potential flow into circumferential openings in drain tubes. Journ. of appl. Physics 21 : 655-660.

KIRKHAM, D. 1958. Seepage of steady rainfall through soil into drains. Trans. Amer. Geophys. Union 39 : 892-908.

KIRKHAM, D. & POWERS, W.L. 1971. Advanced Soil Physics. Wiley-Interscience London : 534 p. (p. 219-228).

KIRKHAM, D. & SCHWAB, G.O. 1951. The effect of circular perforations on flow into subsurface drain tubes. Part I. Theory. Agr. Eng. 32, 4 : 211-214.

KOOPER, J. 1914. Beweging van het water in den bodem bij onttrekking door bronnen. De Ingenieur 38 : 697-706, 39 : 710-716.

KOWALD, R. 1963. Untersuchungen über die Stossfugen normaler Tondränrohre. Z.f. Kult. und Flurber. 20 : 300-307.

KOWALD, R. 1970. Die Strömungsverhältnisse an Tondränrohren und ihre Beeinflussung durch Rohrart, Stossfugenweite und Filter. Z.f. Kult. und Flurber. 11 : 151-161.

KOZENY, J. 1933. Über den Wasserzudrang bei Dränfugen. Wasserkraft und Wasserwirtschaft 2, 28 : 13-17.

KRUIJTZER, G.F.J. 1971. Stijghoogteverliezen in en rond putfilters. H_2O 4, 8 : 162-172.

KUNTZE, H. 1969. Forschritte der Dräntechnik - Grenzen der Dränerfolges. Verfahren zur Untergrundmelioration. Arb. der D.L.G. 126 : 12-33.

LIST, E.J. 1964. The steady flow of precipitation to an infinite series of tile drains above an impervious layer. J. Geophys. Res. 69 : 3371-3381.

LUTHIN, J.N. & HAIG, A. 1972. Some factors affecting flow into drainpipes. Hilgardia 41, 10 : 235-245.

MADELUNG, E. 1918. Das elektrische Feld in Systemen von regelmässig angeordneten Punktladungen. Physik. Zeitschrift 19, 524-533.

MANTEI, C.L. & WINGER, R.J. 1973. Flow into perforated corrugated drain tubing. A.S.A.E.-meeting, Chicago Paper 73-2510 : 8 p.

MEIJER, H.J. 1969. Enkele resultaten met metingen aan plastiek ribbeldrainbuis. Nota 519, I.C.W. Wageningen : 13 p.

MEIJER, H.J. 1972. Intreeweerstanden van ribbeldrainbuizen voorzien van machinaal aangebrachte omhullingsmaterialen. Nota 689, I.C.W. Wageningen : 17 p.

MEIJER, H.J. & FEDDES, R.A. 1972. Afdek- en omhullingsmaterialen bij plastic drainbuizen. Nota 690, I.C.W. Wageningen : 12 p.

MILLER, D.G. & SNYDER, C.G. 1944. Expansion of clay and concrete drain tile due to increasing of temperature and moisture content. Agr. Eng. 25 : 179-180.

MONKE, E.J. 1959. A study of water flow patterns near subsurface drains. Unpublished Ph. D. thesis. University of Illinois : 156 p.

MOODY, W.T. 1960. Effect of gap width on flow into drain tile. U.S. Depart. of the Interior Bureau of Reclamation. Memorandum to Chief, Off. of Drain. and Groundw. Eng. : 6 p.

MUSKAT, M. 1942. The effect of casing perforations on well productivity. Petroleum Technology 5 : 175-187.

MUSKAT, M. 1946. The flow of homogeneous fluids through porous media. 1st Ed. 2d Print. J.W. Edwards, Inc. Ann Arbor, Michigan : 763 p. (p. 258-286).

NIEUWENHUIS, G.J.A. 1976. De invloed van perforatie en filter op de intreeweerstanden van draineerbuizen. Nota 921. I.C.W. Wageningen : 53 p.

NIEUWENHUIS, G.J.A. & WESSELING, J. 1979. Effect of perforation and filter material on entrance resistance and effective diameter of plastic drain pipes. Agric. Water Managem. 2 : 1-9.

OEHLERS, T. 1932. Versuche über die Wasseraufnahme von Dränrohrleitungen. Zweiter Vorbericht. Der Kulturtechniker 4/5 : 299-305.

PESCHL, I.A.S.Z. 1969. Gewelfvorming in bunkers. Ph. D. Thesis. Technical University, Eindhoven : 175 p.

PILLSBURY, A.F.; PELISHEK, R.E. & BURAS, N. 1960. Wetting expansion of drain-tile and its effects on water entry. Trans. A.S.A.E. 3, 1 : 88-89.

RIBBENS, R.W. 1971. Flow into draintiles with pairs of drain holes. Unpublished memorandum to Chief, Drainage and Groundwater Branch, U.S. Bureau of Reclamation : 10 p.

ROTHER, L. 1904. Die Ergiebigkeit unvollkommener Brunnen. Journ. für Gasbeleuchtung und Wasserversorgung : 937-942, 957-962.

SAULMON, R.W. 1971. Need for envelope material above draintile. J. Irr. and Drain. Div. Proc. A.S.C.E. 97, IR4 : 661-663.

SCHWAB, G.O.; DEBOER, D.W. & JOHNSON, H.P. 1969. Effect of openings on design of subsurface drains. J. Irr. Drain. Div. Proc. A.S.C.E. 95, IR1 : 199-209.

SCHWAB, G.O. & KIRKHAM, D. 1951. The effect of circular perforations on flow into subsurface drain tubes. Part II. Experiments and results. Agr. Eng. 32, 5 : 270-274.

SEGEREN, W.A. & ZUIDEMA, F.C. 1969. Ontwikkelingen in de drainagetechniek. Cultuurtechnische Verhandelingen. Min. Landbouw en Visserij. Staatsuitgeverij 's Gravenhage : 325-357.

SISSON, D.R. & JONES, B.A. Jr. 1964. Filter materials for tile drains in a medium sand - A laboratory comparison. Trans. A.S.A.E. : 54-67.

SNEYD, A.D. 1976. Effect of semi-circular arches at drain gaps on drain conductance. J. of Hydrology 30 : 293-294.

SNEYD, A.D. & HOSKING, R.J. 1976. Seepage flow through homogeneous soil into a row of drain pipes. J. of Hydrology 30 : 127-146.

TERZAGHI, K. & PECK, R.B. 1965. Mécanique des sols appliquée aux travaux publics et au bâtiment. Dunod, Paris : 565 p. (p. 53-57).

VAN DEEMTER, J.J. 1950. Bijdrage tot de kennis van enige natuurkundige grootheden van de grond. 11. Theoretische en numerieke behandeling van ontwaterings- en infiltratiestromingsproblemen. Versl. Land. Onderz. 56. 7 : 1-67.

VAN DER BEKEN, A. 1962. De aanwending van plastic bij drainage. Rijkslandbouwhogeschool, Gent : 119 p.

VAN DER BEKEN, A. 1968. Filtermaterialen in de drainagetechniek. Mededelingen Rijksstation voor Landbouwtechniek - Merelbeke/Gent. Publ. nr. 30/WB-3 : 115 p.

VAN SOMEREN, C.L. 1964. De toepassing van plastieken draineerbuizen in Nederland (I). Cultuurtechniek 2, 1 : 4-10.

WATTS, D.G. & LUTHIN, J.N. 1963. Tests of thick fiberglass filters for subsurface drains. Hilgardia 35, 3 : 33-46.

WESSELING, J. 1957. Wanddikte, diameter en aantal perforaties van plastiekdraineerbuizen. Nota I.C.W. Wageningen : 7 p.

WESSELING, J. 1958. Verslag over het onderzoek naar de perforatie van plastic drainbuizen. Nota I.C.W. Wageningen : 6 p.

WESSELING, J. 1959. Enige resultaten van het onderzoek naar de perforatie van plastic draineerbuizen. Nota I.C.W. Wageningen : 9 p.

WESSELING, J. 1961. Toepassing van plastic bij drainage. Landb. Tijdschr. 73, 9 : 355-365.

WESSELING, J. 1964. The effect of using continually submerged drains on drain spacing. J. of Hydrology 2 : 33-44.

WESSELING, J. 1979. The entrance resistance of drains as a factor in design. Proceedings of the international Drainage Workshop. I.L.R.I. Wageningen. Paper 2.08 : 354-366.

WESSELING, J. & HOMMA, F. 1967. Entrance resistance of plastic drain tubes. Neth. J. Agric. Sci. 15 : 170-182 and Technical Bulletin 51, I.C.W. Wageningen.

WESSELING, J. & VAN SOMEREN, C.L. 1972. Drainage Materials - Provisional report of the experience gained in the Netherlands. Irr. and Drainage Paper 9 : Drainage Materials. F.A.O.-Rome : 55-84.

WIDMOSER, P. 1966. Potentialströmung zu geschlitzten Rohren. Schweizerische Bauzeitung 84, 52 : 913-919.

WIDMOSER, P. 1967. Etude de l'écoulement au voisinage immédiat des drains. Exposé dans le cadre du cours de perfectionnement pour ingénieurs du génie rural. E.P.F. Zurich : 28 p.

WIDMOSER, P. 1968. Der Einfluss von Zonen geänderter Durchlässigkeit im Bereich von Drain- und Brunnenfilterrohren. Schweizerische Bauzeitung 86, 9 : 135-144.

WIDMOSER, P. 1972. Etude de l'écoulement au voisinage-immédiat des drains. C.I.I.D. 8th Congress, Varna 28, 1 : 12-31.

WILLARDSON, L.S. 1967. Water entry into partially full subsurface drains. Unpublished Ph. D. Dissertation. Ohio State University, Columbus OH. : 194 p.

WILLARDSON, L.S. & WALKER, R.E. 1978. Protecting subsurface drains from sedimentation. Research paper Utah State Univ. Logan : 16 p.

WILLNER, K. 1961. Uberlegungen zu der Frage der Eintrittsöffnungen von Kunststoff-Dränrohren. Z.f. Kult. 2 : 167.

WINGER, R.J.Jr. & RYAN, W.F. 1971. Gravel envelopes for pipe drains-design. Transaction of A.S.A.E. 14, 3 : 471-474, 479.

YOUNGS, E.G. 1965. A comparison of the performance of some plastic and tile drains. Journ. Agr. Eng. Research 10, 3 : 202-203.

YOUNGS, E.G. 1967. A treatment of the gappy drain problem in drainage theory. Journ. Agr. Eng. Research 12, 1 : 40-47.

ZUNKER, 1932. Arbeitsbericht des Unterausschusses für Dränung. Der Kulturtechniker 4/5 : 272-274.